

Brookhaven National Laboratory's
Annual Report of
Laboratory Directed
Research & Development
Program Activities
For FY 2005

Director's Office

BROOKHAVEN NATIONAL LABORATORY
BROOKHAVEN SCIENCE ASSOCIATES
UPTON, NEW YORK 11973-5000
UNDER CONTRACT NO. DE-AC02-98CH10886
UNITED STATES DEPARTMENT OF ENERGY

December 2005

Acknowledgments

The Laboratory Directed Research and Development (LDRD) Program is managed by Leonard Newman, who serves as the Scientific Director, and by Kevin Fox, Special Assistant to the Assistant Laboratory Director for Finance (ALDF). Preparation of the FY 2005 report was coordinated and edited by Leonard Newman and Kevin Fox, who wish to thank D.J. Greco and Maria Ohlsen for their assistance in organizing, typing, and proofing the document. A special thank you is also extended to the Photography and Graphic Arts Group for their help in publishing. Of course, a very special acknowledgement is extended to all of the authors of the project annual reports and to their assistants.

Table of Contents

Introduction.....	1
Management Process	2
Peer Review	7
Self Assessment	8
Relatedness of LDRD to Laboratory Programs and Initiatives	9
Summary of Metric Data	11
Projects Funding Table.....	13
 Project Summaries	
High-Brightness, High-Power Electron Beams	20
Structural Properties of Methane Hydrates.....	22
Investigation of Neutron and Gamma Probes to Detect Explosives in Sealed Containers.....	24
Structural Studies on the Integral Membrane Protein AlkB	26
The Micro PET Study of Gene Expression in Rodents	28
Hydrogen Atom Transfer from Carbon to Metal - Relevance of a Novel Reaction to Catalyzed Hydrocarbon Conversions	30
Radioprotection in <i>D. radiodurans</i> , a Radiation Resistant Bacterium	32
New Development of Norepinephrine Transporter Radioligands for PET Studies of Substance Abuse, Depression and ADHD.....	35
Condition: Green Chemistry Radiolytic Studies of Ionic Liquids in Service of Security and the Environment	39
Exploring the Use of Powder Diffraction for Proteins	42
Element-Resolved Dynamics of Nanoscale Ferromagnets.....	44

Table of Contents

Membrane Biophysics Using Model Membranes	46
High Pressure in Strongly Correlated Materials - An Optical Investigation	48
Polyoxometalate Giant Molecules: Novel Synthetic Methods, Characterizations and Potential Applications.....	52
Functional Bulk Mn-Based Nanocomposites	55
Radio Wave Detection of Ultra High Energy Cosmic Rays.....	57
New Synthesis Techniques to Control Atomic Defects in Advanced Intermetallic Compounds.....	59
Femtosecond Photoinitiated Nanoparticle Surface Chemistry	61
Chirped Pulse Amplification at the DUV-FEL	65
Overcoming Coherent Instabilities at Medium-Energy Storage Rings	67
Layered Cobaltates with High Thermoelectric Power.....	69
Complex Thin Films and Nanomaterial Properties	71
Lattice QCD Relevant for RHIC and AGS.....	74
Very Long Baseline Neutrino Oscillation Experiment.....	77
Advanced ³ He Detectors for the Spallation Neutron Source.....	80
Genetic NanoTags	82
The Use of Singular Point Genome Sequence Tags to Analyze Community Composition and Metabolic Potential.....	85
3-D Electronic Wave Functions from EM Images	88
Functional MRI Studies in Rats Using Implanted Brain Electrodes	91
Optimizing Functional Neuroimaging Techniques to Study Brain Function in Health and Disease States	93

Table of Contents

Technological Development of a Fluorescence Probe for Optical Detection of Brain Functional Activation <i>in vivo</i>	97
Nuclear Control Room Unfiltered Air In-Leakage by Atmospheric Tracer Depletion (ATD)	100
Perfluorocarbon Tracer Sampling, Tagging and Monitoring Techniques for Use at the Urban Atmospheric Observatory	102
Development of an Aerosol Mobility Size Spectrometer and an Aerosol Hygroscopicity Spectrometer	104
Exploration of Thermal Diffusion Processes in CdZnTe for Improved Nuclear Radiation Detectors	107
An Integrated Approach of High Power Target Concept Validation for Accelerator-Driven Systems	109
Hydrogen Storage Using Complex Metal Hydrides for Fuel Cell Vehicles	112
Full Power Test of the Amplifier for the Optical Stochastic Cooling Using JLAB FEL	114
Study of Photon Coupling to an Electromagnetic Field Gradient	115
Heavy Ion Physics with the ATLAS Detector	117
Superconducting Lead Photoinjector	119
Controlled Formation of Nanostructured RuO ₂ Catalysts	121
Hydrogen Storage in Complex Metal Hydrides	124
Behavior of Water on Chemically Modified Semiconductor Surfaces: Toward Photochemical Hydrogen Production	128
Assembling of Biological and Hybrid Complexes on Surfaces	130
Ultra High Resolution Photoelectron Spectrometer	132
Metal-Metal Oxide Electrocatalysts for Oxygen Reduction	134

Table of Contents

Multifunctional Nanomaterials for Biology	137
Polariton-Enhanced FRET for Device-Integration of Plasma Membranes from Rhodobacter Sphaeroides	141
Intense THz Source and Application to Magnetization Dynamics.....	143
Nano-Imaging of Whole Cells with Hard X-Ray Microscopy	145
Study to Convert NSLS VUV Ring to Coherent IR Source	147
Superconducting Undulator Technology	150
Characterization and Imaging of Amyloid Plaques Using Diffraction Enhanced Imaging.....	153
Development of Methodologies for Analyzing Transcription Factor Binding in Whole Genomes	157
Application of Endophytic Bacteria to Improve the Phytoremediation of TCE and BTEX Using Hybrid Poplar.....	161
Design and Build Two Dimensional Protein-Lipid Thin Film: A First Step Toward Novel Biochips	163
Positron Labeled Stem Cells for Non-Invasive PET Imaging Studies of In-Vivo Trafficking and Biodistribution	165
Breaking the Millimeter Resolution Barrier in fMRI	167
Novel Multi-Modality MRI and Transcranial Magnetic Stimulation to Study Brain Connectivity.....	171
Ovarian Hormone Modulation of ICP: MRI Studies.....	174
Feasibility of CZT for Next-Generation PET Performance.....	176
Biology on Massively Parallel Computers	178
Ionic Liquids in Biocatalysis and Environmental Persistence.....	179

Table of Contents

Single Particle Laser Ablation Time-of-Flight Mass Spectrometer (SPLAT-MS) Enhancements: Aerosol Optical Properties and Increased Particle Detectivity	183
Transition Metals in Oil and Gas Exploration.....	185
An Innovative Infiltrated Kernel Nuclear Fuel (IKNF) for High-Efficiency Hydrogen Production with Nuclear Power Plants.....	187
Development of Green Processes: Catalytic Hydrogenation in Water Utilizing In Situ Biologically-Produced Hydrogen	191
Fast Neutron Imaging Detector.....	193
Giant Proximity Effect (GPE) in High-Temperature Superconductors.....	195
Development of an Observation Based Photochemical-Aerosol Modeling System	197
Exploring Root Physiology in Relation to Uptake of Groundwater Pollutants.....	199
X-ray Absorption Spectroscopic Method for Studying Environmentally-relevant Reaction Kinetics.....	203
Global Cloud Analysis Technologies (G-CAT)	205
Computational Science.....	209
Structural Study of gamma-Secretase by Cryo-EM.....	210
Structural Analysis of Bacterial Pilus Biogenesis	212
Study of High-T _c Nanostructures.....	214
Appendix A - 2006 Project Summaries.....	216
Exhibit A - Call for Proposals for FY 2006.....	223
Exhibit B - LDRD Proposal Questionnaire	225
Exhibit C - LDRD Data Collection Form.....	232

Introduction

Brookhaven National (BNL) Laboratory is a multidisciplinary laboratory that carries out basic and applied research in the physical, biomedical, and environmental sciences, and in selected energy technologies. It is managed by Brookhaven Science Associates, LLC, under contract with the U. S. Department of Energy. BNL's total annual budget has averaged about \$460 million. There are about 2,700 employees, and another 4,500 guest scientists and students who come each year to use the Laboratory's facilities and work with the staff.

The BNL Laboratory Directed Research and Development (LDRD) Program reports its status to the U.S. Department of Energy (DOE) annually in March, as required by DOE Order 413.2A, "Laboratory Directed Research and Development," January 8, 2001, and the LDRD Annual Report guidance, updated February 12, 1999. In FY 2005 the LDRD Program continued to obtain its funds through the Laboratory overhead pool and operates under the authority of DOE Order 413.2A. Based on pending guidance from the DOE-CFO this funding structure will be changing in FY 2006.

The goals and objectives of BNL's LDRD Program can be inferred from the Program's stated purposes. These are to (1) encourage and support the development of new ideas and technology, (2) promote the early exploration and exploitation of creative and innovative concepts, and (3) develop new "fundable" R&D projects and programs. The emphasis is clearly articulated by BNL to be on supporting exploratory research "which could lead to new programs, projects, and directions" for the Laboratory.

As one of the premier scientific laboratories of the DOE, BNL must continuously foster groundbreaking scientific research. At Brookhaven National Laboratory one such method is through its LDRD Program. This discretionary research and development tool is critical in maintaining the scientific excellence and long-term vitality of the Laboratory. Additionally, it is a means to stimulate the scientific community and foster new science and technology ideas, which becomes a major factor in achieving and maintaining staff excellence and a means to address national needs within the overall mission of the DOE and BNL.

The LDRD Annual Report contains summaries of all research activities funded during Fiscal Year 2005. The Project Summaries with their accomplishments described in this report reflect the above goals and objectives. Aside from leading to new fundable or promising programs and producing especially noteworthy research, the LDRD activities have resulted in numerous publications in various professional and scientific journals and presentations at meetings and forums.

All FY 2005 projects are listed and tabulated in the Project Funding Table. Also included in this Annual Report in Appendix A is a summary of the proposed projects for FY 2006. The BNL LDRD budget authority by DOE in FY 2005 was \$10.5 million. The actual allocation totaled \$9.0 million.

The following sections in this report contain the management processes, peer review, and the portfolio's relatedness to BNL's mission, initiatives and strategic plans. Also included is a metric of success indicators and Self Assessment.

Management Process

PROGRAM ADMINISTRATION:

Overall Coordination: Overall responsibility for coordination, oversight, and administration of BNL's LDRD Program resides with the Laboratory's Director. Day-to-day responsibilities regarding funding, oversight, proposal evaluation, and report preparation have been delegated to the dedicated Scientific Director (SD) for the LDRD Program who now reports to the Assistant Laboratory Director for Policy and Strategic Planning. (PSP). The Office of the Assistant Laboratory Director for Finance (ALDF) continues to assist in the administration of the program. This includes administering the program budget, establishment of project accounts, maintaining summary reports, and providing reports of Program activities to the DOE through the Brookhaven Site Office Manager.

Responsibility for the allocation of resources and the review and selection of proposals lies with a management-level group called the Laboratory Directed Research & Development Program Committee. For Fiscal Year 2005, the Program Committee--which selected the 2006 programs--consisted of twelve members. The Scientific Director of the LDRD Program chaired the Committee, and the other members were the Assistant Laboratory Director for Policy and Strategic Planning (PSP), five Associate Laboratory Directors (ALDs), and five members from the scientific departments and divisions (S).

2005 LDRD PROGRAM COMMITTEE

Leonard Newman	Chairperson (SD)
Pat Looney	Assistant Laboratory Director for Policy and Strategic Planning (PSP)
Ralph James	Energy, Environment & National Security (ALD)
Samuel Aronson	High Energy & Nuclear Physics (ALD)
Peter Bond	Life Sciences (Interim ALD)
Steven Dierker	Light Sources (ALD)
Doon Gibbs	Basic Energy Sciences (ALD)
John Dunn	Biology (S)
James Davenport	Computational Science Center (S)
Steven Kettell	Physics (S)
G. Carr	Light Source (S)
Jose Rodriguez	Chemistry (S)

Allocating Funds: There are two types of decisions to be made each year concerning the allocation of funds for the LDRD Program. These are: (1) the amount of money that should be budgeted overall for the Program; and (2) of this, how much, if any, should go to each competing project or proposal. Both of these decisions are made by high-level management.

For each upcoming fiscal year the Laboratory Director, on recommendation by the Deputy Director for Science and Technology (DDS&T) and the Assistant Laboratory Director for Policy and Strategic Planning (PSP) and in consultation with the ALDF, develops an overall level of funding for the

LDRD Program. The budgeted amount is incorporated into the Laboratory's LDRD Plan, which formally requests authorization from the DOE to expend funds for the LDRD Program up to this ceiling amount.

The majority of projects are authorized for funding at the start of the fiscal year. However, projects can be authorized throughout the fiscal year, as long as funds are available and the approved ceiling for the LDRD Program is not exceeded.

The actual level, which may be less, is determined during the course of the year and is affected by several considerations including: the specific merits of the various project proposals, as determined by Laboratory management and the members of the LDRD Program Committee; the overall financial health of the Laboratory; and a number of budgetary tradeoffs between LDRD and other overhead expenses.

At BNL the LDRD Program was historically a much smaller portion of the total budget than at comparable National Laboratories. This prevented the Laboratory from preparing itself for work in emerging areas of research. Accordingly, the LDRD budget has been significantly increased over the past ten years from \$2.0 million to \$9.5 million, or from less than 1% to almost 2% of the Laboratory budget. The target level is to go to about 4%, which would still be significantly less than the DOE mandated maximum of 6%.

Request for Proposals: The availability of special funds for research under the LDRD Program is well publicized throughout the Laboratory. This is done using two methods - one occurring at yearly intervals, the other occurring irregularly. Each year a call letter is sent by the SD for LDRD to the Scientific Staff and as a separate memorandum to all the

Associate Laboratory Directors and Department Chairpersons. The FY 2006 call issued in February 2005 is attached as Exhibit A. This early schedule better facilitated the recruitment of post-doctorate candidates to support LDRD projects. We continued the process initiated in FY 02 that permits the deferral of expending the budget allocation into a third year to permit the full funding of post doctorates for two years, as they might not arrive at the onset of the LDRD project. The call references the BNL LDRD Standards-Based Management System (SBMS) Subject Area, which is available to all employees on the web at https://sbms.bnl.gov/sbmsearch/subjarea/99/99_SA.cfm?parentID=99. The other method is through a feature article in The Bulletin, the Laboratory's weekly newspaper.

The LDRD SBMS Subject Area specifies the requirements necessary for participation in the program. It states the program's purpose, general characteristics, procedures for applying, and restrictions. An application for funding, i.e., a project proposal, takes the form of a completed "Proposal Information Questionnaire," Exhibit B. An application must be approved up the chain-of-command which includes the initiator's Department or Division Budget Administrator and the Department Chairperson or Division Head.

The Chairperson or Division Head reviews the Proposal Information Questionnaire for completeness. This includes the review of responses to questions on National Environmental Policy Act (NEPA) and Environmental Safety and Health (ES&H).

Plans to ensure the satisfactory continuation of the principal investigator's regularly funded programs must also be approved.

The applications are then forwarded to the

LDRD Program Committee for full review and consideration for funding.

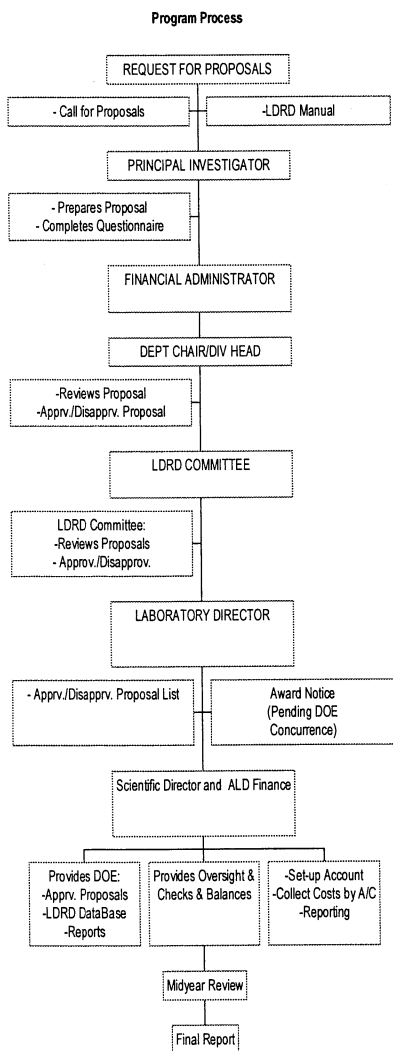
The process that solicits and encourages the development of proposals has evolved into two modes of operation. Specifically, the ideas for proposal development may originate among the scientific staff in response to the general call for proposals. Alternatively, they may be initiated by Laboratory science management. A portion of the LDRD budget was set aside as the Laboratory Directors Fund to address these issues. Eventually, both follow the standard procedures for proposal approval up the chain-of-command to the same decision makers. The fact that all proposals must be approved up the chain-of-command permits BNL managers to consider all ideas together when designing the mix of projects for the LDRD Program.

An initiative from management typically takes the form of a broad topical area or item of special interest such as computational biology. Then these “areas of interest” are communicated broadly to the scientific staff and in particular to staff members who are known to be in a position to pursue and develop their ideas in the form of a more formal proposal.

Proposal Review: Once the cognizant line managers approve the proposals, they are forwarded to the Chairperson of the Committee (SD for LDRD) who transmits a copy of the abstracts of all proposals received to the Committee for review. The Committee considers all proposals that have met certain minimum requirements pertaining to the Department's and BNL's LDRD policies.

Lead proponent responsibility of a proposal is assigned to that Associate Laboratory Director of the Committee who oversees and directs the technical area from which the proposal originated. One other ALD and a S serve as second proponents. The SD and the PSP serve as third proponents for all of the proposals. All of the above receive for review the full proposals for which they are responsible. A description of the process is outlined in the Figure above. All members have several weeks to review the proposals and prepare for a full debate on each proposal. The DOE Project Manager is present during the Committee evaluation sessions as a non-voting member.

Selection Criteria: Minimum requirements for each proposal are: (1) consistency with program purpose; (2) consistency with missions of BNL, DOE, and NRC; (3) approval by Department Chairperson and/or Division Head, and cognizant Associate/Assistant Director; (4) assurance of satisfactory continuation of principal



investigator's regularly funded programs; (5) modest size and generally scheduled for 2 years but limited to no more than 3 years; (6) will not substitute for, supplement, or extend funding for tasks normally funded by DOE, NRC, or other users of the Laboratory; (7) will not create a commitment of future multi-year funding to reach a useful stage of completion; and (8) will not fund construction line-item projects, facility maintenance, or general purpose capital equipment.

The selection criteria used to evaluate and rank individual proposals are stated in broad terms. While the LDRD SBMS Subject Area clearly states that selection is based on (1) scientific or technological merit, (2) innovativeness, (3) compliance with minimum requirements, (4) proposal cost as compared to the amount of available funding, and (5) its potential for follow-on funding. The requirements of DOE Order 413.2A are also carefully considered during the selection process to ensure that proposals are consistent with DOE criteria.

Project Approval: All proposals are rated and then discussed with the discussion of the lower rated proposals kept to a minimum. The Committee selects the highest priority proposals, by concurrence, for detailed discussion. Final selections are made by a vote of the ALDs as recommended for funding. Some funding may be held in reserve earlier in the fiscal year so that funds remain available for proposals submitted at later dates. The funding amount requested in any one specific proposal may be changed or adjusted during the approval process. The Committee's recommendation is then submitted to the Laboratory Director for approval. After approval by the Director all new projects are submitted to the DOE-Brookhaven Site Office (DOE-BHSO) for concurrence by the DOE Project Manager

prior to start. The ALDF then sets up a separate laboratory overhead account to budget and collect the costs for the project.

Project Supervision: The SD for LDRD carries out overall supervision of the projects. Supervision over the actual performance of LDRD projects is carried out in the same way as other research projects at the Laboratory. Each principal investigator is assigned to an organizational unit (Department, Division), that is supervised by a chairperson or manager.

Each chairperson or manager is responsible for seeing that the obligations of the principal investigator are satisfactorily fulfilled and that the research itself is carried out according to standard expectations of professionalism and scientific method. The SD monitors the project's status, schedule, and progress and coordinates with the chairperson or manager as necessary.

The SD organizes a mid-year review of all projects. Each PI presents a progress report on the status of their project. In attendance is the SD, the PSP, the DDS&T, the cognizant ALD and Department Chair, and a representative from the ALDF and DOE-BHSO. This review checks on the progress of the projects including its funding schedule. This allows the SD to ensure that the work be completed in a timely manner.

In addition, the SD conducts a monthly meeting with the DOE LDRD Project Manager to update the progress of the program and to solicit assistance to verify that the BNL LDRD Program is meeting the overall LDRD requirements. This includes providing the DOE-BHSO with copies of all funded proposals, an LDRD Program database, and a project funding and schedules summary report.

Project Reporting: Routine documentation of each project funded under the LDRD Program consists of a file containing: (1) a copy of the written proposal; (2) all interim status reports; (3) notifications of changes in research direction, if any; and (4) reports on costs incurred. Also, a formal LDRD Plan and the Annual Report on the LDRD Program (this Report) are submitted to BNL management and the DOE summarizing work progress, accomplishments, and project status on all projects.

All projects selected for approval are reviewed by the BNL Operations Security (OPSEC) Working Committee chair for classification review and operational security considerations.

Documentation for the overall Program consists of (1) various program history files, (2) a running list of all proposals with their acceptance/rejection status, (3) funding schedule and summary reports for all approved projects, (4) permanent records on cost accounting, and a database containing information on each funded project (description, funding by fiscal year, status and accomplishments, follow-on funding, publications, etc.). We have a Data Collection Form (Exhibit C) so that we can more formally collect information on the impacts of the projects. Each project will be tracked for two years after its completion so as to gather a complete set of data on the impact of the project. Also, we input LDRD data into the DOE-Chief Financial Officer's Laboratory/Plant Directed Research and Development Web Site (<https://ldrdrpt.doe.gov>) to support DOE reporting of LDRD to Congress.

Some of the projects may involve animals or humans. Those projects will have received approval from the Laboratory's appropriate review committees. The projects which involve animals or humans are identified in this report as follows:

Note: This project involves animal vertebrates or human subjects.

This is noted on the summary sheet and also at the end of each report.

Peer Review

LDRD projects have peer reviews performed in several different ways. Primarily, LDRD research is managed and reviewed by the cognizant Department and Division manager. These projects are a part of the activities of their respective Department and Divisions in which they reside. The BNL LDRD Program itself does not solicit formal peer reviews, consisting of written comments by experts outside the normal lines of supervision. Instead, advisory committees that consist of subject matter experts from academia and industry conduct peer reviews of LDRD projects as part of a Department's program review. One such group is the Brookhaven Science Associates' Science Advisory Committee, which performs peer reviews of different Laboratory programs on a rotating basis. There are also periodic reviews of the science at the Laboratory performed by various offices of DOE.

In addition to these outside peer reviews of the BNL program, the members of the LDRD Committee are considered to have sufficient technical knowledge to perform peer reviews of projects during the initial selection process and annual renewal. Also, all LDRD projects go through a formal mid-year review (described in the previous section under project supervision) conducted by the SD that includes the Assistant Laboratory Director for Policy and Strategic Planning, the Deputy Director for Science and Technology, and the cognizant Department Chair and Associate Laboratory Director.

Self Assessment

BNL supports the concept of continued improvement as part of its management of the Laboratory. To achieve this goal every year BNL performs self assessments on various functions at the Laboratory. In FY 2005, BNL conducted self assessments on program processes and accomplishments of the LDRD Program.

In FY 2005, all aspects of the program continue to function efficiently and effectively. The Laboratory added an Assistant Laboratory Director for Policy and Strategic Planning (PSP) who has oversight of the LDRD Program. This better supported the need to align the selected projects with Laboratory Initiatives.

As part of the annual assessment the LDRD Program Director and the PSP met with each ALD to solicit feedback on the LDRD selection process. In general, the comments were positive and the current process will continue in FY 2006 with some logistic changes. The process will continue to move toward a totally paperless process. Proposals will be submitted electronically and maintained on a database that the selection committee can access. In addition, decisions are under way to have improved abstracts to allow for better initial screening of projects.

The LDRD Program continues to emphasize that funding would be made for two years. This permits us to fund more projects in subsequent years. There was a mid-year review of all projects. This review was a factor in determining whether a project would continue into the next fiscal year. The Mid-year review continues to improve in format and quality. Several Directorates now conduct preliminary reviews of the projects prior to the Laboratory formal mid-year review. In

addition, the Scientific Director conducted monthly meetings with the DOE Brookhaven Site Office (BHSO) to update the progress of the program and verify that the BNL LDRD Program is meeting the overall LDRD requirements. Congressional inquiries continue to impact the DOE LDRD Program. This, along with BNL budget uncertainties required that we delay the start of those new programs that were approved for FY 2006.

BNL maintains its support of any new LDRD requirements by:

- Participating in the DOE SC LDRD working group to develop new guidelines
- Participating in changes to the DOE Chief Financial Officer (CFO) LDRD database
- Ensuring that all projects support the DOE security missions and missions of other federal agencies
- Identifying potential use/benefits to the DOE security missions for all projects
- Submitting data sheets for all projects to the DOE-BHSO for concurrence
- Including the DOE-BHSO LDRD Program Manager in all LDRD selection meetings

In FY 2005, BNL received approval from DOE of a \$10.5 million budget, which is approximately 2 percent of BNL operating funds, but is still far less than the maximum of 6 percent permitted by DOE. However, due to financial constraints the allocation was limited to \$9.5 million with 1 million in reserve. There continues to be many success stories in the LDRD Program with projects subsequently receiving direct funding from DOE, NIH, and CRADA agreements. In addition, several patents were submitted based on LDRD research.

Relatedness of LDRD to Laboratory Programs and Initiatives

BNL's mission is to produce excellent science in a safe, environmentally benign manner with the cooperation, support, and appropriate involvement of our many communities. Brookhaven was founded as a laboratory which would provide specialized research facilities that could not be designed, built, and operated at a university or industrial complex, and provides a scientific core effort for these facilities. This still remains a basic mission of the Laboratory.

BNL is committed to cultivating programs (including the LDRD) of the highest quality. These programs address DOE's Strategic Mission which is to conduct programs relating to energy resources, national nuclear security, environmental quality, and science.

Brookhaven National Laboratory has the following elements in its mission which support the DOE programmatic business lines.

The elements of Brookhaven's mission support and cut across the central activities of the Department of Energy as defined in its Strategic Plan.

The Laboratory's breadth of expertise as provides the basis for its contributions to the DOE's missions and focuses on providing extraordinary tools for the pursuit of basic science and technology.

SCIENCE & RESEARCH FACILITIES

Conceive, design, construct, and operate complex, leading-edge, user-oriented facilities in response to the needs of the DOE, and the needs of the international community users.

SCIENTIFIC PROGRAMS

Carry out basic and applied research in long-term high-risk programs at the frontier of science.

ENERGY RESOURCE MISSION, ENERGY TECHNOLOGIES

Perform R&D to provide clean, sustainable energy focusing on basic and applied research, system analysis and technology development.

NATIONAL SECURITY MISSION

Focus on domestic and international programs in nonproliferation and national security.

ENVIRONMENTAL QUALITY MISSION

Remediate the site and decontaminate and decommission of several research reactors.

TECHNOLOGY TRANSFER

Developing, managing, and transferring to industry intellectual property and technical know-how associated with research discoveries.

Overall, the LDRD portfolio supports all of the BNL themes and strategic objectives which in turn supports the DOE strategic initiatives (see table)

THEMES		Number of LDRD Projects
1	Scientific Facilities Operations <ul style="list-style-type: none"> • RHIC • NSLS • ATF • LEAF • STEM • Tandem • BMRR 	0
2	Nuclear Physics <ul style="list-style-type: none"> • Quark/gluon plasma • Spin Physics 	1
3	High Energy Physics <ul style="list-style-type: none"> • Standard Model • Rare Particles & Processes 	2
4	Advanced Accelerator & Detector Concept and Designs - Advanced Instrumentation <ul style="list-style-type: none"> • Muon Collider • DUV-FEL • LHC • SNS 	12
5	The Physics & Chemistry of Materials <ul style="list-style-type: none"> • Superconductivity • Magnetism • Surfaces • Nanostructure 	12
6	Energy Sciences <ul style="list-style-type: none"> • Combustion • Catalysis • Bio-fuels • Batteries • Geothermal • Buildings 	9
7	Environmental Sciences <ul style="list-style-type: none"> • Atmospheric • Terrestrial • Bio-remedial • Waste Technologies • Counter Terrorism 	16
8	Medical and Imaging Sciences & Technology	9
9	Advanced Computation	0
10	Biological Sciences	10
11	Critical Infrastructure	1
Totals		72

Summary of Metric Data

Statistical data is collected on all projects for the annual report. Since the LDRD Program is intended to promote high-risk research, the data collected has nominal value on a project-by-project basis. It does provide a general overall picture of the productivity of the LDRD Program.

Some of the more common indicators/measures of success are: 1) the number of proposed, received and approved projects, 2) amount of follow-on funding, 3) the number of patents applied for, and 4) the number of articles published in peer-reviewed journals.

Historically, statistics on the number of projects approved, compared to those rejected, show an overall approval rate of about 30 percent for new starts (see table). Essentially all of the scientific departments were represented in the FY 2005 LDRD Program. The LDRD Program at BNL is expanding and is generating interest from across the entire Laboratory population.

In FY 2005, the BNL LDRD Program funded 78 projects, 41 of which were new starts, at a total cost of \$8,378,553. Included in this report is the Project Funding Table, which lists all of the FY 2005 funded projects and gives a history of funding for each by year.

FY	DOE AUTH. \$K	BNL AUTH. \$K	COSTED \$K	NO. RECD.	NEW STARTS	TOTAL FUNDED
1985	4,000	1,842	1,819	39	13	13
1986	4,500	2,552	2,515	22	15	25
1987	4,000	1,451	1,443	29	8	17
1988	4,000	1,545	1,510	46	14	23
1989	4,000	2,676	2,666	42	21	29
1990	4,000	2,008	1,941	47	9	26
1991	2,000	1,353	1,321	23	14	21
1992	2,500	1,892	1,865	30	14	25
1993	2,500	2,073	2,006	35	14	28
1994	2,500	2,334	2,323	44	15	27
1995	2,500	2,486	2,478	46	13	31
1996	3,500	3,500	3,050	47	17	31
1997	4,500	4,500	3,459	71	10	28
1998	3,500	4,000	2,564	53	4	20
1999	4,750	4,612	4,526	67	25	33
2000	6,000	6,000	5,534	93	21	45
2001	6,000	6,000	5,345	97	38	70
2002	7,000	7,000	6,732	87	29	70
2003	8,500	8,482	7,830	153	44	83
2004	9,500	8,550	7,209	107	19	72
2005	10,500	9,073	8,379	114	41	78
2006	11,500	9,127		96	29	87
TOTALS	111,750	93,056	76,515	1,388	427	882

An analysis of the FY 2005 projects shows that many of the projects were reported to have submitted proposals for grants or follow-on funding (several received funding), and a multitude of articles or reports were reported to be in publication or submitted for publication. Several of these projects have already experienced varying degrees of success, as indicated in the individual Project Program Summaries that follow. A summary of success indicators for the FY 2005 projects is as follows:

SUCCESS INDICATORS FY 2005	QTY
Number of postdoctoral researchers supported in full or in part by LDRD during the fiscal year.	48
Number of students supported in full or in part by LDRD during the fiscal year.	2
Number of full-time scientific and technical research staff hired as a result of full or partial LDRD support during the fiscal year.	8
Number of LDRD-derived refereed publications (e.g., journal articles, conference papers, book chapters, or other reports) published during the fiscal year. This indicator includes all publications derived in whole or in part from LDRD projects funded in any year.	97
Number of LDRD-derived invention disclosures filed during the fiscal year (disclosure are internal laboratory intellectual property documents). This indicator includes all disclosures derived in whole or part from LDRD projects funded in any year and all subsequent LDRD follow-on activities.	0
Number of LDRD-derived patents issued/granted during the fiscal year. This indicator includes all patents derived in whole or part from LDRD projects funded in any year and all subsequent LDRD follow-on activities.	2
Number of LDRD-derived copyrights (other than publications) issued/granted during the fiscal year. This indicator includes all copyrights derived in whole or part from LDRD projects funded in any year and all subsequent LDRD follow-on activities.	0
Total number of national awards or recognitions received that are attributable in whole or in part from this LDRD.	8
Total number of formal presentations originating in whole or in part from this LDRD, including those that have been accepted for presentation but not yet presented.	401

Total number of reports originating in whole or in part from this LDRD.	27
Total number of review presentations that pertain to this work.	32

In conclusion, the overall LDRD Program has been successful. In FY 2005, the LDRD Program has improved on the level established in FY 2004 which already was at a high level. This increase in size is a consequence of the identification of the LDRD Program by Laboratory Management to be an important part of its future. The LDRD Program is a key component for developing new areas of science for the Laboratory. In FY 2005 the Laboratory continued to experience a significant scientific gain by the achievements of the LDRD Projects.

FUNDING TABLE OF LDRD PROJECTS APPROVED FY 2005

<u>Proj. No.</u>	<u>Project Title</u>	<u>P.I.</u>	<u>Dept./Bldg.</u>	<u>Theme</u>	<u>Actual FY03 \$</u>	<u>Actual FY04 \$</u>	<u>Actual FY05 \$</u>	<u>Approved FY06 \$</u>	<u>Requested FY07 \$</u>	<u>Total</u>
03-004	High-Brightness, High-Power Electron Beams	Ben-Zvi, I.	CAD/817	4	150,000	192,464	190,047			532,511
03-056	Structural Properties of Methane Hydrates	Mahajan, D.	ES&T/815	6	85,000	103,647	14,997			203,644
03-064	Investigation of Neutron and Gamma Probes to Detect Explosives in Sealed Containers	Todosow, M.	ES&T/475B	7	110,000	112,370	90,901			313,271
03-094	Structural Studies on the Integral Membrane Protein AlkB	Shanklin, J.	BIO/463	10	55,000	96,692	37,988			189,680
03-099	The microPET Study of Gene Expression in Rodents	Thanos, P.	MED/490	8	50,000	94,700	51,145			195,845
03-104	Hydrogen Atom Transfer from Carbon to Metal - Relevance of a Novel Reaction to Catalyzed Hydrocarbon Conversions	Bullock, M.	CHEM/555A	6	20,000	56,480	58,039	25,000		159,519
03-105	Radioprotection in D. Radiourans, a Radiation Resistant Bacterium	Cabelli, D.	CHEM/555A	10	57,500	74,668	15,329			147,497
03-107	New Development of Norepinephrine Transporter Radioligands for PET Studies of Substance Abuse, Depression and ADHD	Ding, Y.-S.	CHEM/555A	8	112,000	111,095	93,195			316,290
03-118	Condition: Green Chemistry Radiolytic Studies of Ionic Liquids in Service of Security and the Environment	Wishart, J.	CHEM/555A	7	43,000	79,517	36,945			159,462
03-119	Exploring the Use of Powder Diffraction for Proteins	Allaire, M.	NSLS/725D	10	45,000	79,445	34,880			159,325
03-121	Element-Resolved Dynamics of Nanoscale Ferromagnets	Kao, C.-C.	NSLS/725D	5	30,000	79,558	49,698			159,256
03-122	Membrane Biophysics Using Model Membranes	Pindak, R.	NSLS/725D	10	30,000	79,316	49,740			159,056
03-127	High Pressure in Strongly Correlated Materials - An Optical Investigation	Homes, C.	CMP/510B	5	54,400	66,865	11,000			132,265
03-129	Polyoxometalate Giant Molecules: Novel Synthetic Methods, Characterizations and Potential Applications	Liu, Tianbo	CMP/510B	6	54,000	95,532	45,558			195,090

FUNDING TABLE OF LDRD PROJECTS APPROVED FY 2005

<u>Proj. No.</u>	<u>Project Title</u>	<u>P.I.</u>	<u>Dept./Bldg.</u>	<u>Theme</u>	<u>Actual FY03 \$</u>	<u>Actual FY04 \$</u>	<u>Actual FY05 \$</u>	<u>Approved FY06 \$</u>	<u>Requested FY07 \$</u>	<u>Total</u>
03-138	Functional Bulk Mn-Based Nanocomposites	Lewis, L.	MSD/480	5	28,000	76,906	42,185			147,091
03-151	Radio Wave Detection of Ultra High Energy Cosmic Rays	Takai, H.	PHYS/510A	3	100,000	123,923	17,502			241,425
03-162	New Synthesis Techniques to Control Atomic Defects in Advanced Intermetallic Compounds	Cooley, L.	MSD/480	5	88,000	90,577	70,713			249,290
04-011	Femtosecond Photoinitiated Nanoparticle Surface Chemistry	Camillone, N.	CHEM/555	6		79,532	121,071	41,000		241,603
04-013	Chirped Pulse Amplification at the DUV-FEL	Yu, L.H.	NLSL/725C	4		78,404	119,331	41,000		238,735
04-025	Overcoming Coherent Instabilities at Medium-Energy Storage Rings	Wang, J.-M.	NLSL/725C	4		91,415	128,858	48,000		268,273
04-033	Layered Cobaltates with High Thermoelectric Power	Li, Qiang	MSD/480	6		61,780	103,160	32,300		197,240
04-038	Complex Thin Films and Nanomaterial Properties	Misewich, J.	MSD/480	6		79	190,532	307,000	143,000	640,611
04-041	Physics of Quark Gluon Plasma (QGP)	Petreczky, P.	PHYS/510A	2		69,272	109,751	37,000		216,023
04-043	Very Long Baseline Neutrino Oscillation Experiment	Diwan, M.	PHYS/510E	3		71,099	106,166	36,000		213,265
04-046	Advanced 3He Detectors for the Spallation Neutron Source	Smith, G.	INST/535B	4		72,953	109,650	37,400		220,003
04-055	Genetic Nano Tags	Hainfeld, J.	BIO/463	5		12,933	114,424	99,000		226,357
04-060	The Use of Singular Point Genome Sequence Tags to Analyze Community Composition and Metabolic Potential	van der Lelie, D.	BIO/463	10		121,236	185,509	63,000		369,745
04-061	3-D Electronic Wave Functions from EM Images	Wall, J.	CFN/463	4		98,945	149,814	51,000		299,759
04-062	Functional MRI Studies in Rats using Implanted Brain Electrodes	Gifford, A.	MED/490	8		78,466	119,912	41,000		239,378
04-063	Optimizing Functional Neuroimaging Techniques to Study Brain Function in Health and Disease States	Goldstein, R.	MED/490	8		100,684	144,278	51,000		295,962

FUNDING TABLE OF LDRD PROJECTS APPROVED FY 2005

<u>Proj. No.</u>	<u>Project Title</u>	<u>P.I.</u>	<u>Dept./Bldg.</u>	<u>Theme</u>	<u>Actual FY03 \$</u>	<u>Actual FY04 \$</u>	<u>Actual FY05 \$</u>	<u>Approved FY06 \$</u>	<u>Requested FY07 \$</u>	<u>Total</u>
04-066	Technological Development of a Fluorescence Probe for Optical Detection of Brain Functional Activation <i>in vivo</i>	Du, C.	MED/490	8		27,032	132,570	104,000		263,602
04-069	Nuclear Control Room Unfiltered Air In-Leakage by Atmospheric Tracer Depletion (ATD)	Dietz, R.	ESD/815E	7		59,463	88,764	31,000		179,227
04-073	Perfluorocarbon Tracer Sampling, Tagging and Monitoring Techniques for use at the Urban Atmospheric Observatory	Heiser, J.	ESD/830	7		65,530	98,809	34,000		198,339
04-079	Development of an Aerosol Mobility Size Spectrometer and an Aerosol Hygroscopicity Spectrometer	Wang, J.	ESD/815E	7		65,589	99,415	34,000		199,004
04-086	Exploration of Thermal Diffusion Processes in CdZnTe for Improved Nuclear Radiation Detectors	Bolotnikov, A.	NNS/197C	7		86,077	131,041	44,000		261,118
04-088	An Integrated Approach of High Power Target concept Validation for Accelerator-Driven Systems	Simos, N.	ES&T/475B	4		82,747	121,361	46,000		250,108
04-104	Hydrogen Storage Using Complex Metal Hydrides for Fuel Cell Vehicles	Wegrzyn, J.	ES&T/815	6		70,265	108,592	37,000		215,857
05-003	Full Power Test of the Amplifier for the Optical Stochastic Cooling using JLAB FEL	Yakimenko, V.	PHYS/820M	4			112,488	120,000		232,488
05-005	Study of Photon Coupling to an Electromagnetic Field Gradient	Scarlett, C.	PHYS/510E	4			105,693	132,000		237,693
05-006	Heavy Ion Physics with the ATLAS Detector	Takai, H.	PHYS/510A	2			5,623	103,000	86,000	194,623
05-017	Superconducting Lead Photoinjector	Smedley, J.	INST/535B	5			117,500	118,000		235,500
05-020	Controlled Formation of Nanostructured RuO2 Catalysts	Sutter, P.	CFN/555	6			117,502	115,000		232,502
05-021	Hydrogen Storage in Complex Metal Hydrides	Vogt, T.	CFN/510A	6			123,301	125,000		248,301

FUNDING TABLE OF LDRD PROJECTS APPROVED FY 2005

<u>Proj. No.</u>	<u>Project Title</u>	<u>P.I.</u>	<u>Dept./Bldg.</u>	<u>Theme</u>	<u>Actual FY03 \$</u>	<u>Actual FY04 \$</u>	<u>Actual FY05 \$</u>	<u>Approved FY06 \$</u>	<u>Requested FY07 \$</u>	<u>Total</u>
05-028	Behavior of Water on Chemically Modified Semiconductor Surfaces: Toward Photochemical Hydrogen Production	Fujita, E.	CHEM/555A	6			89,092	120,000		209,092
05-030	Assembling of Biological and Hybrid Complexes on Surfaces	Gang, O./Freimuth, P.	CMP/510B	6			139,859	140,000		279,859
05-033	Ultra High Resolution Photoelectron Spectrometer	Johnson, P.	CMP/510B	4			67,053	67,000		134,053
05-038	Metal-Metal Oxide Electrocatalysts for Oxygen Reduction	Vukmirovic, M.	MSD/555	6			99,510	103,000		202,510
05-041	Multifunctional Nanomaterials for Biology	Wong, S.	MSD/480	5			128,192	130,000		258,192
05-042	Polariton-Enhanced FRET for Device-Integration of Plasma Membranes from Rhodobacter Sphaeroides	Abbamonte, P.	NSLS/725D	10			79,321	80,000		159,321
05-044	Intense THz Source & Application to Magnetization Dynamics	Carr, G. L.	NSLS/725D	4			50,175	100,000	50,000	200,175
05-048	Nano-Imaging of Whole Cells with Hard X-Ray Microscopy	Miller, L.	NSLS/725D	10			19,496	80,000	60,000	159,496
05-050	Study to Convert NSLS VUV Ring to Coherent IR Source	Podobedov, B.	NSLS/725C	4			49,261	130,000	80,000	259,261
05-051	Superconducting Undulator Technology	Rakowsky, G.	NSLS/725D	5			189,451	175,000		364,451
05-057	Characterization and Imaging of Amyloid Plaques Using Diffraction Enhanced Imaging	Zhong, Z.	NSLS/725D	10			100,793	100,000		200,793
05-058	Development of Methodologies for Analyzing Transcription Factor Binding in Whole Genomes	Anderson, C.	BIO/463	10			92,970	112,000	51,300	256,270
05-063	Application of Endophytic Bacteria to Improve the Phytoremediation of TCE and BTEX using Hybrid Poplar	van der Lelie, D.	BIO/463	10			212,900	220,000		432,900
05-064	Design and Build Two Dimensional Proten-Lipid Thin Film: A First Step Toward Novel Biochips	Wei, Y.	BIO/463	4			61,342	60,000		121,342

FUNDING TABLE OF LDRD PROJECTS APPROVED FY 2005

<u>Proj. No.</u>	<u>Project Title</u>	<u>P.I.</u>	<u>Dept./Bldg.</u>	<u>Theme</u>	<u>Actual FY03 \$</u>	<u>Actual FY04 \$</u>	<u>Actual FY05 \$</u>	<u>Approved FY06 \$</u>	<u>Requested FY07 \$</u>	<u>Total</u>
05-068	Positron Labeled Stem Cells for Non-Invasive PET Imaging Studies of In-Vivo Trafficking and Biodistribution	Srivastava, S.	MED/801	8			63,600	165,000	65,000	293,600
05-069	Breaking the Millimeter Resolution Barrier in fMRI	Tomasi, D.	MED/490	8			109,920	110,000		219,920
05-070	Novel Multi-Modality MRI and Transcranial Magnetic Stimulation to Study Brain Connectivity	de Castro Caparelli, E.	MED/490	10			105,571	112,000		217,571
05-071	Ovarian Hormone Modulation of ICP: MRI Studies	Biegan, A.	MED/490	10			107,120	112,200		219,320
05-072	Feasibility of CZT for Next-Generation PET Performance	Vaska, P.	MED/490	8			111,425	110,000		221,425
05-074	Biology on Massively Parallel Computers	Davenport, J. W.	CSC/463B	9			168,787	177,801		346,588
05-078	Ionic Liquids in Biocatalysis and Environmental Persistence	Francis, A. J.	ESD/490	7			99,464	100,000		199,464
05-082	Single Particle Laser Ablation Time-of-Flight Mass Spectrometer (SPLAT-MS) Enhancements: Aerosol Optical Properties and Increased Particle Detectivity	Senum, G.	ESD/815E	7			97,705	100,000		197,705
05-088	Transition Metals in Oil and Gas Exploration	Vairavamurthy, A.	ES&T/815	6			128,489	135,000		263,489
05-092	An Innovative Infiltrated Kernel Nuclear Fuel (IKNF) for High-Efficiency Hydrogen Production with Nuclear Power Plants	Saccheri, J./Bowerman, B	ES&T/475B	6			130,393	130,000		260,393
05-094	Development of Green Processes: Catalytic Hydrogenation in Water Utilizing In Situ Biologically-Produced Hydrogen	Mahajan, D.	ES&T/815	7			274,561	288,000		562,561
05-098	Fast Neutron Imaging Detector	Lemley, J.	NNS/197C	4			124,052	144,000		268,052
05-104	Giant Proximity Effect in High-Temperature Superconductors	Bozovic, I.	MSD/480	14			267,837	275,000	191,000	733,837
05-105	Development of an Observation-based Photochemical-Aerosol Modeling System	Wright, D.	ESD/815E	26			109,033	79,000		188,033

FUNDING TABLE OF LDRD PROJECTS APPROVED FY 2005

<u>Proj. No.</u>	<u>Project Title</u>	<u>P.I.</u>	<u>Dept./Bldg.</u>	<u>Theme</u>	<u>Actual FY03 \$</u>	<u>Actual FY04 \$</u>	<u>Actual FY05 \$</u>	<u>Approved FY06 \$</u>	<u>Requested FY07 \$</u>	<u>Total</u>
05-106	Exploring Root Physiology in Relation to Uptake of Groundwater Pollutants	Ferrieri, R./ Thorpe, M.	CHEM/555	5			165,365			165,365
05-108	X-ray Absorption Spectroscopic Method for Studying Environmentally-relevant Reaction Kinetics	Fitts, J.	ESD/830	26			92,733			92,733
05-109	Global Cloud Analysis Technologies (G-CAT)	Vogelmann, A.	ESD/490D	5			92,858			92,858
05-110	Computational Science	Davenport, J.	CSC/463B	34			109,776	126,000		235,776
05-111	Structural Study of gamma-Secretase by Cryo-EM	Li, H.	BIO/463	26			191,280			191,280
05-112	Structural Analysis of Bacterial Pilus Biogenesis	Li, H.	BIO/463	26			208,405			208,405
05-114	Study of High-Tc Nanostructures	Bozovic, I.	MSD/480	14			265,787	275,000	191,000	731,787
			TOTALS		1,111,900	3,007,256	8,378,553	6,008,701	917,300	19,423,710

LABORATORY DIRECTED RESEARCH AND DEVELOPMENT
2005 PROJECT PROGRAM SUMMARIES

High-Brightness, High-Power Electron Beams

Ilan Ben-Zvi

03-004

PURPOSE:

The objective of this work is to develop bright and high power electron beams from photoinjector electron sources. This is done through the development of CW photoinjectors and critical subcomponents for the photoinjectors. Getting a high brightness and high power electron beam is a risky, cutting edge R&D, but the payoff could be high in enabling new radiation sources such as x-ray Free Electron Lasers (FELs) and Photoinjected Energy Recovery Linacs, electron cooling for RHIC and high-power FELs for defense applications.

APPROACH:

The PI, in collaboration with Triveni Srinivasan-Rao, undertook to carry out the development of a superconducting laser photocathode RF guns and the associated photocathodes. The basic tools of the research were the niobium superconducting RF gun (Figure 1) and photocathode preparation and testing systems (Figures 2 and 3).

TECHNICAL PROGRESS AND RESULTS:

We tested the superconducting photoinjector. As a result we became the first US laboratory to possess a functioning superconducting laser photocathode RF gun. Photoelectrons from an all niobium superconducting injector have been generated for the first time. A quantum Efficiency, QE of 2×10^{-6} at 266 nm and 2×10^{-5} at 248 nm, maximum charge of 10

nC in 10 ns and charge/cycle of 0.8 nC were measured. The relatively small improvement observed in the QE after laser cleaning is attributed to the long distance between the cathode and the closest ion pump and the possibility of the laser ablated material adsorbed back onto the cathode surface at cryogenic temperature. No cavity quenching has been observed even at the maximum laser energy of 3 mJ, maximum repetition rate of 250 Hz and maximum charge of 10 nC from the cathode.

As the program of testing the niobium cathode came to a successful conclusion, we modified the gun to accept an interchangeable photocathode by incorporating a choke-joint in the gun. Figure 1 shows the superconducting, all-niobium photoinjector with the choke-joint. The success of this program led to a decision by the US Navy to construct a high-current (up to 0.5 ampere average current) superconducting photoinjector using BNL expertise in the design of such devices and hand it over to BNL for testing.

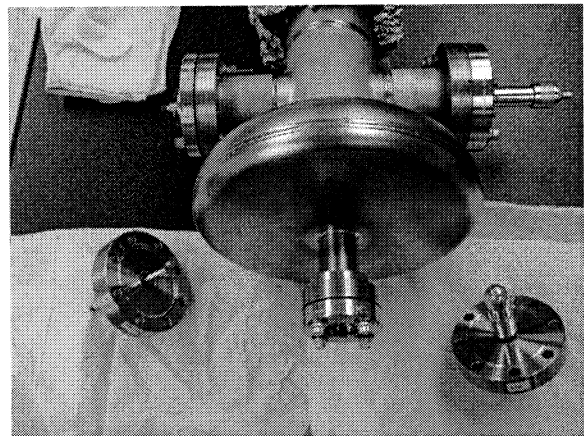


Figure 1. Superconducting photoinjector with choke-joint for insertion of photocathodes.

In turn, the future availability of the new gun (to be completed in March 2007) led the Navy to invest further funding at BNL and construct a high-current demonstration Energy Recovery Linac at Building 912 at

BNL/C-AD, which will use the gun and other components available.

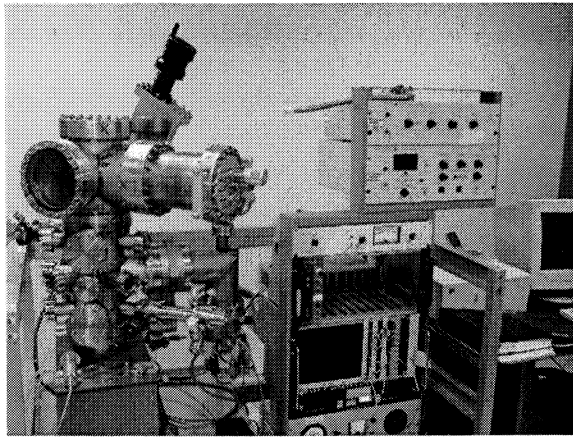


Figure 2. Diamond amplified photocathode test chamber.

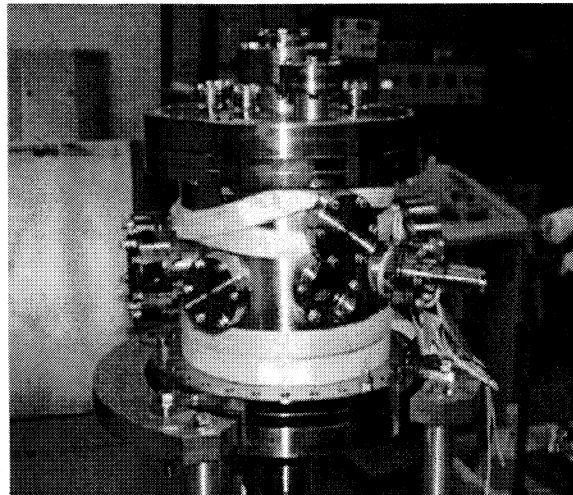


Figure 3. Diamond hydrogenation chamber.

Another development, which stemmed from this LDRD work has been the diamond amplified photocathode invention. In this new concept, a thin (30 micron) diamond window is positioned between the photocathode and the electron gun acceleration region. The electrons released from the photocathode are accelerated by a modest DC voltage of about 5 kV to strike the diamond window through a face, which is covered with a thin metal electrode. The

primary electrons generate a large number of electron-hole pairs. The holes are collected by the thin metal layer, while the secondary electrons are drifted through the diamond and exit it through a Negative Electron Affinity (NEG) face into the accelerating space of the gun. Figure 2 shows the diamond amplifier test chamber and Figure 3 shows the diamond hydrogenation system.

The advantages of this new principle of amplified photocathode are as follows:

- The quantum efficiency of the photocathode is increased by a couple of orders of magnitude.
- The temporal characteristics of the laser pulse are maintained.
- The cathode's lifetime is increased very significantly, due to the protection afforded by the diamond window.
- The gun is protected from the cathode materials, enabling one to use a superconducting RF gun.

SPECIFIC ACCOMPLISHMENTS:

Publication:

J. Sekutowicz, S. A. Bogacz, D. Douglas, P. Kneisel, G. P. Williams, M. Ferrario, I. Ben-Zvi, J. Rose, J Smedley, T. Srinivasan-Rao, L. Serafini, W.-D. Möller, B. Petersen, D. Proch, S. Simrock, P. Colestock, and J. B. Rosenzweig, Proposed continuous wave energy recovery operation of an x-ray free electron laser, Phys. Rev. ST Accel. Beams **8**, 010701 (2005)

LDRD FUNDING:

FY 2003	\$150,000
FY 2004	\$192,464
FY 2005	\$190,047

Structural Properties of Methane Hydrates

Devinder Mahajan

03-056

PURPOSE:

The key to recovering methane from globally abundant methane hydrate is to understand its kinetic stability in host sediments. An uncertainty remains as to the nature of sediment pores in which methane hydrates prefer to form and reside. The purpose of this project is to measure key physical properties of host sediments from methane hydrate sites and then correlate their structural characteristics with the formation of guest (methane hydrate)-host (sediment) complexes.

APPROACH:

Our approach involves: 1) measuring porosity and related properties of the sediment samples, obtained from the methane hydrate sites, using Computed Microtomography (CMT) and 2) obtaining baseline methane hydrate formation/decomposition data on the guest-host complexes in the characterized sediments. Pristine samples of host sediments from Blake Ridge, a well-known hydrate site, were obtained from the United States Geological Survey (USGS). Porosity and other sediment properties were measured at the Beamline X27A at the NSLS. In addition, a unique unit to study methane hydrate kinetics has been brought on-line that mimic subsurface conditions.

TECHNICAL PROGRESS AND RESULTS:

Three sediment samples: two from Blake Ridge, off the coast of the Carolinas (depths of 50 m and 667 m), and one from Georges

Bank (0.2 m), both well-established methane hydrate sites, were obtained through USGS to establish their porosity differential as a function of depth. The CMT technique was used to collect 2-D data on the sediment slices, from which 3-D images of the sediments were reconstructed (Figure 1).

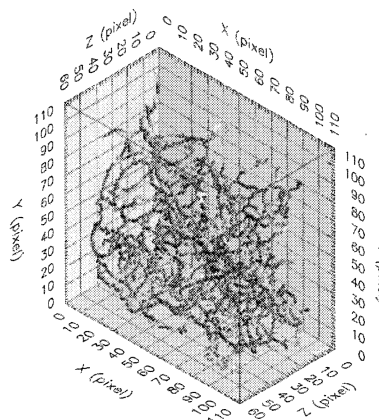


Figure 1. Fluid flow pathways reconstructed from the 2-D data for the 50 meters depth sample. Small diameter pathways correspond to a red color whereas a blue color indicates larger diameter pathways. The pixel sizes for the three axes are .0068 mm.

The calculated porosity values show that sediment porosity decreases as a function of depth: 80.7%, 64.3%, and 58.1% for 0.2, 50 and 667 meters respectively. Further data refinement now continues. In addition, a customized cell, capable of operating at high pressures and low temperatures (those mimicking ocean floor conditions), was obtained from a vendor to study *in situ* methane hydrate formation at the beam line.

A parallel effort was initiated to study the methane hydrates formation/decomposition in the characterized sediments. A unit capable of a flexible, integrated study of the hydrate was constructed and baseline kinetic data of pure methane hydrate formation were collected. The data fits well with the reported literature studies (Figure 2).

In FY05, the work was completed to further test the unit and data dissemination

continued. Further work to establish the effect of sediment porosity on methane hydrate formation kinetics is in progress with follow-up funding from U.S DOE, Office of Fossil Energy.

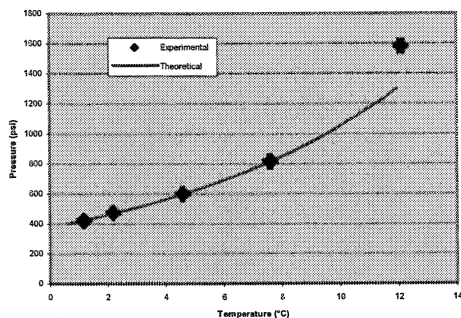


Figure 2. Pure methane hydrates formation in the BNL unit. The line represents theoretical values.

SPECIFIC ACCOMPLISHMENTS:

Refereed Publications

1. M. Eaton, D. Mahajan, and R. Flood. A Novel High-Pressure Apparatus to Study Hydrate-Sediment Interactions. J. Pet. Sci. & Eng., Accepted.
2. Fundamental Challenges to Methane Recovery from Gas Hydrates. P. Servio, M. Eaton, D. Mahajan, and W.J. Winters. Topics In Catal., 101-108 (2005).
3. Methane Hydrate Studies: Decomposition Kinetics and Delineating Properties of Host Sediments. D. Mahajan, P. Servio, K.W. Jones, H. Feng, and W.J. Winters. Chapter 16 in Advances in the Studies of Gas Hydrates, C. E. Taylor and J. T. Kwan, Editors, pp. 239-250, Kluwer Academic Publishers, Inc., New York, New York.

Presentations

1. Hydrate-Sediment Interactions in a Novel High-Pressure Apparatus. Symp. on Gas Hydrates and Clathrates. M. Eaton, D. Mahajan, R. Flood Co-sponsored by the ACS Petroleum Chemistry and Fuel

Divisions. 229th ACS National Meeting, San Diego, CA. March 13-17, 2005.

2. Morphology of methane hydrate host sediments. K.W. Jones, H. Feng, S. Tomov, W.J. Winters, Michael Eaton, and D. Mahajan. Same as in 1.

3. Technical Challenges to Mining Methane Hydrates: The next Energy Frontier". Marine Sciences and Atmospheric Sciences Colloquium Series, Stony Brook University, New York. February 6, 2004.

4. Gulf of Mexico Naturally Occurring Gas Hydrates JIP Workshops. Denver, CO. September 30 - October 1, 2003.

5. Kinetic Reproducibility of Methane Production from Methane Hydrates. P. Servio and D. Mahajan. Symposium on Synthetic Clean Fuels from Natural Gas and Coal-bed Methane: 30 Years Since First Oil Crisis. Co-sponsored by the ACS Fuel and Petroleum Chemistry Divisions. 226th ACS National Meeting, New York, NY. September 7-11, 2003.

6. Methane Hydrate Studies: Delineating Properties of Sediments Using Synchrotron Computed Micro tomography (CMT). D. Mahajan, K. W. Jones, H. Feng, and W. J. Winters. Presented at the Symposium on Gas Hydrates, 2003 AICHE Spring National Meeting, Abstract #78a New Orleans, LA March 30- April 3, 2003.

Review Presentation

- Methane Hydrate Activity at BNL - An Overview. D. Mahajan. To NETL/ DOE. May 5, 2003.

LDRD FUNDING:

FY 2003	\$ 85,000
FY 2004	\$103,647
FY 2005	\$ 14,997

Investigation of Neutron and Gamma Probes to Detect Explosives in Sealed Containers

Michael Todosow
L. Wielopolski

03-064

PURPOSE:

The purpose of the project is to examine options for using neutrons and/or resonance gamma rays to probe airline shipping containers and determine the presence of explosives by reading the characteristic signatures of induced or scattered radiation. These techniques can be specifically designed to probe for contraband in small and large containers. The challenges include the ability to make them simultaneously effective and efficient. This includes issues such as decreasing false positive alarms while retaining a very high detection probability, reducing the time necessary to make the determinations, cost and implementation issues, etc. As a result of interest by DHS in the detection of Special Nuclear Materials (SNM), issues associated with this application have also been addressed.

APPROACH:

It is proposed to use modern Monte Carlo methods (specifically the MCNP/MCNPX codes developed by LANL) to perform "synthetic experiments" to simulate systems based on the use of neutrons and resonance gamma rays to determine the physical and performance characteristics of potential systems to detect explosives. However, because neutrons will activate materials, the focus is on Gamma Resonance Technology (GRT), which has been demonstrated to be a viable solution to intercept concealed

explosives with a low (5%) false alarm rate. A fundamental aspect of the initial phase of the study was to evaluate the adequacy of the basic cross section data needed to evaluate this approach. The use of high-energy, mono-energetic gammas to detect SNM is also being explored.

Based on the results of the initial survey phase, additional analyses will be performed to define the characteristics of a reference system(s) which might be based on neutrons only, gammas only, or a combination. Needed RD&D, including initial experiments to evaluate selected performance characteristics (e.g., intensity, number and orientation of neutron/gamma sources; number and orientation of detectors; characteristics of signatures to be measured/compared, etc.), will be identified.

TECHNICAL PROGRESS AND RESULTS:

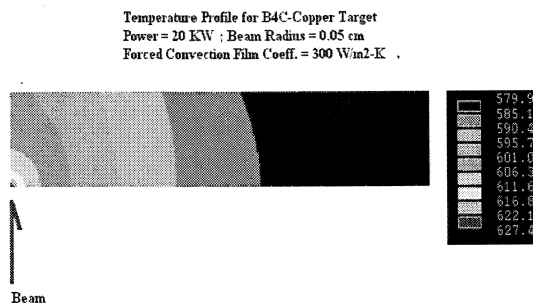
Accomplishments for FY05 includes:

Target (H. Ludewig, N. Simos).

Several target isotopes for the production of high-energy mono-energetic gammas from a few MeV protons were identified. An attractive candidate is boron carbide which could produce mono-energetic beams of 12.8, 9.17, and 4.4 MeV. In addition to detecting explosives via detection of N-14 by GRT, this suite of photons would excite photo-fission in any SNM present, and would allow imaging of high-z materials via γ -radiography. More detailed studies utilizing the ANSYS finite element code considered a boron carbide (50 μm) on copper (1-cm.) target with an assumed flat proton beam. The model employed an extremely fine mesh to capture the thin-layer effects, and differential expansion of the two materials was incorporated into the thermal stress analysis.

Results of some of the thermal calculations are shown in Figure 1. Assuming a 20 kW beam resulting from a typical proton beam energy of 2MeV and a current of 10-mA, the increase in temperature would be acceptable for a beam spot with a radius of ~0.1 cm. However, a beam spot radius > ~0.3 cm. would be required from stress considerations.

Figure 1. Temperature Profile in Target



Monte Carlo Simulations for SNM (G. Raites , M. Todosow, A. Mallen.)

M. Todosow is currently serving as a member of the DHS Active Interrogation Working Group (AIWG). In connection with this activity the ability of a system based on high-energy, mono-energetic gammas to detect SNM hidden in a large shipping container has been considered. Several container configurations with varying contents defined by the AIWG have been simulated at BNL and LANL. Some of the key figures of merit for an Active Interrogation system include: 1) number of fissions induced in the concealed SNM per dose on the surface of the container; 2)

absolute number of fissions induced; and 3) number of neutrons and/or photons which escape the container and are available for detection. High-energy mono-energetic photons are particularly attractive based on the first performance criterion, but the relatively low yield per proton, coupled with the characteristics of present and near-term accelerators present a challenge with respect to criteria 2 and 3.

SPECIFIC ACCOMPLISHMENTS:

Presentations

L. Wielopolski, M. Todosow, H. Ludewig, N. Simos, **“Production of Monoenergetic Gamma Rays for Cargo Container Inspection,”** CAARI-2004, October 2004. (accepted, but not presented due to LW illness).

M. Todosow and H. Ludewig, gave several talks on “Active Interrogation” to potential sponsors.

Proposals

“Target Studies to Support Active Interrogation Options,” submitted to DOE/NA-22.

LDRD FUNDING:

FY 2003	\$110,000
FY 2004	\$112,370
FY 2005	\$ 90,901

Structural Studies on the Integral Membrane Protein AlkB

John Shanklin

03-094

PURPOSE:

The goal of this proposal is to initiate structural studies on the Alkane ω -hydroxylase (AlkB) from *Pseudomonas oleovorans*, exploiting its unique structural organization that is ideally suited to both crystallography and cryo-electron microscopy.

APPROACH:

Approximately 30 percent of all proteins reside in membranes, and with a few notable exceptions little is known about their structures and how those relate to their function. There are two major obstacles to structure determination of membrane proteins. 1) Membrane proteins exist in a lipid bilayer along with many other membrane proteins, which greatly complicates purification because they are all functionally tethered together in the same membrane. 2) Solubilizing proteins from a complex heterogeneous membrane environment while maintaining the functional protein requires precisely defined conditions that are specific to each protein. The solution to this complex problem is difficult, because to purify membrane proteins, they must first be expressed to high levels, solubilized, and the conditions for solubilization often interfere with the conditions needed for purification. A unique property of AlkB is that it forms homogeneous protein vesicles that can be purified in the absence of detergents. This offers a unique opportunity to simplify obtaining structural information for this particular integral membrane enzyme.

TECHNICAL PROGRESS AND RESULTS:

The postdoctoral research associate, I. Abreu replaced I. Heilmann when he took a faculty position in Germany.

While previous efforts were directed at improving the relative abundance of expressed AlkB protein, Dr. Abreu tested several combinations of host strains, media composition, and scale of induction. She arrived at an acceptable expression level and spent several months expressing and purifying the protein. She found that a critical step was in the concentration of resuspended AlkB containing membrane following a differential ultracentrifugation step. Resuspension in too high of a concentration prevented the AlkB from binding to the carboxymethyl phase of high performance liquid chromatography and was resulting in high low AlkB recovery and low purification. Having solved this problem, we were able to increase the yield of recovered AlkB. Because the yield of AlkB was specifically improved, with respect to minor contaminants, the yield increase also facilitated an increase in purity. Thus, we were able to obtain several tens of mg of purified AlkB for detergent solubilization trials. Membrane proteins are notoriously unstable upon the addition of detergents. We undertook a two-step detergent solubilization regime. The first step involved membrane solubilization using a harsh non-ionic detergent, Triton X-100. This is particularly effective for removing integral membrane proteins from the membrane component, but is often responsible for unfolding of the protein once removed from the membrane. Further, Triton X-100 has large micelle size, thus it is very difficult to obtain monodispersed AlkB, i.e., one AlkB per micelle. Thus, we subjected Triton X-100 solubilized

membranes to high performance liquid chromatography with the use of a G3000SW matrix with n-Dodecyl-b-D-maltoside, DDM, as the mobile phase. During the chromatography, the Triton was exchanged for DDM, and the AlkB came off at a retention time consistent with it being a monomer. This is a very significant accomplishment and a prerequisite step for crystallization trials. Now that we have accomplished a monodispersed form at the analytical level, we have to scale up our procedure. The monodispersed protein eluant needs to be concentrated and then subjected to crystallization trials.

The following has been accomplished:

- Identification of strains of AlkB in a pET3a or pET9a plasmids in host cell lines BL21DE3, BL21DE3pLysS.
- Optimization of growths in TB media at the 1.5 lit scale.
- Optimization of purification conditions increasing yield while minimizing contaminants.

- Purification of tens of mg highly enriched and biologically active AlkB protein.
- Demonstration of solubilization from membranes with the use of Triton X-100.
- Demonstration of the ability to exchange the Triton X-100 for DDM with monodispersed AlkB at the analytical level.

SPECIFIC ACCOMPLISHMENTS:

Evidence linking the *Pseudomonas oleovorans* alkane ω -hydroxylase, an integral membrane diiron enzyme, and the fatty acid desaturase family. Shanklin, J. and Whittle, E. FEBS Lett. 545, 188-192 (2003).

LDRD FUNDING:

FY 2003	\$55,000
FY 2004	\$96,692
FY 2005	\$37,988

The Micro PET Study of Gene Expression in Rodents

Panayotis Thanos

03-099

PURPOSE:

The chief objective of this research is to develop methods and assess the potential of micro PET for the investigation of the function of genes in the whole organism. We specifically propose to assess the function of specific genes in the brain of rats in which we will overexpress the gene in specific brain areas and in mice in which through “knock out” or “knock in” technology these genes have been deleted or modified. The implications of these results would be critical in furthering our understanding in several research areas currently at BNL: a) substance abuse, b) aging, c) neurodegenerative disease, d) learning and memory, e) cancer, and f) radiation. More specifically these results will be critical in studies of radiation exposure and treatment of neurodegenerative disease with stem cells.

APPROACH:

Rapid developments in genetic research have given rise to the new field of behavioral genetics and a growing demand for assessing in-vivo the expression and function of genes as well as how they correlate with environmental factors and behavior. Recent PET studies have started to link disease associated genetic mutations with specific brain metabolic and biochemical abnormalities that occur prior to disease presentation (Feigin et al., 2001; Matsuda, 2001). These studies have highlighted the potential of PET as a tool to investigate the consequences of genetic polymorphisms in regional brain function. Mice, through the use of “knock out” and

“knock in” technologies have been particularly valuable in elucidating the role of genes and the proteins they encode in behavior and drug effects. This model is valuable in predicting the genotypic basis of neuropsychiatric disease.

Micro PET technology is a new and exciting area of research. The present research examines the development of methods assessing the feasibility and sensitivity of microPET in genetically engineered mice and genetically modified rodents. We are evaluating the genes involved in brain dopamine (DA) neurotransmission [D2 receptor and DA transporter (DAT)] since this is a system for which we have access to appropriate radiotracers and to transgenic and knockout animals. Finally, methods employed include micro PET and autoradiography.

Collaborators include: Dr. G.-J. Wang and Dr. A. Biegon

TECHNICAL PROGRESS AND RESULTS:

- 1) Measured dopamine receptor and transporter levels in transgenic mice in: (a) D2 wild type, D2 heterozygous, and D2 knockout and (b) DAT wild type, DAT heterozygous, and DAT knockout.
- 2) Measured D2 levels in rats that have regional overexpression of these molecule targets.
- 3) Evaluated the sensitivity of microPET to assess functional brain changes as measured by regional brain glucose metabolism in D2 family transgenic mice that are treated with the psychostimulant MP.
- 4) Evaluated the sensitivity of microPET to assess functional brain changes as measured by regional brain glucose metabolism in: Transgenic DAT mice that were treated with a DAT blocking drug (cocaine).
- 5) Complete the evaluation of the sensitivity of microPET to assess functional

brain changes as measured by regional brain glucose metabolism in rats with regional DAT who are treated with a DAT blocker drug.

This project involves animal vertebrate subjects (rodents).

SPECIFIC ACCOMPLISHMENTS:

Thanos, P.K.; Dimitrakakis, E.S.; Rice, O.; Gifford, A.; Volkow, N.D. Ethanol self-administration and ethanol conditioned place preference are reduced in mice lacking cannabinoid CB1 receptors. Behavioral Brain Research 2005 Nov 7;164(2):206-13.

Volkow, N.D.; Wang, G.-J.; Franceschi, D.; Fowler, J.S.; **Thanos, P.K.;** Maynard, L.; Gatley, S.J.; Wong, C.; Veech, R.L.; Kunos, G.; & Li, T.K. (2005). Low Doses of Alcohol Substantially Decrease Glucose Metabolism in the Human Brain. Neuroimage doi:10.1016/j.neuroimage.2005.07.004.

Heidbreder, C.A.; Gardner, E.L.; **Thanos, P.K.;** & Ashby, C.R. The role of central dopamine D3 receptors in drug addiction: a review of pharmacological evidence. Brain Research Reviews Vol 49(1)77-105

Thanos, P.K. et al., The selective dopamine D3 receptor antagonist SB-277011-A attenuates ethanol consumption in ethanol preferring (P) and non-preferring (NP) rats. Pharm Biochemistry and Behavior 2005 May;81(1):190-7

Thanos, P.K. et al., Dopamine D2R DNA transfer in dopamine D2 receptor-deficient

mice: Effects on ethanol drinking Life Sciences 77 (2005)130-139

Thanos, P.K., et al. (2004). DRD2 Gene Transfer into the Nucleus Accumbens of the Alcohol Preferring (P) and Non Preferring (NP) Rats Attenuates Alcohol Drinking. Alcohol Clin Exp Res. May;28(5):720-8.

Ding, Y.S.; Gatley, S.J.; **Thanos, P.K.;** et al. (2004). Is the *l-threo* Enantiomer of MP (Ritalin) Inactive in the Brain when the Drug Is Given Orally? Synapse 2004 53:168-75.

Alexoff, D.L.; **Thanos, P.K.;** and Volkow, N.D. Reproducibility of ¹¹C-Raclopride binding in the rat brain measured with the MicroPET R4: Effects of photon scatter and tracer specific activity. J Nucl Med.44:815-822. 2003.

Thanos, P.K.; et al. In Vivo Comparative Imaging of Dopamine D2 Knockout and Wild Type Mice with [¹¹C] raclopride & mPET. J Nucl Med. 43: 1570-1577. 2002.

Thanos, P.K.; et al. 2004; 2005. Society for Neuroscience (SfN) Annual Meeting, Washington, DC Nov 12-16. Presented 6 posters at this conference and 6 at last years SfN conference.

LDRD FUNDING:

FY 2003	\$50,000
FY 2004	\$94,700
FY 2005	\$51,145

Hydrogen Atom Transfer from Carbon to Metal — Relevance of a Novel Reaction to Catalyzed Hydrocarbon Conversions

Morris Bullock

03-104

PURPOSE:

The purpose of this project is to investigate the feasibility of a new method for cleavage of the carbon-hydrogen (C-H) bonds in hydrocarbons, through hydrogen (H) atom transfer reactions from a carbon to a metal. We seek to carry out fundamental kinetic and mechanistic studies to investigate this novel chemical reaction that is relevant to homogeneously catalyzed hydrocarbon conversions.

APPROACH:

A fundamental understanding of reaction mechanisms is required for the rational design of new homogeneous catalysts. Both kinetic and thermodynamic issues are important in assessing the viability of new proposed steps that might be used in catalytic cycles. We seek an improved understanding of the reactivity of metal complexes that catalyze organic reactions. Synthetic, kinetic and mechanistic studies on organometallic complexes are performed towards this goal.

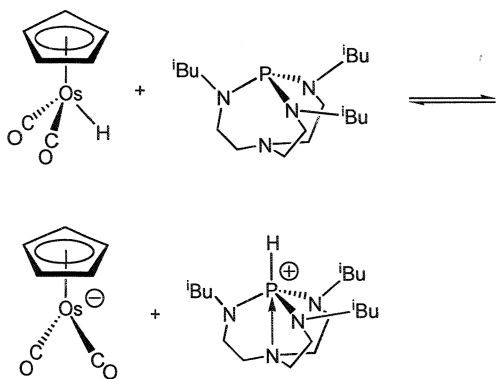
Selective conversion of hydrocarbons to functionalized organic compounds presents a formidable scientific and practical challenge, and is a major goal of organometallic chemistry and homogeneous catalysis. We are examining a novel reaction in which cleavage of a C-H bond proceeds by hydrogen atom transfer from a hydrocarbon to a photochemically generated metal-centered radical.

Jie Zhang, a post doc funded through this project, carries out synthesis and characterization of the metal complexes used in this study, along with photochemical studies using continuous irradiation. Experiments using laser flash photolysis and transient infrared spectroscopy measurements are carried out in collaboration with Etsuko Fujita and David Grills. Kuo-Wei Huang, a Goldhaber Fellow at BNL, carries out computations to determine energetics of the reactions, and bond strengths of the bonds being cleaved or formed in the reactions.

TECHNICAL PROGRESS AND RESULTS:

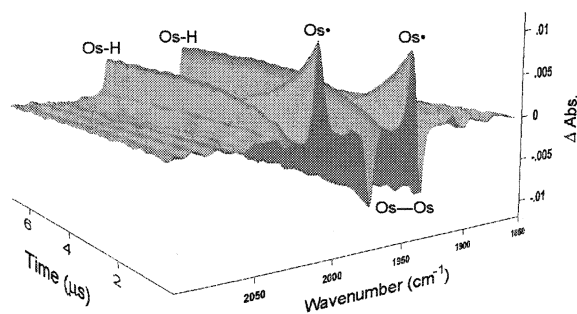
Metal complexes containing osmium (Os) are the primary focus of our efforts, since Os is known to form strong bonds to carbon and to hydrogen. Our previous report gave details of the successful efforts to develop reliable, high-yield synthetic methods for preparation of the Os-Os bonded complexes used in our photochemical experiments, $[\text{Cp}(\text{CO})_2\text{Os}]_2$ ($\text{Cp} = \eta^5\text{-C}_5\text{H}_5$) and $[\text{Cp}^*(\text{CO})_2\text{Os}]_2$ ($\text{Cp}^* = \eta^5\text{-C}_5\text{Me}_5$).

Photolysis ($\lambda > 300$ nm) of a solution of $[\text{Cp}(\text{CO})_2\text{Os}]_2$ and 1,4-cyclohexadiene produces two equivalents of $\text{Cp}(\text{CO})_2\text{OsH}$, together with benzene as the organic product, thus documenting that the proposed metal-to-carbon hydrogen atom transfer occurs. A key issue was physical measurements on the Os-H bond being formed in this reaction. The acidity of this osmium hydride was determined by measuring the equilibrium constant for deprotonation by a very strong base, as shown above.

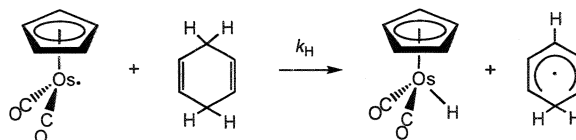


The pK_a of $Cp(CO)_2OsH$ was determined as 32.7 in CD_3CN solvent, indicating it is far less acidic than its first and second row congeners $Cp(CO)_2FeH$ ($pK_a = 19.4$) or $Cp(CO)_2RuH$ ($pK_a = 20.2$). The osmium anion, $[Cp(CO)_2Os]^-Li^+$, was prepared, and its oxidation potential was determined by electrochemical measurements. Use of these data in a thermochemical cycle leads to an estimated lower limit of the Os-H bond dissociation energy as 82 kcal/mol, which is exceptionally strong for a transition metal hydride.

Laser flash photolysis (355 nm) of a solution of $[Cp(CO)_2Os]_2$ leads to an instantaneous bleaching of the $\nu(CO)$ IR bands of the dimer and appearance of new bands assigned to the osmium-centered radical $Cp(CO)_2Os^\bullet$. These experiments were carried out by time-resolved infrared (TRIR) spectroscopy using a step-scan FTIR spectrometer. The figure below shows the spectroscopic changes observed in the presence of 1,4-cyclohexadiene.



The kinetics of the metal-to-carbon hydrogen atom transfer (shown below) were determined to be first-order in osmium radical and first-order in 1,4-cyclohexadiene.



The second-order rate constant for the hydrogen atom transfer was determined to be $k_H = (2.1 \pm 0.2) \times 10^6 M^{-1} s^{-1}$ at 23°C.

Future research will seek to determine further mechanistic details and to measure the rate constants and kinetic isotope effects for a range of metal complexes, including metals that form weaker M-H bonds. Hydrocarbons with stronger C-H bonds will be studied to determine the limits on how strong of a C-H bond can be ruptured using such reactions.

SPECIFIC ACCOMPLISHMENTS:

An invited talk was given at a symposium at the 229th National American Chemical Society Meeting (San Diego, CA, March 13-17, 2005) entitled Ionic Hydrogenations Using Proton and Hydride Transfer Reactions of Metal Hydrides, and Hydrogen Atom Transfers of Osmium Complexes.

A communication on these results was published, Carbon-to-Metal Hydrogen Atom Transfer: Direct Observation Using Time-Resolved Infrared Spectroscopy, Zhang, J.; Grills, D. C.; Huang, K.-W.; Fujita, E.; Bullock, R. M. *Journal of the American Chemical Society*, **2005**, *127*, 15684-15685.

An invited talk was presented at a symposium on metal hydrides held at the Pacificchem 2005 conference (Dec. 15-20, 2005) entitled Carbon-to-Metal Hydrogen Atom Transfers in the Formation of Metal Hydrides.

LDRD FUNDING:

FY 2003	\$20,000
FY 2004	\$56,480
FY 2005	\$58,039
FY 2006 (budgeted)	\$25,000

Radioprotection in *D. radiodurans*, a Radiation Resistant Bacterium

Diane Cabelli

03-105

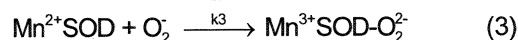
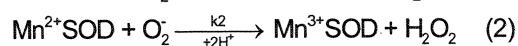
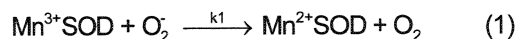
PURPOSE:

Deinococcus radiodurans is a bacterium that is extremely resistant to gamma radiation. Great interest in this organism led to its complete genomic sequencing in 1999. When the superoxide dismutase (SOD), metalloenzyme that dismutates superoxide (O_2^-) to O_2 and H_2O_2 is cloned out of the organism, the radiation resistance drops significantly. Understanding the mechanism of this bacterial superoxide dismutase (MnSOD) would help us to understand a large component of radioresistance exhibited by this organism and to address possibly engineering radioresistance into other organisms. The use of bacteria for the remediation of heavy metal and radioactive waste (e.g. isotopes of uranium, plutonium and mercury) is very promising and has, in some cases, been translated into reality. The involvement of this particular bacterium lies in its extreme radiation resistance and efforts to engineer remediation function into *D. radiodurans* or to enhance the bacterium's existing ability to reduce heavy metals is underway elsewhere. Understanding the basic differences between *D. radiodurans* and other organisms with regards to MnSODs, membrane components and membrane surfaces may allow us to engineer radiation resistance into other bacterial systems that are already useful in non-radioactive cleanup.

APPROACH:

It has been proposed that Mn-SOD eliminates superoxide through the mechanism shown below, where the reduced

enzyme can react with superoxide through an outer or inner sphere reaction (2 or 3). The gating between the rates of these two-steps will determine the efficiency of the enzyme, depending on the concentration of superoxide present.



In order to understand an aspect of the extreme radioresistance of *Dr*, we studied the reactivity of its Mn-SOD with superoxide using the fast kinetic technique of pulse radiolysis found at BNL. This technique allows us to measure the rates of the individual reactions in the overall dismutation mechanism. We compared the reactivity of *Dr* MnSOD with that of *e coli* MnSOD and human MnSOD.

We then studied a mutant of MnSOD where the tyrosine in the second coordination sphere that had been mutated to a phenylalanine. This mutation helps test what factors might control the gating between outer-sphere and inner-sphere reduction of superoxide.

Finally, we performed Density Functional Theory (DFT) calculations aimed at providing a detailed understanding of the energetics of each step, the transition state structures and the differences between the various enzymes and mutants.

Collaborators are:

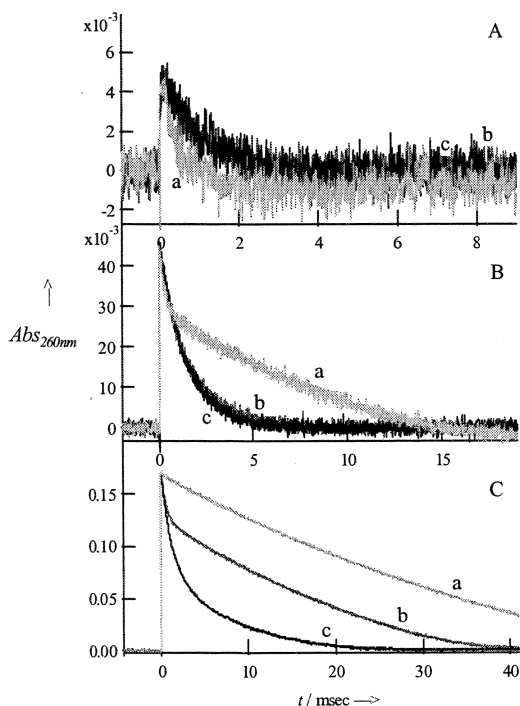
Professor David Silverman, University of Florida for the expression, isolation, and purification of MnSOD from *D. radiodurans*.

Professor Geoff Jameson, University of New Zealand for determination of the crystal structure of the MnSOD.

Dr. Jose Rodriguez, BNL for the DFT calculations.

TECHNICAL PROGRESS AND RESULTS:

These results show that when compared to both the *E. coli* and human enzymes, the *Dr* Mn-SOD is able to deal with higher superoxide concentrations.



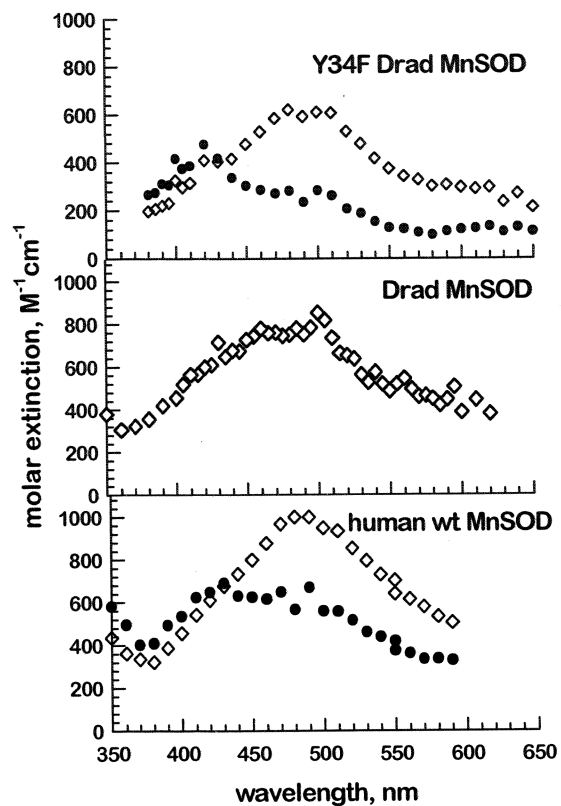
The traces show the disappearance of various concentrations of superoxide in the presence of varying amounts of MnSOD. In panel A, the superoxide and MnSOD are there in identical concentrations ($5\mu\text{M}$). Here, O_2^- disappears at equally fast rates for all of the enzymes; hMnSOD, *e coli* MnSOD and DrMnSOD. In equimolar concentrations, only k_1 or k_2 are accessed and the rate constants are identical. Under catalytic conditions, however, where the ratio of O_2^- to MnSOD is 7:1 (panel B), the human enzyme is already noticeably less efficient at removing superoxide. In the

hMnSOD, the O_2^- is partitioning equally between the inner sphere and outer sphere mechanism and release of the bound peroxide becomes rate limiting.

In the presence of $43\mu\text{M}$ superoxide and $1\mu\text{M}$ MnSOD (Panel C), the *E. coli* enzyme is now also partitioning between an inner sphere and outer sphere mechanism. The dramatic difference observed here is that within 3 milliseconds, over half the superoxide has disappeared in the presence of DrMnSOD while less than 25% has disappeared in the presence of *e coli* MnSOD and only a few percent has disappeared in the presence of human MnSOD.

This uniquely efficient dismutation ability of DrMnSOD will be physiologically relevant in an organism such as *Dr*, since the high levels of radiation it endures will have a primordial effect on the enhancement of intracellular ROS. It has been shown that *Dr* Mn-SOD plays a role in radioresistance, since *Dr* cells lacking the enzyme are more susceptible to radiation.

The three panels below show the spectra generated when a substoichiometric amount of superoxide is generated in the presence of an excess of Mn(II)SOD. Clearly, the *Drad* Mn(II)SOD is rapidly converted to Mn(III)SOD, consistent with the ratio of reactions 2:3 of 15. In contrast, the human Mn(II)SOD is converted to a 50:50 ratio of Mn(III)SOD (absorption maximum at 480 nm) and the transient MnSOD-superoxide adduct (absorption maximum at 420 nm). Interestingly, the *Drad* Y34FMn(II)SOD now reacts in a manner identical to the human MnSOD, with a 50:50 gating of k_2 and k_3 . The role of the tyrosine 34 in this system needs to be further addressed both experimentally and theoretically.



SPECIFIC ACCOMPLISHMENTS:

Isabel A. Abreu, José A. Rodriguez, and Diane E. Cabelli “Bonding of O₂⁻ to Manganese and Iron Superoxide Dismutases: Role of the Second-Sphere of Coordination around the Metal Centers” J Phys Chem, ASAP.

“MnSOD and Radiation Resistance in *Deinococcus radiodurans*: A Pulse Radiolysis Study” Seminar given by D. Cabelli at CERM, Florence, Italy, February 23, 2005

LDRD FUNDING:

FY 2003	\$57,500
FY 2004	\$74,668
FY 2005	\$15,329

New Development of Norepinephrine Transporter Radioligands for PET Studies of Substance Abuse, Depression and ADHD

Yu-Shin Ding

03-107

PURPOSE:

Research on dopamine (DA) and serotonin (SER) systems related to various Central Nervous System (CNS) disorders has benefited from the availability of suitable radioligands. The norepinephrine transporter (NET) has long been recognized in relation to the pathophysiology and treatment of Attention Deficit Hyperactivity Disorder (ADHD), substance abuse and depressive disorders. However, brain imaging of NET has been hampered by lack of suitable radioligands. The fact that all three transporters (NET, DAT and SERT) are involved in various neurological and psychiatric diseases places a sense of urgency on the development of new NET ligands so that we will be able to tease out the roles of individual transporters underlying specific CNS disorders.

APPROACH:

Reboxetine, (RS)-2-[(RS)- α -(2-ethoxyphenoxy)-benzyl]morpholine (RB), is a specific NET inhibitor with a high affinity and high selectivity (IC_{50} DAT/NET = 4000), and it has been approved for the treatment of depressive illness in several European countries. The purpose of this project is to synthesize and evaluate positron emitter labeled analogues of reboxetine for PET imaging studies of NET in non-human primates.

TECHNICAL PROGRESS AND RESULTS:

As indicated in our last report, we have identified a number of reboxetine (RB) analogues that are potential radioligands for PET studies of brain NET. We continue to make significant progress, and we have synthesized and evaluated several new ligands that we proposed in our submission, including RB, 3-Cl-MRB, oxaprotiline and lortalamine. These results provide valuable information in our design to develop more promising NET ligands.

Synthesis of [^{11}C]Reboxetine ([^{11}C]RB):

Currently, there is no satisfactory method for the preparation of [^{11}C]ethyl labeled radiopharmaceuticals. We proposed a new synthetic approach to the preparation of aryl [^{11}C]ethyl ethers from [^{11}C]CH₃I with an in situ generated aryloxymethyl lithium reagent, and its application to the radiosynthesis of [^{11}C]RB. We were able to obtain the desired product RB by using this strategy in an overall yield of 71%.

Synthesis and evaluation of 3-Chloro-[^{11}C]O-methylreboxetine (3-Cl-[^{11}C]MRB):

The precursor and the unlabeled standard, 3-Cl-MRB have been synthesized. We used the same chiral resolution strategy, followed by radiosynthesis to obtain pure (S,S) & (R,R)-3-Cl-[^{11}C]MRB. Comparative PET studies were then carried out in baboons. It showed that (S,S)-3-Cl-[^{11}C]MRB displayed appropriate regional specificities and signal to noise ratio, with TH uptake significantly higher than ST; in contrast, high uptakes in both ST and TH were observed for the (R,R)-enantiomer. This suggests that (S,S)-3-Cl-[^{11}C]MRB is a promising ligand for imaging brain NET.

Synthesis and evaluation of [^{11}C]Oxaprotiline (Oxap):

Oxap and its normethyl precursor were prepared in our lab according to reported methods. Racemic [^{11}C]Oxap was then synthesized and subjected

to initial evaluation with PET. The tracer uptake in baboon brain, in general, was high; however, the distribution did not match with the known NET distribution. The fact that Oxap has the highest uptake in ST and low S/N ratio suggested strongly to us that an analogue with this type of molecular structure is probably not desirable for in vivo imaging of NET, despite the fact that its measured log P is ideal (2.1).

Synthesis and evaluation of [¹¹C]Lortalamine (Lort): The precursor and the unlabeled standard, Lort, have been synthesized. Racemic [¹¹C]Lort was then synthesized and subjected to initial evaluation with PET in baboon. In terms of regional specificity and signal-to-noise ratio, [¹¹C]Lort is better than [¹¹C]Oxap; however, [¹¹C]Lort still suffers high non-specific uptake in ST.

These results clearly indicated the superiority of (S,S)-[¹¹C]MRB and the suitability of the MRB analogs ((S,S)-[¹¹C]MRB >(S,S)-[¹¹C]3-CI-MRB >(S,S)-[¹⁸F]FERB) as NET ligands for PET. In addition to high uptake in ST (higher than TH), Nis, Oxap and Lort displayed high non-specific binding and poor S/N. (R)-[¹²³I]iodoNis, which has high affinity as a promising in vitro ligand, also has high non-specific binding and lack of selectivity in vivo.. **Thus, (S,S)-[¹¹C]MRB remains by far the most promising NET ligand for PET studies.**

Asymmetric synthesis to obtain single enantiomer (S,S)-[¹¹C]MRB: Since (S,S)-[¹¹C]MRB is superior to any existing in vivo NET ligands, it's currently used for many of our baboon studies and will be used for our future human studies as well. We, therefore, investigated the feasibility of preparing a single enantiomerically pure precursor that can be used directly, without the need of chiral separation by HPLC, for the radiosynthesis of (S,S)-[¹¹C]MRB. We have succeeded in an asymmetric synthesis via Sharpless asymmetric epoxidation and consequently to obtain the desired precursor,

with the enantiomeric purity >99 % as checked by chiral HPLC, that leads to (S,S)-[¹¹C]MRB.

Evaluation of tracer metabolism: All of the radiolabeled plasma metabolites of MRB were polar species and are not expected to enter the brain. To confirm this, mice were injected with (S,S)-[¹¹C]MRB, and their brains were removed at 10 min after injection and homogenized. Radiolabeled species were extracted and analyzed by radio-HPLC. It was determined that >95% of radioactivity present in the homogenates was unmetabolized parent compound, indicating very low brain entry of the radiolabeled metabolites of MRB.

Transgenic mice study: This study was designed to test the in vitro specificity and selectivity of (S,S)-[¹¹C]MRB in NET knockout and wildtype mice. The results showed that the mean specific counts in LC were 129±15 vs 28±4 (p<0.001) in wild type compared to knockout mice. Cerebellar counts were 34±5 and 20.6±2 (p=0.05) in wild type and knockout mice, respectively; the difference in non-specific binding was not statistically significant. These results further support our previous experiments demonstrating that (S,S)-[¹¹C]MRB is a selective ligand for brain NET.

Co-registration with MRI: PET-MRI co-registration can guide and improve the reliability of ROI placement. We have conducted MRI scans on our baboons and will use Pixel-wise Modeling (PMOD) to do the co-registration and then draw the ROIs. Further data analysis such as DV can also be performed with this PMOD technology.

Improved Kinetic Analysis (a new modeling approach to the identification of a reference region and its Application to the Occupancy Studies): Our improved kinetic analysis method using DVR calculated by using an average of OCC and BG as the reference region has provided more reliable quantification in our occupancy studies. It's

important to point out that the estimated NET occupancies by the tracer alone were not significant and we would not anticipate any significant mass effects.

Taken together, the knowledge and expertise we gained from our preliminary studies has set the stage for further investigation of the role of NET in psychostimulants in human subjects.

IND Application for (S,S)-[¹¹C]MRB: Upon completion of the toxicology study and receipt of the report for (S,S)-[¹¹C]MRB, an IND application was submitted on March 4, 2005. We received IND approval from the FDA on April 11, 2005. In the meantime, an application for human PET studies was made to the Brookhaven Institutional Review Board and this was approved on April 19. We then began our human PET studies in normal subjects using (S,S)-[¹¹C]MRB.

Test/Retest Studies in normal controls: As the FDA requested that our initial study has to be restricted to normal subjects only and without other drugs (i.e. methyl-phenidate), and we are committed to submit all the dosimetry and safety data to the FDA agency for review prior to initiating new studies. Currently, test/retest studies in the brain in normal subjects to assess the reproducibility of the tracer, along with the torso studies to obtain dosimetry, are ongoing. The preliminary data shows promising results.

Summary:

Two areas, substance abuse and ADHD, desperately require further investigation since, in spite of the massive public health problems associated with drug abuse and the fact that ADHD is the major psychiatric disorder in children, effective treatments remain elusive and the neurochemical mechanisms are poorly understood. Our successful development of selective NET radioligands would allow us to measure occupancies and duration of action by pharmacologically relevant doses of Coc and MP. This will provide a pivotal tool to investigate the role of NET in the reinforcing

as well as the therapeutic properties of stimulants.

To our knowledge, (S,S)-[¹¹C]MRB is by far the most promising in vivo NET radiotracer with adequate pharmacokinetic and metabolism and is expected to provide specific and functional maps of NET in the brain.

This project involves animal vertebrate subjects.

SPECIFIC ACCOMPLISHMENTS:

Publications not previously reported:

Lin, K.S.; Ding, Y.-S.; Kim, S.W.; Kil, K.E. Synthesis, enantiomeric resolution, F-18 labeling and biodistribution of reboxetine analogs: promising radioligands for imaging the norepinephrine transporter with Positron Emission Tomography. Nucl. Med. Biol. 32:415-22, 2005.

Ding, Y.-S.; Lin, K.S.; Benveniste, H.; Carter, P. Comparative evaluation of PET radiotracers for imaging the norepinephrine transporter: (S,S) and (R,R) enantiomers of reboxetine analogues ([¹¹C]MRB, 3-Cl-[¹¹C]MRB and [¹⁸F]FRB), (R)-[¹¹C]nisoxetine, [¹¹C]oxaprotiline, and [¹¹C]lortalamine. J. Neurochem. 94:337-51, 2005.

Logan, J.; Ding, Y.-S.; Lin, K.S.; Pareto, D.; Fowler, J.S.; Biegon, A. Modeling and analysis of PET studies with Norepinephrine transporter (NET) ligands: The search for a reference region. Nucl. Med. Biol. 32:531-42, 2005.

Lin, K.S.; Ding, Y.S. Synthesis and C-11 labeling of three potent norepinephrine transporter selective ligands ((R)-nisoxetine, lortalamine, and oxaprotiline) for comparative PET studies in baboons. Bioorg Med Chem. 13:4658-66, 2005.

Lin, K.S.; Ding, Y.S. Synthesis and C-11 labeling of three potent norepinephrine transporter selective ligands ((R)-nisoxetine, lortalamine, and oxaprotiline) for comparative

PET studies in baboons. *Bioorg Med Chem.* 13:4658-66, 2005.

Chapters and Reviews (invited):

Ding, Y.-S.; Fowler, J.S. New Generation Radiotracers for nAChR and NET. In proceedings of the third La Jolla Conference "The Magic Bullet a Century Later." *Nucl. Med. Biol.* 32:707-718 (2005) Review.

Ding, Y.-S.; Lin, K.S.; Logan, J. PET imaging of Norepinephrine transporter. *Current Pharmaceutical Design* (2005) Review, in press.

Ding, Y.-S. and Gatley, S.J. Positron Radiopharmaceuticals and their Chemistry in "NUCLEAR MEDICINE," R. Henkin, M. Boles, G. Dillehay, J. Halama, S. Karesh, R. Wagner, A.M. Zimmer, eds. Elsevier Press, (2005).

Presentations to international scientific symposia (2005 only):

Modeling and analysis of PET studies with NET ligands. Logan, J.; Lin, K.S.; Ding, Y.-S.; Pareto, D.; Fowler, J.; Biegon, A. 52nd Annual Meeting of the Society of Nuclear Medicine. Toronto, CA, June 18-23, 2005.

Synthesis, C-11 labeling and in vivo evaluation of a potent and selective reboxetine analog as PET tracer for the norepinephrine transporter. Lin, K.S. and Ding, Y.-S. 52nd Annual Meeting of the Society of Nuclear Medicine. Toronto, CA, June 18-23, 2005.

New generation radiotracers for nAChR and NET, Ding, Y.-S. MIRT Workshop (DOE). Toronto, CA, June 17-18, 2005.

Recent development in new generation radiotracers for PET imaging of the norepinephrine transporter. Ding, Y.-S.; Lin, K.S.; Logan, J.; Benveniste, H.; Carter, P. 52nd Annual Meeting of the Society of Nuclear Medicine. Toronto, CA, June 18-23, 2005.

Synthesis and in vivo evaluation of C-11 labeled mazindol analogs for imaging the norepinephrine transporter with PET. Lin, K.S. and Ding, Y.-S.; Betzel, T.; Quandt, G. 16th International Symposium on Radiopharmaceutical Chemistry. Iowa, June 23-28, 2005.

Synthesis and C-11 labeling of three potent norepinephrine transporter selective ligands (lortalamine, oxaprotiline and (R)-nisoxetine) for comparative PET studies in baboons. Lin, K.S. and Ding, Y.-S. 16th International Symposium on Radiopharmaceutical Chemistry, Iowa, June 23-28, 2005.

Recent development in new generation radiotracers for PET imaging of the norepinephrine transporter. Ding, Y.-S.; Lin, K.S.; Logan, J. 16th International Symposium on Radiopharmaceutical Chemistry. Iowa, June 23-28, 2005.

Invited talks (2005 only):

Plenary speaker for the third La Jolla Workshop on Receptor-Binding Radiopharmaceuticals, entitled *The Magic Bullet: A Century Later*. La Jolla, CA, Feb 24-28, 2005.

Plenary speaker for the Molecular Imaging and Radionuclide Therapy (MIRT) workshop, entitled, "Translational Applications of Molecular Imaging and Radionuclide Therapy," June 17-18, 2005, Toronto, Canada.

LDRD FUNDING:

FY 2003	\$112,000
FY 2004	\$111,095
FY 2005	\$ 93,195

Condition: Green Chemistry.

Radiolytic Studies of Ionic Liquids in Service of Security and the Environment

James Wishart

03-118

PURPOSE:

The objective of this project is to understand the radiation chemistry of ionic liquids (low-melting salts), a new class of solvents that can be safer and more environmentally benign alternatives to present technology. Radiolysis studies are needed to determine the radiation stability of ionic liquids for applications as media for nuclear fuel processing and for developing methods to study chemical kinetics in these novel solvents. Results of this study may lead to new, ionic liquid-based initiatives in photochemical energy storage, including (H₂ and methanol production), nanoscience, chemistry related to actinide processing, and a large, multi-investigator, multi-institution project to study the physical chemistry of ionic liquids.

APPROACH:

Ionic liquids have broad applications as media for chemical transformations and in the study of chemical reaction mechanisms. Pulse radiolysis is an important and in some ways unique method of studying chemical kinetics. In order to use pulse radiolysis to study reactions in ionic liquids, the yields and chemistry of the primary radiolysis products must be known. The time resolution of BNL's Laser-Electron Accelerator Facility (LEAF) facility is uniquely suited to identify reactive species and measure their reaction rates. Subsequently, we will use our findings to study charge transport and other reactions that are relevant to chemical conversion of solar energy.

The physical properties of ionic liquids can be varied over an extremely wide range, with dramatic effects on reactivity. We design and prepare ionic liquids with desired properties in our lab and through collaborations with Profs. Robert Engel and Sharon Lall-Ramnarine of City University of New York (CUNY). We characterize the physical properties of our liquids by several techniques including AC conductivity and viscometry. Solvation dynamics is a very important facet of reactivity in ionic liquids. We collaborate with Prof. Edward Castner of Rutgers to measure the solvation response of our ionic liquids using time-resolved emission spectroscopy of solvatochromic dyes, with Prof. Mark Kobrak of Brooklyn College, CUNY on molecular dynamics simulations of solvation phenomena, and with Prof. Steven Greenbaum of Hunter College, CUNY, on nuclear magnetic resonance (NMR) studies of transport phenomena in ionic liquids.

"Criticality safe" ionic liquids (containing high concentrations of thermal neutron scavengers boron and/or chlorine) with good fluid properties would be useful as safer alternatives for nuclear processing applications. It is important to find out what kinds of radiolysis products are formed in these liquids and how can the liquids be made radiation-stable. We collaborate with Prof. Christopher Reed of U. C. Riverside to design ionic liquids containing inert carborane anions and study their radiation chemistry.

TECHNICAL PROGRESS AND RESULTS:

Pre-solvated electron spectra and relaxation dynamics in ionic liquids were observed by visible and Near Infra Red (NIR) pulse-probe spectroscopy using the LEAF accelerator. Pulse-probe spectroscopy of three NTf₂⁻ salts (N-methyl-N-(n)-butyl-pyrrolidinium (P₁₄⁺), N-methyl-N-methoxyethyl-pyrrolidinium (P_{1EOM}⁺) and N-methyl-N-ethoxyethyl-pyrrolidinium (P_{1EOE}⁺)) between 600 and 1600 nm clearly shows the decay of a pre-solvated

electron species and growth of the fully solvated electron. In $P_{14}^+NTf_2^-$, the average electron solvation time is 260 ps, comparable to the average Stokes shift solvation time of 220 ps for coumarin 153 in the same liquid (see below). Further comparisons of electron and coumarin solvation times are being sought in order to validate the estimation of electron solvation times in ionic liquids that are too viscous to use in the pulse-probe flow system, pending implementation of the single-shot ultrafast detection methods at LEAF. Knowing electron solvation times is important to understanding how dry electron scavenging in ionic liquids affects radiolysis product yields.

Time-resolved fluorescence of coumarin 153 (C153) was used to study solvation dynamics in several ionic liquids over a wide temperature range. Microviscosity was characterized using fluorescence anisotropy measurements, while the time-dependent Stokes shift of the C153 emission provides a measure of the solvent reorganization. Both C153 anisotropies and Stokes shifts display multi-exponential dynamics, reminiscent of glassy behavior.

In another collaboration with Prof. Ed Castner, the ultrafast molecular dynamics of pyrrolidinium cation ionic liquids were investigated using femtosecond optical heterodyne-detected Raman-induced Kerr effect spectroscopy. Their picosecond relaxation processes are best fit with a triexponential model. The fast and intermediate relaxation time constants are about 2 and 20 ps and are almost the same for all liquids. The slow relaxation time constant is consistent with the Stokes-Einstein-Debye hydrodynamic model for orientational friction. The Fourier transform Kerr spectra of the liquids were also obtained. The intermolecular spectral densities of P_{1EOE}^+/NTf_2^- , P_{1EOM}^+/NTf_2^- , and P_{14}^+/NTf_2^- show maxima at lower frequencies than those of P_{1EOE}^+/Br^- and P_{1EOE}^+/DCA^- , indicating weaker anion-cation interactions in the NTf_2^- liquids.

A summer student project studied the effects of ionic liquids on charge-transport reactions in dipeptide-bridged donor-acceptor systems. Preliminary results indicate that specific ionic liquid anion-cationic acceptor interactions influence the observed electron transfer processes. This project will form the basis for further study of the characteristics and advantages of ionic liquids in devices for photochemical energy storage.

SPECIFIC ACCOMPLISHMENTS:

Publications:

Ultrafast Dynamics of Pyrrolidinium Cation Ionic Liquids H. Shirota, A. M. Funston, J. F. Wishart, E. W. Castner, Jr. *J. Chem. Phys.* **122**, 184512 (2005), selected for the *Virtual Journal of Ultrafast Science* (6/05)

Dynamics of Fast Reactions in Ionic Liquids A. M. Funston and J. F. Wishart in "Ionic Liquids IIIA: Fundamentals, Progress, Challenges and Opportunities" Rogers, R. D. and Seddon, K. R., Eds.; *ACS Symp. Ser.* **901**, Ch. 8, American Chemical Society, Washington, DC, (2005).

Radiation Chemistry of Ionic Liquids J. F. Wishart, A. M. Funston, and T. Szreder in "Molten Salts XIV" Mantz, R. A., et al., Eds.; The Electrochemical Society, Pennington, NJ, in press.

A group of New York Regional Alliance for Ionic Liquid Studies (NYRAILS) investigators including this PI submitted an NSF Research Experience for Undergraduates proposal (pending) to establish a summer research program in ionic liquids, with the help of the BNL Office of Educational Programs.

Invited talks:

Radiation Chemistry of Ionic Liquids, at the 2004 Joint International Meeting of the

Electrochemical Society, Honolulu, HI, Oct. 7, 2004

Picosecond Pulse Radiolysis of Ionic Liquids - Complex and Structured Materials, at the conference on "Sanken International Symposium on Scientific and Industrial Nanotechnology 2004," Osaka, Japan, Dec. 7, 2004

Picosecond Radiolysis of Ionic Liquids, at the conference on "Transient Chemical Structures in Dense Media," Paris, France, March 14, 2005

Technical Progress and Research Activities at BNL's Laser-Electron Accelerator Facility, Laboratoire de Chimie Physique, Université de Paris-Sud, Orsay, France, April 8, 2005

The Radiation Chemistry of Ionic Liquids via Picosecond Electron Radiolysis,

Commissariat d'Energie Atomique, Marcoule, France, April 13, 2005

Solvation Dynamics of Excess Electrons in Ionic Liquids, at the symposium "Spectroscopy of Biomolecules, Interfaces, and Materials," ACS Mid-Atlantic Regional Meeting, New Brunswick, NJ, May 24, 2005

Ionic Liquids: Radiation Chemistry, Solvation Dynamics and Reactivity Patterns, at the 2nd DOE Condensed Phase and Interfacial Molecular Science Meeting, Airlie, VA, October 26, 2005

Future talks on this work are scheduled for meetings in Mumbai, India; Clausthal, Germany; and Shanghai, China.

LDRD FUNDING:

FY 2003	\$43,000
FY 2004	\$79,517
FY 2005	\$36,945

Exploring the Use of Powder Diffraction for Proteins

Marc Allaire

03-119

PURPOSE:

The discoveries of ligands that bind specifically to targeted proteins have a dramatic impact in Life Sciences. We could infer, from the chemical nature of these ligands, possible biochemical activity and assign function to proteins. These ligands could also be used as probes, e.g. to observe phenotype in cellular assay, and identify cellular activity and function of these proteins. Moreover these ligands could be exploited in the process of drug discovery. The purpose of this proposal is to develop an X-ray based method such as Protein Powder Diffraction (PPD) to identify protein/ligand complexes.

APPROACH:

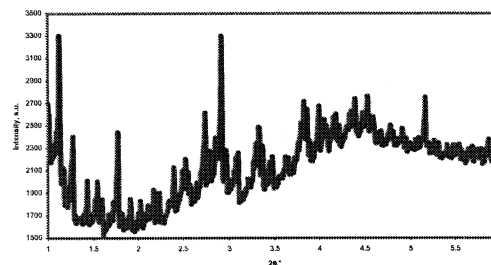
The goal of our approach is to use PPD to identify protein/ligand complexes from High-Throughput Screening (HTS) of a large library of chemicals. The approach is based on the idea that PPD data of bound and unbound proteins should be different. The work done by R. Von Dreele on lysozyme suggests the potential of PPD to locate ligands and infers the possibility of using PPD and HTS to describe the binding modes of a protein target. In our study we want to develop a simple method based on PPD data to identify protein/ligand complexes.

TECHNICAL PROGRESS AND RESULTS:

Our initial effort has shown that powder diffraction data could be acquired from a solution of a lysozyme sample with the

addition of NaCl. This data has been subjected to restrained-Rietveld refinement and converged with a final χ^2 of 3.85 and good stereochemistry. We then tested the hypothesis that changes in PPD data should be observed in the presence of bound ligand. Our results indicated that we could identify lysozyme/ligand complexes in comparing their PPD profile. We have also shown that the signal obtained from powder diffraction data even at a d-Bragg spacing of $\sim 3\text{\AA}$ is sample-dependant.

Our goal over the last year was to produce protein powders in preparation for HTS assays. Samples were prepared in a 96-well plate format with 10ul of lysozyme at a concentration of 200mg/ml in an acetate buffer of pH 4.5 mixed with 10ul of 2.0M NaCl. Protein powder was readily produced and measured at the NSLS beamline X3B1 using a crystal analyzer. The data acquisition was done with the X-ray beam passing directly through the plate. The powder profile, as shown below, was of comparable quality to profiles obtained with samples in capillaries.



SPECIFIC ACCOMPLISHMENTS:

Producing diffraction quality powders from soluble lysozyme and thaumatin. (2005) The IUCR meeting. Florence, Italy.

X-ray based assays in chemical genetics and ligand discovery. (2005) BioSciences

Division, Argonne National Laboratory,
Argonne, IL.

X-ray based assays in chemical genetics and
ligand discovery. (2005) Department of
Microbiology and Immunology, McGill
University, Montreal, Canada.

LDRD FUNDING:

FY 2003	\$45,000
FY 2004	\$79,445
FY 2005	\$34,880

Element-Resolved Dynamics of Nanoscale Ferromagnets

Chi-Chang Kao

03-121

Dario A. Arena

PURPOSE:

The dynamical properties of engineered magnetic materials (that is, alloys and multilayer structures) are increasing in importance and relevance, with the emphasis to develop faster hard drives, advanced magnetic memory for computers and novel magneto-electronic components. However, most experimental probes require magnetization dynamics, such as conventional ferromagnetic resonance (FMR). The purpose of this LDRD is to develop elementally resolved magnetization measurements in the pico second time regime.

APPROACH:

All our measurements are based on X-ray magnetic circular dichroism (XMCD), which is a standard synchrotron-based spectroscopic technique. XMCD provides the element-specificity and high magnetic contrast that are critical for our experiments. A benefit of using synchrotron spectroscopy is that the photon beam consists of short bunches that arrive with a fixed frequency. Thus, the instantaneous state of the magnetization may be probed by synchronizing the arrival of the photon bunches with a magnetic excitation (described below). Time resolution is achieved in a pump-probe fashion by varying the delay between the excitation source and the arrival of the photons. The combination of a pump-probe architecture and the synchrotron based spectroscopy is time-resolved XMCD (tr-XMCD).

Our approach for providing the perturbation which initiates the magnetization dynamics has evolved over the course of this LDRD. Initially, we introduced a magnetization pulse

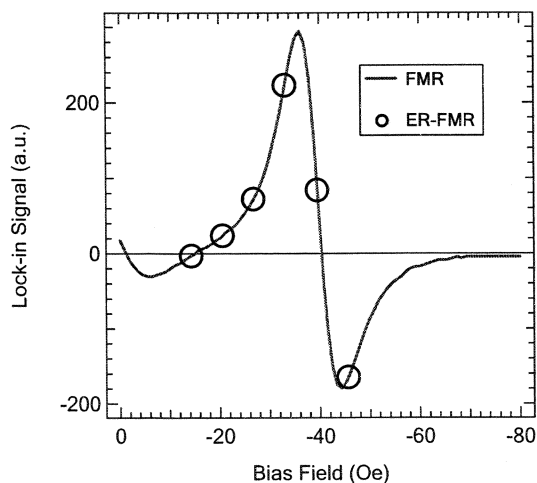
with a fast rise time (~ 100 ps) into the central conductor of a co-planar waveguide. A magnetic alloy thin film has been deposited at the central constriction (width ~ 100 μm) in the waveguide. The microwave pulse initiates a rotation of the magnetization of the thin film about an axis perpendicular to the applied field. The magnetization of the sample then precesses around the applied field with an amplitude whose decay is described by a phenomenological damping constant, α . Because the magnetic film must be deposited directly on the co-planar waveguide, the tr-XMCD measurements must be made in reflectivity mode. While we have successfully used the technique to measure the dynamic response of magnetic thin film alloys and multi-layer structures, sample preparation is difficult, tedious, and results in samples with considerable surface and interface roughness.

To overcome these difficulties, and also to expand the capabilities of tr-XMCD, we recently undertook a complete redesign of the experimental approach. Instead of using a pulsed excitation source, we utilized a synthesized sinusoidal RF excitation that was phase-locked with the photon bunch clock with the synchrotron. Our initial measurements used a fixed frequency (2.3 GHz) excitation, although in the future we plan to modify the set up to perform measurements at variable frequencies. The advantage of using a sinusoidal excitation is that the magnetization of the sample precesses at the same frequency as the driving RF. All magnetic materials have a natural precession frequency that depends on fixed internal fields and external bias fields and thus the system can be driven into resonance with the driving RF field by varying the external field. The system is exactly analogous to a forced, driven harmonic oscillator such as a mass on a spring, and indeed very similar changes in the amplitude and phase of the precession oscillations are observed as the system is driven through resonance. This approach using forced oscillations, which we term *element-resolved* ferromagnetic resonance

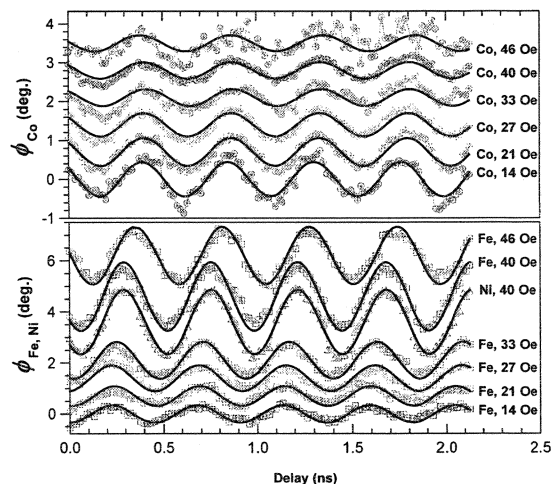
(ER-FMR), has an additional advantage in that sample preparation is much simpler as planar films can be grown on suitable substrates instead of relying on patterned waveguide structures.

TECHNICAL PROGRESS AND RESULTS:

Our initial results using pulsed excitation sources have been described elsewhere (refer to the publications listed below). The re-designed ER-FMR measurements have been extremely successful. A novel feature of these measurements is that conventional FMR spectra can be measured, and tr-XMCD measurements can determine the amplitude and phase of the precession for the various ferromagnetic elements in the sample. An example of conventional FMR is shown below; the sample was a FM tri-layer ($\text{Ni}_{81}\text{Fe}_{19} / \text{Cu} / \text{Co}_{93}\text{Zr}_7$):



The red curve shows the conventional FMR measurements, and the circles indicate the field values that were used in subsequent tr-XMCD scans. These scans are shown below with the photon energy tuned to either the Fe or Co L3 core level:



As the system is driven through the main resonance near 40 Oe, the increase in the amplitude of the Fe oscillations and the decline of the Co oscillations is clear. Also, there is a clear shift in the phase of the oscillations as the system is driven through resonance. These types of measurements will be used shortly to directly investigate several long-standing controversies on the nature of energy loss mechanisms from oscillatory precession modes such as the ones shown above.

SPECIFIC ACCOMPLISHMENTS:

Publications

“Precessional dynamics of elemental moments in a ferromagnetic alloy,” W.E. Bailey, L. Cheng, D. J. Keavney, C.-C. Kao, E. Vescovo, and D.A. Arena, *Phys. Rev. B* **70**, 172403 (2004)

“Comparison of time-resolved XMCD measurements in reflection and transmission for layer-specific precessional dynamics measurements,” Y. Guan, W. E. Bailey, C. -C. Kao, E. Vescovo, and D. A. Arena, *Journal of Applied Physics*, *in press*.

LDRD FUNDING:

FY 2003	\$30,000
FY 2004	\$79,558
FY 2005	\$49,698

Membrane Biophysics Using Model Membranes

Ronald Pindak

03-122

L. Yang

PURPOSE:

Structural studies on biological membranes are important to understand the function and regulation of membrane proteins and other membrane structures that carry out important biological functions. However, unlike soluble proteins that can be crystallized and studied at atomic resolution, these membrane structures are normally fluid and cannot be crystallized. This LDRD project aims to explore different forms of model membranes that are suitable for studying membrane structures and establish the infrastructure that is needed to characterize these structures.

APPROACH:

The model systems to be explored are solid supported multi-bilayers, solid supported single bilayers, and freestanding multi-bilayers. In the previous fiscal year, we used x-ray scattering to study substrate-supported and free-standing lipid film under controlled environmental conditions (temperature and relative humidity), which lead to a variety of temperature- and hydration-dependent lipid structures and lipid-peptide complexes. In FY04, we started to study substrate supported single bilayers, which most resemble biological membranes, but also are the most difficult among the three model systems to prepare and characterize. We successfully measured x-ray reflectivity data that showed the formation of a lipid bilayer, and the subsequent adsorption of a protein layer, on a silicon substrate submerged in a buffer solution. Since then, we have shifted our focus to the development of resonant/

anomalous scattering techniques to examine the periodic lipid structures formed in multi-bilayers.

TECHNICAL PROGRESS AND RESULTS:

Our previous work on lipid structure in substrate-supported films resulted in the discovery of a lipid phase in which a modulated structure with square symmetry forms within each one of the stacked lipid bilayers. This square phase structure belongs to a class of more generally modulated structures. Clarifying the exact shape of the modulation and how the lipid chains pack is essential to understanding the energetics that drive the formation of the modulated phases in general. We have collected high-resolution scattering data (Fig.1) that correspond to the organization of lipid chains and are currently analyzing the data.

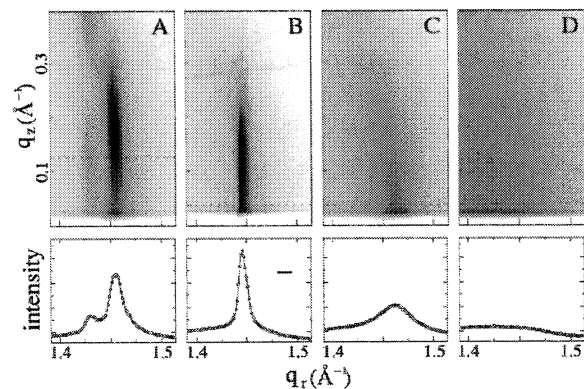


Figure 1. The chain-packing peaks and their q_r profiles observed in (A) L_{β}' (30 °C, 48%RH); (B) L_{β} (43 °C, 31% RH); (C) square (30 °C, 54% RH); and (D) L_{α} (30 °C, 61%RH) phases of DTTPC.

We have also started to explore, utilizing resonant/anomalous scattering at the K-edge of phosphorous (~ 2.1 KeV), atoms that are naturally present in lipid molecules. Measurements at such low energies are challenging, and there are a number of technical issues that have to be resolved.

Firstly, the x-ray beam normally contains higher energy photons that must be filtered out. To do this, we utilized a compact plane mirror that is positioned at an incident angle that is between the critical angles of the fundamental and higher harmonic photons. Anomalous/resonant scattering is also often polarization dependent. For this reason, a compact x-ray polarization analyzer was developed by a visiting graduate student researcher, Suntao Wang. While developing the polarization analyzer, the new polarization analyzer was recently commissioned and applied to unambiguously determine the structure exhibited by bent-core liquid crystal molecules. With this success in hand, we will next focus our x-ray polarization analysis on the lipid bilayer systems.

SPECIFIC ACCOMPLISHMENTS:

L. Yang and M. Fukuto, "A Modulated Phase of Phospholipids with Two-Dimensional Square Lattice," *Phys. Rev. E*, 72 (1): 010901, 2005.

N. W. Roberts, S. Jaradat, M. S. Thurlow, Y. Wang, S. T. Wang, Z.Q. Liu, C.C. Huang, J. Bai, R. Pindak and H. F. Gleeson, "The temperature dependence of inter-layer periodicities in antiferroelectric liquid crystal mixtures as revealed by resonant x-ray scattering," accepted for publication in *Europhysics Letters*

LDRD FUNDING:

FY 2003	\$30,000
FY 2004	\$79,316
FY 2005	\$49,740

High Pressure in Strongly Correlated Materials – An Optical Investigation

Christopher C. Homes

03-127

PURPOSE:

The goal is to study the effect of pressure on the complex optical properties of highly-correlated electronic systems and to look for novel behavior. The use of the diamond anvil cell (DAC) in optical high-pressure studies is a rapidly expanding field. However, much of this work has focused on insulating materials such as minerals. Poorly conducting systems should be quite sensitive to changes in pressure (i.e. metal-insulator transitions, etc.) due to the poor screening and the possibilities for correlated behavior. The primary objective is to devise a reliable method for measuring the reflectance and transmission of the material and to then determine the complex optical properties. If successful, this project may constitute the basis for a new fieldwork proposal in the optical properties of materials under high pressure.

APPROACH:

Studies of highly-correlated materials are numerous, but there is little in the way of high-pressure optical work. We have encountered numerous problems in spectroscopy where there appears to be accidental degeneracies that might be removed with the application of pressure. This served as a motivation to attempt an in-house solution.

While diamond is the almost perfect optical window, the small gasket (or aperture) size in the DACs makes it difficult to pass light through the cell. However, the synchrotron

provides an extremely bright source; through the use of optics that condenses the image size, it is possible to pass a significant amount of light through a small (100 micron) aperture. The combination of such an ideal source and the expertise in infrared spectroscopy and reflecting optics suggested the viability of this project.

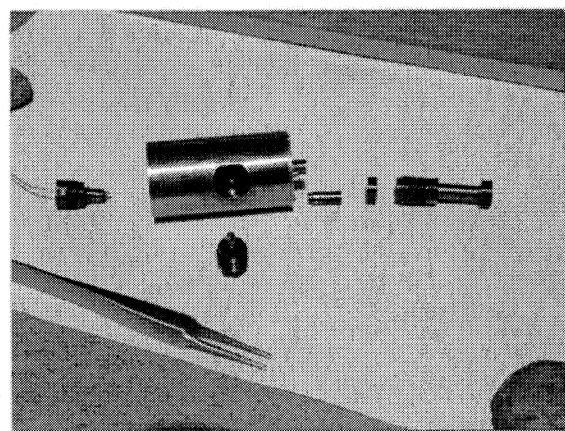
The high-pressure studies performed by the Materials Synthesis Group (until recently led by T. Vogt) allowed us to exploit an existing knowledge base, rather than begin from scratch. Our interest has also shifted to a clamped pressure cell through a collaboration with the University of Budapest (G. Mihaly), which allows larger samples, in particular single crystals, to be examined.

TECHNICAL PROGRESS AND RESULTS:

Initial actions were the hiring of a postdoctoral fellow, Dr. Sasa Dordevic, who arrived in December 2004. A DAC suitable for optical studies was purchased, and a vacuum optical bench was constructed using off-axis parabolic mirrors (outlined in the first status report).

In FY 2004 the transmission bench was fully commissioned, and initial studies of the effects of pressure on the high-dielectric constant material $\text{CaCu}_3\text{Ti}_4\text{O}_{12}$ were performed using quartz as a pressure calibration (quartz is preferable to ruby as it avoids having to use powerful class 3b lasers to determine the pressure in the cell). The transmission cell is well suited for insulating materials that are mainly transparent in the infrared region. However, it does not work well with metallic systems that are opaque. To this end, we have collaborated with Prof. G. Mihaly's group (Budapest, Hungary), to construct a clamped pressure cell with a large wedged diamond window. While this

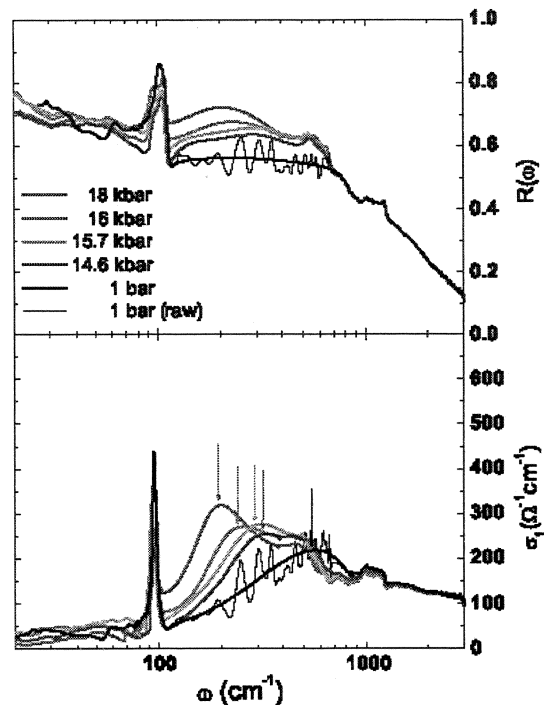
cell has a lower ultimate pressure (~25 kbar) than is achievable in a DAC (~80 kbar), it has a large sample volume that allows single crystals to be examined, rather than powders (shown in the figures below).



The cell is compact and threads into the bottom of a flow cryostat, allowing the effects of both temperature and pressure to be examined.

In FY 2005 work was performed mainly on the pressure studies of the polarized reflectance of BaVS_3 (R. Gaal, Lausanne; I. Kezsmarki, Budapest) using the clamped pressure cell. There has been considerable success in the construction of a simple optical bench for high-pressure studies, and work in this area will continue.

A further important result has been the measurement of the complex optical properties of the strongly-correlated material BaVS_3 , which has a metal-insulator transition below ~70 K.



The conductivity (shown above, lower panel) at ~60 K indicates that the charge-transfer band shifts to zero frequency above a critical pressure ~20 kbar, resulting in the recovery of the metallic state. Additional work on the polarized optical properties of this anisotropic material are now underway. During the course of this work, a new scaling relation for high-temperature superconductors was also developed between the superfluid density, the critical temperature, and the normal-state dc conductivity close to the critical temperature.

SPECIFIC ACCOMPLISHMENTS:

FY 2004

“Energy scales in the high- T_c superconductor $\text{YBa}_2\text{Cu}_3\text{O}_{6+x}$.” C.C. Homes, S.V.

Dordevic, D.A. Bonn, Ruixing Liang and W.N. Hardy, *J. Superconductivity* **17**, 93-96, (2004).

“Sum rules and energy scales in the high temperature superconductor $\text{YBa}_2\text{Cu}_3\text{O}_{6+x}$,” C.C. Homes, S.V. Dordevic, D.A. Bonn, Ruixing Liang and W.H. Hardy, *Phys. Rev. B* **69**, 024514 (2004).

“Signatures of bilayer splitting in the c -axis optical conductivity of double layer cuprates,” S.V. Dordevic, E.J. Singley, J.H. Kim, M.B. Maple, T. Room, Ruixing Liang, D.A. Bonn, W.N. Hardy, J.P. Carbotte, T. Timusk, C. C. Homes, M. Strongin and D.N. Basov, *Phys. Rev. B.* **69**, 094511 (2004).

“A universal scaling relation in high-temperature superconductors,” C.C. Homes, S.V. Dordevic, M. Strongin, D.A. Bonn, Ruixing Liang, W.N. Hardy, Seiki Komiya, Yoichi Ando, G. Yu, N. Kaneko, X. Zhao, M. Greven, D.N. Basov, and T. Timusk, *Nature* **430**, 539-541 (2004).

FY 2005

“Pressure induced suppression of the singlet insulator phase in BaVS_3 : infrared optical study,” I. Kezsmarki, G. Mihaly, R. Gaal, N. Barisic, H. Berger, L. Forro, C.C. Homes, and L. Mihaly, *Phys. Rev. B* **71**, 193103 (2005).

“Coherence, incoherence and scaling relations along the c axis of $\text{YBa}_2\text{Cu}_3\text{O}_{6+x}$,” C.C. Homes, S.V. Dordevic, D.A. Bonn, R. Liang, and W.N. Hardy, submitted to *Phys. Rev. B* **71**, 184515 (2005).

“Scaling of the superfluid density in high-temperature superconductors,” C.C. Homes, S.V. Dordevic, T. Valla and M. Strongin, *Phys. Rev. B* **72**, 134517 (2005).

“Extracting the electron-boson spectral function $\alpha^2F(\omega)$ from infrared and photoemission data using inverse theory,” S.V. Dordevic, C.C. Homes, J.J. Tu, M. Strongin, T. Valla, P.D. Johnson, G. Gu, and D.N. Basov, *Phys. Rev. B* **71**, 104529 (2005).

“Electrodynamics of the nodal metal state in weakly doped high- T_c cuprates,” Y.S. Lee, K. Segawa, Z.Q. Li, W.J. Padilla, M. Dumm, S.V. Dordevic, C.C. Homes, Y. Ando, and D.N. Basov, *Phys. Rev. B* **72**, 054529 (2005).

“Scaling laws in high-temperature superconductors as revealed through infrared spectroscopy,” C.C. Homes, *Synchrotron Radiation News* **18**, 9-14 (2005).

“Scaling of the superfluid density in high-temperature superconductors,” C.C. Homes, *Strongly Correlated Electron Materials: Physics and Nanoengineering*, SPIE International Symposium on Optics and Photonics, San Diego, CA, 31 July – 4 August 2005. SPIE Proceedings, Vol. **5932**, 59320M1-9 (2005).

Conferences:

FY 2004

“Signatures of charge inhomogeneities in IR spectra of high- T_c cuprates,” S.V. Dordevic (invited talk), March Meeting of the American Physical Society, Montreal, P.Q., Canada, 22-26 March 2004.

“A new method of extracting electron-boson spectral function $\alpha^2F(\omega)$ from infrared and ARPES spectra using inverse theory,” (contributed talk) S.V. Dordevic, C.C. Homes, J.J. Tu, T. Valla, M. Strongin, P.D. Johnson, G.D. Gu, and D.N. Basov, *Bull. Am. Phys. Soc.* **49**, 818 (2004). March

Meeting of the American Physical Society, Montreal, PQ, Canada, 22-26 March 2004.

“Infrared optical properties of $\text{HgBa}_2\text{CuO}_{4+\delta}$,” (contributed talk) C.C. Homes, S.V. Dordevic, G. Yu, X. Zhao, and M. Greven, *Bull. Am. Phys. Soc.* **49**, 818 (2004). March Meeting of the American Physical Society, Montreal, PQ, Canada, 22-26 March 2004.

“A new method of extracting electron-boson spectral function $\alpha^2F(\omega)$ from infrared and ARPES spectra using inverse theory,” (contributed talk) S.V. Dordevic, C.C. Homes, J.J. Tu, T. Valla, M. Strongin, P.D. Johnson, G.D. Gu, and D.N. Basov, International conference on the Low Energy Electrodynamics of Solids, Kloster Banz, 18-23 July 2004.

FY 2005

“A universal scaling relation in high-temperature superconductors,” (invited talk) Aspen Winter Conference in Condensed Matter Physics: High-Temperature Superconductivity, 9-15 January 2005.

“Probing strong coupling effects in high- T_c superconductors using infrared spectroscopy

in high magnetic field,” (contributed talk) Y. Lee, Z.Q. Li, W.J. Padilla, D.N. Basov, S.V. Dordevic, C.C. Homes, K. Segawa, and Y. Ando, *Bull. Am. Phys. Soc.* **50**, 1243 (2005). March Meeting of the American Physical Society, Los Angeles, CA, 21-25 March 2005.

“Universal scaling relation in high-temperature superconductors,” (invited talk) C.C. Homes, *Bull. Am. Phys. Soc.* **50**, 1135 (2005). March Meeting of the American Physical Society, Los Angeles, CA, 21-25 March 2005.

“Scaling of the superfluid density in high-temperature superconductors,” (invited talk) C.C. Homes, Strongly Correlated Electron Materials: Physics and Nanoengineering, SPIE International Symposium on Optics and Photonics, San Diego, CA, 31 July – 4 August 2005.

LDRD FUNDING:

FY 2003	\$54,400
FY 2004	\$66,865
FY 2005	\$11,000

Polyoxometalate Giant Molecules: Novel Synthetic Methods, Characterizations and Potential Applications

Tianbo Liu

03-129

PURPOSE:

The purpose of this LDRD project is to study the new physical properties of giant polyoxomolybdate (POM) molecules. The important fundamental scientific problem: that is being explored can be stated as “*When the size of single inorganic molecules reach the orders of nanometers in size, what new sciences can we expect?*” Particularly focusing on the unique solution properties of the giant POM anion, this project fits in well with BNL efforts on nanoscience and condensed matter physics.

APPROACH:

Since the last decade, inorganic chemists have continuously synthesized giant POM molecules, pushing the size of inorganic compounds to the nanometer scale (The largest one was discovered by the PI at BNL). However, their physical properties have not been systematically studied. In the fields of nanoscience, the giant POMs offer “dual personality” benefits: that possess the advantages of single molecules (well-defined structures and uniform size and mass), and those of nanoparticles (complex and variable electronic, magnetic, and colloidal properties). This combination of properties, especially the molecules’ monodispersed nature and adjustable chemical and physical properties, could help to develop more diverse nanomaterials than were previously thought possible.

The first priority is to study the fascinating solution behavior of these giant POM anions, which would provide a valuable link to connect those of simple ions, polyelectrolytes (e.g., proteins and DNAs) and hydrophilic colloids.

Laser and small-angle X-ray scattering techniques (X21C, NSLS), TEM (H. Li, Biology, BNL) and AFM (Y. Cai, Physics, BNL) are used for the study. Some samples were provided by Prof. Achim Müller at U. of Bielefeld, the leading synthetic chemist in the field of POM.

TECHNICAL PROGRESS AND RESULTS:

We have found that although highly soluble and fully hydrophilic, POM and POM-based macroions still tend to self-associate into unknown supramolecular structures, this obviously contradicts our common understanding on soluble ions. Successfully determined that such strange structures actually had unique single-layer vesicle structure, and named it “blackberry.” This discovery leads to the identification of a new type of self-assembly in nature and finally solves the historical “blue water” puzzle. A new universal solute state has been identified, resulting in the opening of a new field – macroionic solution, which lies between simple ions and colloidal suspensions.

Expect that in the near future, the term of “macroionic solutions” may become a new direction in condensed matter physics and Chemistry curriculum, paralleling those of some other well-established areas such as ionic solutions, polymer solutions, and colloidal suspensions. Discussions on how to incorporate the new results into Chemistry textbook are underway with the *Journal of Chemical Education*. A lot of new physical phenomena have been

discovered, such as usual thermodynamic and dynamic properties; tuning macroionic charge density via pH and solvent; as well as the bio-membrane like materials formed by pure inorganic species. Have also systematically studied the effects of additional salts, temperature, solvent quality, pH, size and charge density of macroions on the formation of "blackberry," and have basically identified the nature of the strong attractive force among macroanions.

Four high school students have been working during the summer. They have been very successful in various national competitions.

Brandon Imber: Intel finalist (top 40 in the nation); Siemens-Westinghouse semifinalist; Champion, Long Island Science Fair (physics); Champion, Naval Research Contest.

Clara Tow: Intel semifinalist (top 300 in the nation); Siemens-Westinghouse semifinalist. Matthew Cons & Mike Bigesno, *Siemens-Westinghouse* Regional finalist (top 30 in the nation).

SPECIFIC ACCOMPLISHMENTS:

Tianbo Liu*, Ekkehard Diemann, Huilin Li, Andreas Dress and Achim Müller, "Self-Assembly in Aqueous Solution of Wheel-Shaped Mo_{154} Oxide Clusters into Vesicles," *Nature*, **2003**, 426, 59.

Guang Liu, Yuguang Cai and **Tianbo Liu***, "An Automatic and Continuous Dissolution and Precipitation Process in Inorganic Macroionic Solutions," *J. Am. Chem. Soc.*, **2004**, 126, 16690.

Guang Liu and **Tianbo Liu***, "Thermodynamic Properties of the Unique Self-Assembly of $\{\text{Mo}_{72}\text{Fe}_{30}\}$ Inorganic Macroions in Salt-Free and Salt-Containing

Aqueous Solutions," *Langmuir*, **2005**, 21, 2713.

Tianbo Liu*, "An Unusually Slow Self-Assembly of Giant Inorganic Ions in Aqueous Solution," *J. Am. Chem. Soc.*, **2003**, 125, 312-313.

Tianbo Liu*, "Supramolecular Structures of Polyoxomolybdate-Based Giant Molecules in Aqueous Solution," *J. Am. Chem. Soc.*, **2002**, 124, 10942-10943.

Tianbo Liu*, "Surfactant-Induced Trans-Interface Transportation and Complex Formation of Giant Polyoxomolybdate Clusters," *J. Clust. Sci.*, **2003**, 14, 215.

Guang Liu, Matthew Cons and **Tianbo Liu***, "The Ionic Effect on Supramolecular Aggregates in Polyoxomolybdate Solution," *J. mol. Liq.*, **2005**, 118, 27.

Anatoly I. Frankel*, Shira C. Frankel and **Tianbo Liu**, "Structural Stability of Giant Polyoxomolybdate Molecules as Probed by EXAFS," *Physica Scripta* **2005**, T115, 721-723.

Our work has been reported in over 15 top scientific public magazines in different countries, such as:

"Singin' the Blue," *Chemistry – American Chemical Society's Award-Winning Publication*, pp.4, Winter **2003**. (USA)

"Magnetic Molecules Take Better Pics – Sharper Scans Out of the Blue," *New Scientist*, vol. 175, issue 2359, pp. 17, September 7, **2002** (U.K.).

"Molybdän und Brombeersöße," *Wissenschaft-online* (German edition of the *Scientific American*), August 28th, **2002**.

"Rounding Up Nanoclusters," *Materials*

Today, January 2004 (U.K.).

“Unique Molecular Structure Offers Insight Into Nanoscale Self-assembly, Solution Chemistry,” *Science Daily*, Nov. 6th, 2003 (USA).

“Mo’s Better Blues,” *Reactive Reports*, Issue #35, 2004 (U.K.).

“Researchers Track New Solute State,” *Tcetoday*, September 10th, 2002 (U.K.).

“Old Chemical Enigma Solved,” *Popular Mechanics*, pp. 34, December Issue, 2002 (USA).

“Molecular Structure Offers Insight Into Nanoscale Self-Assembly,” *Space Daily*, Nov. 7th, 2003 (USA).

“Metal-oxide nanowheels roll up into vesicles,” *NanoTechWeb*, Nov. 7th, 2003 (USA).

Science & Technology Trends, Dec. 2003 (Japan).

“Molibdénkéssel,” *Nepszabadsag* (Hungary), January 18th, 2003.

- “Distinguished Oversea Young Scientists Award” from National Science Foundation of China in 2004 (8 per year in chemistry and chemical engineering related fields).

- Symposium organizer and co-Chair (From polyoxomolybdate to complex ions), 28th International Conference on Solution Chemistry, Debrecen, Hungary, August 23-28th, 2003.

- 18 invited talks.

LDRD FUNDING:

FY 2003	\$54,000
FY 2004	\$95,532
FY 2005	\$45,558

Functional Bulk Mn-Based Nanocomposites

Laura H. Lewis
Chi-Chang Kao

03-138

PURPOSE:

This work includes scientific and strategic objectives and is innovative in that it addresses a topic that is new within the DOE BES research portfolio. The scientific objective is to synthesize and characterize the materials attributes and response of magnetic nanosystems with a magneto-structural transition. While properly selected bulk magnetostructural material systems are anticipated to exhibit an extreme functional response, such as a giant magnetocaloric or colossal magnetoresistive effect, the nature of the response remains unknown in the nanostructured counterpart. Understanding the fundamental nanomagnetism will advance the science as well as foster new technology that supports selected missions of the DOE. The strategic objective of this work is to enhance the metastable or nanomaterials synthesis capabilities resident in the Materials Science Department by installation of a commercial Melt Spinner.

APPROACH:

The research focus is directed towards ferromagnetic equiatomic MnBi, chosen due to its well-known novel bulk magnetic properties such as a record magneto-optical Kerr effect and a magnetostructural transition underlying a large magnetocaloric effect and a giant magnetoresistive effect. This compound was successfully prepared in nanostructured form by employing the rapid solidification method of melt-spinning to a nominal eutectic Mn_5Bi_{95} alloy, resulting in unusual MnBi nanorods in a coarse-grained

Bi matrix (in collaboration with A. R. Moodenbaugh, MSD). Materials characterization was carried out from a variety of perspectives with a variety of probes. Structural characterization was achieved by standard laboratory x-ray diffraction and high-resolution transmission electron microscopy (HRTEM) (in collaboration with Yimei Zhu (CFN)). Characterization of the transport properties was carried out with a superconducting quantum interference device (SQUID) magnetometry and magneto-resistance measurements (with Qiang Li, MSD). Advanced characterization of the phase constitution structural details has been investigated with the synchrotron x-ray (NSLS X7B). Additionally, discussions with the BNL Computational Science Center are ongoing.

TECHNICAL PROGRESS AND RESULTS:

A commercial Melt Spinner (Edmund-Buhler GmbH, model SC) was installed and optimum processing conditions were established in 2003 and 2004. *Ex-situ* annealing of the quenched samples at 530 K/1 hour produced isolated, atomically coherent uniform MnBi nanorods of diameter 10 nm and length 30 nm. Magnetic properties reported in the bulk MnBi, such as a spin reorientation $T_S \sim 90$ K and positive temperature coefficient of coercivity were preserved in the nanostructured materials in this study, indicating that those effects are not closely related to the nanoscaling effect. However, a reduction in the Curie temperature of 100 K from the bulk value of ~ 650 K and a new first-order magnetic phase transition have been verified in this nanostructured material, confirming the proof of concept of the research. Studies of the behavior of MnBi nanorods in the presence of a magnetic field during heating revealed development of a

crystallographic nanorod texture and thus a tailored anisotropy. Synchrotron x-ray diffraction showed that the magnetic behavior introduced above is related to the crystal structure changes during *in-situ* heating. Additionally, an extremely high magnetoresistive effect (~300 % at 300 K) is found in *ex-situ* annealed ribbons, which may be further enhanced in samples with aligned nanorods (Fig. 1).

SPECIFIC ACCOMPLISHMENTS:

Publications:

1) K. Kang, L. H. Lewis, and A. R. Moodenbaugh, "Crystal structure and magnetic properties of MnBi/Bi nanocomposite," *J. Appl. Phys.*, **97** (2005) 10K302. [Also in Virtual Journal of Nanoscale Science & Technology, vol. 11, Issue 20, May 23 (2005)]

2) K. Kang, L. H. Lewis, and A. R. Moodenbaugh, "Alignment and analyses of MnBi/Bi nanostructures," *Appl. Phys. Lett.* **87** (2005) 062505.

3) Kyongha Kang, Y. F. Hu, L. H. Lewis, Qiang Li, A. R. Moodenbaugh, and Young-Suk Choi, "Large ordinary magnetoresistance in melt-spun Bi thin ribbons," *J. Appl. Phys.* **98** 073704 (2005).

4) Kyongha Kang, Y. F. Hu, L. H. Lewis, Qiang Li, A. R. Moodenbaugh, and Young-Suk Choi, "Magnetic and transport properties of MnBi/Bi nanocomposites," *J. Appl. Phys.*, (2005) (accepted).

5) L. H. Lewis and Kyongha Kang *et al.*, "MnBi Nanocomposites: Magnetostructural Size Dependence and Matrix Templating" (to be submitted).

Presentations:

1) K. Kang, L. H. Lewis and A. R. Moodenbaugh, "Crystal structure and magnetic properties of MnBi/Bi nanocomposite," at the 49th Conference on Magnetism and Magnetic Materials, Nov. 7-11, 2004, Jacksonville, Florida.

2) Kyongha Kang, L. H. Lewis, Y. F. Hu, Qiang Li, A. R. Moodenbaugh and Young-Suk Choi, "Magnetic and transport properties of MnBi/Bi nanocomposites," 50th Annual Conference on Magnetism & Magnetic Materials, San Jose, CA, Oct. 30-Nov. 3, 2005.

LDRD FUNDING:

FY 2003 (partially refunded)	\$28,000
FY 2004	\$76,906
FY 2005	\$42,185

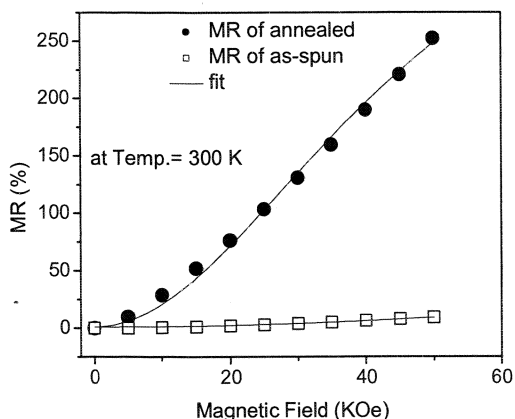


Figure 1. Room-temperature perpendicular magnetoresistance (MR) data and fits to the MR data using the Pippard-Fawcett two-carrier expression for Mn₅Bi₉₅ *ex-situ* annealed.

Radio Wave Detection of Ultra High Energy Cosmic Rays

Helio Takai

03-151

PURPOSE:

This project seeks the detection of ultra high energy cosmic rays via radio (radar) detection. It is well known that micro-meteors when vaporized in the upper atmosphere produce ionization trails that reflect radio waves in the 30-100 Mhz range. Ultra high energy cosmic rays with energies larger than 10^{18} eV produce ionization densities similar to micro-meteors and hence their detection via radio (radar) should, in principle, be possible. To prove the concept, an experiment where a radio echo is detected simultaneously with muons produced in the shower is being built. If proven successful a dedicated experiment can be built to cover an area near to 10^6 km² at a reasonable cost for the study of ultra high energy cosmic rays.

APPROACH:

In recent years cosmic rays of energies larger than 10^{20} eV have been detected. The origin and nature of the acceleration mechanism that can accelerate particles to such high energies is unknown. To put it in perspective these energies are four orders of magnitude larger than what the Large Hadron Collider, schedule to be operational in 2007, will accelerate. What are the acceleration mechanisms that can accelerate particles at these extreme energies? What sources of energy are available to accelerate particles at these energies? To study this problem large area detectors are required due to the very low event rate. The largest detector now under construction the Auger observatory, will cover an area of 3,000km².

Radar allows for the construction of detectors with coverage of the order of 10^6 km². This project seeks the detection of Radio waves from commercial transmitters, e.g. TV stations, in coincidence with compact shower detectors. Because of the distances involved, detection sites will be located far apart. Each detection site will acquire data independently and register the detection time using a GPS clock. Off line all the event times will be scanned and coincidences sought.

We collaborate in this project with U. of Stony Brook (M. Rijssenbeeck, M. Marx), the Suffolk County Community College (B. Warasila, T. Breeden and M. Inglis), and 12 high school physics teachers from Long Island and Maryland.

TECHNICAL PROGRESS AND RESULTS:

The array now available for studies is comprised of 10 scintillator detectors and one radar site. At the moment 4 of the scintillator sites are operational and 6 are being commissioned. The problem we face in the installation is primarily access to the network in High Schools.

The radar site in BNL has undergone several design changes. The most fundamental change was the antenna design which is based on existing antennas used in low-frequency radio astronomy. This addresses the issue of flat frequency response and impedance mismatch.

We spent time to model the radio response from an ionization cloud produced by a cosmic ray shower. This model includes the free electron lifetime performed at the NSLS. The modeling shows that the footprint of the signal will be widespread on the ground and short in duration. The signal

will be present for 10 microseconds which is well within the range of detectability.

We have attracted a group of the Electrical Engineering department in Stony Brook who are interested in the development of a dedicated radar system. Collaboration with the Astrophysics group from the Argonne National Laboratory is also underway.

SPECIFIC ACCOMPLISHMENTS:

We have presented results of our experiment at the following conferences and invited talks:

"Detecting UHECR via RADAR," Colloquia given to ASTRON, The Dutch Centre for Radioastronomy, Dwingeloo, The Netherlands, June 2, 2005.

"Detecting EAS with RADAR" Seminar given to the Auger collaboration, in Malargue, Argentina, November 11, 2004.

We have submitted and obtained funds of \$205,000 from the NSF for the continuation of this project. This project will be performed together with the Stony Brook Physics Department.

LDRD FUNDING:

FY 2003	\$100,000
FY 2004	\$123,923
FY 2005	\$ 17,502

New Synthesis Techniques to Control Atomic Defects in Advanced Intermetallic Compounds

Lance D. Cooley

03-162

PURPOSE:

Advanced intermetallic superconductors need to balance the delicately structural perfection, which enhances superconductivity, and structural disorder, which adds electron scattering and improves the upper critical field H_{c2} . This project explores new synthesis techniques that manipulate this balance in a controllable manner.

APPROACH:

Techniques to alloy MgB_2 received significant focus. Substitution of carbon for boron was explored because carbon alloying produces $\mu_0 H_{c2}(0)$ values well above the ~ 30 T limit of Nb_3Sn . This makes $Mg(B,C)_2$ a potential new material for energy science applications. Also, substitution of Al for Mg or C for B produces changes in the underlying physics of the two-band superconductivity that are not fully understood.

During FY2004, synthesis techniques were set up to control the volatility of Mg. Substitution of Al for Mg was then explored to understand the changes to the physics when an extra electron is added to the band structure. Since Al does not enter interstitial sites, a baseline for determining the homogeneity of alloying elements could also be obtained.

Alloying with carbon was more complicated because C can either enter an interstitial site or substitute for B. The much higher energies of B defects than for Mg defects, and

the presence of other Mg-B-C ternary intermetallics, made intended arrangements of carbon in MgB_2 more difficult to control. Characterization thus built upon the work established for Al alloying. Also, mixtures of boron and carbon were specially prepared using a plasma torch to reach very high temperatures, in collaboration with the Center for Thermal Spray Research at Stony Brook and with Specialty Materials, Inc. This provided higher uniformity of the carbon content in the boron carbide precursor.

This LDRD project supported a postdoc, Antonio Zambano, who led much of the work. Electromagnetic and heat capacity measurements, which probe the different bands participating in superconductivity, were coordinated with electron energy-loss spectroscopy (EELS) to compare property changes to the electronic structure. The latter measurements were done in collaboration with Y. Zhu's group in the Center for Functional Nanomaterials.

TECHNICAL PROGRESS AND RESULTS:

In FY2004, we made many Al and C alloyed samples using reactions typically used to make pure MgB_2 . These initial samples indicated that interesting changes in 2-band superconductivity were occurring because of the extra electrons provided by either Al or C, which filled the important hole states in the boron σ band. However, the physics was difficult to understand because there was significant scatter in property trends as a function of Al or C composition. Also, many samples were porous and not well suited for electron microscopy.

During FY2005, we discovered that the reactions above, which have been widely used by other researchers, were not sufficient to produce homogeneously alloyed samples. Detailed analyses of x-ray diffraction spectra

revealed evidence for compositional gradients. We were able to remove these gradients by altering our synthesis approach. In doing so, we discovered that the scatter in property trends analyzed as a function of composition could be removed when analyzed as functions of crystallographic data. This important discovery allowed us to approach the underlying physics despite the presence of sample inhomogeneities.

The combination of EELS with heat capacity measurements revealed a curious inversion of the hierarchy of the two superconducting bands for heavy Al alloying. EELS data indicated that 33% Al doping provided enough electrons to fill the σ band, which is the stronger band in pure MgB_2 . But this did not destroy superconductivity; rather it persisted at a low level up to 55% doping. Heat capacity measurements showed that the π band became the stronger band at high doping levels. This suggested that heavily Al-alloyed MgB_2 is akin to intercalated graphite. Thus, we concluded that the extraordinary superconductivity in pure MgB_2 is not an isolated occurrence, but it is a result of the favorable positioning of the σ band with electron removal. This important result implies that other high-temperature superconductors might be possible in graphite analogs by suitably adjusting their σ bands.

As expected, carbon alloying was found to be significantly poorer in homogeneity than Al alloying of MgB_2 . However, the x-ray diffraction analyses revealed huge strains, more than 2%, indicating a possible separation of reaction pathways between Mg and B_4C . Annealing at very high temperatures, too high for many applications, was required to produce the level of homogeneity comparable to those in Al-alloyed MgB_2 and in pure MgB_2 . This implies that far-from-equilibrium synthesis routes are needed to

achieve high H_{c2} values in practical forms of carbon-alloyed MgB_2 .

SPECIFIC ACCOMPLISHMENTS:

Funding: Renewal of “Superconducting Materials,” DOE-BES Field Work Proposal (Li and Cooley), \$729k. The LDRD project provided the seed for a central task. This work was the subject of a DOE-BES panel review 6/22/05.

Publications:

- A. J. Zambano, A. R. Moodenbaugh and L. D. Cooley, “Effects of different reactions on composition homogeneity and superconducting properties of Al-doped MgB_2 ,” *Supercond. Sci. Technol.* **18** (2005) 1411.
- L. D. Cooley, A. J. Zambano, A. R. Moodenbaugh, R. F. Klie, Jin-Cheng Zheng, and Yimei Zhu, “Inversion of two-band superconductivity at the critical electron doping of $(Mg,Al)B_2$,” to appear in *Phys. Rev. Lett.*
- R. F. Klie, J. C. Zheng, Y. Zhu, A. J. Zambano and L. D. Cooley “Electron energy-loss spectroscopy study of electron-doping in MgB_2 ,” submitted to *Phys. Rev. B*
- L.D. Cooley, Kyongha Kang, R. F. Klie, Qiang Li, A. M. Moodenbaugh, and R. Sabatini, “Low-temperature synthesis of MgB_2 from B_6Si ,” *Supercond. Sci. Technol.* **17** (2004) 942. (FY2004 result.)

LDRD FUNDING:

FY 2003	\$88,000
FY 2004	\$90,577
FY 2005	\$70,713

Femtosecond Photoinitiated Nanoparticle Surface Chemistry

Nicholas Camillone III

04-011

PURPOSE:

The goal of this project is to bring together the ultra-fast and the ultra-small to understand the physics behind the unique chemistry of nanostructured materials. In this pursuit we are developing capabilities to probe with femtosecond time resolution the chemical dynamics of molecules adsorbed on supported nanoparticles. This involves ultrafast laser-based techniques for initiating and following chemical transformations in real time in ultra-high vacuum (UHV), an undertaking that brings new capabilities and expertise to BNL. This project is seeding the growth of Ultrafast Surface Dynamics research within the Surface Chemical Dynamics component of the Chemical Physics Program. In addition, this project is nucleating discovery in an important area with the promise of continued growth in a number of different venues at BNL, such as the Center for Functional Nanomaterials, the Laser-Electron Accelerator Facility, and the Catalysis on the Nanoscale Program.

APPROACH:

About ten years ago a new class of surface chemistry, involving excitation driven by femtosecond light pulses, was demonstrated¹ and has recently begun to be exploited to study reaction dynamics on planar surfaces.² However, little has been done to explore these phenomena on nanoscale materials,³ where size-dependent properties are expected to impact the surface chemical dynamics.⁴ In particular, on supported metal nanoparticles, spatial confinement of electrons, size-dependent electronic structure⁵

and changes in electron-phonon coupling⁶ are expected to significantly affect hot electron lifetimes in small nanoparticles. Furthermore, enhancements in photoelectron yield from nanoparticles have been indicated.⁷ These effects are expected to impact the dynamics of adsorbates on nanoparticles. We aim to explore these dynamics as the size of the nanoparticles is varied through the regime spanning the non-metal to metal transition.

Our experiments employ the two-pulse correlation (2PC) technique^{2,8} wherein, the photoexcitation pulse is split into two pulses separated in time by a variable delay and directed to impinge upon the target. The photoinduced desorption yield is measured by a quadrupole mass spectrometer (QMS). In part because the relaxation times of the electronic and lattice temperatures differ by an order of magnitude, the 2PC desorption yield correlation width depends upon the desorption mechanism. This enables distinctions to be drawn among possible reaction mechanisms² and allows for quantification of their timescales.

Such time-resolved measurements on nanoparticles require a high energy (~ 1 mJ) source of 100 fs laser pulses, a UHV environment, a well-characterized substrate surface, manipulation and introduction of the pulses into the UHV, an ion counting scheme to detect photodesorbed species, and the capability to grow nanoparticles in UHV.

Development of this project, and design, assembly and operation of the experiment has depended heavily on the efforts of postdoctoral research associate Paul Szymanski (Chemistry) and has involved the collaboration of Alexander Harris (Chemistry) and James Misewich (Materials Science). In addition, components crucial to the effort have been supplied through collaboration with

Michael White (Chemistry BNL and SUNY Stony Brook).

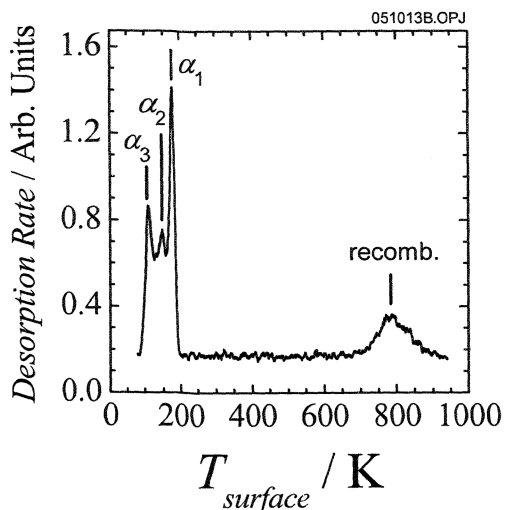


FIG. 1. TPD spectrum for O_2 desorbing from Pd(111).

TECHNICAL PROGRESS AND RESULTS:

During fiscal year 2005 several important milestones towards achieving our stated goals have been reached:

- Protocols were developed and executed to prepare Pd(111), a model surface chosen for this work. The thermal surface chemistry with molecular oxygen was surveyed with temperature-programmed desorption (TPD, see Fig. 1). Results were in agreement with the literature.⁹
- Our first femtosecond photoinduced desorption measurements of O_2 from Pd(111) were made. This involved the development of a detection protocol and new software.
- Our first 2PC measurements for photoinduced desorption of O_2 from Pd(111) were made (Fig. 2). This involved alignment of optical components to manipulate and characterize the laser pulses, including: installation of a new frequency-resolved optical gating second-harmonic (SHG)-based pulse-

width measurement device; construction of a separate SHG-based device to characterize the temporal profile of the pulses at a location approximating that of the target surface; construction of an autocorrelator incorporating an optical delay line; installation of a CCD camera to measure the spatial profile and alignment of the incident pulses at a location approximating that of the target, and the development of new software to control the optical delay line and acquire SHG and 2PC data.

- Measurements of the dependence of the desorption yield upon adsorbed fluence were made. At low O_2 coverage, these data are in reasonable agreement with those found in the literature⁸ (Fig. 3). At coverages greater than those used in the previously published work, our measurements suggest a significantly higher photodesorption cross section. Other preliminary measurements suggest that the desorption dynamics may be coverage dependent. Changes in the 2PC response and the photon fluence-dependence of the cross section with O_2 coverage are areas of ongoing detailed investigation.

- We researched and purchased an evaporative doser for physical vapor deposition (PVD) of Pd and Au nanoparticles.

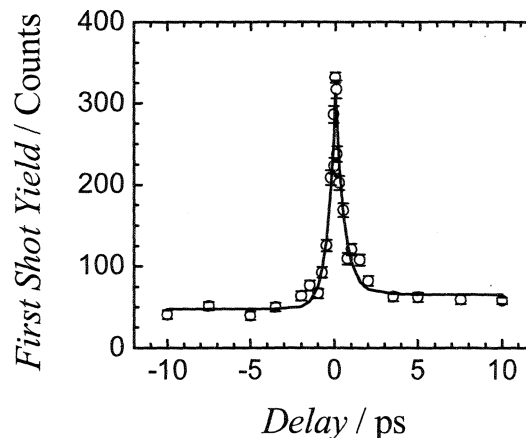


FIG. 2. Subpicosecond-resolution two-pulse correlation measurements of photoinduced desorption of O_2 from Pd(111).

Projected milestones for FY 2006 include:

- optimization of the detection scheme including shot-to-shot pulse energy measurements and isotopic substitution,
- exploration of the coverage dependence of the dynamics of photoinduced desorption of O₂ from Pd(111),
- measurements of the photoinduced desorption of CO from Pd(111),
- characterization of rutile TiO₂ (110) surfaces to serve as substrates for the nanoparticle experiments,
- TPD studies of CO and O₂ from Pd nanoparticles grown on TiO₂, and
- 2PC measurements of the photoinduced desorption of CO and O₂ from Pd nanoparticles.

Reaching the last two milestones will require completion of the final major step in construction of the apparatus. This will involve installation of the evaporative metal source for PVD of nanoparticles, and a quartz crystal microbalance to monitor the deposition rate.

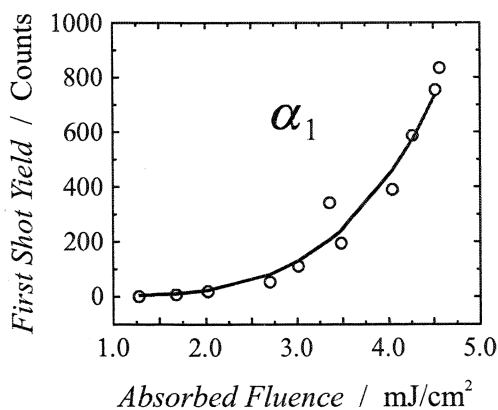


FIG. 3. Photoinduced desorption yield for O₂ from Pd(111) when prepared with a coverage such that only the α_1 feature is observed in the TPD.

Our longer term goal is to explore the size-dependence of the desorption dynamics of molecular adsorbates from nanometer scale metal particles. It has been shown that Au and Pd nanoparticles can be grown on TiO₂ with a relatively narrow size dispersion by PVD with mean particle diameters on the order of 1 to 50 nm.^{5,10} This size regime is of interest because the reactivity of the particles for the catalytic oxidation of CO shows a marked peak for particles approximately 3 nm in diameter, and this peak in reactivity coincides with the non-metal to metal transition.¹¹ Our aim is to measure the desorption dynamics of CO from nanoparticle assemblies as a function of nanoparticle size to begin to probe the chemical dynamics behind the marked size-dependence of the reactivity of this model catalytic system.

SPECIFIC ACCOMPLISHMENTS:

Strategic Accomplishments

- Based in part on extension of this LDRD work, a proposal for “Ultrafast Investigations of Surface Chemical Dynamics” was made at the DOE Chemical Sciences Review of the BNL Chemical Physics Program in October of 2003. The proposal was approved for funding of \$955,000 available in FY 2005 through 2007.

- As a result of the success of the October 2003 proposal to DOE, we have formed a new Surface Chemical Dynamics Group. The group includes principal investigators M. White and R. Beuhler, A. Harris, and N. Camillone (all BNL Chemistry).

LDRD-Related Presentations

- “Ultrafast Investigations of Surface Chemical Dynamics,” N. Camillone III, oral presentation at the *DOE Chemical Sciences Review of the BNL Chemical Physics Program* (BNL, October 28, 2003).

• “Femtosecond Photoinitiated Nanoparticle Surface Chemistry,” N. Camillone III, oral presentation at the *Mid-Year Review of LDRD Projects* (BNL, May 3, 2004).

• “Femtosecond Photoinitiated Nanoparticle Surface Chemistry,” N. Camillone III, oral presentation at the *Mid-Year Review of LDRD Projects* (BNL, April 13, 2005).

REFERENCES:

- ¹ J.A. Misewich, T.F. Heinz, D.M. Newns, *Phys. Rev. Lett.*, **68**, 3737 (1992).
- ² M. Bonn, S. Funk, C. Hess, D.N. Denzler, C. Stampfl, M. Scheffler, M. Wolf, G. Ertl, *Science*, **285**, 1042 (1999).
- ³ A. Wille, R. Buchwald, K. Al-Shamery, *Appl. Phys. A*, **78**, 205 (2004).
- ⁴ A. Wille, K. Al-Shamery, *Surf. Sci.*, **528**, 230 (2003).
- ⁵ M. Valden, X. Lai, D.W. Goodman, *Science*, **281**, 1647 (1998).

- ⁶ T. Valla, M. Kralj, A. Šiber, M. Milun, P. Pervan, P.D. Johnson, D.P. Woodruff, *J. Phys.: Condens. Matter*, **12**, L477 (2000).
- ⁷ P.V. Kamat, M. Flumiani, G.V. Hartland, *J. Phys. Chem. B*, **102**, 3123 (1998).
- ⁸ J.A. Misewich, A. Kalamarides, T.F. Heinz, U. Höfer, M.M.T. Loy, *J. Chem. Phys.*, **100**, 736 (1993).
- ⁹ X. Guo, A. Hoffman, J.T. Yates, Jr., *J. Chem. Phys.*, **90**, 5787 (1989).
- ¹⁰ X. Lai, T.P. St.Clair, M. Valden, D.W. Goodman, *Prog. Surf. Sci.*, **59**, 25 (1998).
- ¹¹ S.B. DiCenzo, S.D. Berry, J. E.H. Hartford, *Phys. Rev. B*, **38**, 8465 (1988); C. Binns, *Surf. Sci. Rep.*, **44**, 1 (2001).

LDRD FUNDING:

FY 2004	\$ 79,532
FY 2005	\$121,071
FY 2006 (budgeted)	\$ 41,000

Chirped Pulse Amplification at the DUV-FEL

Li Hua Yu

04-013

PURPOSE:

We propose to investigate the Chirped Pulse Amplification (CPA) by free-electron laser at the DUV-FEL (Deep Ultra-Violet Free Electron Laser) facility. In a seeded FEL, when the seed laser is chirped and the electron bunch is also chirped accordingly, the output radiation is also amplified and chirped. When the chirped output is compressed by an appropriate optical system, the output can have a very short pulse with very high peak power.

APPROACH:

Our approach is to use the HGHG (High Gain Harmonic Generation) process to carry out CPA (Charge Pre Amp) at the DUVFEL. The HGHG approach utilizes a laser-seeded FEL to produce amplified, longitudinally coherent, Fourier-transform-limited output at a harmonic of the seed laser. Since the output wavelength is reduced by the harmonic number but with the same percentage of chirp as the seed. The pulse length is also reduced by the harmonic number when compared with the bandwidth limited seed pulse length. This makes it possible to achieve ultra-short pulse lengths with high peak power. With the existing laser technology of 6% bandwidth (most updated techniques allow for 9% bandwidth), with the possible energy chirped chirp range of 3% at the DUVFEL, our calculation showed that it is possible to achieve 7 fs with 6 GW peak power at 266 nm. Recently we have carried out the HGHG experiment at 266 nm using the NISUS (Near Infra Red Scalable Undulator System) at the DUVFEL. The results agree

with the theory very well. Short pulse amplification is also an important part of the cascaded HGHG experiment to achieve x-ray FEL. Here, we plan a first CPA experiment to confirm this principle, with the ultimate goal of providing an intense, highly coherent ultra-short pulse source of hard x-rays.

TECHNICAL PROGRESS AND RESULTS:

We have made significant progress towards achieving CPA in FEL.

Since we have achieved stable HGHG output at 266 nm using an 800 nm seed, we started to chirp the seed and the electron beam energy within the electron bunches. By varying the energy chirp, we change the matching between the seed and the electron bunch, and in the mean time measure the bandwidth. The results showed a maximum bandwidth at a certain chirp rate of the electron bunch, and the bandwidth is 1.5nm, which is quite close to the theoretically expected maximum bandwidth achievable, i.e. 1.8 nm. This gave us confidence for the desired CPA.

We then proceeded to install the SPIDER (Spectral Interferometry for Direct Electric-Field Reconstruction) to measure the phase distortion of the HGHG output. We were able to carry out the SPIDER measurement on the HGHG output, and start to vary the chirp and change the bandwidth. The results showed the output is chirped agreeing with theory, and hence should be able to be compressed.

After the shut-down for an energy upgrade at the SDL (Source Development Lab) from May 2004-June 2005, we started to repeat what had been achieved in FY2003-2004. We are still continuing to improve the electron beam quality to the level before the

shut-down. Evidence showed that the photo-cathode laser pulse length is shorter than what is optimized for the operation, causing a larger space charge effect and degraded the performance. We are in progress to improve on this.

SPECIFIC ACCOMPLISHMENTS:

Our works acquired funding of \$400K from the Air Force Office of Scientific Research/Finance Dept. (AFOSR/PIF), Medical FEL Research Program, Agreement Number NMIPR015203751.

We have obtained funding of \$1M from the NAVY on high energy free electron lasers, which is related to the recent works on HGHG.

Publications:

- H. Loos, A. Doyuran, J. B. Murphy, J. Rose, T. Shaftan, B. Sheehy, Y. Shen, J. Skaritka, X.J. Wang, Z. Wu, L.H. Yu, "ELECTRO-OPTIC LONGITUDINAL ELECTRON BEAM DIAGNOSTIC AT SDL," PAC 2003
- T. Shaftan, Z. Huang, A. Doyuran, L. Carr, W.S. Graves, C. Limborg, H. Loos, J. Rose, B. Sheehy, Z. Wu, L.H. Yu, "Experiments with electron beam modulation at the DUVFEL accelerator," Volume 528, Issues 1-2, 1 August 2004, Pages 397-401
- J. Rose, B. Podobedov, J. Murphy, T. Shaftan, B. Sheehy, X.J. Wang, L.H. Yu, "A SCRF Linac as a FEL Driver and Storage Ring Injector," PAC2003
- T. Shaftan, L.H. Yu, "HGFG with Variable Wavelength," BNL-72034-2004-JA
- Adnan Doyuran, Louis DiMauro, William Graves, Richard Heese, Erik D. Johnson, Sam Krinsky, Henrik Loos, James B. Murphy, George Rakowsky, James Rose, Timur Shaftan, Brian Sheehy, Yuzhen Shen, John Skaritka, Xijie Wang, Zilu Wu, and LiHua Yu, "Experimental study of a high-gain harmonic-generation free-electron laser in the ultraviolet," Phys. Rev. ST Accel. Beams 7, 050701 (2004)
- L.H. Yu, A. Doyuran, L. DiMauro, W. S. Graves, E. D. Johnson, R. Heese, S. Krinsky, H. Loos, J.B. Murphy, G. Rakowsky, J. Rose, T. Shaftan, B. Sheehy, J. Skaritka, X.J. Wang, Z. Wu "First Ultraviolet High-Gain Harmonic-Generation Free Electron Laser," PRL, 91, 7, 074801 (2003)
- Adnan Doyuran, Louis DiMauro, Richard Heese, Erik D. Johnson, Sam Krinsky, Henrik Loos, James B. Murphy, George Rakowsky, James Rose, Timur Shaftan, Brian Sheehy, Yuzhen Shen, John Skaritka, Xijie Wang, Zilu Wu, Li Hua Yu, "Preliminary Chirped Pulse Amplification of HGFG-FEL at DUV-FEL Facility in BNL," NIM, A, Volume 528, Issues 1-2, Pages 467-470 (2004)
- L.H. Yu, "R&D experiments at BNL to address the associated issues in the Cascading HGFG scheme," Proceedings of International FEL Conference, 2004, Trieste, Italy
- Z. Wu, H. Loos, Y. Shen, B. Sheehy, E. D. Johnson, S. Krinsky, J. B. Murphy, T. Shaftan, X.-J. Wang, L. H. Yu, "Spectral Phase Modulation and chirped pulse amplification in High Gain Harmonic Generation," Proceedings of International FEL Conference, 2004, Trieste, Italy

LDRD FUNDING:

FY 2004	\$ 78,404
FY 2005	\$119,331
FY 2006 (budgeted)	\$ 41,000

Overcoming Coherent Instabilities at Medium-Energy Storage Rings

Jiunn-Ming Wang

04-025

PURPOSE:

In the United States, Europe and Japan, new light sources are being designed which are comprised of medium energy storage rings with twenty or more Mini Gap Undulators (MGUs) with magnet gaps of 5 mm. The mini-gap undulator provides a means of producing X-rays with high brilliance from a medium-energy storage ring. Unfortunately, it has been observed in many light sources throughout the world that the tapered vacuum vessels for such undulators tend to excite transverse mode-coupling instability (TMCI) of the electron beam. In order to avoid operational complications, the effects of transverse mode-coupling instability in the new storage rings must be minimized. The purpose of this LDRD is to analyze the impedance and study the potential coherent instabilities for medium energy storage rings containing Mini Gap Undulators.

APPROACH:

In this LDRD project we plan to carry out:

1. numerical and analytical analyses of the coupling impedance for the most critical storage ring components;
2. investigations of the electrodynamic properties of the identified components in order to reduce their impedance contribution to the total impedance of the ring;
3. analytical verification of the calculated data from the electromagnetic simulation program GdfidL;
4. comparison of the received data for the critical components with results obtained at other laboratories.

analysis of the preliminary impedance budget for the NSLS-II storage ring.

The collaborators of this work include Alexei Blednykh, Samuel Krinsky, James Rose, Stephen Kramer, Toshiya Tanabe, George Rakowsky and Joe Greco.

TECHNICAL PROGRESS AND RESULTS:

- a) In the future medium energy storage rings it is planned to install both superconducting and in-vacuum room temperature MGU (RTMGU). Investigation of the transverse impedance of the in-vacuum RTMGU shows that the driving charge can excite in the structure some strong resonant modes. All modes in the structure were identified and classified. Existence of the resonant mode at low frequencies can give rise to coupled bunch instabilities. This type of instability requires additional research, which can be done experimentally using the X25 RTMGU after it's installed into the NSLS X-Ray ring.
- b) The tapered elliptic vacuum chamber for Superconducting MGU has smaller contribution to the transverse impedance than RTMGU, as can be seen from comparison of the kick factors. The kick factor for the tapered elliptic vacuum chamber is a factor of 4 smaller than for the RTMGU.
- c) Investigation of the electrodynamic properties of the tapered elliptic vacuum chamber uncovered the existence of trapped modes. These modes were identified and classified.
- d) To verify existence of the trapped modes in the tapered vacuum chamber, a rectangular prototype was manufactured for microwave measurements. The obtained experimental results are in agreement with analytical and numerical calculations. All identified modes correspond to the TE_{mn} -Mode (mode with transverse electric field).

- e) For some components of the future storage rings, we have carried out a series of the analytical verifications of the received numerical code calculated data. For example, it has been found that analytical results for the dipole vacuum chamber using the theoretical Bethe-hole predictions, and the theoretical studies of A. Fedotov, L. Gluckstern, S. Kurennoy and G. Stupakov, are in agreement with the GdfidL calculations.
- f) One of the most important parts of our research has been to compare GdfidL results with already evaluated data of other laboratories. For this purpose we chose identical geometries to make sure that the results calculated using difference methods were in agreement. Results for two geometries, the tapered elliptic vacuum chamber and the SOLEIL's BPM, were compared in collaboration with Ryutaro Nagaoka from SOLEIL. In both cases we used the GdfidL code; however, the methods of the transverse impedance calculations were different. R. Nagaoka applied the method, which was introduced by G. Nassibian and F. Sacherer, in 1979 in CERN (European Organization for Nuclear Research). Our method is the computation of the impedances using a quarter of the structure with appropriate boundary conditions. After uncovering a factor of two corrections to the method of computing the impedance from GdfidL using a quarter structure, we found that our computations were in good agreement with SOLEIL. The transverse impedance in the low-frequency limit for the SOLEIL BPM has a value of $\text{Im}Z_y(\omega \rightarrow 0) = 50 \text{ k}\Omega/\text{m}$. This result depends very strongly on the BPM's button geometry, due to excitation of resonant modes.

A preliminary impedance budget including the most important components has been generated for a medium energy storage ring. All data have been entered into a table, which

can serve as a useful starting point for future light source projects such as NSLS-II.

SPECIFIC ACCOMPLISHMENTS:

Collective Effects for NSLS-II. A. Blednykh, S. Krinsky, B. Podobedov, J. Rose, N. A. Towne, J. -M. Wang. PAC 2005 – Proceedings, Knoxville, Tennessee, USA, May 16-20.

A Model Study of Transverse Mode Coupling Instability at NSLS-II. A. Blednykh, J. -M. Wang. PAC 2005 – Proceedings, Knoxville, Tennessee, USA, May 16-20.

Harmonic Cavity Performance for NSLS-II. A. Blednykh, S. Krinsky, B. Podobedov, J. Rose, N. A. Towne, J. -M. Wang. PAC 2005 – Proceedings, Knoxville, Tennessee, USA, May 16-20.

Insertion Device Upgrade Plans at the NSLS. T. Tanabe, A. Blednykh, D. A. Harder, M. Lehecka, G. Rakowsky, J. Skaritka. PAC 2005 – Proceedings, Knoxville, Tennessee, USA, May 16-20.

NSLS II: The Future of the NSLS. J. B. Murphy, J. Bengtsson, R. Biscardi, A. Blednykh, G. L. Carr, W. R. Casey, S. Chouhan, S. B. Dierker, E. Haas, R. Heese, S. Hulbert, E. D. Johnson, C. C. Kao, S. L. Kramer, S. Krinsky, I. P. Pinayev, S. Pjerov, B. Podobedov, G. Rakowsky, J. Rose, T. V. Shaftan, B. Sheehy, J. Skaritka, N. A. Towne, J. -M. Wang, X. J. Wang, L. -H. Yu. PAC 2005 – Proceedings, Knoxville, Tennessee, USA, May 16-20.

NSLS-II Injection Concept. T. V. Shaftan, A. Blednykh, S. Chouhan, E. D. Johnson, S. L. Kramer, S. Krinsky, J. B. Murphy, I. P. Pinayev, S. Pjerov, B. Podobedov, G. Rakowsky, J. Rose, T. Tanabe, J. -M. Wang, X. J. Wang, L. -H. Yu. PAC 2005 – Proceedings, Knoxville, Tennessee, USA, May 16-20.

Comparison of Bethe-Hole and GdfidL Calculations of the Horizontal Beam Impedance of a Long Slot. NSLS-II Technical Note 0005. A. Blednykh, J. -M. Wang.

LDRD FUNDING:

FY 2004	\$ 91,415
FY 2005	\$128,858
FY 2006 (budgeted)	\$ 48,000

Layered Cobaltates with High Thermoelectric Power

Qiang Li

04-033

PURPOSE:

We carried out a systematic study of the fundamental thermoelectric and related material properties of layered cobaltates necessary for their effective practical utilization. Through coordinated research on synthesis and characterization, we will be able to understand the mechanism controlling the thermoelectric properties, as well as gaining the ability to tune various materials parameters in order to optimize their thermoelectric performance. The proposed research can lead to the discovery of new phenomena in strongly correlated electron systems, novel functionality, and many practical applications. This project is aligned with the BNL Grand Challenge to understand strongly correlated phenomena.

APPROACH:

Cobaltates (A_xCoO_y) are transition-metal misfit layered oxides, that feature self-assembled alternatively-stacked blocks with incoherent layer boundaries, producing highly anisotropic properties along their crystallographic directions. Recently, it was discovered that some cobaltates have thermoelectric a performance challenging that of conventional thermoelectric materials. Though preliminary studies have shown that cobaltates hold great promise to be the first choice thermoelectric materials operated at high temperature and in hazardous environments, the synthesis and characterization of this class of material in various forms are largely unexplored. In particular, the role of self-assembly in the growth of cobaltates thin films is poorly

understood. To address this key issue, we focused our study on the properties and structure of $Ca_3Co_4O_9$ single crystals, and thin films grown on various single crystalline, polycrystalline, and amorphous substrates. A coordinated Transmission Electron Microscope (TEM) and thermoelectric property characterization is performed to understand the growth mechanism and the correlation between the structures and thermoelectric properties.

TECHNICAL PROGRESS AND RESULTS:

A post-doctoral research associate was hired in February 2004 to participate in this project. In the summer of 2005, a graduate student from the State University of New York at Stony Brook was supported to participate in this project. Specifically:

- 1) We set up the three zones furnace and successfully grew Na_xCoO_2 and $Ca_3Co_4O_9$ single crystals, which were characterized by x-ray diffraction and magnetometry, and used electron correlation studies, in collaboration with the photoemission group of BNL.
- 2) A new thermoelectric and transport characterization system was purchased from Quantum Design with BES capital funding. It became the main instrument for evaluating the thermoelectric properties.
- 3) Thin films of $Ca_3Co_4O_9$ have been successfully grown on various substrates, including single crystalline $SrTiO_3$, $LaAlO_3$, Si, Al_2O_3 , polycrystalline Al_2O_3 , and glass, using pulsed laser deposition, in collaboration with Dr. W. Si of Physics Department of BNL.
- 4) High resolution TEM was used to characterize the microstructures of

Ca₃Co₄O₉ films, in collaboration with Dr. E, Sutter of the Center for Functional Nanomaterials at BNL.

5) High-quality *c*-axis oriented Ca₃Co₄O₉ thin films were grown directly on Si (100) and Si (111) wafers by pulsed laser deposition without pre-chemical treatment of the substrate surface. Cross-sectional transmission electron microscopy shows excellent crystallinity of the Ca₃Co₄O₉ films. The Seebeck coefficient and resistivity of the Ca₃Co₄O₉ thin films on Si (100) substrate are 126 μV/K and 4.3 micro-Ohm.cm respectively at room temperature. This is comparable to the single crystal samples. This advance demonstrated the possibility of integrating the cobaltate based high thermoelectric materials with the current state-of-the-art silicon technology for thermoelectricity-on-a-chip application, such as thermochemistry-on-a-chip, biothermoelectric chip, and active cooling for microelectronic processors.

6) *c*-axis oriented Ca₃Co₄O₉ thin films have been grown directly on glass (fused silica) substrate by pulsed laser deposition. Detailed microstructure analysis showed stacking faults abundant throughout the films. However, the Seebeck coefficient (~ 130 μV/K) and resistivity (~ 4.3 mΩ•cm) of these films on a glass substrate at room temperature were found comparable to the single crystal samples. The presence of these structural defects could reduce thermal conductivity, and thus enhance the overall performance of cobaltate films to be potentially used in the thermoelectric devices.

7) A box furnace was purchased and used exclusively for single crystal growth of cobaltates.

SPECIFIC ACCOMPLISHMENTS:

- 1) Two peer-reviewed papers published in Applied Physics Letter. “*In situ* growth of *c*-axis oriented Ca₃Co₄O₉ thin films on Si (100)” Y. Hu, et al, Appl. Phys. Lett. **86** 082103 (Feb. 2005), and “Thermoelectric properties and microstructure of *c*-axis oriented Ca₃Co₄O₉ thin films on glass substrates” Y. F. Hu, et al, Appl. Phys. Lett. **87** 171921 (Oct. 2005)
- 2) One patent application “Cobalt Oxide Thermoelectric Compositions and Uses Thereof” Y. Hu, Q. Li, and W. Si
- 3) A research collaboration was established with GM R&D Lab on the high performance thermoelectric materials
- 4) Two invited presentations: 1) “Layered Cobaltates with High Thermoelectric Power” in 6th Pacific Rim Conference on Ceramic and Glass Technology, organized by American, Australia, Japan, China, Korean Ceramic Society, Maui, Hawaii, September 11-16, 2005; 2) “Layered Cobaltates with High Thermoelectric Power” in Materials Research Society 2005 Fall meeting, Boston MA, Nov. 28 - Dec. 2, 2005

LDRD FUNDING:

FY 2004	\$ 66,780
FY 2005	\$103,160
FY 2006 (budgeted)	\$ 32,300

Complex Thin Films and Nanomaterial Properties

J. Misewich

04-038

PURPOSE:

The purpose of this program is twofold: (1) to explore novel methods of high-quality perovskite nanomaterial synthesis, in particular to study the untapped solid-state approach to nano-oxide synthesis. (2) the development of innovative approaches to the high-sensitivity characterization of nanomaterials, in particular to pursue the first simultaneous structural and spectroscopic characterization of *individual* nanotubes.

APPROACH:

Many of the most interesting and extreme examples of physical properties are exhibited in the perovskite oxide family of materials. For example, high-temperature superconductivity, the highest electro-optic coefficients, colossal magnetoresistance, and high polarization ferroelectricity are all demonstrated in perovskite oxide materials. Remarkably, the exploration of this important family of materials in nanoscale form is largely unexplored. A problem has been that there are only limited approaches in synthesis. To date, the synthesis of nanoscale oxides has been wet-chemistry oriented and therefore subject to impurities which has made reliable characterization more of a challenge.

In part (1) of this project we have undertaken an exploration of the solid-state synthesis of perovskite oxides to explore whether higher-quality nanostructured forms of oxides can be attained in this important class of materials. In part (2) of this project we address the challenge of nanomaterial characterization.

One of the problems of nanoscience lies in the wide distribution of nanomaterial structures usually obtained from even the best syntheses. Carbon nanotubes are a prime example, where even the best dispersed samples contain hundreds of varieties of the chiral (or wrapping) vector, with each species having different electronic and optical properties. Therefore, the challenge is to develop capabilities to characterize both the properties and structure of an individual nanotube or nanoparticle. We have developed spectroscopic and transport characterization techniques in this project that allow the properties of an individual nanotube to be determined. In addition, we have explored the use of diffraction to characterize the structure of individual nanotubes. The successful combination of individual nanotube structural and spectroscopic characterization represents a solution to a grand challenge in nanoscience. Collaborators here include Stan Wong and Yimei Zhu and their groups, and Columbia University (for spectroscopy).

TECHNICAL PROGRESS AND RESULTS:

In 2004, the main accomplishment was the establishment of nanofabrication capabilities at Brookhaven and the development of synchrotron characterization techniques for nanomaterials (NEXAFS). By working with electron-beam lithography capabilities at the Center for Functional Nanomaterials, we developed nano-patterned structures that are the basis for individual nanotube transport and optical characterization. Also in 2004, success was achieved in the solid-state synthesis of nanostructured forms of perovskite oxide materials. This included the synthesis of nanocubes of strontium titanate and nanowires of barium titanate. Figure 1 is a high-resolution Transmission Electron Microscope (TEM) image of a section of a barium titanate nanowire

showing the high degree of crystallinity and high quality of the material.

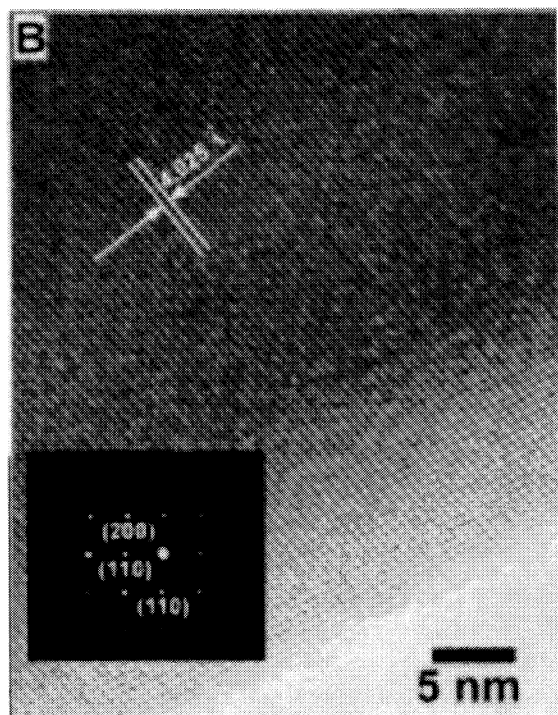


Figure 1. Hi-resolution TEM of BaTiO₃ nanorod.

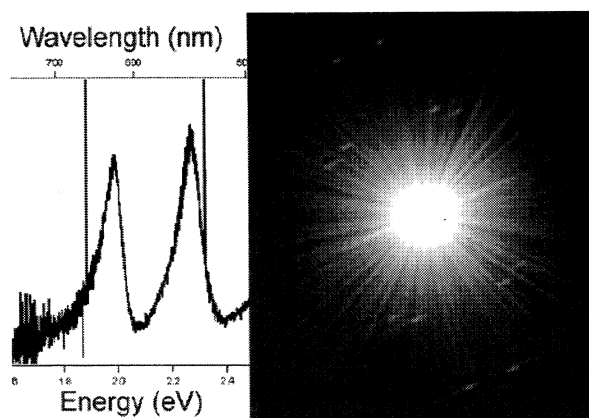


Figure 2. Left: Spectrum of an individual nanotube, Right: Electron diffraction pattern for the same nanotube.

The 2005 progress included the first simultaneous structural and spectroscopic characterization of an individual carbon nanotube which was a major accomplishment.

For the first time the spectra of different species of carbon nanotubes were studied individually AND directly correlated with structure. Figure 2 left shows the optical spectrum for an individual nanotube and Figure 2 right shows the electron diffraction pattern for the same nanotube, which was used to determine uniquely the chiral vector of the nanotube.

We also started work to characterize the oxide nanowires shown in Figure 1. In 2005 we used nonlinear spectroscopy to show that ensembles of the oxide nanowires remained ferroelectric in nanoscale form. In FY 2006 we started work to characterize the nonlinear response of an individual oxide nanowire which is necessary to sort out ensemble perturbations to ferroelectric properties of nanomaterials.

Additional work in 2006 is aimed at the synthesis of novel nanomaterial heterostructures, and the extension of the property characterization of chirally identified individual carbon nanotubes to include photoconductivity studies (for potential in solar energy applications) and transport studies.

SPECIFIC ACCOMPLISHMENTS:

Commitment for future programmatic funding obtained from DOE (FWP MA-507-MAAA), which was reviewed by DOE in June 2005.

Refereed publications: Surface chemistry and structure of purified, ozonized, multiwalled carbon nanotubes probed by NEXAFS and vibrational spectroscopy, S. Banerjee, T. Hemraj-Benny, M. Balasubramanian, D.A. Fischer, J.A. Misewich, and S.S. Wong, *Chem. Phys. Chem.*, 5, 1416, 2004.

Oxidized single-walled carbon nanotubes investigated using NEXAFS spectroscopy, S. Banerjee, T. Hemraj-Benny, M. Balasubramanian, D.A. Fischer, J.A. Misewich, and S.S. Wong, Chem. Commun. 772, 2004.

Hot Carrier Electroluminescence from a single carbon nanotube, M. Freitag, V. Perebeinos, J. Chen, A. Stein, J.C. Tsang, J.A. Misewich, R. Martel, and Ph. Avouris, Nano Letters, 4, 1063 (2004).

Near-edge x-ray absorption fine structure investigations of order in carbon nanotube based systems, S. Banerjee, T. Hemraj-Benny, S. Sambasivan, D.A. Fischer, J.A.

Misewich, and S.S. Wong, J. Phys. Chem. B 109, 8489, 2005.

Optical Spectroscopy of Individual Single-Walled Carbon Nanotubes of Defined Chiral Structure Matthew Y. Sfeir, Tobias Beetz, Feng Wang, Limin Huang, X.M. Henry Huang, J. Hone, Stephen P. O'Brien, J.A. Misewich, Tony F. Heinz, Yimei Zhu, and Louis E. Brus, submitted to Nature.

LDRD FUNDING:

FY 2004	\$ 79
FY 2005	\$190,532
FY 2006 (budgeted)	\$307,000

Lattice QCD Relevant for RHIC and AGS

Péter Petreczky

04-041

PURPOSE:

The purpose of this LDRD project was to identify and in the long run solve lattice QCD (Quantum Chromo Dynamic) problems relevant for the physics program at RHIC and AGS, especially those related to the Quark Gluon Plasma (QGP) created at RHIC. One of the main motivations for the project was the creation of the Center for Lattice Gauge Theory at BNL with a 10Tflop QCD on a chip (QCDOC) supercomputer as well as the availability of the 10Tflop QCDOC machine at the RIKEN-BNL Research Center.

APPROACH:

The central questions for the RHIC heavy ion program are related to the creation of new states of strongly interacting matter and investigation of its properties. Lattice QCD can contribute to answering these questions by first principles calculations of the relevant quantities, for example, critical temperature and the associated energy density for QGP formation and the quarkonium yield from a QGP.

To address the problem of the critical temperature and energy density finite temperature, lattice calculations with improved staggered fermions need to be carried out. At the moment it is not clear which version of the improved staggered formulation is the most appropriate for reaching the outlined goals.

To gain insight on the fate of different quarkonium states in hot and dense strongly interacting matter, the corresponding meson

spectral functions have been calculated in quenched lattice QCD (where the effect of dynamical quarks is neglected) and spectral functions have been extracted using the *Maximal Entropy Method*. It is not completely clear how reliably the spectral function can be reconstructed from the lattice data and to what extent the effects of finite lattice spacing (cutoff effects) can be controlled in those calculations.

In addition, the heavy quark potentials have been calculated in full QCD which should help to gain insight on the effects of dynamical quarks on dissociation of heavy quarkonia states at high temperatures.

The following problems were addressed in FY05:

- Quenched lattice QCD calculations of charmonia and bottomonia spectral on anisotropic lattices
(P. Petreczky, K. Petrov)
- Detailed investigation of heavy quark potentials in full QCD for relatively large dynamical quark masses
(F. Zantow)
- Study of QCD phase transition at finite temperature with improved staggered fermion formulation
(P. Petreczky, K. Petrov, C. Schmidt)

TECHNICAL PROGRESS AND RESULTS:

Detailed calculations of charmonia and bottomonia correlators and spectral functions at several lattices spacings have been done. Numerical calculations have been performed on the QCDOC supercomputer.

The use of different lattice spacings allowed us to estimate the importance of the cutoff

effects in quarkonia correlators at finite temperature. The reliability of the *Maximum Entropy Method* in extracting quarkonia spectral functions has been investigated.

Calculations of meson spectral functions for the charm quark mass confirmed earlier results on survival of the J/ψ and η_c states in the plasma and dissolution of χ_c states. In addition, it has been found that the bottomonium χ_b state is strongly modified or possibly dissolved at unexpectedly low temperatures, $T = 1.15T_c$ (T_c being the transition temperature). We also investigated the possibility of extracting the heavy quark diffusion constant from quarkonium correlators.

A detailed calculation of heavy quark free energy in full QCD at relatively large quark masses (corresponding to pion masses of about 700 MeV) on $N_t = 4$ lattices has been performed. This allowed us to extract the running coupling constant at finite temperatures in full QCD for the first time, as well as to fully isolate the entropy contribution of the heavy quark free energy. The screening radius in full QCD was also estimated for the first time. This is a first step toward a more detailed study of this quantity in full QCD on the new QCDOC supercomputer using smaller lattice spacing (larger N_t). This can have important consequences for the quarkonium physics at finite temperature in full QCD.

We have started the investigation of the QCD phase diagram at finite temperatures using improved staggered quarks with the QCDOC supercomputer. We developed the code for molecular dynamics evolution for the so-called p4 lattice action, which largely reduces the effects of finite lattice spacing.

In addition, programs for the analysis of the lattice data were developed. We have investigated the nature of the phase transition and the corresponding transition temperature. To determine the nature of the transition calculations, different volumes have been used. We found quite unexpectedly that the nature of the deconfinement transition strongly depends on the lattice spacing even when an improved staggered fermions formulation is used.

The value of the transition temperature obtained so far, on the other hand, is compatible with earlier estimates and less sensitive to the effects of finite lattice spacing.

SPECIFIC ACCOMPLISHMENTS:

Publications

Static quark anti-quark interactions in zero and finite temperature QCD I: Heavy quark free energies, running coupling and quarkonium binding. O. Kaczmarek and F. Zantow, *Physical Review D* 71, 114510 (2005)

Static quark anti-quark interactions at zero and finite temperature QCD II: Quark anti-quark internal energy and entropy. O. Kaczmarek and F. Zantow, submitted to *Physical Review*

Presentations

Bottomonia correlators and spectral functions at zero and finite temperature. Petrov, K.; Jakovác, A.; Petreczky, P.; and Velytsky, A.; *Proceedings of Science (LAT2005)* 153

Heavy quark diffusion and lattice correlators. Petreczky, P.; Petrov, K.;

Teaney, D.; and Velytsky, A. Proceedings of Science (LAT2005) 185

Screening lengths of hot QCD. Kaczmarek, O. and Zantow, F., Proceedings of Science (LAT2005) 177

Static quark anti-quark free and internal energy in 2-flavor QCD and bound states in the QGP. Kaczmarek, O.; and Zantow, F.; Proceedings of Science (LAT2005) 192

Charmonia correlators and charm diffusion, Petreczky, P.; Petrov, K.; Teaney, D., and Velytsky, A., Quark Matter 2005, Budapest, Hungary, August 4-9, 2005

QCD Thermodynamics with an almost realistic quark mass spectrum, Schmidt, C., PANIC 2005, Particles and Nuclei International Conference, Santa Fe, New Mexico, October 24-28, 2005

LDRD FUNDING:

FY 2004	\$ 69,272
FY 2005	\$109,751
FY 2006 (budgeted)	\$ 37,000

Very Long Baseline Neutrino Oscillations Experiment

Milind V. Diwan

04-043

PURPOSE:

We studied in detail the physics capabilities of a very long baseline neutrino oscillation experiment based at BNL. Preliminary engineering designs and costs were also studied. We have a good understanding of how well such a facility will perform for the following goals: precise determination of the oscillation parameters Δm^2_{32} and $\sin^2(2\theta_{23})$ in ν_μ disappearance mode, detection of $\nu_\mu \rightarrow \nu$ appearance, sensitivity to $\sin^2(2\theta_{13})$, measurement of Δm^2_{21} and $\sin^2(2\theta_{12})$ in appearance mode (independent on the value of θ_{13}), verification of matter enhancement and determination of the sign of Δm^2_{32} , determination of the CP-violation parameter δ_{CP} in the neutrino sector, and confirmation of CP violation by dedicated anti- ν running. We examined the detector design to reach the required resolution and background capability. We have also optimized the neutrino beam spectrum and the length of the baseline to reach these goals. The needs of a near and far detector have been examined and a scheme to optimize the running time based on current and possible future physics understanding developed.

APPROACH:

Future neutrino oscillation experiments must be much more ambitious to precisely measure the parameters and, for the first time, observe violation of CP symmetry in the lepton sector. We recently studied the feasibility of a neutrino beam produced by an upgraded AGS sent over 2500 km to a massive underground detector. We

concluded that such an experiment could indeed achieve the above goal. In addition, the large underground detector will be the most important facility for the study of proton decay, and atmospheric, solar and supernova neutrino physics. This bold program of experiments will put BNL and the United States in a leading position in the field of neutrino physics.

Our study is in three parts: 1) The spectrum and intensity of neutrinos from the BNL AGS accelerator. The beam-related work is in collaboration with Bill Weng and others in the Collider-Accelerator Department (CAD). It includes simulations of various geometries for producing the neutrino beam. 2) The strategy for running the beam and obtaining the best possible physics results: The beam spectrum, the length of the baseline, and the capabilities of the detector are coupled in a complex way. We now understand the requirements on each so that the goals of the project can be realized, in particular the goal of measuring the CP-violation parameter. This work is carried out by both theoretical analysis (with help from Bill Marciano) and parametric simulations that attempt to approximate the detector response. 3) Simulation of detector response and detector design: Ultimately, we will need a detailed design of a large detector with mass greater than 100 kT. Brett Viren has worked with colleagues from Stony Brook University (SBU) to create a simulation program while Chiaki Yanagisawa, a collaborator from SBU, has used existing simulations of water Cherenkov detectors to understand the performance of such a detector.

TECHNICAL PROGRESS AND RESULTS:

We started by reviving software that required many changes to make these programs suitable for the current study. We

designed a new geometry for the target and horn systems to accommodate a new, longer graphite target and to produce a more energetic beam. The spectrum that resulted from this simulation was used for the detector and physics work. Better optimization and understanding of the beam spectrum is, however, still needed.

For the physics results, initial estimates were based on analytical calculations. We performed more detailed numerical calculations by adapting old simulation codes. We parameterized the detector response using published data on water Cherenkov detectors as well as estimates produced by preliminary detector simulations.

We determined that the most important requirement of these detectors was the ability to distinguish electrons from other showering background events, in particular neutral pion decays.

The most important accomplishment this year was the demonstration by simulation that the background to electron events could be controlled in a water Cherenkov detector. This work was carried out in collaboration with Stony Brook and Colorado State Universities (part of the UNO Underground Nucleon Decay and Neutrino Observatory Collaboration). Collaborators Chiaki Yanagisawa and his student, Le Phoc Trung performed the background calculation using a large sample of Super-Kamiokande atmospheric neutrino Monte Carlo events re-weighted to the BNL flux. Special software was developed that searched for extra particles besides the main electron shower in a water Cherenkov event. The pattern of the extra ring (low energy particle) was then subjected to a likelihood criteria that included the energy, angle, and quality of reconstruction as inputs. An energy dependent cut on the likelihood resulted in

reduction of the background by approximately a factor of 10 while about 0.5 of the electron signal was lost. The final performance yields a neutral current background that is roughly the same in magnitude as the irreducible beam electron neutrino background.

We need to develop reconstruction software (independent of the Superkamiokande software), the UNO Monte Carlo program and associated software framework. The UNO collaboration has chosen to focus on the problem of electron appearance background, and has formed a group dedicated to using UNO as a far detector for the BNL VLBL (Very Long Baseline). This group includes Brett Viren. Work on a vertex fitter, the initial step of the reconstruction chain, has finished and has shown that the UNO software framework is maturing. For the time being, many of the reconstruction steps, including vertex fitting, can and will be "faked" by smearing Monte Carlo truth information with very well known reconstruction resolutions. This allows the effort to be focused on pushing the state of the art in water Cherenkov reconstruction. Such improvements will be needed to assure that electron appearance background rejection levels can be achieved. This work is very computationally intensive, but is necessary for reducing the backgrounds.

SPECIFIC ACCOMPLISHMENTS:

The AGS Based Super Neutrino Beam Facility BNL-73210-2004-IR is a conceptual design and a cost estimate for the 1 MW upgrade of the AGS accelerator complex and a super neutrino beam.

Publications

Very long baseline neutrino oscillation experiments for precise measurements of mixing parameters and CP violating effects, M. V. Diwan, et al., Physical Review D 68, 012002 (2003).

Conference Proceedings

THE CASE FOR A SUPER NEUTRINO BEAM, Talk given at Heavy Quarks and Leptons 2004, San Juan, Puerto Rico, June 1 - June 5, 2004. hep-ex/0407047

Very Long Baseline Neutrino Oscillations, The BNL VLBNO concept, B. Viren, Proceedings of NuFact05, 7th International Workshop on Neutrino Factories and Superbeams, Frascati, June 21-26, 2005. hep-ex/0510018.

Spectrum from the proposed BNL very long baseline neutrino facility, S. A. Kahn and M. V. Diwan, Proceedings of 2005 Particle Accelerator Conference. Knoxville, TN, May 16-20, 2005.

Laboratory reports

THE AGS BASED SUPER NEUTRINO BEAM FACILITY (CONCEPTUAL DESIGN REPORT), W. T. Weng et al., BNL-73210-2004-IR, Oct. 1, 2004. 206 pp.

Proposals granted

SBIR, Very Large High Gain APDs for Particle Physics, Phase II, FY2005-FY2006, PI: Mike Sivertz, April 2004, DOE high energy physics, 2 yr duration.

LDRD 06-004, Detector Development for Very Long Baseline Neutrino Experiment, Grant of \$111k for FY2006.

Proposal to use the Homestake Mine in South Dakota as the site for the Deep Underground Science and Engineering Laboratory and conceptual design. NSF-05-506. PI: Kevin Lesko from LBNL. (Milind Diwan is part of the group that prepared this proposal for the National Science Foundation.)

LDRD FUNDING:

FY 2004	\$ 71,099
FY 2005	\$106,166
FY 2006 (budgeted)	\$ 36,000

Advanced ^3He Detectors for the Spallation Neutron Source

Graham C. Smith

04-046

Bo Yu

PURPOSE:

Instruments presently under construction for first operation of the Spallation Neutron Source (SNS) will, in general, require eventual upgrades to exploit fully the expected flux and capabilities of the new facility. The technical goal of this LDRD project is to investigate an innovative readout method for ^3He -based neutron detectors that possesses extremely high rate capability and accurate position determination in two-dimensions and with large solid-angle coverage. Small angle neutron scattering (SANS), in particular, is one several fields that will benefit.

APPROACH:

The highest counting rate of presently available ^3He detectors for SANS is limited to $<5 \times 10^5 \text{ n s}^{-1}$ on a $1 \times 1 \text{ m}^2$ area. The SNS foresees rate requirements of 10^8 s^{-1} , and a promising new technical approach is a detector that operates in ionization mode, with discrete pixels, or pads, read-out in parallel. This approach has potential benefits over ^3He detectors operating with some level of gas gain, particularly with respect to space-charge saturation, long-term stable performance, and electronic pulse pile-up. The innovative nature of this method includes operation in pulse mode with a gas gain of unity, a high density of readout pads, and inclusion of much of the microelectronics inside the detector gas volume. The latter feature, never before attempted, is important in this approach to ensure that channel capacitance is small enough for accurate analysis of the primary

electrons from neutron conversion. The payoff, however, is enormous: a range of geometries will be easily achievable, long-term stability would be much more likely than with existing approaches, and rate and resolution will satisfy the demanding requirements of several SNS instruments.

Collaborators are G. DeGeronimo and N. Schaknowski (BNL).

TECHNICAL PROGRESS AND RESULTS:

Using stainless-steel vacuum flanges and spacers as the gas containment vessel, a test cell comprising a 40 mm deep, parallel plate, ionization chamber has been fabricated. This is shown in figure 1. The window, removed for the picture, represents the negatively biased cathode, a field cage defines the uniform electric field in the 40 mm drift depth, and an array of thirteen pads on the anode plane are connected, through a hermetic feed-through on the rear

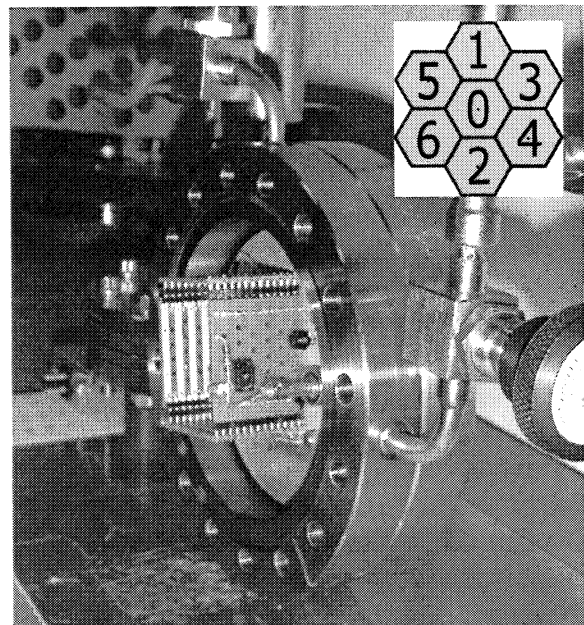


Figure 1. Picture of test cell for evaluation of ionization mode operation in two-dimensions. The stainless steel window is removed to show the field cage, at the bottom of which is a thirteen pad anode plane (inset shows numbering of middle seven pads). Total gas depth is 40mm.

flange, to preamplifiers, shaping amplifiers, and multiplexed to a pc-based ADC card. The cell is filled with 3 bar of ^3He and varying pressures of propane. The latter determines the range of the proton and triton created after neutron interaction with ^3He . Typically a mm or so, the range of these particles determines the degree of charge sharing between pads, a key element to quantify for a full-fledged instrument, and a primary goal of this project. Figure 2

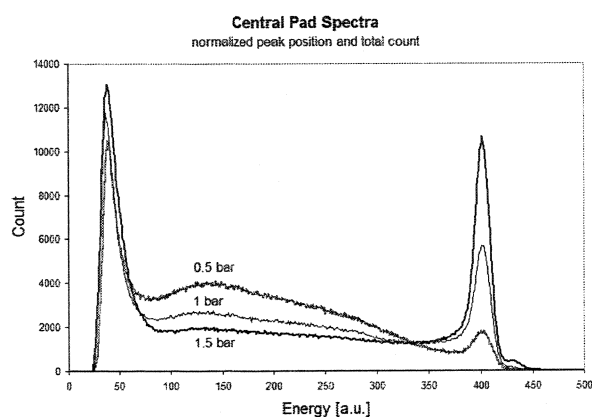


Figure 2. Pulse height distributions from central pad (#0), under uniform irradiation with thermal neutrons, at three different pressures of propane.

illustrates the pulse height spectrum from the central pad (#0 in figure 1) for three different propane pressures: at 1.5 bar, the thermal neutron peak around Ch 400, corresponding to events in which the full charge of about 30,000 electrons is collected by a single pad, dominates the spectrum, with few events, in the lower signal amplitude plateau, that share their charge among two or more pads. At 0.5 bar, the reverse occurs, i.e. most events occur in the low amplitude plateau, with very few in which all charge is collected by a single pad. This behavior is demonstrated in Figure 3, which shows pulse height correlation plots, for 0.5 bar propane, for a) events shared between two adjacent pads (#0 and #1) and b) events where the primary ionization extends to non-neighbor pads (#2 and #5). Since our goal is limit charge collection to

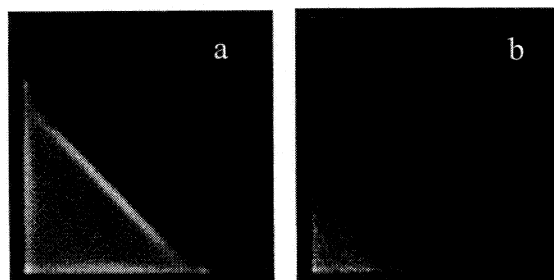


Figure 3. Correlation plots of pulse heights from a) pads #0 and #1 (adjacent pads), and b) pad #2 and #5 (next closest pair of pads), for a propane pressure of 0.5 bar.

only one, two or three adjacent pads, we require zero events of the type in figure 3(b). This occurs around a pressure of 1 bar propane, which we have established is about the optimum condition. Thus, provided the threshold level in each channel is placed at about channel 100 (figure 2) to inhibit triggers from electron induced signals on non-electron collecting pads, we have established conclusively the validity of the original concept proposed for this LDRD. The remainder of the project will focus on reading out all pads of the prototype to quantify position linearity, and operation with electronics inside the gas volume.

The results from this LDRD project are critical to future DOE BES support, and have helped place BNL's Instrumentation Division in a key role for SNS neutron detector development.

SPECIFIC ACCOMPLISHMENTS:

A contributed talk, "Two-dimensional He3 Detectors with Pad Readout for High Rates" was presented at the IEEE Nuclear Science Symposium in Puerto Rico, October 2005 and is being prepared for submission as a peer-reviewed article to Transactions on Nuclear Science.

LDRD FUNDING:

FY 2004	\$ 72,953
FY 2005	\$109,650
FY 2006 (budgeted)	\$ 37,400

Genetic NanoTags

James F. Hainfeld

04-055

PURPOSE:

Genomics and proteomics have advanced to where it is of interest to identify and characterize cellular complexes or “machines.” In order to isolate these complexes from cells for study, genetically engineered tags have been developed to bind the desired proteins to columns for purification. Unfortunately, most larger complexes do not crystallize for x-ray studies, so these are then studied by electron microscopy (EM). A difficulty exists in identifying component proteins (which protein is where?), and orienting smaller complexes, necessary for 3-D image reconstruction and solving the structure.

We propose to use the tags commonly genetic engineered into recombinant proteins for the purpose of biochemical purification to construct complementary gold labels that will bind to these tags. This could break the 500 kDa barrier for cryoEM by identifying subunits and enabling their orientation and analysis. Currently, complexes < 500 kDa are not generally solvable by cryoEM since at the low dose required, distinctive features are not perceived, and the alignment with other molecules, necessary to solve the 3-D structure, is not possible. The work we propose should make it possible for cryoEM to solve < 500 kDa protein complexes at a 10 Å resolution, which would be a significant advance for biology.

The four genetically engineered sequences investigated will be programmed into and expressed in target proteins. Gold nanoparticles will be designed that will bind to these four sequences: 1) Ni-NTA-gold

binding to 6x-His tags, 2) negatively charged gold to 6x Arg tags, 3) monomaleimido gold linked to cysteine, and 4) gold targeted to a gold-binding sequence.

This work will be applied to three important molecular machine complexes required for life: Ku70/Ku80/DNA-PK complex, human chromatin remodeling complex ACF, and the human ligase IV/Xrcc4 complex, all being currently worked on in the biology department. CryoEM single particle data will be collected in ice and reconstructions done.

This work is cogent to the DOE Genomes to Life (GTL) Initiative. The first goal of GTL is: “Identify and characterize the molecular machines of life.” NIH is investing heavily in imaging (with their new National Institute for Biomedical Imaging and Bioengineering, NIBIB) with support for cryoEM. Preliminary results from this LDRD would provide convincing evidence for follow-on funding. It would also help establish BNL as a unique cryoEM center of excellence, especially since label development is deemed highly necessary for the field. We are in a unique position to answer this need, having established both nanoparticle labeling expertise and genetic production of tagged protein complexes.

APPROACH:

The three genetically engineered sequences investigated will be programmed into and expressed in target proteins. Gold nanoparticles will be designed that will bind to four sequences: 1) Ni-NTA-gold binding to 6x-His tags, 2) negatively charged gold to 6x Arg tags, 3) maleimido gold to link to cysteine residues, and 4) gold targeted to a gold-binding sequence.

This work will be applied to two important molecular machine complexes required for life: Ku70/Ku80/DNA-PK complex, and the human ligase IV/Xrcc4 complex. CryoEM single particle data will be collected in ice and computer reconstructions done to find the three-dimensional structures.

TECHNICAL PROGRESS AND RESULTS:

Protein production and genetic engineering: several proteins in the complexes that we are to study have now been expressed in insect cells using the baculovirus method. This includes Ku70, Ku80, Xrcc4, ISWI, and the ACF chromatin remodeling complex. These have been engineered with the 6x-Histidine (His) tag and for a control, without the His tag, by substituting the Flag tag. Purification of these proteins is also underway, and various columns and buffer conditions explored to maximize yield and maintain protein integrity. Under many conditions, the proteins aggregate or do not purify well. The conditions for Ku70/Ku80, ISWI, ACF1 and the complete ACF complex have now been worked out to reasonable satisfaction. ISWI has been expressed now with a Genome Sequence Tag (GST). Additional genetic tags have now been designed and are being expressed: the Arg tag, Cysteine tag, and streptavidin tag.

Gold particle synthesis: 1.8 nm gold particles with the nitrilotriacetic acid functional ligand were synthesized. These were then charged with nickel. Binding to Ku70, Ku80, and ISWI was evaluated both by blots and column chromatography. Labeling with the gold targeted to the His tag was compared to gold binding to the same proteins without the His tags. A significant problem to overcome is that we found some binding of the gold particles to

proteins without the His tag, even though there was more binding to those with the His tag. Methods to eliminate this “non-specific” binding are being addressed, and include: high salt to reduce electrostatic binding, and use of detergents to reduce hydrophobic interactions. We found that high salt (0.3-0.5 M NaCl) was effective in reducing background by blocking charge interactions. We also found pre-reaction of the protein with N-ethylmaleimide also reduced background by blocking free thios that can interact with gold nanoparticles. Finally, a 10-20 molar excess of nickel ions was particularly useful in eliminating background binding. Changing the metal from nickel to copper, mercury, cobalt, zirconium, and gadolinium was explored to give different binding affinities. A gold cluster with glutathione attached was synthesized to bind to GST-tagged proteins. We are still trying to overcome some background binding with this approach. Larger gold nanoparticles (3-5 nm) were synthesized and functionalized since they are more visible by electron microscopy. Initial positive results of specific binding to His-tagged proteins was obtained.

Electron microscopy and image analysis: Individual proteins, Ku70/80, ISWI, ACF1 and the ACF complex were prepared for negative stain EM. Various stains were investigated. The ACF complex visualization was successful and about 7,000 particles obtained and are being processed to find the three-dimensional structure of this important protein which has never been solved. We will then label the various subunits with gold to identify their position and the architecture of the complex.

SPECIFIC ACCOMPLISHMENTS:

Follow-On Funding:

High Resolution Gold Labels for EM, J. F. Hainfeld (PI), NIH, 9/30/03 - 8/31/08, \$2,400,000 for 5 years. The gold will play a large part in this initiative.

Develop a Hybrid Electron Cryo-Tomography Scheme for High Throughput Protein Mapping in Whole Bacteria, H. Li and J. Hainfeld (co-PIs), DOE, KP1102010, BO-122, \$1,700,000 for FY 2005-2007.

FY 2005 Publication:

5 nm gold-Ni-NTA binds His tags. Reddy, V.; Lyman, E.; Hu, M.; and Hainfeld, J. F. *Microsc. Microanal.* 11 (Suppl. 2), 1118-1119 (2005).

LDRD FUNDING:

FY 2005	\$114,424
FY 2006 (budgeted)	\$ 99,000

The Use of Singular Point Genome Sequence Tags to Analyze Community Composition and Metabolic Potential

Daniel van der Lelie

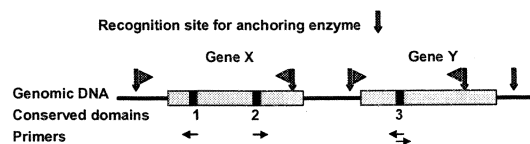
04-060

PURPOSE:

This project aims at developing a high-throughput approach to compare closely related microbial strains and to analyze microbial communities and their metabolic potential. The proposed technique is a unique spin-off of the Genome Sequence Tag (GST) technology that was recently developed and patented by BNL.

APPROACH:

Figure 1: Schematic representation of the SP-GST approach on a conserved gene domain. Only one



- Digest with anchoring enzyme
- Ligate *MmeI* linker cassette to ends
- Linear amplification with 5' biotinylated domain specific primer (→)
- Exponential amplification with *MmeI* cassette and domain specific primers
- Solid phase capture and release of tags (▶) adjacent to proximal sites for the anchoring enzyme

conserved region per gene of interest is required to generate genome signature tags. Tags (▶) can, depending on the orientation of the primer, be generated from the anchoring enzyme site located upstream or downstream of the primer annealing site. Different steps involved in generating tags are indicated in the figure. Numbers (1-3) indicate three different conserved regions located in genes X and Y.

To overcome the major limitation of the GST technology, namely the large number of tags, we used the 16S rRNA gene to develop the singular point GST technology, as it is ideal for the following reasons:

- 16S rRNA gene present in all prokaryotes.
- 16S rRNA copy number will define number of distinct GSTs per species.

- Database available with >100,000 16S rRNA gene entries.
- Tag frequencies will reflect community composition.
- Each tag will allow direct coupling with a 16S rRNA gene for species identification.

The principle of the SP-GST protocol we developed is presented in Figure 1. In addition to the 16S rRNA gene, it can be employed for any gene as long as one conserved domain is available. As anchoring enzyme we determined *Csp6I* as our best choice.

TECHNICAL PROGRESS AND RESULTS:

16S rRNA based SP-GST tags of pure strains. To investigate whether 16S SP-GST tags generated would allow us to discriminate between closely related strains of *Bacillus cereus* and *Bacillus anthracis*. As the rDNA operons of the *B. anthracis* species are nearly identical, none of the 59 chosen anchoring enzymes yielded internal or upstream SP-GST tags from 16S rDNA that distinguished between the *B. anthracis* strains Ames, Ames 0581 and Sterne. Internal 16S SP-GST tags and SARST tags also failed to discriminate between *B. cereus* and *B. anthracis* on the species level. However, *Csp6I*-based identifier tags generated upstream of the 16S rDNA clearly do distinguish between *B. cereus* and *B. anthracis* species, as well as between different *B. cereus* strains. Therefore, when comparing closely related members of the genus *Bacillus*, *Csp6I* SP-GST tags generated upstream of the 16S rDNA have better specificity than internal 16S SP-GST and SARST tags.

16S rRNA based GST tags obtained from a "simple" microbial community. A microbial community containing 4 species was used to validate the SP-GST concept and to compare it with classical molecular ecological techniques. The members of this community were *Deinococcus radiodurans* R1, whose genome

has been sequenced, *Bacillus licheniformis* B-6-4J, whose close relative ATCC 14580 was sequenced, *Pseudomonas stutzeri* strains Stanier 221 and BRW1, and *Arthrobacter globiformis* DSM 20124. *Csp6I* was chosen as the fragmenting enzyme.

Sequence analysis of the resulting library of concatenated tags demonstrated that we were successful in obtaining 16S-linked tags from all species. We accurately found the two tags adjacent to the *Csp6I* sites upstream of *D. radiodurans*' three 16S rRNA genes: GST-DR1, which is present in both sections 8 and 213 of the complete chromosome 1 sequence, and GST-DR2 from section 198 of the chromosome 1 sequence. These two *D. radiodurans* tags were present in a ratio of approximately 2:1, demonstrating that tag frequency can provide quantitative information concerning the relative abundance of the target sequence from which they were derived.

As was the case for the *D. radiodurans* R1 tags, tag frequencies for *B. licheniformis* B-6-4J reflected the relative abundances of the target sequences from which they were derived. Q-PCR showed that GST-BL3, GST-BL4 and GST-BL5 were present once in the *B. licheniformis* B-6-4J genome, while GST-BL1 and GST-BL2 were observed twice as frequently. This indicates that the *B. licheniformis* B-6-4J genome contains, like strain ATCC14580, 7 copies of its 16S rDNA. These tag frequencies were compared to that of the fully sequenced genome of *B. licheniformis* ATCC 14580 (Genbank Accession N° AE017333) and proved that these two species had four tags in common although their frequencies differed between strains. Three copies of GST-BL2, two copies of GST-BL3, one copy of both GST-BL4 and GST-BL5 were identified in *B. licheniformis* ATCC 14580, while GST-BL1 turned out to be a tag unique to *B. licheniformis* B-6-4J.

Tag frequencies for *P. stutzeri* also reflected the relative abundances of the target sequences from which they were derived. Q-PCR showed that GST-PS2, GST-PS3 and GST-PS4 were present once in the *P. stutzeri* genome, whilst GST-PS1 was observed twice as frequently. These data were consistent for both *P. stutzeri* Stanier 221 and BRW1 and indicate that both *P. stutzeri* strains contain five copies of the 16S rDNAs, one more than previously found for this species. SP-GST tag distributions in *A. globiformis* suggested that this species has 3 copies of a 16S rRNA gene with 2 copies of GST-AG1 and a single copy of GST-AG2. Tags for *A. globiformis* DSM 20124 may possibly have been harder to obtain due to this species high genomic GC content. Due to the small number of tags recovered from this species, SP-GST was specifically carried out on *A. globiformis* DNA to determine if these results were accurate. Two additional tags were discovered belonging to this species which were linked to two additional copies of the 16S rRNA gene. Q-PCR on *A. globiformis* DSM 20124 confirmed that GST-AG1 was present twice as frequently on the genome as GST-AG2. Q-PCR further suggested that *A. globiformis* DSM 20124 has a total of 15 copies of its 16S rDNA, 8 of which were linked to GST-AG1, 4 to GST-AG2, 2 to GST-AG3 and 1 to GST-AG4.

SPECIFIC ACCOMPLISHMENTS:

The SP-GST concept on the 16S rRNA gene was part of a patent application entitled "Genome Signature Tags."

The GST technology will also be applied in the following DOE funded project: Composition of Microbial Communities Used for *In Situ* Radionuclide Immobilization: Natural Gene Transfer to Develop Resistance to Metal Toxicity. J. Fitts and D. van der Lelie (PIs), NABIR – DOE/BER, \$900,000, FY 2005-2007.

Publications:

The application and molecular tools to follow up bioremediation. Geets, J.; Vangronsveld, J.; Diels, L.; and van der Lelie, D. J. Soil Sediments 3, 251 (2003).

Molecular monitoring of SRB community structure and dynamics in batch experiments to examine the applicability of *in situ* precipitation of heavy metals for groundwater remediation. Geets, J.; Borremans, B.; Vangronsveld, J.; Diels, L.; and van der Lelie, D. J. Soil Sediments 5, 149-163 (2005).

Factors influencing the composition of bacterial communities found at abandoned copper-tailings dumps. De la Iglesia, R.; Castro, D.; Ginocchio, R.; van der Lelie, D.; and González, B. J. Appl. Microbiol. (in press).

Column experiments to assess the effects of electron donors on the efficiency of *in situ* precipitation of Zn, Cd, Co and Ni in contaminated groundwater applying the biological sulfate removal technology. Geets, J.; Vanbroekhoven, K.; Borremans, B.; Vangronsveld, J.; Diels, L.; and van der Lelie, D. Environ. Sci. & Pollut. Res. (in press).

Single point genome signature tagging (SP-GST), a general simplified tagging method for microbial genome surveys. van der Lelie, D.; McCorkle, S.; Lesaulnier, C.; Geets, J.; Taghavi, S.; and Dunn, J. Appl. Environ. Microbiol. (under revision).

LDRD FUNDING:

FY 2005	\$185,509
FY 2006 (budgeted)	\$ 63,000

3-D Electronic Wave Functions from EM Images

Joseph S Wall
Y. Zhu

04-061

PURPOSE:

Presently available detectors in the Scanning Transmission Electron Microscope (STEM) record only a small fraction of the available information. We have designed a new detector to record over 1000 signals simultaneously, instead of the present 3. We are using image simulation to understand how to combine these signals in order to determine atom locations and charge distribution in the specimen. The TEAM Project (Transmission Electron Aberration-corrected Microscope) is a major DOE/BES effort to improve the resolution of both conventional and STEM instruments. Development of better detectors is an important aspect of that project and our efforts, if successful, should enhance BNL's position to obtain the second TEAM Instrument (the first is already committed to Lawrence Berkeley National Lab).

APPROACH:

STEM makes an image by scanning a finely focused probe over a thin specimen while recording the number of electrons deflected as a result of striking atoms in the object. The scan is a TV-type raster and all signals are stored and displayed digitally. The 3 signals recorded currently give a quantitative map of the mass distribution, and this is the basis of our BNL STEM user facility with over 50 active projects.

The three signals presently used are obtained by integration over annular regions of the detector plane using scintillators and photomultipliers to give quantum detection

efficiency. Large-angle and small-angle scattering detectors give dark-field images proportional to the mass of atoms in the path of the beam. These signals are useful for quantitative microscopy and imaging of atom columns in thin specimens. As valuable as this information is, it is only a small fraction of what could be used.

The new approach supported by this LDRD is to utilize the additional information present in the detector plane, which is now discarded. The actual intensity distribution consists of three components: 1) a convergent beam electron diffraction (CBED) pattern outside the disc of the transmitted beam giving information about the 3-D spatial arrangement of atoms within the probe, 2) an in-line hologram within the disc of the transmitted beam and 3) lateral displacement of the central beam disc due to electric or magnetic fields within the area probed by the beam.

We have adapted image-simulation software to study: 1) information available, 2) detector properties needed to record it, 3) methods to extract specimen information, and 4) results to be expected on scientifically interesting specimens. The software uses the multi-slice method to accurately simulate propagation of an electron wave through a specimen containing up to 10^6 atoms, as well as the wave optics of image formation. This allows simulated imaging of all atoms in a 25 nm cube. Objects can be any known structure and can be placed on an amorphous or crystalline support and embedded in an amorphous or crystalline matrix.

In a previous LDRD we designed a high-resistivity Si detector with 32x32 elements, high detection efficiency and high speed, suitable for STEM use. The first manifestation fabricated in the Instrumentation Division had a serious

defect. The second attempt was not perfect, but appears adequate to demonstrate the utility of the approach. Testing on STEM revealed a problem with the electronics, which is being corrected by the Instrumentation Division. This prototype will play a key role in future applications of the TEAM instruments and strengthen BNL's case for hosting the second TEAM instrument.

To test our approach, we have selected two specimens of interest to the NanoScience community and available at BNL: 1.4 nm diameter gold particles (catalysts) and nanotubes.

TECHNICAL PROGRESS AND RESULTS:

To aid in this project, we recruited a postdoc, Xiadong Tao. His tasks were to critique previous work in this area, work on reconstruction algorithms, and aid in data analysis. Unfortunately, he left for a permanent position elsewhere in July 2005. Steve Volkov, a postdoc in Y. Zhu's group, took his place, but with some loss of continuity.

The high-risk component is the attempt to retrieve asymmetric electronic charge distributions as well as atomic coordinates for ordered and "amorphous" objects.

Thus far, we improved the simulation program and generated simulated data for gold particles and nanotubes. This data is free of practical limitations (such as vibration, finite dose, radiation damage, etc.) and is being used to test reconstruction algorithms.

Tao repeated work by Cowley, adapting and revising a standard algorithm. However, simulation shows this method doesn't work

for "unknown" crystals and amorphous materials.

Tao found that the idea of oversampling could be used to solve the reconstruction problem for "in-line" holography for STEM.

John Rodenburg's early research suggested that the complex potential (projection) of any object could be retrieved from collecting and analyzing a series of CBED patterns. This technique is called "Ptychography." Tao wrote a program to test this idea.

Tao also proposed to use the new Complementary Metal Oxide Semiconductor (CMOS) detector to characterize magnetic materials. This method will be an extension of the Differential Phase Contrast Technique. Through measuring and mapping the shift of the central beam (or one reflection) through using the new CMOS detector, we can map the magnetic field in one magnetic structure. Quantitative comparison can be made between this method, other standard techniques and holography.

In the remainder of the LDRD we expect to test the version 2 STEM CBED detector in STEM1 in Biology and produce real data for comparison to the simulations. We will investigate the effect of charged atoms and asymmetrical charge distributions in simulation and reality. We will define the extent to which we can extract 3-D atomic positions and charge distributions from data acquired with the STEM CBED detector and the increase in value of the data relative to that available with the standard integrating annular detector.

SPECIFIC ACCOMPLISHMENTS:

Microscopy Society of America Meeting, Honolulu, Hawaii, Aug. 2-5, 2005

“Coherent Scattering in the STEM,” J. S. Wall (poster)

“Direct Detectors of Electrons for STEM and TEM,” P. Rehak, J. S. Wall, Y. Zhu (platform)

“An Alternative Explanation for Diffractive Imaging Technique,” X. Tao, J. S. Wall, Y. Zhu (poster)

“Using Iteration Algorithm to Solve the Twin Image Problem for Shadow Imaging,” X. Tao, J. S. Wall, Y. Zhu (poster)

LDRD FUNDING:

FY 2004	\$ 98,945
FY 2005	\$149,814
FY 2006 (budgeted)	\$ 51,000

Functional MRI Studies in Rats Using Implanted Brain Electrodes

Andrew Gifford

04-062

PURPOSE:

The overall goal has been to determine the feasibility of using the animal MRI to identify regions of the brain that become activated by direct stimulation of the brain via an implanted electrode. These experiments are performed on anesthetized rats. Using the implanted electrode it is possible to activate very localized areas or specific fiber tracts in the brain to determine their effects on other regions of the brain to which they are connected. Having developed this new approach to functional brain mapping, we have been using it to address specific issues that remain unresolved in the neurobiology field. For example, a question we are currently investigating is to determine the effect of neuronal activity in the striatum on functional activity in the substantia nigra, a brain region that receives direct neuronal input from this area.

The implications of a successful completion of this project in terms of the BNL institutional strategy will be the development of a new and relatively powerful approach to using the animal MRI (and PET) instrumentation at BNL to perform functional brain imaging experiments in rodent models.

APPROACH:

The previous fMRI studies performed in rats and mice have mostly involved mapping the changes in fMRI signals in the sensory cortex of the brain produced by sensory

stimulation, such as pain signals or olfactory signals, in the anesthetized animal.

Although these studies have been valuable in examining the fMRI response in the sensory cortex, they have been of little value in examining neuronal activity outside of this region. In our approach we have been using an electrode implanted in the brain of the animal to provide direct and selective focal activation of regions outside of this one area. Our studies to date have focused on electrical stimulation in the striatum and motor cortex, since the anatomical connections of these regions to other brain areas is well documented and of significant clinical importance. Also, together with the MRI studies, we have been using ^{18}F -fluorodeoxyglucose (FDG) and *ex vivo* autoradiography to verify activation of the brain tissue by electrical stimulation via the implanted electrode.

Since this is a new approach to producing brain activation for rodent MRI studies, there are significant technical obstacles and risks inherent in the project. Amongst these are the potential susceptibility artifact created by the electrode on the region of the brain being imaged and the possibility of an effect of the passage of current through the electrode in degrading the MRI signal.

The electrode development and surgeries have been performed by Dr. Jasbeer Dhawan (senior research associate). Dr. Congwu Du and her student assisted us with setting up the MRI imaging.

TECHNICAL PROGRESS:

Over the past year we made progress on a primary goal of the project, which was the development of an electrode suitable for electrically stimulating the brain whilst the animal is in the magnet. Our specific

progress (and difficulties encountered) is as follows:

Required changes to the electrode design. Development of an electrode that can both pass sufficient current to activate the surrounding brain tissue and have a sufficiently low susceptibility artifact not to affect the image quality in the MRI has been the major part of our efforts to date on this project. Our initial electrode design, developed in FY 2004 as part of this LDRD, consisted of a central carbon fiber surrounded by a thin walled polyamide tube for insulation. However, in studies on phantoms conducted earlier this year, it became apparent that this electrode would not be suitable for the fMRI studies without modification. Thus, although the electrode showed a low susceptibility artifact and good passage of current, a totally new and unexpected problem encountered was that the tip of the electrode appeared to be moving in the magnetic field. This is presumably a result of the force generated by the current pulses passing through it interacting with the strong static magnetic field of the magnet. Although this movement was small any movement of the electrode in the brain is undesirable since it may cause hemorrhaging and injury to the surrounding tissue.

New electrode design: To solve the problem of bending the electrode whilst in the MRI, we have constructed and tested a wide variety of new electrode designs. The design we have found most suitable continues to employ a central carbon fiber surrounded by thin-walled polyamide tubing. However, in order to provide increased structural strength to the electrode but without introducing an increased susceptibility artifact, the carbon fiber is coated with a viscous protein solution as it is threaded through the polyamide tubing. The

protein is then cross-linked using a chemical fixative to make it rigid. Our tests so far indicate that this electrode has the required properties for conducting electrical stimulation of the brain in the MRI.

Electrical stimulation parameters: In parallel with the construction of new electrode designs, we have conducted trials on the ability of the electrodes to activate the surrounding brain tissue. We have conducted these trials using FDG to measure brain activation due to the limited availability of time on the MRI itself and due to the fact that FDG is readily available via the PET program at BNL. However, although initially intended as a way to test our electrodes and stimulation parameters, these experiments have proved to be of value in their own right by producing a map of brain activation following stimulation with the implanted electrodes that can be compared to the fMRI signal.

Objectives for FY2006: Employ the new electrode design to obtain electrical stimulation in the brain without potential tissue damage resulting from movement of the electrode.

This project involves animal vertebrates

SPECIFIC ACCOMPLISHMENTS:

Presentations: Mapping functional neural pathways in the rat brain using intracranial electrical stimulation. Dhawan, J.; Kanderappa, S.; and Gifford, A.N. Society for Neuroscience 35th Annual Meeting. Washington DC, Nov 12-16, 2005.

LDRD FUNDING:

FY 2004	\$ 78,466
FY 2005	\$119,912
FY 2006 (budgeted)	\$ 41,000

Optimizing Functional Neuroimaging Techniques to Study Brain Function in Health and Disease States

Rita Z. Goldstein

04-063

PURPOSE:

The optimal study of functioning human brain circuits would reveal both the location and progression of the neural activities underlying mental processes. We combine simultaneously the high spatial resolution of functional magnetic resonance imaging (fMRI) with the high temporal resolution of event-related potential (ERP) brainwave analyses. This project brings a highly innovative technique (performed in fewer than five centers around the world) to BNL for development as a high-resolution spatiotemporal functional neuroimaging for the assessment of cognitive-behavioral (e.g., sustained attention, working memory, inhibitory control) and emotional (e.g., salience/reward attribution) brain functions in addiction and other medical science research. Our goal is to further the central role of the *Brookhaven Center for Translational Neuroimaging* as a multidisciplinary international center for neuroscience research and education.

APPROACH:

A combination of the complementary fMRI and ERP techniques is a very attractive aim in neuroscience, and a number of research groups have taken up the challenge.

Goldman et al. (*UCLA Brain Mapping Center*) developed a method for acquiring simultaneous electroencephalography (EEG) and fMRI by combining analog preprocessing and digital post-processing to strongly suppress common artifacts. Their group implemented a functional scan protocol that yields windows of artifact-free EEG between

short gradient and radio frequency bursts during functional scanning.

Bonmassar et al. (*NMR Center at Massachusetts General Hospital*) recorded sensory ERPs using interleaved EEG and fMRI techniques. Although ERP amplitudes are much smaller than the raw EEG, their group demonstrated the feasibility of recording even small exogenous ERP components.

Kruggel et al. (*Max-Planck Institute of Cognitive Neuroscience*) has conducted combined ERP-fMRI experiments under cognitive stimulation using a 3 T MR scanner. Their group has studied later endogenous processes including Gestalt perception and target processing.

Other groups in the United Kingdom (Lemieux et al., *Wellcome Department of Cognitive Neurology*; Allen et al., *National Hospital for Neurology and Neurosurgery*) reported on the basic science and clinical utility of the EEG/fMRI combination for localization of the generators of interictal epileptiform discharges.

Our laboratory has developed a response inhibition paradigm for examining reward processing and motivation in both fMRI and ERP environments. We have recorded control subjects as they performed the task during separate fMRI and ERP sessions. Amplitudes of the cognitive P300 ERP component were significantly larger in monetarily motivating conditions, and corresponded with subjective ratings of interest and excitement about the task. During fMRI in controls and cocaine addicts the task produced a distinct pattern of activation in the orbitofrontal cortex of cocaine addicts that mirrored subjective reports showing deficits in reward processing. We expected to find similar reward processing deficits in cocaine addicts under our ERP paradigm, as reflected by P300 amplitude and self-report measures.

TECHNICAL PROGRESS AND RESULTS:

During 2004 the hardware and software components required to acquire and analyze human cognitive ERPs were identified and acquired. After consideration of several state-of-the-art alternatives - which included extended discussions, site visits to the fMRI centers at Yale University and Massachusetts General Hospital and an invited presentation by Giorgio Bonmasser here at BNL - a leading commercial ERP system from NeuroScan was ultimately selected. Modifications of the existing research protocol (#328) to incorporate ERP testing were completed and have been approved by the BNL IRB.

Since the last progress report, the NeuroScan system has been installed for independent use outside the fMRI environment to begin operator training and for the development of cognitive tasks that will be used during simultaneous fMRI/ERP recordings. Indeed, novel task development has been initiated and in a short time has produced 3 new tasks: the drug Stroop, threat Stroop, and the punishment Stroop. Further, ERP data was collected for 16 cocaine-addicted subjects (of the planned 20) and 5 healthy controls. We have also participated in preparing an R01 grant together with Giorgio Bonmassar, a simultaneous ERP-fMRI expert at MGH, and pending final system modifications, we are about to purchase Dr. Bonmassar's unique system. Specifically, we are interested in taking advantage of the open software source written mostly in high-level language (Labview) and the open hardware schematics by customizing the system to our internal needs.

We are further very excited about the fact that the current development of the MRI-compatible EEG system will enable us to use the planned 128 Channel System for even higher resolution EEG recordings. This future system will include a 128 Channel InkCap that will allow for safe EEG/MRI recordings

at this highest spatio-temporal resolution. We think these current and future systems will become leaders in the cognitive neuroscience market, as currently other available systems have not proved sufficiently reliable for our research purposes.

By using this advanced system, we anticipate becoming one of the leading sites around the world to apply simultaneous EEG-fMRI recordings to clinical research. This integration of the EEG data with anatomical and functional MR images is essential for advancing our cognitive neuroscience studies by including highly accurate sampling of the scalp recorded electric field. Specifically, the EEG/fMRI multimodality will enable us to perform experiments where the number of stimuli is limited and where consequently it is impossible to repeat the same experiment with the same subject using the two modalities separately. Studies of the effect of sleep deprivation or pharmacological intervention (e.g., methylphenidate) on long-term priming or learning are a prime example. Furthermore, scanner noise in the MRI environment (mostly during EPI) can influence the timing and amplitude of ERPs making the separate measurements incongruent.

This project involves human subjects.

SPECIFIC ACCOMPLISHMENTS:

Presented in a symposium on "Inhibitory Control in fMRI Studies: Application of Basic Cognitive-Behavioral Research to the Study of Psychopathology;" Organization for Human Brain Mapping 2005, Toronto, Canada.

Invited talk for a NIDA/APA-sponsored symposium for the APA Annual Meeting in Washington DC on "Neurobiological Aspects of Drug Addiction: Implications for Treatment" (8/05).

Other invited talks: 12/04 "Imaging the Addicted Human Brain," in the International Conference on Counseling and Treating People of Color, Bermuda; 12/04 "Neuropsychological tools to imaging cocaine addiction and aggression," The Joseph Sagol Neuroscience Center,

Sheba Health Center, Ramat Gan, Israel; 04/05 "The emotional reward-related mechanisms that bias behavioral control in cocaine addiction," Department of Psychology, New York University, Memory and Brain series, Cognitive Neuroscience Journal Club; 05/05 "Functional Neuroimaging of Human Cocaine Addiction," the fifth Italian Society on Addiction conference, on "Addiction in Medicine and Society," Bari, Italy; 12/05 "The prefrontal cortex in the I-RISA syndrome of drug addiction," Dept. of Psychology, Beer Sheva University, Emotion symposium.

09/05 As collaborator, PI is part of a funded R01 from NIDA, D. Samaras of Stony Brook PI, for applying novel machine learning techniques to analyze multimodal data sets. An additional R01 with G. Bonmassar as PI, was recently submitted for concurrent EEG and fMRI studies of human brain activity.

Publications

- **Goldstein, R.Z.**; Leskovjan, A.C.; Hoff, A.L.; Hitzemann, R.; Bashan, F.; Khalsa, S.S.; Wang, G.-J.; Fowler, J.S.; Volkow, N.D. (2004). Severity of neuro-psychological impairment in drug addiction: association with metabolism in the brain reward circuit. *Neuropsychologia*, 42, 1447-1458. *The 5th most heavily downloaded articles from the journal, 7/05.*
- **Goldstein, R.Z.**; Alia-Klein, N.; Leskovjan, A.C.; Fowler, J.S.; Wang, G.-J.; Gur, R.C.; Hitzemann, R.; Volkow, N.D. (2005). Anger and depression in cocaine addiction: association with the orbitofrontal cortex. *Psychiatry Res: Neuroimaging*, 138, 13-22.
- Alia-Klein, N.; O'Rourke, T.; **Goldstein, R.Z.**; Malaspina, D. Insight into illness and adherence to psychotropic medications predict violence severity in a forensic sample. *Aggressive Behavior*, *accepted*.

REFEREED FULL-LENGTH PROCEEDINGS

- Zhang, L.; Samaras, D.; Volkow, N.D.; **Goldstein, R.Z.** Machine Learning for Clinical Diagnosis from Functional Magnetic Resonance Imaging (#169). In *IEEE Proc. of Computer Vision and Pattern Recognition*, I:1211-1217, 2005.
- Zhang, L.; Samaras, D.; Tomasi, D.; Alia-Klein, N.; Cottone, L.A.; Leskovjan, L.C.; Volkow, N.D.; **Goldstein, R.Z.** Exploiting Temporal Information in Functional Magnetic Resonance Imaging Brain Data. *Medical Image Computing and Computer Assisted Intervention*, *accepted*.
- Zhang, L.; Samaras, D.; Alia-Klein, N.; Volkow, N.D.; **Goldstein, R.Z.** Modeling Neuronal

Interactivity using Dynamic Bayesian Networks. Neural Information Processing Systems Conference, *accepted*.

SUBMITTED MANUSCRIPTS

- **Goldstein, R.Z.**; Tomasi, D.; Cottone, L.A.; Zhang, L.; Leskovjan, A.L.; Alia-Klein, N.; Telang, F.; Caparelli, E.C.; Chang, L.; Ernst, T.; Samaras, D.; Squires, N.K.; and Volkow, N.D. Loss of sensitivity to relative value of money in cocaine abusers is associated with disrupted activity in lateral orbitofrontal cortex. *NeuroImage*, *under review after revision*.
- **Goldstein, R.Z.**; Alia-Klein, N.; Tomasi, D.; Cottone, L.A.; Zhang, L.; Maloney, T.; Telang, F.; Caparelli, E.C.; and Volkow, N.D. Decreased prefrontal cortical sensitivity to monetary reward in cocaine addiction is associated with impaired motivation and self-control. *American Journal of Psychiatry*, *final decision pending*.
- Volkow, N.D.; Wang, G.-J.; Begleiter, H.; Porjesz, B.; Fowler, J.S.; Telang, F.; Ma, Y.; Wong, C.; Logan, J.; **Goldstein, R.Z.**; Thanos, P.K.; Alexoff, D. High Dopamine D2 Receptors in Unaffected Members of Alcoholic Families: Possible Protective Factors. *Archives of General Psychiatry*, *under review*.
- Alia-Klein, N.; **Goldstein, R.Z.**; Tomasi, D.; Zhang, L.; Telang, F.; Wang, G.-J.; Fowler, J.S.; Volkow, N.D. Role of the orbitofrontal cortex in valence attribution to "No!" and emotional control. *NeuroImage*, *submitted*.
- Tomasi, D.; **Goldstein, R.Z.**; Telang, F.; Maloney, T.; Caparelli, E.C.; Volkow, N.D. Cocaine abusers have abnormal brain response during working memory tasks. *PNAS*, *submitted*.
- **Goldstein, R.Z.**; Tomasi, D.; Rajaram, S.; Cottone, L.A.; Zhang, L.; Maloney, T.; Telang, F.; Alia-Klein, N.; and Volkow, N.D. Role of the anterior cingulate in negative valence attribution and accuracy on a drug Stroop in crack/cocaine addiction. *Journal of Neuroscience*, *submitted*.

BOOK CHAPTERS

- **Goldstein, R.Z.**; Alia-Klein, N.; Cottone, L.A.; Volkow, N.D. (2005). Addiction and the Orbitofrontal Cortex. In D Zald & S Rauch (Eds.), *The Orbitofrontal Cortex*. Oxford University Press, *in press*.
- Volkow, N.D.; Wang, G.-J.; Fowler, J.S.; **Goldstein, R.Z.** Imaging the Addicted Brain. In: *The Cellular Biology of Addiction*. Cold Spring Harbor Press. *in press*.

CONFERENCE ORAL PRESENTATIONS

- **Goldstein, R.Z.** "The Lateral Orbitofrontal Cortex and Inhibitory Control in Cocaine Addiction." Human Brain Mapping 2005, Toronto, Canada, June 2005.
- J. S. Fowler, N. Klein, A. Kriplani, J. Logan, I. W. Craig, F. Telang, R. **Goldstein**, N. D. Volkow, G.-J. Wang. Brain MAO A Activity and MAO A Genotype in Healthy Male Subjects. Society of Nuclear Medicine, Annual Meeting, Toronto, Canada, June 2005.
- G.-J. Wang, N. Alia-Klein, F. Telang, Y. Ma, M. Jayne, W. Zhu, R. Z. **Goldstein**, N. D. Volkow, J. S. Fowler. Brain metabolic response to violent video presentation. Society of Nuclear Medicine, Annual Meeting, Toronto, Canada, June 2005.
- **Goldstein, R.Z.** "Neuropsychological impairment in drug addiction and its association with prefrontal cortical activity." A NIDA/APA-sponsored symposium for the American Psychological Association Annual Meeting in Washington DC on ""Neurobiological Aspects of Drug Addiction: Implications for Treatment," August 2005.

CONFERENCE POSTER PRESENTATIONS

- Alia-Klein, N.; **Goldstein, R.Z.**; Tomasi, D.; Zhang, L.; Cottone, L.; Fowler, J.; Wang, G.-J.; Volkow, N.D. Role of Genotype in Cingulate Function and Inhibitory Control: a Functional Magnetic Resonance Imaging (fMRI) Study. Cognitive Neuroscience Society, Annual Meeting, New York, NY, April 2005; in Journal of CN, 33-34 Suppl.
- Leskovjan, A.C.; Tomasi, D.; Zhang, L.; Cottone, L.A.; Telang, F.; Caparelli, E.C.; Samaras, D.; Chang, L.; Ernst, T.; Volkow, N.D.; and **Goldstein, R.Z.** Modulation of neural response in the prefrontal cortex and cerebellum by monetary reward and instrumental response on a GO/NO-GO task. Cognitive Neuroscience Society, Annual Meeting, New York, NY, April 2005. in Journal of CN, 36 Suppl.
- Delosh, D.; Leskovjan, A.C.; Cottone, L.A.; Alia-Klein, N.; and **Goldstein, R.Z.** Cocaine Addiction is associated with impaired learning on the Wisconsin Card Sort Task: findings in high functioning individuals. Cognitive Neuroscience Society, Annual Meeting, New York, NY, April 2005. in Journal of CN, 226 Suppl.
- Tomer, R.; **Goldstein, R.Z.**; Wang, G.-J.; Christopher, W.; Volkow, N.D. Incentive

motivation is associated with striatal dopamine asymmetry. Cognitive Neuroscience Society, Annual Meeting, New York, NY, April 2005 in Journal of CN, 167 Suppl.

- Alia-Klein, N.; **Goldstein, R.Z.**; Tomasi, D.; Zhang, L.; Cottone, L.; Fowler, J.; Volkow, N.D.; Wang, G.-J. Increased amygdala and decreased anterior cingulate responses to a signal to stop behavior (emphatic vocalizations of the word "No!") in aggression-prone individuals. Human Brain Mapping Annual Meeting, Toronto, Canada, June 2005.
- Cottone, L.A.; Maloney, T.; Delosh, D.; Leskovjan, A.; Alia-Klein, N.; Telange F.; Squires, N.K.; Fowler, J.S.; Volkow, N.D.; **Goldstein, R.Z.** The effect of monetary reward on event-related potentials in cocaine addiction. Society for Neuroscience, Washington, 2005.
- **Goldstein, R.Z.**; Delosh, D.; Cottone, L.A.; Leskovjan, A.C.; Alia-Klein, N.; Fowler, J.S.; Wang, G.-J.; Telang, F.; Maloney, T.; and Volkow, N.D. Relationship between cognitive functioning and recent cocaine use: evidence from neuropsychological testing and urine toxicology. Society for Neuroscience, Washington, 2005.
- Zhang, L.; Samaras, D.; Alia-Klein, N.; Cottone, L.; Maloney, T.; Leskovjan, A.; Tomasi, D.; Fowler, J.; Volkow, N.D.; **Goldstein, R.Z.** Using Advanced Computational Methods to Analyze Neuroimaging Data to Diagnose Psychopathology. Society for Neuroscience, Washington, 2005.
- **Goldstein, R.Z.**; Tomasi, D.; Cottone, L.A.; Zhang, L.; Alia-Klein, N.; Maloney, T.; Telang, F.; Caparelli, E.C.; Swanson, J.M.; Volkow, N.D. Decreased Frontolimbic sensitivity to monetary reward in cocaine addiction is associated with motivation and trait control of behavior. ACNP, Hawaii, 2005.

LDRD FUNDING:

FY 2004	\$100,684
FY 2005	\$144,278
FY 2006 (budgeted)	\$ 51,000

Technological Development of a Fluorescence Probe for Optical Detection of Brain Functional Activation *in vivo*

Congwu Du

04-066

H. Benveniste

PURPOSE:

The objective of this project is to develop an optical probe that concurrently tracks blood volume, tissue oxygenation, and intracellular calcium changes in the rodent brain *in vivo*. The new optical probe will provide new modalities for future brain functional studies by measuring calcium transients from a brain surface, and will compliment other strategic and planned 'Life and Physical Science interface' initiatives in drug addiction and developmental research at BNL.

APPROACH:

Based on our previous success with calcium fluorescence studies in the whole perfused heart using the calcium indicator Rhod2, we further integrated multi-instrumentation functions including blood volume; oxygenation and intracellular calcium into a single system. Besides the implementation of the system design, we still need to characterize its systematical sensitivity because the signal gets distorted while the photons propagate through the highly scattering biological tissue. This is due to the complexity of tissue absorption, scattering and physiological interferences caused by the variation in blood volume and oxygenation of the tissue. Such interferences impose obstacles to detection of calcium transients at the cellular level (i.e., Ca^{2+}_i) because they interfere with signal-to-noise ratios and sensitivity of the calcium

indicator binding properties to calcium. Therefore, one of the aims in this LDRD project is to examine the detection sensitivity threshold by means of phantoms and animal studies. The animal studies are most important in order to demonstrate instrumental feasibility.

Milestones for FY2005 were 1) examining the systematic sensitivity of detecting brain activity by measuring the changes in blood volume, oxygenation and intracellular calcium in the living animal; 2) characterizing the intracellular localization of the calcium signal when labeling calcium by the indicator Rhod2; 3) experimentally analyzing the influence of drugs (e.g., cocaine) on brain function using this new ODF probe.

TECHNICAL PROGRESS AND RESULTS:

In vivo animal studies to examine the system sensitivity and validate instrumental feasibility of detecting the three parameters simultaneously. The transient ischemia

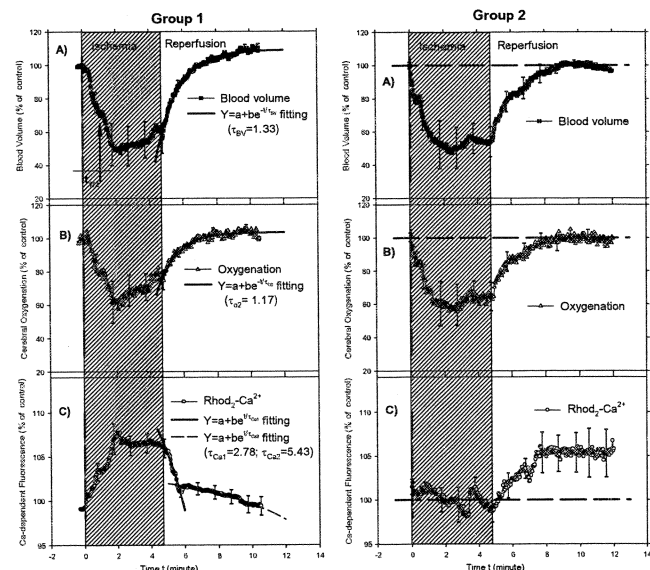


Fig. 1.: Experimental results of the changes in A) Blood volume; B) Cerebral Oxygenation; and C) Ca^{2+} -dependent fluorescence of Rhod2; obtained from the brain cortex of rat during ischemia and reperfusion. Values are mean \pm s.d. a) **Left plots** are from rat Group 1 (n=8), i.e., without Ca^{2+} blocker pretreatment before ischemia; and b) **Right plots** are Group 2 (n=4) with the Ca^{2+} blocker pretreatment before ischemia induction.

animal model was suggested by Dr. H. Benveniste to provide predictable and simultaneous changes in cerebral blood volume, oxygenation, as well as elevation of intracellular calcium to validate the techniques proposed. Fig. 1a (left graphs, Group 1) summarizes the ischemia-induced mean changes (n=8) in blood volume, cerebral oxygenation and Rhod2-Ca²⁺ fluorescence as a function of time obtained from Group 1. Our results are in agreement with previous measurements of cerebral ischemia-induced extracellular calcium changes performed by calcium-sensitive electrodes in rat brain. This demonstrates the feasibility of the Optical Diffusion and Fluorescence (ODF) system in performing measurements of the three parameters *in vivo*.

Studies in vivo and in vitro to characterize the localization of the calcium signal obtained from the cortex of the rat brain. Fig. 1b above (right plots, Group 2) shows the mean time course of blood volume, oxygenation, and Ca-fluorescence during ischemia and reperfusion obtained from the cortex of rats pre-treated with nimodipine (a Ca channel blocker) prior to the ischemic insult. There were no significant Ca-dependent fluorescence increases during the ischemic insult (Fig. 1b.C) although both blood volume (Fig.1b.A) and hemoglobin oxygenation (Fig.1b.B) display the typical ischemia changes. The nimodipine data indicates that the elevation of Ca²⁺-fluorescence is predominately due to an intracellular calcium increase and not to an activated Rhod2 leaking into the extracellular space. In addition, cryostatic frozen sections of the brain were prepared and examined using a fluorescence microscope. The fluorescence micrographs also indicate an intracellular localization of Rhod2-Ca binding (data not shown) although the exact cell type cannot be determined as yet.

Animal studies with cocaine administration has also been initiated in parallel to examine the ODF probes role in pharmacological and pathophysiological applications. The experiments are performed to detect the brain responses to a cocaine challenge in the living rat brain. The experimental results will not only validate the techniques but also be used as primary results for further grant application from other funding agents, e.g., NIH.

This project involves animal vertebrates

SPECIFIC ACCOMPLISHMENTS:

Publications:

1. Du, C.; Koretsky, A.P.; Igor, Izrailtayan; Benveniste, H. "Simultaneous detection in vivo of changes in cerebral blood volume, oxygenation and intracellular calcium during cerebral ischemia and reperfusion using diffuse reflectance and fluorescence." *J. of Cerebral Blood Flow & Metabolism*, 25, 1078-1092, (2005).
2. Luo, Z.; Benveniste, H.; Yu, M.; and Du, C. "Activation-blood flow coupling during direct somatosensory cortical stimulation in living rat brain," *Proceedings of 2nd International IEEE EMBS Conference on Neural Engineering*, 664-666, (2005).

Abstracts and Presentations:

1. Du, C.; Thanos, P.K.; Yu, M.; Rivera, S.; Koretsky, A.P.; Volkow, N.; Benveniste, H.; "Cerebrovascular and intracellular calcium effects of cocaine on brain function in the living rat," Accepted to present at Society for *Neuroscience* annual meeting, Washington, Maryland, Nov. 12-16, 2005.
2. Du, C.; Thanos, P.K.; Yu, M.; Rivera, S.; Benveniste, H.; "Optical brain monitoring of cocaine-induced cerebrovascular and intracellular calcium effects in the living rat," *International Narcotics Research*

Conference, Annapolis, Maryland, July 10-15, 2005.

3. Wolf, A.; Du, C.; Pan, Y.; Benveniste, H.; "Imaging rat brain function using calcium-sensitive fluorescent dye Rhod2," *Biomedical Engineering Society Annual Meeting*, Oct 13-17, Philadelphia, 2004.

Grant Proposal Pending:

NIH-K25 "Optical and fMRI Studies of Cocaine in the Rat Brain," 04/01/06-03/31/11, 743,000 (direct cost).

NIH-RFA "New Optical Diffusion and Fluorescence Probe for Measurement of Neural Activity," 09/01/2006-08/31/2011, \$1,274,724 (total direct cost)

LDRD FUNDING:

FY 2004	\$ 27,032
FY 2005	\$132,570
FY 2006 (budgeted)	\$104,000

Nuclear Control Room Unfiltered Air In-Leakage by Atmospheric Tracer Depletion (ATD)

Russell N. Dietz

04-069

PURPOSE:

Nuclear plants with a licensing based, in part, on low control room (CR) unfiltered air in-leakage (UI) rates (<50 cfm), needed to use a tracer approach that directly measured this value as the standard tracer approach, which determines this value by difference, often results in an unacceptably large uncertainty. The goal was to use the ATD approach at actual low in-leakage nuclear plants as the method for generating results mandated by the Nuclear Regulatory Commission (NRC). New programs, supported at BNL by specific nuclear plants for generating these NRC-required results, were a measure of the success of this project; results were reported to the NRC. There is a further mandate that such UI determinations be repeated on a tri-annual basis; once applied to a particular plant, repeat testing could be conducted less expensively by utility personnel employing ATD with BNL only performing the state-of-the-art analyses. Improved analyses would also benefit new homeland security and CO₂ sequestration tracer projects.

APPROACH:

Background. The mathematical hypothesis of this project was that the efficient removal of the ambient background concentration of certain perfluorocarbon tracers (PFTs) by the charcoal filters in a nuclear plant's dual control room emergency ventilation system (CREVS) provides the means for the direct determination of UI. At steady state (SS), CR concentrations equal to those out of the charcoal implies no UI; a slight increase in the CR concentration means a slight amount of UI. The CR concentration relative to that in normal ambient air times the rate of charcoal-filtered air provides the UI quantification. This ATD

approach had not been previously applied. The exploratory issues pertained to an assessment of the likely performance of installed charcoal systems for the nearly 100% removal of certain PFTs and the development of the sampling and analysis strategies for the successful quantification of the expected few one thousandths of the normal 5 to 10 parts per quadrillion ambient concentrations – a significant extension of the PFT technology.

Scope. **1)** Testing of commercial-grade nuclear charcoals for nearly 100% removal of PFT was needed with ASTM-type test cells & sampling apparatus. **2)** Nuclear plant charcoal filtration system tracer tent testing was to be compared to ATD testing. **3)** Accelerated depletion of PFT backgrounds in a large-volume nuclear facility required testing commercial portable charcoal-filtration units. **4)** The resulting low concentrations ($\sim 10^{-3}$ of ambient) required efficient high sampling rate systems. **5)** Such low-level analyses required enhancements to the gas chromatograph (GC) system. **6)** ATD needed testing at commercial nuclear plants.

Methods. Standard laboratory procedures were used to conduct this research – with the exception of the state-of-the-art GC system and the use of nuclear control room facilities for conducting final demonstrations of ATD.

TECHNICAL PROGRESS AND RESULTS:

FY 2004 results included: **1)** Charcoal testing that showed PFT removal efficiencies adequate for ATD – 99.90 to 99.94%. **2)** Four installed charcoal systems at an actual nuclear plant, tested for UI by ATD, and demonstrated that they perfectly tracked the traditional results. **3)** As expected, that ATD testing in nuclear plants was expedited with 1000-cfm portable charcoal systems – rapidly depleting ambient PFT concentrations. **4)** Four types of low- to high-rate (50- to 500-mL/min) adsorbent sampling tube systems and that these showed good efficiency **5)** Analyses of actual nuclear plant samples that showed quantification difficulties with critical PFT peaks and that GC enhancements improved results. **6)** The first

ATD testing, where the utility relied solely on this technique. This was conducted at two nuclear plants, one in August and the second in Sept 2004.

FY 2005 results. The modeling and interpretation of the ATD results demonstrated the ability to determine UI in the complex case of a CR inside a control building (CB) – both with their own charcoal-filtration systems; conventional tracer testing was not applicable. The replication of 2 different samplers used in the 4 elevations of Plant-1 CB was excellent:

Coincident BATS vs PAS Conc. (cts/L)			
Elevation	Sampler	15 – 19 h	19 – 21 h
2073' (80,000 ft ³)	BATS (1)	280 ± 6	219 ± 9
	PAS (3)	239 ± 11	200 ± 5
2032' (95,000 ft ³)	BATS (1)	311 ± 15	267 ± 6
	PAS (3)	278 ± 14	278 ± 20
2016' (95,000 ft ³)	BATS (1)	362 ± 9	362 ± 9
	PAS (4)	445 ± 59	445 ± 49
2000' (95,000 ft ³)	BATS (1)	446 ± 20	446 ± 12
	PAS (4)	406 ± 46	406 ± 25

Surrogate ambient PFT conc of 7700 cts/L ≡ 10.2 ppq
(surrogate PFT is the average of 3 PFTs)

Train B: not at steady state (SS), attained after 30 to 36 h

Only 1 sampler per elevation collected sequential samples to assure steady state was obtained; personal air samplers checked the concentration uniformity on the floor. The precision of these low levels (375 cts/L ≡ 0.5 ppq) was excellent. At steady state, measured levels were significantly lower – especially in the CR and out of the charcoal systems (EVSs):

Surrogate PFT Conc (cts/L) at Two Plants				
	Plant 1		Plant 2	
	Train A	Train B	Train A	Train B
CR	21 ± 1	74 ± 4	36 ± 3	17 ± 4
EVS	2 ± 1	46 ± 5	<1	<1
(net)	19 ± 1	28 ± 7	36 ± 3	17 ± 4
CB	<500	160 ± 25	599 ± 20	1094 ± 22
EVS	1 ± 1	49 ± 7	10 ± 2	21 ± 3
(net)	<500	111 ± 26	589 ± 20	1073 ± 22

Plant 1 CB Train-A test did not achieve steady state

The net CR and CB concentrations were used in the developed models to compute UI rates as shown in the next table. The plants, built as identical units but located in two different states, had the same CR rates but somewhat different CB rates. For both, UI met licensing specifications in the CRs (~10 cfm or less) and was much lower in the CBs than required (<300 cfm).

	Unfiltered In-Leakage (UI) Rates (cfm)			
	Plant 1		Plant 2	
	Train A	Train B	Train A	Train B
CR	6.9 ± 0.4	10.5 ± 2.6	10.1 ± 0.9	4.7 ± 1.1
CB	<63	14.2 ± 3.0	69.0 ± 3.4	109 ± 4

The goal of quantifying low UI rates was achieved; rates of 5 to 10 cfm were quantified with 10 to 20% uncertainty. The ATD approach will likely replace conventional tracer testing over the next year or two as the results become more widely disseminated.

Other suppliers' charcoals will be lab tested. Further efficiency evaluation of samplers at high flow rates in the presence of organic vapors from charcoals will be extracted from field measurements. Some evidence indicates that installed systems could be leaking; field data will be reviewed to see if ATD can quantify this. Results from the first two nuclear plants using ATD only were sent to the NRC this summer.

SPECIFIC ACCOMPLISHMENTS:

The most significant accomplishment was the acceptance of the ATD approach by the two nuclear plants (with their concomitant funding of \$350K) to provide testing and results to be submitted to the NRC.

LDRD FUNDING:

FY 2004	\$59,463
FY 2005	\$88,764
FY 2006 (budgeted)	\$31,000

Perfluorocarbon Tracer Sampling, Tagging and Monitoring Techniques for Use at the Urban Atmospheric Observatory

John Heiser

04-073

PURPOSE:

As part of the Department of Homeland Security (DHS) initiatives, the Urban Dispersion Program (UDP) was designed to enhance emergency response capabilities in the event of airborne releases of harmful contaminants. An essential component of UDP is conducting field studies in NYC to provide data for improving and validating atmospheric models to simulate contaminant dispersal.

Perfluorocarbon tracers (PFTs) are uniquely qualified to provide the data necessary for model validation. PFTs can be used to safely simulate behavior of contaminants under actual conditions within urban environments where it is particularly difficult to accurately predict fate and transport. This project is developing the crucial engineering hardware and methodology required to fully exploit the capabilities of PFTs to study transport of airborne contaminants in the deep urban canyons of NYC.

APPROACH:

The BNL Tracer Technology Group has done pioneering work in the development and practical use of PFTs. This expertise is being used to develop the equipment, methods, and protocols for PFT sampling and tagging in the deep urban canyon. BNL was able to design, develop, and deploy sampling and release equipment and methodologies in conjunction with the UDP NYC field studies.

TECHNICAL PROGRESS AND RESULTS:

In the spring of 2005, the initial UDP field study was conducted in Midtown Manhattan. Six PFTs were released from five locations (for QA/QC, two at one location). Two 30-minute releases occurred each day, separated by 1-½ hours of no release to allow the tracer to clear out prior to the next release. Dispersion of the tracers was determined by collecting air samples at various locations within a 400m radius. Activities focused on vertical sampling protocol and personal dose monitoring.

The vertical extent and transport time of the tracer plume was measured by placing air samplers on surrounding buildings at various heights. To achieve a better time resolution at several of these sites two samplers were co-located, with one sampler collecting 30-minute samples and the second collecting 5-minute samples. Results proved tracer transport occurred rapidly with significant levels seen in as little as 12 minutes.

During the summer of 2005 a second, larger UDP tracer study was conducted in NYC between Times Square and Central Park and bounded by 10th and 3rd Avenues. As in the first study, the Brookhaven Atmospheric Tracer Sampler (BATS) served as the primary air sampling device. Current BATS are over 25 years old and prone to failure. While the lids containing the collection tubes are still “state-of-the-art,” the operational bases are long past their prime and offer little versatility or convenience.

During FY2004 we developed a prototype of a new BATS base. This unit operated off a personal digital assistant using Embedded Visual C++ to have the functionality of the BATS logic through a graphical user interface. During FY2005 a final prototype was designed and built and included a new pumping system with variable, controlled air flow, mass flow measurement and logging,

simplified programming using a web-based interface, greater program versatility such as variable sampling intervals, and variable flow rates. The unit can be addressed via cable or through wireless communication. The PDA (personal digital assistant) was replaced with a single rugged chip.

As part of the UDP Summer '05 study, we were able to build and deploy three of the new BATS bases (Figure 1). The new BATS prototype performed flawlessly and represents a major improvement over the existing bases. The mass flow measurement and logging capability has fully addressed quality assurance concerns of the older units.

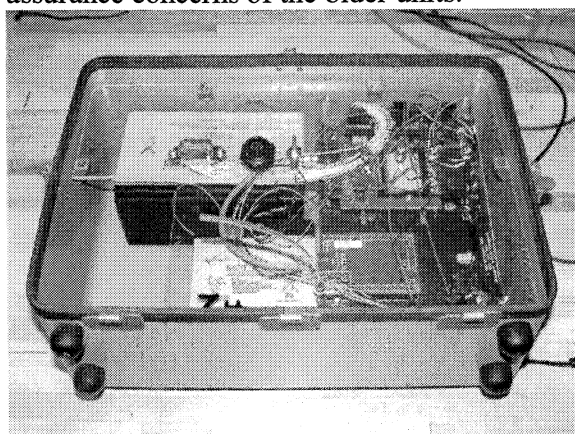


Figure 1. New Brookhaven Atmospheric Tracer Sampler base.

The Summer '05 study also required tracer release quantities considerably higher than those used in Spring '05 which precluded cylinder releases. A new release system was developed (Figure 2). The system is battery operated, low power and portable and is based on a commercially available syringe pump. The liquid PFT is dispensed onto a piece of filter paper via a battery operated, fully programmable syringe pump. The PFT wicks into the filter paper and spreads out in a thin layer. A high air flow, low power fan is used to evaporate the liquid from the filter paper. The syringe pump allows for programmed on/off times as well as highly controlled flow rates and dispense volumes. Additional QA/QC is gained by being able to weigh the syringe before and after each release. A

prototype unit was built and tested. Release rates up to 15 g/min were achieved, which was much higher than required for the 4 sq km study area used in the Summer '05 tests.

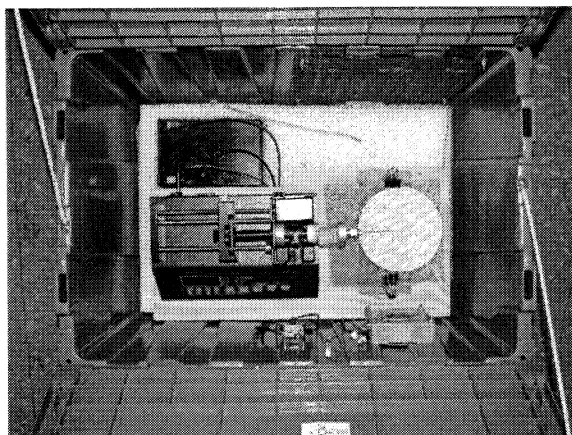


Figure 2. Syringe pump based portable Tracer Release System

For the UDP Summer '05 study six units were built (using DHS funding) and deployed. The units performed flawlessly, gave accurate, reproducible releases and were very well received by the UDP program manager and science community involved in the study.

SPECIFIC ACCOMPLISHMENTS:

Plans for the Madison Square Garden 2004 (MSG04) Tracer Experiment in Manhattan, S. Hanna, M. Reynolds, J. Heiser, and R. Bornstein, Fifth Conference on Urban Environment, American Meteorological Society, Vancouver, BC, Canada, August 2004.

T. Watson, J. Heiser, P. Kalb, R. Dietz, R. Wilke, and R. Wieser, The New York City Urban Dispersion Program March 2005 Field Study: Tracer Methods and Results, Brookhaven National Laboratory, Formal Report, July 2005.

LDRD FUNDING:

FY 2004	\$65,530
FY 2005	\$98,809
FY 2006 (budgeted)	\$34,000

Development of an Aerosol Mobility Size Spectrometer and an Aerosol Hygroscopicity Spectrometer

Jian Wang

04-079

PURPOSE:

The technical objective of this project is to develop two novel instruments. The first instrument, referred to as the Aerosol Mobility Size Spectrometer (AMSS), will be capable of measuring aerosol size distributions for the entire diameter range of 15 nm to 1000 nm within ~1 second. AMSS offers a factor of 50 improvement in time resolution over current state-of-the-art research instruments. The second proposed system, referred to as the Aerosol Hygroscopicity and Volatility Spectrometer (AHVS), will be capable of measuring size-resolved aerosol hygroscopicity and volatility over the diameter range 15 nm to 600 nm within ~2 minutes. Both instruments will significantly improve our ability to characterize atmospheric aerosol properties and to study the evolution of aerosols (e.g. size distribution, hygroscopicity, and chemical compositions) as they are transported downwind of their sources.

APPROACH:

The current incomplete understanding of atmospheric aerosol properties and their controlling processes necessitates further intensive field projects involving aircraft-based measurements. As a result of slow measurement speed of current techniques, accurate measurements of aerosols with high spatial variation, such as aerosols in the vicinity of clouds or inside a pollution plume, are not possible onboard research

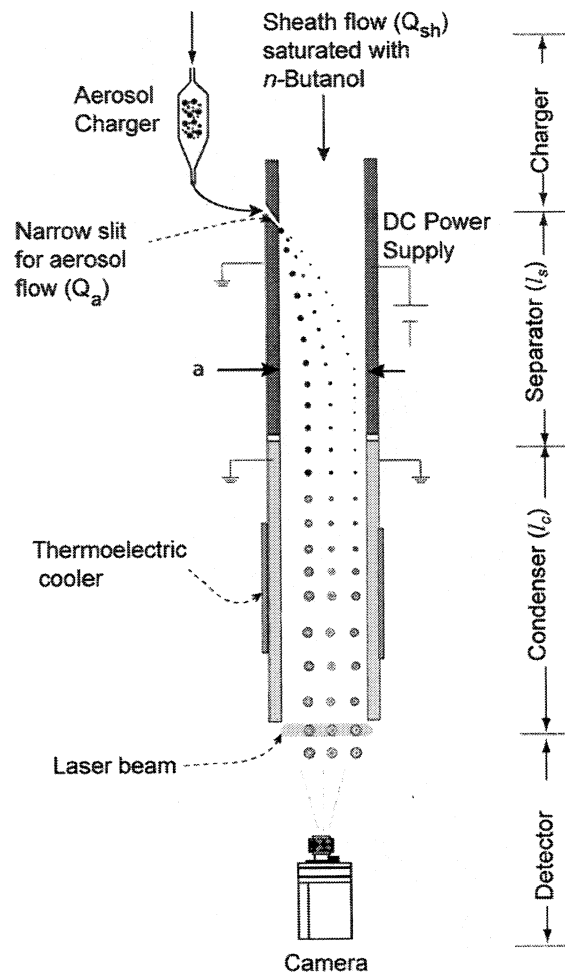


Figure 1. Schematic of the Aerosol Mobility Size Spectrometer (AMSS).

aircraft. The proposed AMSS addresses the issue of measurement speed by measuring charged particles of different sizes simultaneously. Figure 1 shows the schematic of the proposed AMSS, which consists of four major sections. Aerosol samples are first charged in a bipolar aerosol charger. The charged aerosol particles then enter a separator through a narrow slit. Particle-free sheath flow saturated with n-butanol is introduced into the separator from its top as shown in Figure 1. A constant electric field perpendicular to the flow direction is established inside the separator by applying a high voltage to one side of the chamber and grounding the other side.

Under the influence of this electric field, the charged particles are separated into different flow streams/locations according to their mobilities (sizes). The separated particles then enter a subsequent condenser. As no electrical field is applied in the condenser, the positions of the particles in the direction of electric field remain unchanged after particles exit the separator. Inside the condenser, the cooling of the flow generates a high supersaturation of butanol that activates particles as small as 5 nm in diameter. After aerosol particles grow into supermicron droplets, they are detected by an imaging system. A laser beam is collimated into a sheet of light, which illuminates the particles as they cross. The images of particles are recorded by a high-speed CCD camera. Recorded particle images provide both the size dependent position and the concentration of particles, which are then used to derive aerosol size distributions.

Dr. Pramod Kulkarni and Dr. Peter Takacs participated in this project.

TECHNICAL PROGRESS AND RESULTS:

During FY05, we constructed a prototype AMSS basing it on the theoretical analyses and simulations. The performance of the prototype AMSS, including the sizing accuracy, counting efficiency, and mobility resolution have been characterized in detail. In our characterization experiments we used a differential mobility analyzer (DMA) to generate monodisperse aerosols of desired sizes, which were then simultaneously measured by the prototype AMSS and a commercial Condensation Particle Counter (CPC, TSI Inc., model 3760). Figure 2(a) shows that the particle sizes measured by the AMSS agree well with the DMA classified sizes over a wide size range, which indicates the AMSS is capable of measuring particle

size with high accuracy. Figure 2(b) compares the simultaneous measurements of the particle concentrations by the AMSS and the CPC. When particle diameter was greater than 15 nm, close agreements were found between the two measured concentrations, which suggest the AMSS has a counting efficiency of nearly 100% for particles larger than 15 nm. For particles smaller than 15 nm, the particle concentrations measured by the AMSS were higher than those measured by the CPC, indicating even higher counting efficiencies of the AMSS for small particles.

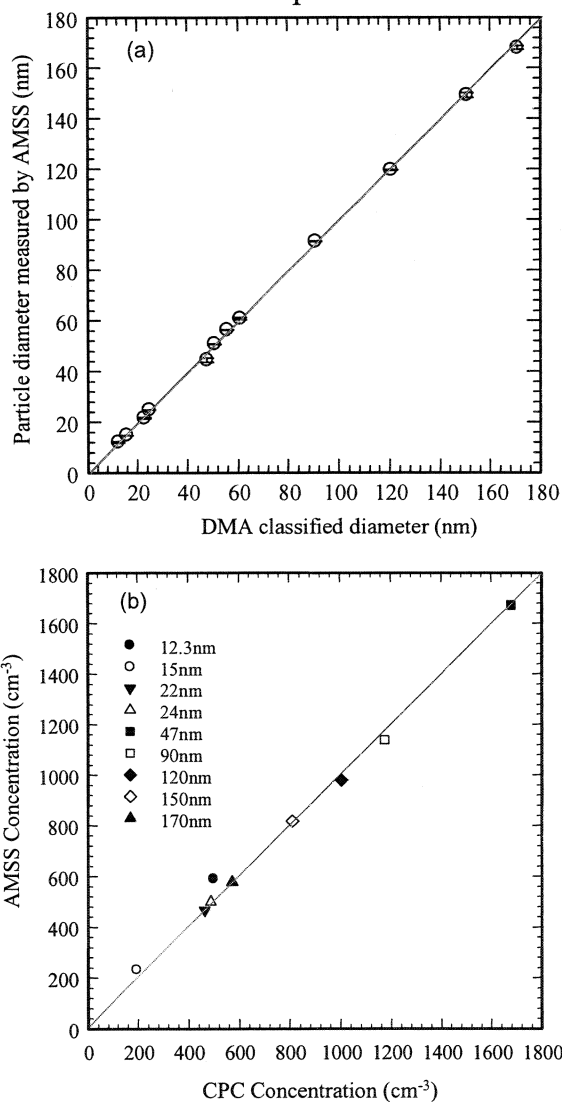


Figure 2. (a) Comparison of the particle diameters measured by AMSS to the DMA classified diameters. (b) Comparison of the particle concentrations measured by the AMSS to those measured by a CPC.

The characterization results showed that the prototype AMSS is capable of measuring aerosol size distributions with high speed, sizing accuracy, and counting statistics. Based on the prototype, the construction of an AMSS suitable for aircraft deployment has started. The body of the airborne AMSS has been fabricated based on an improved design, which further minimizes the flow disturbance within the AMSS and provides better seal against leaks. A more compact optics design is completed and the fabrication of the optics is underway.

The focus in FY06 will be finishing the construction of the AMSS that is suitable for aircraft deployment. Significant efforts will be made to ensure that the airborne AMSS meets the constraints of space, weight, and power for deployment onboard the DOE G-1 aircraft. Automation software will be completed for unattended airborne AMSS operations. The software will also include a first order data inversion routine that analyzes and displays real-time aerosol size distributions. Once the airborne AMSS is built, it will be tested rigorously on the ground before its first aircraft-based deployment.

SPECIFIC ACCOMPLISHMENTS:

Meetings:

J. Wang. "Fast Measurements of Aerosol Size Distribution, Hygroscopicity, and Volatility for Aircraft Deployment," *Atmospheric Science Program science team meeting*, January (2005).

P. Kulkarni and J. Wang. "A New Aerosol Mobility Size Spectrometer: Design, Calibration, and Performance Evaluation,"

Gordon Research Conference-Atmospheric Chemistry, Big Sky, (2005)

P. Kulkarni and J. Wang. "A New Aerosol Mobility Size Spectrometer: Design, Calibration, and Performance Evaluation," *Annual Conference of American Association of Aerosol Research, Austin, (2005)*

Publications:

P. Kulkarni and J. Wang, 2005. "A New Fast Mobility Spectrometer for Real-Time Measurement of Aerosol Size Distribution: I. Concept and Theory," *Submitted to Journal of Aerosol Science*.

P. Kulkarni and J. Wang, 2005. "A New Fast Mobility Spectrometer for Real-Time Measurement of Aerosol Size Distribution: II. Design, Calibration, and Performance Characterization," *Submitted to Journal of Aerosol Science*.

Funding for deployment of the AMSS during future field projects was obtained from the Department of Energy Office of Science through the Atmospheric Science Program and from the National Oceanic and Atmospheric Administration through the Office of Global Programs.

LDRD FUNDING:

FY 2004	\$65,589
FY 2005	\$99,415
FY 2006 (budgeted)	\$34,000

Exploration of Thermal Diffusion Processes in CdZnTe for Improved Nuclear Radiation Detectors

Aleksey Bolotnikov

04-086

PURPOSE:

The goal of the project is to achieve the high detection efficiency and high spectral resolution of virtual Frisch-grid CdZnTe (CZT) detectors by extending the high uniformity response over the entire volume of the bar-shaped CZT crystals.

APPROACH:

We propose to employ a PIN junction structure for CZT devices (similar structures were developed for Ge and Si detectors) to achieve full depletion of the active volume of the semiconductor detectors (virtual Frisch-ring detectors in this case) with minimum leakage current. This provides uniform response of CZT detectors and ensures their high performance.

Two approaches to produce PIN junction are to be investigated: (1) by making the Schottky barrier contacts, and (2) by thermal diffusion of p-type dopants at high temperatures >500 C. The later approach leads to the formation of PN junctions near the contacts, which is equivalent to the first approach, but it provides a more reliable and controllable way of fabrication of blocking contacts on CZT surface.

TECHNICAL PROGRESS AND RESULTS:

During FY 2004-2005, we investigated the first approach by showing improvement in spectroscopic properties of PIN junction CZT detectors. We fabricated several

devices with virtual Frisch-grid. Such contact configuration gives us an opportunity to study improvements in both the uniformity of the electric field and spectral resolution. We developed the pulse shape analyses and x-ray scan system to study the lateral and depth uniformity of the charge collection efficiency inside the Frisch-ring detectors. We developed the process of making high-quality Schottky contacts and surface passivation for the Frisch-ring detectors. With long (> 10 mm) CZT devices achieved the energy resolution of less than 1.2% at 662 keV.

We investigated the possibility to thermally diffuse p-type dopants at > 500 C. It is known, that unlike Si and Ge, detector-grade CZT could not withstand high temperatures. We found experimentally that CZT material irreversibly loses its semi-insulating property already above ~140 C (HPB material) and above ~200 C (MB material). Thus, we consider the first approach to be more reliable and practically usable for CZT detectors.

In addition, during FY 2005 we started the investigation of the role of Te-precipitates on the CZT device performance, and the possibility of using high-temperature post-growth annealing process to minimize the concentration of the precipitates (together with Yinnel Tech, Inc.).

In FY 2006 we will continue to pursue our goal to fabricate high-efficiency and high-energy resolution CZT detectors.

SPECIFIC ACCOMPLISHMENTS:

A.E. Bolotnikov, G.S. Camarda, G.A. Carini, G.W. Wright, R.B. James, D.S. McGregor, W. McNeil, "New Results from Performance Studies of Frisch-Grid CdZnTe Detectors," SPIE, 5540, pp. 33-45, 2004.

A.E. Bolotnikov, G.C. Camarda, G.A. Carini, M. Fiederle, L. Li, D.S. McGregor, W. McNeil, G.W. Wright, and R.B. James, *Fellow, IEEE*, "Performance Characteristics of Frisch-Grid CdZnTe Detectors," to be published in IEEE, 2004.

G.A. Carini, A.E. Bolotnikov, G.S. Camarda, G.W. Wright, R.B. James, "Effect of Te-precipitates on performance of CdZnTe detectors," to be published in APL, 2005.

Received a 2005 100R&D Award together with KSU and Yinnel Tech., Inc.

LDRD FUNDING:

FY 2004	\$ 86,077
FY 2005	\$131,041
FY 2006 (budgeted)	\$ 44,000

An Integrated Approach of High Power Target Concept Validation for Accelerator Driven Systems

Nicholas Simos

04-088

PURPOSE:

The success of a number of proposed high-power accelerators is strongly linked to the ability of a few, non-conventional materials and composites to withstand high levels of irradiation damage combined with severe shock from intercepting energetic protons. The objective of this project is to explore, through a systematic and detailed experimental effort, the feasibility of a number of innovative new materials as accelerator production targets. Specifically, assessment of the irradiation effects on key physical and mechanical properties, which make these materials attractive in the first place, is sought through controlled irradiation exposure and post-irradiation tests.

Proof of irradiation and shock resilience of these novel materials will form the basis for a BNL program development related to,

- Accelerator initiatives such as the Muon Collider, the Neutrino Superbeam, the Next Linear Collider, etc.
- NASA's search for multifunctional materials performing shielding and structural functions while maintaining properties under irradiation exposure.
- Special industrial applications of these materials, including material surface treatment (irradiation effects on nano-film deposition, and plating).

APPROACH:

The challenge, common to all high-power accelerator initiatives, is the feasibility and availability of materials that can meet the ever-increasing demand of power and energy deposition on targets. Recent irradiation damage studies showed that special materials exhibiting superb behavior in the non-irradiated state lose their distinct properties very rapidly with radiation. Results of these studies, combined with the requirements of recent accelerator initiatives (i.e. BNL Neutrino Superbeam), prompted the idea of focusing attention on a narrow material matrix and answering questions regarding the serious implications a material choice might have when used as an accelerator target as it experiences irradiation damage and severe shock.

To reach the goal materials need be selected based on a figure of merit which combines the material Z value with properties like conductivity, coefficient of thermal expansion, fracture toughness, etc. Specimens appropriate for the experiment, the available apparatus and the facility constraints are to be designed and fabricated then irradiated with 200 MeV protons in order to reach irradiation damage of approximately 0.25 displacements-per-atom (dpa). Specimens are to be allowed to "cool-down" and then transferred to the BNL Hot Cell facility for activation measurements and post irradiation testing. Through a series of tests the irradiation effects on (a) mechanical properties such as loss of ductility, failure load and stress-strain relationship, (b) coefficient of thermal expansion and conductivity, and (c) degradation of the special surface treatment of aluminum will be assessed. A material shock experiment using a high-power laser is to be performed alongside the irradiation and post-irradiation studies.

Collaborators contributing in this effort are, Dr. Harold Kirk, Dr. Hans Ludewig, Dr. Peter Thieberger, and Dr. Leonard Mausner (all of BNL), Prof. Kirk McDonald (Princeton U.), Dr. John Sheppard (SLAC) and Dr. Kojii Yoshimura (KEK, Japan).

TECHNICAL PROGRESS:

- The irradiated specimens that comprise the test matrix (3-D weaved carbon-carbon composite, graphite IG-43, "GUM METAL" alloy, AlBeMet, Beryllium, Vascomax, Ti-6Al-4V) was tested for changes of thermal expansion coefficient due to irradiation and changes in the mechanical properties (stress-strain relation, ductility)
- Post-analysis of some of the data has been performed. Rigorous data analysis is currently under way.
- Irradiation damage assessment in dpa of the specimens, based on the protons received during irradiation and their distribution, was completed
- Irradiation of a special 2-D carbon-carbon composite used in the Large Hadron Collider (LHC) proton beam collimators at CERN has been performed at the BNL BLIP facility, including activation measurements.
- The Class IV Nd:YAG laser has been conditioned and has been interfaced with an ultrasonic system for shock generation on target materials and measurements. Actual laser-induced shock tests are planned for this year.

The following are planned tasks for FY06:

- Completion of the irradiation damage assessment for the entire test matrix based on the calculated damage and observed property changes.

- Upgrade of the dilatometer set-up in the hot cell to enable measurements of thermal conductivity and diffusivity
- Assessment of surface bonding degradation for nickel-plated aluminum
- Completion of laser-induced shock tests on targets and applicability of laser interferometry for surface effects
- Completion of the planned irradiation test at the anti-proton facility at Fermi Lab where the 120 GeV protons will be used to assess the possible effects of the proton energy on the material damage.

SPECIFIC ACCOMPLISHMENTS:

Refereed Journals/Refereed Proceedings:

1. *Material Studies for Pulsed, High Intensity Proton Beam Targets*, N. Simos, H. Kirk, P. Thieberger, et. al., *Nuclear Physics B Proceedings Supplements*, Volume 149, p. 259-261
2. *Solid Target Studies for Muon Colliders and Neutrino Beams*, N. Simos, H. Kirk, H. Ludewig, et al., *Nuclear Physics* (submitted September 2005)
3. *A Free Jet Hg Target Operating in a High Magnetic Field Intersecting a High Power Proton Beam*, V.B. Graves, P.T. Spampinato, N. Simos, et al., Elsevier Science (submitted August 2005)
4. *Post-Irradiation Properties of Candidate Materials for High Power Targets*, H. Kirk, H. Ludewig, N. Simos, et. al., Proceedings of PAC05, Paper ID: 1703-ROAD003, May 2005
5. *A High Power Target Experiment*, H. Kirk, S. Kahn, N. Simos, et. al., Proceedings of PAC05, Paper ID: 1698-RPPT067, May 2005

Eight (8) LDRD-relevant presentations at international meetings and have been made.

Target Material Studies – Status, Muon Collider Collaboration Meeting, LBNL, February 2005

Material Irradiation Studies for LHC Collimators – Phase I & II, LHC Accelerator Research Program Collaboration Meeting, Port Jefferson, NY, April 2005

POST-IRRADIATION PROPERTIES OF CANDIDATE MATERIALS FOR HIGH POWER TARGETS, Poster Presentation, PAC 2005, ORNL, TN, May 2005

BNL Target Studies for 2-4 MW Proton Driver, Neutrino Beam Instrumentation 2005 Conference, Fermi National Laboratory, June 2005

Irradiation Studies for High-Intensity Proton Beam Targets, Neutrino Beam Instrumentation 2005 Conference, Fermi National Laboratory, June 2005

US Solid Target Program. Neutrino Factory/ Neutrino Super Beam. NuFact 2005 Conference, Frascati, Italy, July 2005

The LARP Collimation Program – Task 4 Summary, US LHC Accelerator Research Program Review, N. Simos and N. Mokhov, Fermi National Laboratory, September 2005.

A funding commitment through the US-LHC (LARP) of \$50K per year has been made (FY04- FY07). Also, proposals to (a) NuSAG for R&D on Targets/Materials for Future Neutrino Physics Program (\$900K/yr-3yrs) and (b) Neutrino T2K Beam Collaboration (\$240 K/yr-3yrs) have been generated and are pending.

LDRD FUNDING:

FY 2004	\$ 82,747
FY 2005	\$121,361
FY 2006 (budgeted)	\$ 46,000

Hydrogen Storage Using Complex Metal Hydrides for Fuel Cell Vehicles

James Wegrzyn

04-104

PURPOSE:

The purpose of the study is to build upon the expertise and unique capabilities at BNL in the development of a practical hydrogen storage system for fuel cell vehicles. The goal is to enhance our fundamental understanding of the kinetics and thermodynamic properties of both metal and complex metal hydrides. This knowledge serves as the foundation in responding to the President's and Brookhaven's Hydrogen Initiatives.

APPROACH:

The renewed interest in the "concept of a hydrogen economy" provides the motivation for this study. The approach is to synthesize and test novel hydrogen storage materials. Materials of interest have been aluminum hydride, alkali hydrides, and alanates. The role titanium plays as a catalyst has also been investigated.

TECHNICAL PROGRESS AND RESULTS:

Technical progress was realized for this past year in three areas: 1) the kinetic properties of aluminum hydride, 2) the thermodynamic properties of various complex metal hydrides, and 3) the functionality of the titanium catalyst.

The potential of using aluminum hydride as a hydrogen storage medium has been explored, in which accelerated desorption rates have been measured by the addition of

small levels of alkali metal hydrides. DOE's 2010 gravimetric and volumetric system targets can be met, but off board regeneration of spent Al back to AlH_3 still needs to be addressed.

The thermodynamic properties of various complex metal hydrides have been investigated. The alanates ($\text{Na}_2\text{LiAlH}_6$, KAlH_4 , K_3AlH_6 , K_2NaAlH_6 , etc.) were synthesized by mechanical alloying, and the enthalpy and entropy of decomposition was determined by measuring pressure-composition isotherms. Results have demonstrated that the equilibrium pressures can be changed substantially by partial substitution of the alkali metal. A better understanding of the thermodynamic effects of alkali-metal substitutions may lead to the development of new classes of high-capacity alanates with thermodynamic properties that are more favorable for PEM fuel cell applications.

At the NSLS, Ti *K*-edge x-ray absorption near-edge spectroscopy was used to determine the Ti valence and coordination in Ti-activated sodium alanate. These results demonstrated that the formal titanium valence is zero in doped sodium alanate and nearly invariant during H_2 cycling. A qualitative comparison of the edge fine structure suggests that the Ti is present on the surface in the form of amorphous TiAl_3 .

SPECIFIC ACCOMPLISHMENTS:

Publications:

Accelerated thermal decomposition of AlH_3 for hydrogen-fueled vehicles. Sandrock, G.; Reilly, J.; Graetz, J.; Zhou, W.-M.; Johnson, J.; and Wegrzyn, J., *Appl. Phys. A*, **80** 687 (2005).

Nanoscale energy storage materials produced by hydrogen-driven metallurgical

reactions. Graetz, J. and Reilly, J.J., *Adv. Eng. Mat.*, 7 597 (2005).

Structure and thermodynamics of the mixed alkali alanates. Graetz, J.; Lee, Y.; Reilly, J.J.; Park, S.; and Vogt, T., *Phys. Rev. B*, 71 184115 (2005).

Decomposition kinetics of the AlH_3 polymorphs. Graetz, J. and Reilly, J.J., *J. Phys. Chem. B*, accepted (2005).

Alkali metal hydride doping of $\alpha\text{-AlH}_3$ for enhanced H_2 desorption kinetics. Sandrock, G.; Reilly, J.; Graetz, J.; Zhou, W.-M.; Johnson, J.; and Wegrzyn J., *J. Alloys Comp.*, accepted (2005).

Thermodynamics of the α , β and γ polymorphs of AlH_3 . Graetz, J. and Reilly, J.J., *J. Alloys Compd.*, submitted (2005).

Presentations:

X-ray absorption study of Ti-doped sodium aluminum hydride. Graetz, J.; A. Y. Ignatov; T. A. Tyson; J. Reilly; and J. Johnson, Materials Research Society Fall Meeting, Boston, MA, Nov. 29-Dec.3, 2004.

Hydrogen driven metallurgical reactions (HDMR) to produce reactive, nano-scale and nano-composite materials. Reilly, J.; J.

Johnson; J. Graetz; R. Klie; G. Sandrock; and J. Wegrzyn; Materials Research Society Fall Meeting, Boston, MA, Nov. 29-Dec. 3, 2004.

Metal Hydrides, Materials R&D, Heat Transfer & Engineering. Reilly, J. (invited panelist) IPHE International Conference on Hydrogen Storage; Lucca, Italy, June 20-22, 2005.

New Reversible Complex Metal Hydrides, March Meeting of American Physical Society, Los Angeles, CA, 2005.

Doping of AlH_3 with alkali metal hydrides for enhanced decomposition kinetics, March Meeting of the American Physical Society, Los Angeles, CA, 2005.

Synthesis and Characterization of the AlH_3 Polymorphs, Gordon Research Conference: Hydrogen-Metal Systems, July 10-July 15, 2005.

LDRD FUNDING

FY 2004	\$ 70,265
FY 2005	\$108,592
FY 2006 (budgeted)	\$ 37,000

Full Power Test of the Amplifier for the Optical Stochastic Cooling using JLAB FEL

Vitaly Yakimenko

05-003

PURPOSE:

We intend to develop and test an optical amplifier that would be suitable for the optical stochastic cooling (OSC) at RHIC. Our calculations demonstrate that OSC operated at a 12-micron wavelength can effectively improve RHIC performance. OSC can successfully replace microwave stochastic cooling (SC) that is currently proposed for RHIC and experiments planned for the near future. OSC has the potential to affect the whole beam contrary to SC, which only deals with a small portion of the beam. OSC is complimentary to electron cooling (EC), which is another RHIC cooling project. EC is more effective for the particles with small amplitudes, while OSC works faster at large amplitudes. Thus addition of the OSC to the EC would dramatically reduce the requirements of the electron current in the EC project.

APPROACH:

Using an optical parametric amplifier (OPA) pumped by the second harmonic of the Accelerator Test Facility high power pulsed CO₂ laser, we characterized the amplification of a CW CO₂ laser at 9.6 microns. Demonstration of successful amplification using this OPA allowed us to extrapolate the performance expected under the conditions required for optical stochastic cooling of RHIC. Experiments aimed at characterization of the amplification under thermal load would allow developing of the full power optical amplifier.

TECHNICAL PROGRESS AND RESULTS:

Extensive calculations and initial measurements of the amplification of the OPA for OSC were previously performed. We use an OPA based GaGeAs₂ crystal as an optical amplifier for the OSC. A test stand was designed and assembled to verify performance of the OPA in the low repetition (low thermal load) mode of operation. Amplification was observed and characterized including gain length, angular acceptance, and bandwidth measurements for different pumping intensities. An understanding of the very challenging alignment procedure led to a significant modification of the test stand. Experimental verification of the phase preservation during OPA with relaxed alignment requirements, due to enlarged laser sizes, is in their final stages of development.

We started the design of the CO₂ based pump source. It consists of a mode locked CO₂ based oscillator at 10 MHz and a commercially available CW CO₂ welding laser. Experimental tests of the mode locked CO₂ based oscillator is the last item in the optical amplifier part of OSC project that needs verification.

SPECIFIC ACCOMPLISHMENTS:

Phys. Rev. ST Accel. Beams volume 7, issue 1, 012801 (2004).

1. M. Babzien, I. Ben-Zvi, I. Pavlishin, I. V. Pogorelsky, V. E. Yakimenko, A. A. Zholents, and M. S. Zolotorev, Optical Stochastic Cooling for RHIC, Workshop on Beam Cooling and Related Topics, Mt. Fuji, Japan, 2003.
2. I. Ben-Zvi, R&D on Cooling of RHIC Workshop on Beam Cooling and Related Topics, Mt. Fuji, Japan, 2003.

LDRD FUNDING:

FY 2005	\$112,488
FY 2006 (budgeted)	\$120,000

Study of Photon Coupling to an Electromagnetic Field Gradient

Carol Y. Scarlett

05-005

PURPOSE:

This experiment is designed to search for anomalous coupling between a photon and an electromagnetic field. For the field strengths achievable with a RHIC dipole, QED predicts a coupling which induces an ellipticity change of order 10^{-12} rads. However, a previous experiment conducted at BNL has observed an effect of order 10^{-8} rads. In this experiment, we use a RHIC Quad. in two configurations, with and without a mirror cavity, designed to both reproduce E949's results and to determine if the interaction was due to the strength of the field or its gradient. If such a large effect were due to an electro magnetic gradient, it may explain excess 'gravitational lensing' of galaxies believed to contain Dark Matter (DM). This would shed new light on the phenomena of DM in the universe. Follow up experiments could then introduce stronger field gradients to measure the coupling as a function of $\nabla \cdot B$. Alternatively, if the effect is due to the presence of axions, scaling with the field strength, we would be in a unique position to see their effects on propagating photons.

APPROACH:

We have expanded on the approach taken in E949's search for axions. Our goal is two fold: search for a deeper connection between photon interactions in a gravitational and magnetic field gradient and confirmation/ruling out of the previous observations of E949. This experiment was

inspired by both DM research and the signal observed in E949.

Our experimental scope covers a field gradient of $\sim 99\text{T/m}$, over 5000 times what was achieved with a dipole magnet, and a magnetic field strength of $\sim 1\text{T}$. Introduction of a mirror cavity will increase the length through the field to 10-100 km, giving us comparable field strength parameters to E949 – with a gradient in excess of 10^7 of that seen in the previous experiment.

Thus far, data collection has been conducted using only a 'single-pass' through the field. For a second year of running, we are preparing to build a mirror cavity to increase transits through the field to $\sim 10^5$ - 10^6 to achieve the running conditions of E949. This cavity will also allow us to simultaneously probe a larger field gradient than that used in similar experiments.

TECHNICAL PROGRESS AND RESULTS:

The most significant accomplishment for this funding year is the collection of data in the single pass mode. We have collected ~ 6950 mins of data thus far. The first 5900 mins were taken with a displacement in the horizontal direction, while the remainder of the time it was taken with both a vertical and horizontal displacement.

As with all experimental setups, we also completed calibrations of our photo-receivers, conducted systematic studies of the change in laser energy output with changes in temperature, and studied the frequencies of floor vibrations with the magnet current on. These measurements have allowed us to understand the systematics of our detector.

A Fast Fourier Transform analysis program has been tailored to read in and analyze our data. The program was developed concurrently with the actual data taking and has already been used to analyze much of the existing data. The data has been packaged carefully in terms of running conditions and made available to the other collaborators (Yannis Semertzidis, Don Lazarus and Mike Sivertz) on line.

To date we have evidence for a peak at the frequency at which the magnet was ramped. This evidence has appeared in several different runs. We will continue our analysis and include a background study, a shunt measurement, to verify that the effect is coming from within the cavity. A short note is being prepared at this time on all results.

LDRD FUNDING:

FY 2005	\$105,693
FY 2006 (budgeted)	\$132,000

Heavy Ion Physics with the ATLAS Detector

Helio Takai

05-006

PURPOSE:

The ATLAS experiment slated to initiate operation at CERN in the fall of 2007 at the Large Hadron Collider (LHC), is designed to study the origins of the spontaneous symmetry breaking, or the origins of quark mass. The experiment is designed for the detection of high-energy particles, especially jets. As demonstrated by RHIC, jets are very effective probes of the quark gluon plasma created in heavy ion collisions. LHC will accelerate lead nuclei and heavy ion runs scheduled for 2008. The unprecedented energy densities that it will be possible to create at the LHC in heavy ion collisions will open a unique opportunity to study the quark-gluon plasma (QGP) via jets and other hard probes with the ATLAS detector at RHIC. Its large acceptance and fine calorimeter segmentation makes the detector an ideal tool for this study. Because the detector was designed for proton-proton collisions, its effectiveness in the high multiplicity heavy ion environment needs to be understood. Initial simulation studies indicate that ATLAS will perform well in this study; however, it also indicates that dedicated algorithms both for trigger and analysis need to be developed. The goal of this LDRD is to address these issues.

APPROACH:

The scope of this proposal is to develop algorithms to allow ATLAS to study heavy ion physics. These algorithms will be used in the high level trigger and data analysis as well. One particular example is to perform jet finding and reconstruction in the high multiplicity environment of heavy ion

collisions. Unlike the case of proton-proton events, jets will be "riding" on a background of soft particles. The ultimate goal in this particular case is to extract enough information that would allow us to perform quantum chromodynamics studies in the heavy ion environment. One big issue to be solved is the development of dedicated analysis tools for the data that will be collected. This has to be developed within the ATLAS software framework. Progress towards this has been slow, and there is some urgency in developing this tool for the preparation of the Physics Progress Report, due October 2006. Dr. Arthur Moraes will be joining this effort in the capacity of Research Associate to aid in this effort.

TECHNICAL PROGRESS AND RESULTS:

Dr. Arthur Moraes has accepted a Research Associate position to work on this project. In the meantime the ATLAS heavy ion physics working group has made significant progress in laying out a coherent plan for the physics to be performed for the heavy ion specific runs. Initial simulation work has started. In spite of the initial success it is more than evident that dedicated manpower needs to be put in place to meet several deadlines within the ATLAS collaboration.

A physics plan outlining the goals for the heavy ion run has been completed by the ATLAS heavy ion working group. This plan has milestones such as the preparation of a Physics Performance Report for the CERN scientific committee in October 2006. This plan has been discussed within the collaboration presented in a recent PANIC 2005 conference to the general audience.

SPECIFIC ACCOMPLISHMENTS:

ATLAS Heavy Ion Physics Program,
Presented at PANIC 2005, Santa Fe, New
Mexico, October 27-29, 2004.

LDRD FUNDING:

FY 2005	\$ 5,623
FY 2006 (budgeted)	\$103,000

Superconducting Lead Photoinjector

John Smedley

05-017

PURPOSE:

The aim of this project is to investigate the photoemission properties of lead with the goal of improving the capabilities of superconducting (SC) photoinjectors. SC photoinjectors represent an important emerging class of electron sources, with the potential to deliver high average current and high peak current simultaneously. Before this investigation began, the choice of cathode for these injectors was limited to two options. The niobium wall of the injector could be used, but the low quantum efficiency (QE) of niobium limited the maximum current. Alternatively, a radio-frequency (RF) choke joint could be used to introduce a non-SC cathode. While this technique allows a high-QE cathode to be used, the choke negatively impacts the RF properties of the cavity, and greatly increases the complexity of the device. This project has introduced the concept of a hybrid lead-niobium injector, combining the superior SC and RF properties of a niobium cavity with the higher QE of a SC lead cathode. Since all of the materials in this design are superconductors, a choke joint is not necessary, making the device simpler to manufacture.

APPROACH:

This project can be broken into three distinct challenges that must be addressed. The first is to establish methods by which lead can be deposited onto a niobium substrate. This work has been done in collaboration with R. Lefferts and A. Lipski (Stonybrook University) and J. Langner and P. Strzyżewski (INS-Świerk, Poland).

The second is the measurement of the QE and surface properties of the various surfaces prepared in part one. This work has been

performed in the BNL instrumentation division. Existing systems for the measurement of the photoemission properties of metals have been significantly upgraded as part of this project, enabling the material QE to be measured over a broad range of incident wavelengths.

The third portion of this project is the construction of an SC-RF cavity with a lead cathode. This will be the prototype hybrid lead-niobium injector. A niobium cavity has been designed and constructed for this purpose by J. Sekutowicz (DESY, Germany). Existing infrastructure in Collider Accelerator Department (CAD) will be used to perform the RF and photoemission measurements on this cavity. An existing niobium cavity (built by Advanced Energy Systems in collaboration with CAD) will also be used to tests aspects of the hybrid cavity design.

TECHNICAL PROGRESS AND RESULTS:

The first and second phases of the project outlined above have been completed (in FY 2005). Four methods of depositing lead onto niobium have been established (electroplating, vacuum deposition, arc deposition and sputtering). All of these coatings have been shown to be thermally stable, and all can provide QE significantly superior to that of niobium (see Fig. 1). Two of the coating methods (electroplating and arc deposition) have surface finish qualities that appear to be consistent with operation inside a SC photoinjector. In addition to the four-coated lead surfaces, solid lead has been investigated for comparison. A procedure for laser cleaning has been established for each of the lead samples to maximize the QE without damaging the cathode surface.

For the deposition methods, which show promise for use in a hybrid injector (electroplating and arc deposition), tests were performed to measure the QE at low temperature (-170 C). In a good vacuum (8 nTorr), the QE at cryogenic temperatures was

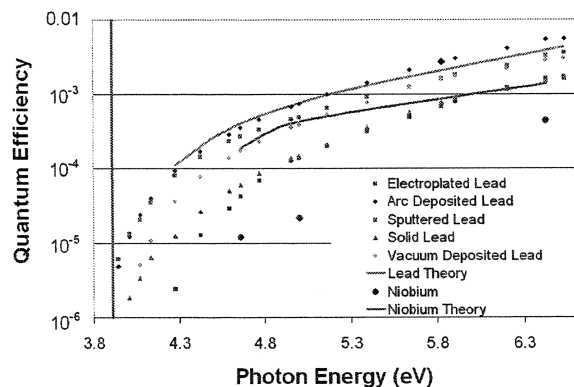


Figure 1: QE vs Photon energy for five lead samples. Niobium data is included for comparison.

comparable to the QE at room temperature. However, poor vacuum ($1.6 \mu\text{Torr}$) degraded the QE of cryogenic cathodes on the scale of hours, while in the same vacuum system room temperature cathodes were unaffected. This measurement emphasizes the importance of good vacuum techniques in the assembly and operation of the hybrid injector.

In addition to the measurements of the photoemission properties of lead, a theoretical investigation of the expected QE of lead has been performed using the three-step model of photoemission. This analysis has produced good agreement with the experimental data.

In the third stage of the project, construction and measurement of a prototype hybrid injector has begun. A niobium cavity has been constructed (Fig. 2) and is currently awaiting coating via arc deposition. The measurements of this cavity will occur during FY2006.

SPECIFIC ACCOMPLISHMENTS:

Publications:

Nb-Pb superconducting RF-gun. J. Sekutowicz, J. Iversen, G. Kreps, W.-D. Möller, W. Singer, X. Singer, I. Ben-Zvi, A. Burrill, J. Smedley, T. Srinivasan-Rao, M. Ferrario, P. Kneisel, J. Langner, P. Strzyzewski, R. Lefferts, A. Lipski, K. Szałowski, K. Ko, L. Xiao. Submitted to Phys. Rev. ST-AB.

Photocathodes for the Energy Recovery Linacs. T. Rao, A. Burrill, X.Y. Chang, J. Smedley, T. Nishitani, C. Hernandez Garcia, M. Poelker, E. Seddon, F.E. Hannon, C.K. Sinclair, J. Lowellen, and D. Feldman; BNL 74711-2005CP; Submitted to Nucl. Inst. and Methods

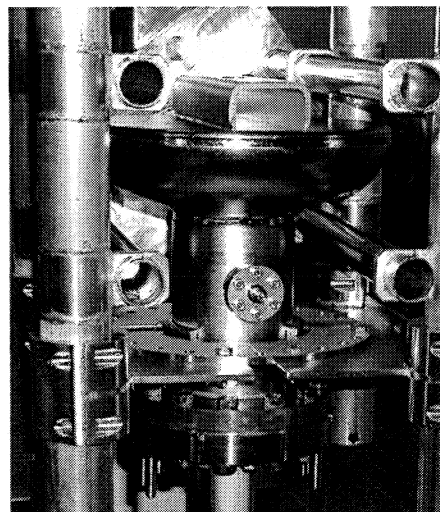


Figure 2: Niobium cavity

Presentations:

John Smedley, Triveni Rao, Jacek Sekutowicz, Peter Kneisel, J. Langner, P. Strzyzewski, Richard Lefferts, and Andrzej Lipski; Progress on Lead Photocathodes for Superconducting Injectors; BNL 75034-2005CP; pres. Particle Accelerator Conf., Knoxville, TN, 16-20 May (2005)

John Smedley, Superconducting Photo-injectors; Workshop on The Physics and Applications of High Brightness Electron Beams 2005, Erice, Sicily, October 9-14, (2005)

John Smedley, Superconducting Photo-injectors; DESY seminar, Hamburg, Germany, 18 October, (2005)

LDRD FUNDING:

FY 2005	\$117,500
FY 2006 (budgeted)	\$118,000

Controlled Formation of Nanostructured RuO₂ Catalysts

Peter Sutter
Jan Hrbek

05-020

PURPOSE:

RuO₂/Ru(0001), a low temperature oxidation catalyst with exceptional activity, has recently become a model system for studying the perceived “pressure gap” in catalysis. A RuO₂ surface oxide, forming in oxidizing environments at high pressure, was identified as the catalytically active phase, while Ru metal, present in UHV experiments, is inactive. Catalytic reactions on the active RuO₂(110) have been studied for the past few years, yet the atomic-scale oxidation pathway of Ru(0001) leading to the formation of the RuO₂ surface oxide remains poorly understood. *In-situ* microscopy of the Ru surface during oxidation, pursued under this LDRD project, has the potential of identifying the atomistic oxidation mechanism, thus answering long-standing questions on the nature of the oxidation reaction.

APPROACH:

Previous studies of Ru oxidation were entirely based on spatially averaging techniques, such as photoelectron spectroscopy or thermal desorption spectroscopy. These techniques are unable to capture the nanoscale dynamics involved in the initial nucleation and growth of a surface oxide. We used low-energy electron microscopy (LEEM), capable of real-time observations of surfaces with sub-10 nm resolution during exposure of Ru(0001) to oxygen. This approach provides quantitative data on the nucleation, growth and coalescence of individual nanoscale RuO₂

islands from which the overall oxidation mechanism and its kinetics can be derived. For the theoretical interpretation of the data, a collaboration was established with N.C. Bartelt (Sandia Livermore).

TECHNICAL PROGRESS AND RESULTS:

The oxidation of Ru(0001) was studied using NO₂ as a source of atomic oxygen over a range of sample temperatures. At low temperatures (< 400°C), the oxidation proceeds via highly anisotropic oxide islands nucleating at surface steps, suggesting step edges as sites for preferential oxygen uptake. At higher temperatures, RuO₂ nucleates and grows at steps and on terraces, and the oxide islands become progressively less elongated.

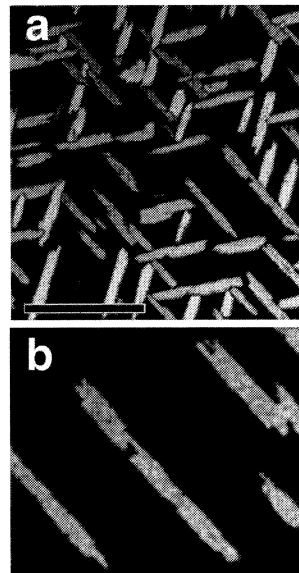


Figure 1: (a) Distribution of three orientations of RuO₂ islands (color) on Ru(0001). Scale bar: 1 μm. (b) Close-up, showing domain structure of RuO₂ islands.

The growing monolayer-thick surface oxide patches consist of smaller (110)-oriented RuO₂ domains separated by domain boundaries (Fig. 1). The RuO₂ lattice aligns with high-symmetry directions of the underlying metal surface, giving rise to 3 rotational domains, but grows without a well-defined epitaxial relationship to the

substrate surface. The prevailing theory on Ru oxidation suggests a sequence of elementary steps: the initial incorporation of several equivalent monolayers of oxygen into sub-surface sites of the Ru crystal, the decoupling of a O-Ru-O trilayer from the underlying metal, ultimately followed by the transformation of the trilayer into a rutile RuO_2 surface oxide. Most importantly, the suggested oxidation pathway would involve only bulk diffusion of oxygen into Ru and local structural transformations but no surface diffusion of Ru. Our observations of the time-dependent growth of individual nanoscale RuO_2 islands suggest that this theoretical picture may not represent the real oxidation mechanism. Our data demonstrate clearly that Ru atoms are removed from the metal surface during the oxidation process. These metal atoms in turn may participate directly in the formation of surface RuO_2 islands. Surface diffusion of both O and Ru appears to be fast, such that the oxidation kinetics is limited by the rate of attachment to the edges of existing oxide patches.

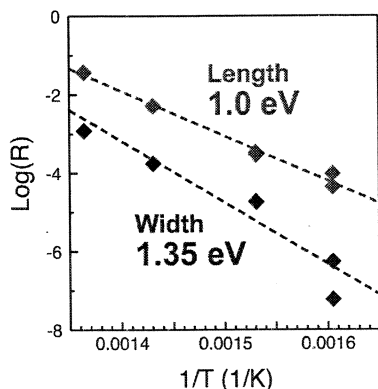


Figure 2: Arrhenius plot of the temperature dependent linear growth rate of RuO_2 islands.

Arrhenius analysis of the temperature-dependent growth rate gives significant activation energies of 1.0 eV and 1.35 eV for incorporation into the short and long edge of the RuO_2 islands, respectively (Fig. 2). While our preliminary observations of the oxidation of Ru have already provided

unique insight into the microscopic mechanisms at the early stages of metal oxidation, several key questions remain unanswered and will be investigated in the second year:

- (i) Are indeed, as suggested by theory, several monolayers of oxygen incorporated into sub-surface sites of the metal crystal prior to formation of the RuO_2 surface oxide? How is the sub-surface oxygen distributed, and how does the oxygen distribution affect the formation of the surface oxide? To answer these questions, quantitative work function maps obtained by LEEM will be compared with predictions of the work function for the various sub-surface oxygen phases.
- (ii) Can the deposition of other metals, e.g., Au, be used to decorate step edges and affect their reactivity and rate of oxygen uptake? Step decoration could be a versatile tool for tailoring (slowing or accelerating) the oxidation rate of $\text{Ru}(0001)$, and of a broader class of other metal surfaces.
- (iii) Does the catalytic activity of nanoscale RuO_2 islands in low-temperature oxidation reactions depend on their size and/or morphology? To answer this question, we will complement our observations of the Ru oxidation process by measurements of the rate of CO oxidation over RuO_2 islands with well-defined size and shape.

SPECIFIC ACCOMPLISHMENTS:

Coadsorption of oxygen, gold and carbon monoxide on $\text{Ru}(0001)$ and CO_2 formation: A thermal desorption study. Wu, Q. and Hrbek, Surf. Sci., 588, 117 - 126 (2005).

Early stages of surface oxidation of $\text{Ru}(0001)$. Sutter, P. and Hrbek, J., in preparation.

Observation of the oxidation of $\text{Ru}(0001)$ by low-energy electron microscopy. Sutter, P.;

Hrbek, J.; and Hwang, R. Symposium P, Materials Research Society Spring Meeting, San Francisco, CA, March 28 – April 1, 2005

Manipulation of nanoparticle growth on surfaces. Hrbek, J and Sutter, P. American Chemical Society Mid-Atlantic Regional Meeting, Piscataway, NJ, May 21-24, 2005.

CO oxidation catalysis on Ru and RuO₂. Wu, Q.; Sutter, P.; and Hrbek, J. North

American Catalysis Society Meeting, Philadelphia, May 2005.

In-Situ Microscopy of the Oxidation of Ru(0001). Sutter, P.; Hrbek, J.; and Hwang, R.Q. Abstract for Symposium MM, Materials Research Society Fall Meeting.

LDRD FUNDING:

FY 2005	\$117,502
FY 2006 (budgeted)	\$115,000

Hydrogen Storage in Complex Metal Hydrides

Peter Sutter

05-021

J. Muckerman

J. Reilly

J. Wegrzyn

D. Welch

L. Cooley

(T. Vogt)

PURPOSE:

Hydrogen storage has been identified as a key bottleneck on the way to a hydrogen-based economy. Complex metal hydrides have the potential to become the material of choice for large-scale hydrogen storage if a compound with a gravimetric hydrogen density near 10 weight % is found that can be hydrogenated safely and reversibly near ambient conditions. The re-hydrogenation reaction, which transforms the spent material back into a hydrogen-rich compound, is particularly problematic and occurs for most materials only under extreme environmental conditions, e.g., at very high pressures. The pivotal discovery that the decomposition of a specific hydride, NaAlH_4 to NaH into Al and hydrogen can be made reversible at moderate temperatures and pressures by *adding small amounts of Ti* has demonstrated a possible path towards a solution of this problem. Recent evidence suggests that the active Ti dopants occupy surface or near-surface sites. Yet, their role in the different elementary steps of the re-hydrogenation ("refueling") reaction remains largely unknown.

APPROACH:

Under this LDRD project, combined experimental and theoretical research is performed to assemble key data underpinning hydrogen storage in NaAlH_4 ,

and in particular to understand the role of transition metal dopants and alkali substitutions in making this process reversible. The general approach is to *apply the multifaceted capabilities of an interdisciplinary research team* to the complex problem of hydrogen storage, a strategy for which a large laboratory such as BNL provides an ideal environment. Our unique experimental approach emphasizes the *use of well-defined model systems to obtain quantitative results* that are readily compared with theory. Specific groups of experiments include: (i) The use of advanced materials synthesis, e.g., of NaAlH_4 single crystals, and characterization to extract intrinsic materials properties; (ii) The investigation of mixed alanates, derived from NaAlH_4 or cryolite Na_3AlH_6 to search for new reversible complex hydrides with favorable hydrogen uptake/release kinetics; and (iii) the systematic study of sites occupied by transition metal dopants, such as Ti, and of the effect of such dopants on the kinetics of hydrogen uptake and release.

TECHNICAL PROGRESS AND RESULTS:

A key step in the re-hydrogenation reaction of NaAlH_4 is the dissociation of H_2 adsorbed from the gas phase on the spent material, consisting of NaH and Al . Since in pure form none of these materials easily dissociate H_2 , we speculate that a major role of Ti dopants is in fact to catalyze H_2 dissociation. Using ab-initio density functional theory, we have identified at least one Al:Ti complex on the (001) surface of Al that dissociates H_2 . Substitution of Ti for Al in third-nearest-neighbor positions on the Al(001) surface in either the first or second surface layer leads to dissociative chemisorption of molecular hydrogen.

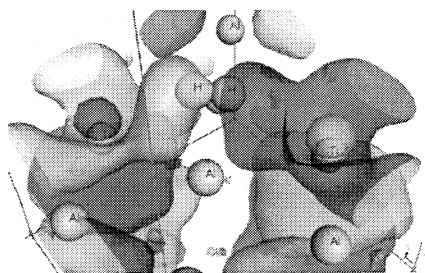


Figure 1: Calculated HOMO of the Ti-doped surface/ H_2 system showing the inclusion of σ^* anti-bonding molecular orbital character of the incoming hydrogen molecule prior to the dissociation of the H-H bond.

The highest occupied molecular orbital (HOMO) of the doped-surface/ H_2 adduct at both active sites exhibits a characteristic nodal symmetry in the entrance channel. So far we have not found any other active site with this characteristic on Ti-doped aluminum.

Parallel to the ab-initio calculations, we have started experiments on well-defined model systems in ultrahigh-vacuum (UHV) to study the interaction of hydrogen with Al in the presence of Ti, and to search for catalytically active Al:Ti sites. In these experiments, an Al(001) single crystal simulates the dehydrogenated (“spent”) material. In a very difficult process, an Al(001) crystal has been prepared successfully in UHV, and scanning tunneling microscopy (STM) has been used to image its surface with atomic resolution. In the second year, the controlled dosing of atomic-H, molecular H_2 , and Ti on this sample, combined with STM imaging will allow us to establish the structure of sites for dissociative chemisorption of H_2 , and to determine their contribution to the overall rate of atomic-H production at Al surfaces. The growth of $NaAlH_4$ single crystals, part of the proposed materials synthesis experiments, has so far been unsuccessful. However, a number of mixed alانات were successfully prepared by mechanochemical synthesis and their crystal structure and lattice parameters determined at the NSLS.

Among these new alانات are Na_2LiAlH_6 , K_2LiAlH_6 , and K_2NaAlH_6 .

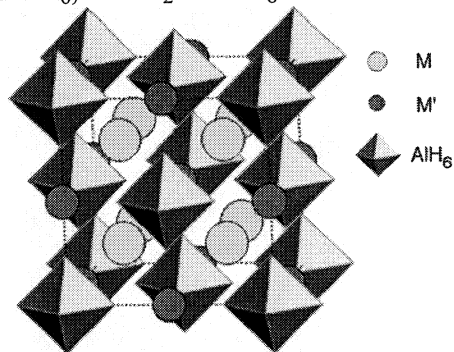


Figure 2: Crystal structure of mixed $M_2M'AlH_6$ alانات. M, M': alkali metal atoms.

The studied mixed alانات prefer the $Fm\bar{3}m$ space group, with the smaller ion (M') occupying an octahedral site and the larger ion (M) in 12-fold coordination. The larger ions tend to stabilize the alانات. The reaction thermodynamics of the mixed alانات was determined by isothermal hydrogenation & dehydrogenation measurements. Most notably, the *mixed alkali alانات were reversible without a catalyst*.

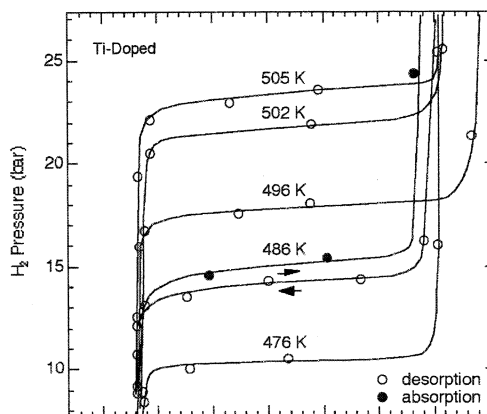


Figure 3: Isotherms for Na_2LiAlH_6 .

Enthalpy (ΔH) and decomposition temperature (T_d) increased with the size of the alkali metal. Compositions with $M' > M$ were unstable and showed a phase separation to cryolite or stable elpasolite. In the second year, we will systematically pursue the two most promising groups of experiments identified so far: (1) Continued

search for potential new light-weight hydrogen storage compounds by combined synthesis, crystallography, and thermodynamic measurements. These experiments, which will be linked closely with theory, will shed light on our surprising finding of reversible hydrogen storage in *undoped* mixed alانات, and have the potential of identifying new classes of reversible storage materials. And (2) surface imaging experiments on Al single crystals combined with density-functional theory to identify Al:Ti sites which catalyze the dissociation of H₂. These activities aim at understanding, at a fundamental level, reversible hydrogen storage in doped NaAlH₄. Such a fundamental understanding of the role of the transition metal dopant can then be used in a rational search for optimized hydrogen storage materials.

SPECIFIC ACCOMPLISHMENTS:

The work performed under this LDRD was part of the foundation of a successful DOE-“Hydrogen Fuel Initiative” (HFI) proposal on “Atomistic Transport Mechanisms in Reversible Complex Metal Hydrides,” and is being extended as part of the funded program.

First-principles study of Ti-catalyzed hydrogen chemisorption on an Al surface: A critical first step for reversible hydrogen storage in NaAlH₄. Chaudhuri, S. and Muckerman, J. J. *Phys. Chem. B* 109, 6952 (2005).

A Density Functional Theory Study of the Catalytic Role of Ti Atoms in Reversible Hydrogen Storage in the Complex Metal Hydride, NaAlH₄. Chaudhuri, S. and Muckerman, J. *Materials and Technology for Hydrogen Storage and Generation*, edited by G-A. Nazri, C. Ping, R.C. Young, M. Nazri, and J. Wang (Mater. Res. Soc.

Symp. Proc. 884E, Warrendale, PA, 2005) GG2.1.

A combined first-principles theory and experimental x-ray absorption study of Ti-activated hydrogen storage reaction in metallic aluminum, Chaudhuri, S.; Graetz, J.; Ignatov, A.; Reilly, J.T.; and Muckerman, J. Manuscript in preparation.

A density functional theory study of Ti-assisted catalytic hydrogenation of terminal alkenes on nanometric NaH particles. Chaudhuri, S. and Muckerman, J. Manuscript in preparation.

Structure and thermodynamics of the mixed alkali alانات. Graetz, J.; Lee, Y.; Reilly, J.J.; Park, S.; and Vogt, T., *Phys. Rev. B* 71 184115 (2005).

“Nanoscale energy storage materials produced by hydrogen-driven metallurgical reactions,” Graetz, J. and Reilly J.J., *Adv. Eng. Mat.* 7, 597 (2005).

Accelerated thermal decomposition of AlH₃ for hydrogen-fueled vehicles. Sandrock, G.; Reilly, J.J.; Graetz, J.; Zhou, W.-M.; Johnson, J.; and Wegrzyn, J. *Appl. Phys. A* 80, 687 (2005).

Characterization of the local titanium environment in doped sodium aluminum hydride using X-ray absorption spectroscopy, Graetz, J.; Ignatov, A.Y.; Tyson, T.A.; Reilly, J.J.; and Johnson, J. *Mat. Res. Soc. Conf. Proc.* 837 (2005).

X-ray absorption and density functional theory study of hydrogen chemisorption on an Al surface: The influence of local surface structure, Chaudhuri, S. and Muckerman, J. 230th National Meeting, Washington, DC, Aug 28-Sept 1, 2005.

A Density Functional Theory Study of the Catalytic Role of Ti Atoms in Reversible Hydrogen Storage in the Complex Metal Hydride, NaAlH₄, Chaudhuri, S. and Muckerman, J.; MRS Spring Meeting 2005, San Francisco, CA, March 28-April 1, 2005.

Ti-Catalyzed selective hydrogenation of terminal alkenes in nanometric NaH: A first principles study of the catalytic reaction on Ti-doped NaH nanoclusters. Chaudhuri, S. and Muckerman, J. 230th ACS National Meeting, Washington, DC, Aug 28-Sept 1, 2005.

A Density Functional Theory and First-Principles Simulation Study of Ti-Assisted Hydrogen Storage in NaAlH₄. Chaudhuri, S. and Muckerman, J. Gordon Research Conference on Chemical Reactions on Surfaces, Ventura, CA, February 13-18, 2005.

First-Principles Study of Ti-Catalyzed Hydrogen Chemisorption on an Al Surface: A Critical First Step for Reversible Hydrogen Storage in NaAlH₄. J. Muckerman and S. Chaudhuri. Frontiers in Nanocatalysis meeting of the Catalysis and Chemical Transformations Program, Division of Chemical Sciences, Office of Basic Energy Sciences, U.S. Department of Energy, Rockville, MD, May 18-21, 2005.

New Reversible Complex Metal Hydrides, J. Graetz et al., March Meeting of American Physical Society, 2005.

Doping of AlH₃ with alkali metal hydrides for enhanced decomposition kinetics. J. Graetz et al. March Meeting of the American Physical Society, 2005.

The Potential of Aluminum Hydride for Vehicular Hydrogen Storage. J. J. Reilly et al. IPHE International Hydrogen Storage Conference, 2005.

X-ray absorption study of Ti-doped sodium aluminum hydride. J. Graetz et al. Fall Meeting of the Materials Research Society, Dec. 2004.

The Use of Hydrogen-Driven Metallurgical Reactions (HDMMR) to Produce Reactive, Nano-Scale and Nano-Composite Materials. J. J. Reilly et al. Fall Meeting of the Materials Research Society, Dec. 2004.

Preparation of Nanoscale/Nanocomposite Materials Using Hydrogen-Driven Metallurgical Reactions (HDMMR). J. J. Reilly et al. International Symposium on Metal-Hydrogen Systems: Fundamentals and Applications, Sept. 2004.

LDRD FUNDING:

FY 2005	\$123,301
FY 2006 (budgeted)	\$125,000

Behavior of Water on Chemically Modified Semiconductor Surfaces: Toward Photochemical Hydrogen Production

Etsuko Fujita

05-028

J. Rodriguez

J. T. Muckerman

PURPOSE:

Photochemical water splitting to hydrogen, a renewable and non-polluting fuel, and oxygen using energy from solar radiation is extremely important for a sustainable source of energy. Hydrogen and oxygen have been successfully produced by UV irradiation of aqueous suspensions of various semiconductor catalysts including TiO_2 (and transition metal-loaded TiO_2) and SrTiO_3 , but a detailed mechanism of the conversion at the active catalytic center remains unclear. Recently nitrogen and carbon doped materials, $\text{TiO}_{2-x}\text{N}_x$, and $\text{TiO}_{2-x}\text{C}_x$, have been synthesized and used as photocatalysts that utilize visible light (> 420 nm). We are carrying out coordinated experimental and theoretical studies of behavior of water on these band-gap-narrowed semiconductors (BGNSCs) toward photochemical hydrogen production with attached multi-electron catalysts (*i.e.*, metal oxides such as RuO_2 and MnO_2). We focus on the coupling between the materials properties and the water redox chemistry, with an emphasis on attaining a fundamental understanding of the individual elementary steps in the processes.

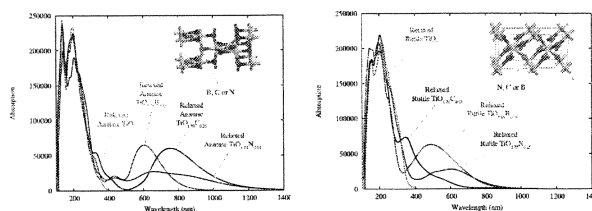
APPROACH:

The key issues associated with the doped semiconductors are their controlled synthesis, band gaps, absorption spectra (and other electronic properties), stability, resistance to

photocorrosion, and reactivity with water and other molecules in ultrahigh vacuum (UHV) and aqueous solution. We prepare N-doped films of TiO_2 and SrTiO_3 , modify single-crystal semiconductor surfaces with N, C, and/or B, prepare nanoparticles of BGMSCs, characterize them by surface/materials science techniques under UHV conditions and at solid/water interface, and elucidate through both experiments and theory the electronic and proximal structure of adsorbed water and its reactions at active centers under irradiation at the atomic level.

TECHNICAL PROGRESS AND RESULTS:

We have calculated the geometric and electronic structures of both anatase and rutile TiO_2 as well as the properties of the nitrogen-, carbon- and boron-doped materials $\text{TiO}_{1.75}\text{N}_{0.25}$, $\text{TiO}_{1.75}\text{C}_{0.25}$ and $\text{TiO}_{1.75}\text{B}_{0.25}$ for both phases using the CASTEP program. Analogous calculations are in progress for SrTiO_3 . Our results are in general agreement with the density functional theory (DFT) calculations previously published. We employed a scissors operator to increase the DFT-computed band gap by 1.14 eV prior to the computation of electronic properties. Our study confirms the expected trend in the computed density of states: the more electropositive the dopant element that replaces oxygen is, the smaller the band gap and the more the Fermi energy is shifted towards the conduction band. While the

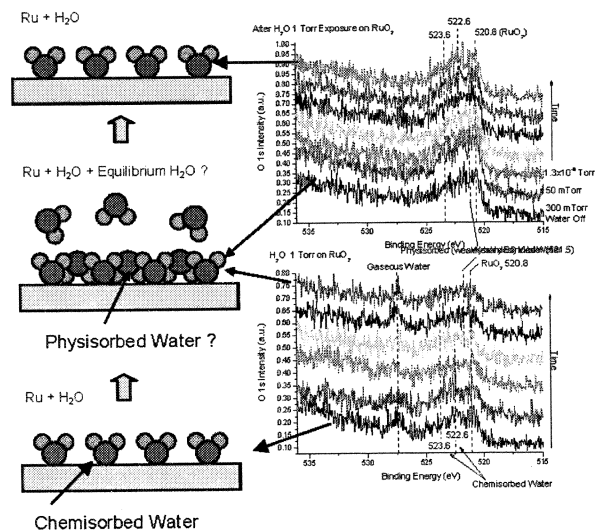


results show that doping places donor states progressively higher in the band gap in the order $N < C < B$, they raise the question of how high in the band gap dopant states can be placed before they become bleached by visible radiation and become traps for electrons moving to the surface of the semiconductor material. The absorption spectra (Fig. 1) were computed through the calculation of the dielectric constant. The effect of doping for both anatase and rutile TiO_2 , as is evident from the figures, is large in the important 400-700 nm portion of the spectra. Unlike the density of states, the positions of the subsidiary peaks of the doped systems do not correlate with the electronegativity of the dopant atom or the calculated band gap. While the high level and (especially) the periodicity of the dopant atoms in these calculations are not truly realistic, the results represent an idealized upper limit for the effect of dopants.

We have prepared N-doped TiO_2 by reacting Degussa TiO_2 (15-20 nm particles) in triethylamine for over 4 days at 90 °C, followed by washing twice with fresh triethylamine. Upon vacuum drying, tan crystallites were obtained. While this material is air stable, the color changes to almost black upon heating to 330 °C. The physical and chemical properties of these materials are currently under investigation using transmission electron microscope, X-ray diffraction, and X-ray photoemission spectroscopy.

One of our primary model catalysts for studying the mechanisms of water oxidation is ordered rutile $\text{RuO}_2(011)$, which can be produced routinely, e.g., by epitaxial oxidation of $\text{Ru}(0001)$ in O_2 or NO_2 . We anticipate that our results will translate easily to other transition metal oxide catalysts, such as MnO_2 which are less available in ordered crystalline form. In order to overcome the pressure gap, we have

started ambient pressure X-ray photoemission spectroscopy (XPS) experiments of $\text{Ru}(0001)$ oxidation and water adsorption on $\text{RuO}_2(011)$. Comparing the XPS spectrum of adsorbed water under 1 torr water ambient pressure to that in UHV, we found a new oxygen signal between RuO_2 and chemisorbed water. As shown in the figure below, we detected differences in the O 1s XPS signal between UHV and ambient pressure condition. The “new” state of adsorbed water may play an important role in “real” catalytic reactions under irradiation.



SPECIFIC ACCOMPLISHMENTS:

DOE Basic Research for the Hydrogen Fuel Initiative, LAB 04-20, “Catalyzed Water Oxidation By Solar Irradiation of Band-Gap-Narrowed Semiconductors” Awarded \$800,000/yr for three years

A poster was presented at the Workshop on Opportunities on Nanocatalysis, Terrytown, NY (Oct. 19-21, 2005)

LDRD FUNDING:

FY 2005	\$ 89,092
FY 2006 (budgeted)	\$120,000

Assembling of Biological and Hybrid Complexes on Surfaces

Oleg Gang

05-030

Paul Freimuth

PURPOSE:

Versatile biological functions and highly specific interaction of viral proteins makes them an attractive component for functional self-assembled systems. Functionalized nanoparticles can specifically interact with cell receptors, and can be potentially used for the directed assembly of biological and inorganic objects, targeted drug delivery, and labeling. In the first stage of our research program, we have investigated the functionalization of silica surfaces and nanoparticles with the receptor-binding protein of adenovirus, through the use of physical adsorption. The main focus of these studies is understanding the role of hydrophobic and electrostatic forces in the receptor-binding protein of adenovirus and to elucidate the conditions when its biological function is retained. In the second stage of our studies, we plan to develop methods for attachments of this protein to gold and silica nanoparticles. The developed approaches are integrated in the BNL-wide activity studies and synthesis of nanomaterials and surfaces with biological functionalization.

APPROACH:

We investigated the adsorption of adenovirus knob protein of serotype 12 (Ad12) and 5(Ad5) on silica surface using Atomic Force Microscopy (AFM). Both serotypes have similar structure, but different distributions of charged groups on the surface, and therefore, this is a good model to address a question of the role of

different types of interactions for the protein adsorption at surfaces.

TECHNICAL PROGRESS AND RESULTS:

We measured the change in adsorbed film morphology with time of adsorption and the type of protein. For the adsorption times where adsorption plateaus, the change in film morphology was investigated after the addition of affinity-purified antibodies. The effect of surface hydrophobicity on the Ad12 protein adsorption was also investigated. By treating silica surfaces in different organic solvents, we obtained surfaces with varying contact angles of water drop from 5 to 70°. Ad12 film morphologies were studied on the surfaces having advancing contact angle of 5, 15, 25 and 45°. The obtained morphology results were contrasted with the adsorbed layer thicknesses measured by X-ray reflectivity. With fluorescent microscopy we have measured the extent of adsorption and the ability of Ad12 protein to keep its native conformation by exposing the adsorbed protein layer to fluorescently tagged protein antibodies. This study was done for the silica surfaces of different hydrophobicity as well as for glass surfaces. To better understand the adsorbed protein orientation on the surface, we carried out a study of CAR protein (specific receptor for Ad12) binding to Ad12 protein. CAR protein binds to a different region on Ad12 protein than Ad12 antibodies used in the experiments described above. CAR protein binding was investigated for Ad12 protein adsorbed on hydrophilic silica surfaces, silica surfaces covered with self-assembled organic monolayers, and glass surfaces. CAR binding was detected by chemiluminescence Ad12 protein adsorption and its interaction with antibodies were also studied on silica particles (350nm in size). We also explored the possibility to construct

functional cross-linked protein cages around silica particles – 350nm and 24nm diameter. To contract shell around particles we used Ad12 protein and bovine serum albumine. Different cross-linking strategies were explored – chemical homofunctional crosslink, chemical heterofunctional cross-link (UV initiated), and UV initiated self-crosslinking.

Using AFM and fluorescence techniques showed that Ad12 adsorption increases with the surface hydrophobicity and, while adsorbed, the protein can keep its native conformation – is able to interact with antibodies – on silica particles and glass surfaces and, to a lesser degree, on silica surfaces.

CAR protein is expressed at high levels on normal prostate epithelium, but its levels decrease by about 50% on prostate tumors. We recently found evidence that knob protein injected into the mouse bloodstream efficiently binds to CAR in the prostate. With Drs. Fowler and Dewey in Chemistry, we have begun writing a grant application to develop knob as a probe for PET imaging of prostate tumors, which we plan to submit to

DOD. One component of this project will use knob-coated nanoparticles to block CAR proteins in liver, using methods for knob adsorption that were developed during the first year of this LDRD project. During the next year we will collect preliminary results to produce knob-coated nanoparticles and investigate their targeting to mouse liver using the animal PET camera and other imaging resources unique to BNL.

SPECIFIC ACCOMPLISHMENTS:

“Functionalization of silica surfaces with receptor-binding protein of adenovirus,” NIBIB/DOE Workshop on Biomedical Applications of Nanotechnology Bethesda, MD, March, 2005

“Functionalization of silica surfaces with receptor-binding protein of adenovirus,” DOE Biomolecular Materials Workshop, August 2005

LDRD FUNDING:

FY 2005	\$139,859
FY 2006 (budgeted)	\$140,000

Ultra High Resolution Photoelectron Spectrometer

Peter D. Johnson

05-033

PURPOSE:

This project is aimed at the development of a new ultra high resolution (≤ 100 meV) photoelectron spectrometer for use with lasers or any other photon source having a high rep rate. Examples of the latter might be a Ti-Sapphire laser with a rep rate of 100Mhz or the proposed NLS II storage ring with rep rate of 500 Mhz. The design involves the use of novel time-of-flight (TOF) techniques that may ultimately find use in other TOF spectroscopies. The development of this new capability will greatly enhance our abilities to study the electronic structure and dynamics of strongly correlated sys materials.

APPROACH:

In 1999, the BNL group introduced a new methodology into the long established photoemission technique, namely the momentum distribution curve (MDC) measurement. Here one measures the intensity of photoemitted electrons as a function of momentum at constant energy as opposed to the intensity as a function of energy at constant momentum. A measurement at constant energy is equivalent to a measurement at constant time. Hence, the new methodology points to the possible advantage of TOF spectrometers.

A completely new type of TOF spectrometer has, therefore, been designed and is now in the fabrication phase. The design of the spectrometer includes a parabolic mirror that reflects the electrons into a velocity

selecting filter that is the electronic equivalent of the velocity selecting chopper used in neutron scattering beamlines at neutron sources.

Several new experimental capabilities are being developed in order to test and ultimately use the spectrometer. This includes new capabilities for generating higher harmonics from a Ti-Sapphire laser to obtain light in the UV range, a means of transporting the light from the laser to the experimental chamber and the spectrometer itself. Each of these is a unique challenge in of itself.

TECHNICAL PROGRESS AND RESULTS:

The output from the Ti-Sapphire laser has been frequency doubled and then sum frequency mixed with the fundamental to give the third harmonic. The latter will be sum frequency mixed with the fundamental again to give the fourth harmonic. However, the latter can only be achieved in high vacuum. To this end a new optical table has been designed, constructed, and installed in a vacuum chamber. The latter is now being commissioned.

The new electron spectrometer presented two immediate technical challenges. How to produce high quality flexible grids that could be bent to the parabolic shape and how to manufacture a series of slits 0.2 mm wide that could be aligned accurately with each other over a distance of 20 cms. Both of these challenges have now been successfully achieved.

SPECIFIC ACCOMPLISHMENTS:

None

LDRD FUNDING:

FY 2005	\$67,053
FY 2006 (budgeted)	\$67,000

Metal-Metal Oxide Electrocatalysts for Oxygen Reduction

Miomir Vukmirovic

05-038

PURPOSE:

The goal of this study is to explore platinum monolayers deposited on several metal oxides as electrocatalysts for the oxygen reduction reaction (ORR). The objectives of the study are: i) enhancing ORR kinetics, ii) preventing Pt dissolution, and iii) reducing Pt content in ORR electrocatalysts. The success of this work could ameliorate three major corresponding problems of existing fuel cell technologies. Since there are no such studies of Pt deposited on well-defined single crystal metal oxide surfaces, a knowledge gained in this study can provide the basis for further work with far-reaching consequences for this potentially important area of electrocatalysis.

APPROACH:

Fuel cells are expected to become one of the major sources of clean energy in the not too distant future. Despite definitive advances in recent years, existing fuel-cell technology still has several drawbacks. The inadequate efficiency of energy conversion and the high Pt content of electrocatalysts are connected to the electrocatalytic ORR. Even on the best Pt-based ORR catalysts, the kinetics of ORR is rather slow. Slow ORR kinetics significantly decreases fuel cell efficiency because, for practical current densities, the potential of oxygen cathodes is 0.3 to 0.4 V below the reversible thermodynamic value of 1.23V. For the same reason, practical current densities require a large number of reaction sites, i.e. a large Pt content in oxygen cathodes. A related major problem

is the dissolution of platinum nanoparticles at open circuit potentials of oxygen cathodes. This process has to be drastically reduced to achieve long-term fuel cell performance stability.

To meet the above objectives, the following investigations were carried out: i) synthesis and characterization of oxide substrates, ii) deposition and characterization of Pt monolayers on oxide surfaces, and iii) determining the electrocatalytic activity and stability of Pt monolayers.

Oxide surfaces were synthesized by electrochemical and chemical methods. Electrochemical deposition of Pt monolayers was used including programmed potential pulses that first generate a high density of nuclei and then grow the nuclei to the desired particle size.

In situ electrochemical scanning tunneling microscopy (ECSTM) was used to determine the shape and size of Pt islands and clusters. The electronic properties of Pt deposits were studied by *in situ* X-ray absorption near edge spectroscopies (XANES). Kinetics of the ORR on single crystal samples was determined by potentiostatic methods. A thin film rotating disk electrode, which allows a realistic test of the catalytic properties needed for an actual fuel cell, was used for high surface area samples.

The study was done in collaboration with R. Adzic and K. Sasaki.

TECHNICAL PROGRESS AND RESULTS:

We have found that Pt-OH inhibits the ORR kinetics. Therefore, to enhance the kinetics, the Pt-OH coverage should be decreased. This can be achieved by replacing some of

the Pt atoms with metal atoms, M, that is oxidized at lower potentials than Pt. In that way, higher OH or O coverage on M than on Pt in the Pt-M mixed monolayer would increase lateral repulsion between the OH adsorbed on Pt and the OH or O adsorbed on a neighboring surface metal atom, M. As a consequence, an increased activity for the ORR should be observed. This hypothesis was verified by the enhanced ORR activity for $(\text{Re}_{0.2}\text{Pt}_{0.8})_{\text{ML}}$ mixed monolayer deposited on Pd(111) compared to Pt(111). The enhancement was observed also with the nanoparticle electrocatalyst (Fig. 1). The voltammetry and *in situ* XANES experiments showed that Pt-OH coverage on Pt-Re was considerably decreased compared to pure Pt.

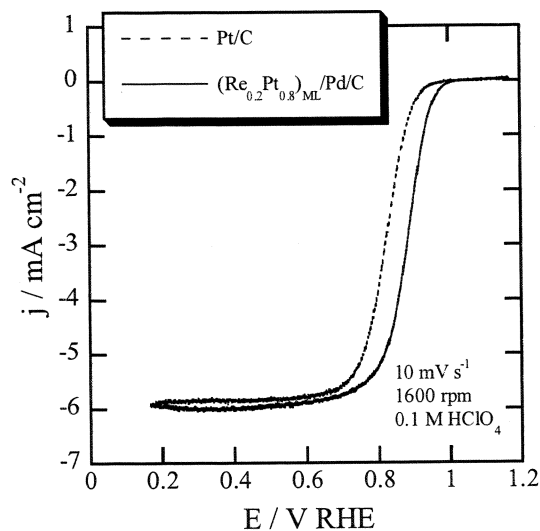


Figure 1. Polarization curves for $(\text{Re}_{0.2}\text{Pt}_{0.8})_{\text{ML}}/\text{Pd}/\text{C}$ and Pt/C, containing $3.8 \mu\text{g Pt cm}^{-2}$ and $12.2 \mu\text{g Pt cm}^{-2}$ respectively.

The RuO_2 film was formed on Pt(111) by electro-oxidation of electro-deposited Ru. The ECSTM revealed closely spaced RuO_2 islands of a monolayer in height and 5 nm in diameter. The voltammetry study showed that the half-wave potential of the ORR on RuO_2/Pt is 30-40 mV less positive than that of Pt(111), suggesting high activity.

Pt was electrochemically deposited from 1 mM K_2PtCl_4 onto electrochemically or chemically grown RuO_2 . Electrochemically grown RuO_2 was obtained by oxidizing Ru(0001). The ECSTM reveals that the Ru(0001) surface is covered with RuO_2 islands. Their size and population could be controlled by the potential. Also, ECSTM revealed that Pt deposits exclusively on RuO_2 , but not on surrounding OH-covered Ru surface. The half-wave potential of the ORR on Pt/ RuO_2 is 60 mV less positive than that on Pt(111), suggesting high activity of this surface. Chemically grown RuO_2 , shown in Fig. 2., was obtained by our newly developed induction heating setup. The ECSTM showed an extremely low population of Pt islands. Pt islands were more than 200 nm in diameter and 20 nm in height. Electrochemical studies showed that the nucleation was instantaneous. This deposit has lower activity for ORR than Pt, which is expected for such size of Pt islands.

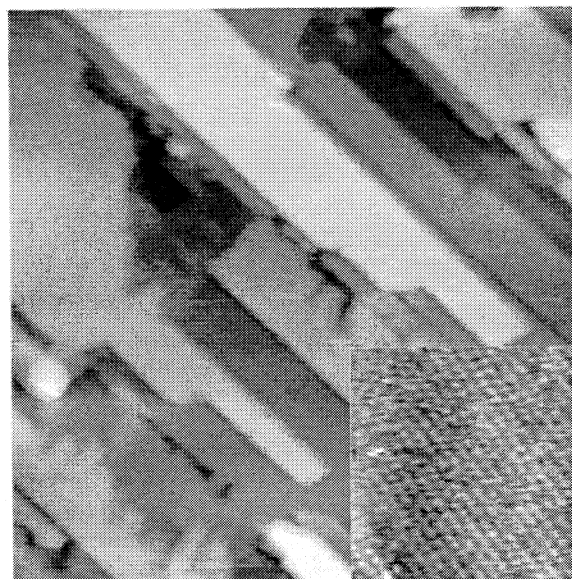


Figure 2. ECSTM image of chemically oxidized Ru(0001). Size 200 x 200 nm. Inset shows the atomically resolved $\text{RuO}_2(110)$ surface.

Synthesis and evaluation of new electrocatalysts comprising monolayer-level Pt on niobium oxide nanoparticles (NbO_2)

for ORR were also carried out. The average diameter of the niobium oxide nanoparticles was *ca* 11 nm determined by TEM and XRD. Preliminary electrochemical tests using the rotating disk electrode technique indicated that the Pt/NbO₂/C electrocatalyst (5 μg cm⁻² Pt) showed more than 5 times higher Pt mass activity for the ORR compared with that of a commercial Pt/C electrocatalyst (Fig. 3.). The half-wave potential for the ORR on the Pt/NbO₂/C electrocatalyst was 40 mV higher than that for the commercial Pt/C electrocatalyst. This is a new promising system for practical applications.

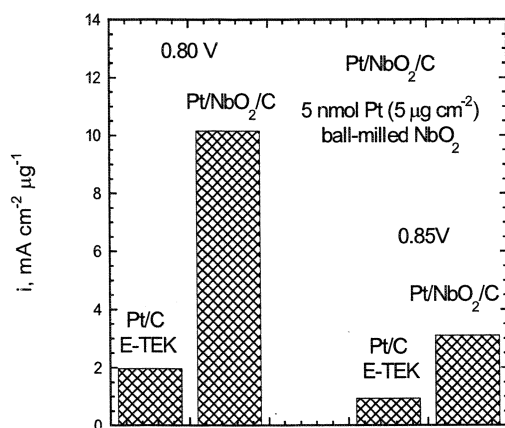


Figure 3. Pt mass activities for Pt/NbO₂/C and commercial Pt/C electrocatalysts for the ORR in 0.1 M HClO₄. Data obtained by K. Sasaki.

The plan for FY 2006 is to deposit Pt on well defined Nb₂O₃, NbO₂, Na_xWO₃ and ReO₃, as well as an investigation of their activity for ORR. *In situ* XANES studies of the electronic properties of Pt induced by the metal oxide substrate, as well as, the atomic structure of Pt deposition are also planned. A durability test using a real operating fuel cell will be carried out.

SPECIFIC ACCOMPLISHMENTS:

Funding obtained for the DOE proposal on ORR on metal-metal oxides that evolved from this project. \$703,000 less \$90,000 subcontract with Illinois Institute of Technology

One patent application submitted for H&B Docket No. 369-215, BNL No. BSA 05-12, Request No. 2118): Electrocatalyst for Oxygen Reduction with Reduced Platinum Oxidation and Dissolution Rates.

Expected funding from GM, certain DuPont. (\$85,000 for one year) for Synthesis and Characterization of Low Platinum Content Electrocatalysts for Methanol Oxidation.

J. Zhang, M. B. Vukmirovic, K. Sasaki, A. U. Nilekar, M. Mavrikakis, and R. R. Adzic, *Mixed-Metal Pt Monolayer Electrocatalysts for Enhanced Oxygen Reduction Kinetics*, J. Am. Chem. Soc., **127** (2005) 12480.

LDRD FUNDING:

FY 2005	\$99,510
FY 2006 (budgeted)	\$103,000

Multifunctional Nanomaterials for Biology

Stanislaus S. Wong

05-041

PURPOSE:

We would like to synthesize nanomaterials with simultaneous biological and physical functions for application in life sciences. As a starting point we will explore the use of carbon nanotubes as a platform for integrating biological specificity with physical function such as fluorescence or conductivity. We seek to put Brookhaven in a position of leadership in the field of *highly-specific* biochemical detection.

This will allow us to probe biological systems in ways that are not readily accessible using other methods.

APPROACH:

Single-walled carbon nanotubes (SWNTs) can be functionalized with biomolecules both inside their internal cavities as well as on their external surface. For instance, proteins such as cytochrome C can be immobilized inside the internal cavities of SWNTs retaining their native conformation and biological activity. Similarly, enzymes, proteins, peptides, antigen-antibody complexes, viruses and oligonucleotides can readily bind to the SWNT surface either nonspecifically by noncovalent interactions or through covalent sidewall functionalization of SWNTs. For instance, proteins have been successfully attached onto the surfaces of SWNTs functionalized with 1-pyrenebutanoic acid succinimidyl ester. An alternative method of immobilization is associated with the binding of proteins onto oxidized SWNTs via diimide linkage in aqueous solution.

In the present work we have investigated the biocompatibility and feasibility of a ligand-receptor protein system bound to oxidized SWNTs via a diimide linkage. The proteins of interest in our study include an adenovirus protein, Ad12 Knob, and its complementary human 'coxsackievirus and adenovirus receptor,' i.e. CAR. Adenoviruses are one of many subclasses of viruses that can cause infection such as the common cold as well as mild ailments associated with the upper respiratory and gastrointestinal tracts. Unlike viruses such as HIV, ebola and poliovirus, adenoviruses do not use envelope proteins or capsid domains to infect cells. Rather, infection is initiated by the formation of a high affinity complex between the Knob trimer and its complementary adenovirus CAR receptor present in the human cell. Upon CAR binding, the Knob coated virus replicates within the cell nuclei, causing infections. Adenoviruses are currently leading candidates as vectors in gene therapy.

TECHNICAL PROGRESS AND RESULTS:

Raw Hipco SWNTs were purified and air oxidized with a modification of a known gasification-dissolution method. This process generates surface functionalities particularly carboxylic acids at the ends and side walls of the nanotubes. The air oxidized (AO) SWNTs were then suspended in 50 mM pH 8 phosphate buffer at a concentration of 1 mg/mL. Both Ad 12 Knob and YieF were labeled using an Alexa Fluor protein labeling kit. Fluorescently labeled anti-Knob antibodies were provided by Dr. Paul Freimuth (BNL). Labeled proteins were collected carefully into the collection tubes and were stored at -4°C .

The proteins were then attached to the AO SWNTs via a two-step process of diimide-activated activation as previously described.

The detailed expression, purification and labeling of proteins and preparation of SWNT-protein hybrids have been determined. Confirmation of protein binding to SWNTs was revealed by atomic force microscopy (AFM) analysis.

We have also studied the interaction of these aggregates with both complementary and non-complementary-labeled proteins with our SWNT-protein conjugates, enabling us to test the activity and specificity of the bound, attached proteins.

The biological activity of bound Ad 12 Knob was investigated by targeting rhodamine labeled anti-Knob antibodies to the AO-SWNT- Knob constructs. These antibodies were purified by using wild type Ad 12 Knob and hence, targeted only Knob proteins folded in specifically active conformations. Non-specific binding of rhodamine-labeled anti-Ad 12 Knob protein attached to carbon nanotubes was prevented by using 4% milk as a blocking agent. The presence of fluorescent carbon nanotubes confirms that Ad 12 Knob bound to SWNTs indeed retains its biological activity. As control experiments, labeled anti-Knob antibodies were targeted to SWNTs in the absence of protein, both in the presence and absence of milk blocking. We observed sample fluorescence in both controls, indicating the presence of binding of labeled antibodies onto the SWNTs. Conversely, there was little or no fluorescence observed for SWNTs that had been blocked with milk, suggesting the efficacy of milk as a blocking agent. Hence, we demonstrated that labeled anti knob antibodies could specifically target bound Knob proteins on SWNTs.

By analogy, to investigate the biological activity and specificity of bound CAR, we used fluorescently labeled Knob and YieF in separate experiments. Whereas, Ad12 Knob is specific to CAR, YieF is nonspecific to

CAR. Hence, the presence of bound CAR proteins will show specificity to Knob proteins. SWNT-CAR constructs were blocked by 0.4 % milk to avoid any non-specific binding of the labeled proteins to the nanotubes. The sample of SWNT-CAR constructs targeted by Ad 12 Knob fluoresces, indicating the presence of binding of Knob to bound CAR proteins. On the other hand, the samples did not fluoresce at all when the labeled Ad 12 knob was replaced by labeled YieF. This observation satisfied three purposes: (1) this experiment gave additional evidence that CAR is bound to the carbon nanotubes; (2) the bound CAR is biologically active; and (3) CAR functionalized nanotubes are specific to the presence of Ad 12 knob. Thus, this idea can be used as the basis of a biological sensor for the determination of the presence of Ad 12 Knob viral protein.

Goal for FY 2006

We will use proteins involved in mercury resistance as a model system. Many of these proteins are also found as part of other heavy metal resistance systems, such as lead resistance, which will allow us to extrapolate our results for the construction of new sensors with different metal specificity. These proteins will be integrated with nanotubes to obtain a functional biosensor.

SPECIFIC ACCOMPLISHMENTS:

Publication:

Vasiliki Zorbas, Mandakini Kanungo, Sukhmine A. Bains, Yuanbing Mao, Tirandai Hemraj-Benny, James A. Misewich, and Stanislaus S. Wong, "Current-less Photoreactivity Catalyzed by Functionalized AFM Tips," *Chem. Comm.*, (36), 4598-4600 (2005).

"Oxide Nanostructures," New York Nano-science Discussion Group. Joint Meeting

with the Nanoscience Topical Group (New York Section) of the American Chemical Society, New York University, New York, NY, September 20, 2005.

230th *American Chemical Society National Meeting*, Washington, DC, August 28-September 1, 2005.

- "Demonstration of Diameter-Selective Reactivity in the Sidewall Ozonation of SWNTs by Resonance Raman Spectroscopy."

Poster presentations given at 2005 Gordon Research Conference, entitled *Chemistry of Electronic Materials*. Connecticut College, New London, CT, July 17-22, 2005.

- "General, room-temperature method for the synthesis of isolated as well as arrays of single-crystalline ABO₄-type nanorods"
- "Synthesis and Characterization of Multiferroic BiFeO₃ nanotubes"
- "Large-Scale Synthesis of Single-Crystalline Perovskite Nanostructures"

"Nanovision: Nanotubes, Nanorods, and Nanoparticles," presentation at the following universities/governmental institutions:

- Department of Chemistry, University of California at Irvine, June 7, 2005.
- Department of Chemistry, University of California at Los Angeles, June 6, 2005.
- 404th Brookhaven Lecture, Brookhaven National Laboratory, May 18, 2005.

Competitive Grants Received:

Department of Energy (Office of Science – Office of Basic Energy Sciences, Materials Sciences and Engineering Division)

Grant Title: Synthesis and Characterization of Individual Carbon and Perovskite Oxide Nanotubes

PIs: James Misewich and Stanislaus Wong.
Proposal: \$1,347,000 – 8/31/04 to 9/30/06;
20% effort

(ii) *SUNY Stony Brook - BNL Seed Grant Program*

Title: Probing Potential Cellular Toxicity of Purified Carbon Nanotubes and Perovskite Nanotubes

PIs: Stanislaus S. Wong with Barbara Panessa-Warren (collaborator at BNL Materials Science Dept)

Proposal - \$20,000 – 09/01/04 to 08/31/05;
5% effort

(iii) *National Science Foundation*

Grant Title: NER: Large-scale synthesis of boron-containing nanostructures

PI: Stanislaus S. Wong. Proposal: \$100,000
– 09/01/04 to 08/31/05; 10% effort

(iv) *National Science Foundation*

Grant Title: CAREER: Rational Synthesis and Studies of Functionalized Carbon Nanotubes

PI: Stanislaus S. Wong. Proposal: \$568,352
– 01/01/04 to 12/31/08; 20% effort

(v) *3M Nontenured Faculty Awards (competitively renewed twice already)*

Title: Bioadhesion

PI: Stanislaus S. Wong. Proposal – \$45,000
– 09/01/02 to present; 5% effort

(vi) *SUNY Stony Brook - BNL Seed Grant Program*

Title: Microscopy for Biomolecular Structure Analysis

PI: Stanislaus S. Wong with Joseph S. Wall (collaborator at BNL Biology Department)

Proposal - \$14,000 – 09/01/02 to 08/31/04;
5% effort

(vii) *American Chemical Society Petroleum Research Fund – Type 'AC' grant*

Grant title: 'Catalytic Probe Microscopy'

PI: Stanislaus S. Wong. Proposal: \$79,985
– 9/01/03 through 8/31/05; 10% effort

(viii) American Chemical Society Petroleum Research Fund – Type ‘G’ Starter grant (completed)

Grant title: ‘A Strategy for Photoreactivity at the Nanometer Scale’

PI: Stanislaus S. Wong. Proposal: \$25,000 – 9/01/01 through 8/31/03; 10% effort

(ix) Individual Development Award – United University Professions (completed)

PI: Stanislaus S. Wong. Proposal: ~\$450 – 9/01/02 through 6/30/03. 5% effort

(x) SUNY Stony Brook - Presidential Mini-grant Award for Innovative Teaching Projects (completed)

Title: A Pilot Program for Improving Undergraduate Physical Chemistry Laboratory Courses

PI: Stanislaus S. Wong. Proposal: \$650 – 7/01/01 to 7/01/02; 5% effort

LDRD FUNDING:

FY 2005	\$128,192
FY 2006 (budgeted)	\$130,000

Polariton-Enhanced FRET for Device-Integration of Plasma Membranes from Rhodobacter Sphaeroides

Chi-Chang Kao

05-042

PURPOSE:

The purpose of this project is to investigate the influence of surface plasmon polaritons on the fluorescence resonance energy transfer (FRET) between chromophores on metal surfaces. The suspicion is that the nonlocality of surface plasmons will enhance FRET over large distances, which could become a means to exploit this phenomenon in a device. It was our intention to investigate plasma membranes from the photosynthetic bacteria rhodobacter Sphaeroides, as well as free fluorescent dyes, deposited on metal surfaces.

APPROACH:

FRET occurs between donor acceptor pairs, i.e. pairs of molecules in which the absorption energy of one (the acceptor) is matched to the emission energy of the other (the donor). If they are sufficiently close together ($< 100 \text{ \AA}$), energy can be transferred nonradiatively from donor to acceptor. The way FRET is measured experimentally is to excite the donor and look for fluorescence from the acceptor.

Our strategy for this project was to first build a fluorescence spectroscopy setup consisting of a solid state dye laser and emission spectrometer. The plan was to deposit dyes and membrane proteins on metal surfaces by suspending them in volatile solvents (e.g. methanol) at controlled concentrations and depositing them on the surfaces with a micropipette.

The intention was to also experiment with self-assembly techniques for the membrane proteins. We would then measure the efficiency of FRET in these samples as a function of density, morphology etc., to see if FRET might occur, for example, over a larger distance than in solution. The plasma membranes were to be grown in the lab of James Shapleigh in the Microbiology Department at Cornell University.

TECHNICAL PROGRESS AND RESULTS:

Recruited Serban Smadici, a graduate of Rick Osgood's group Columbia. In the first four months we constructed the complete fluorescence setup for FRET measurements (Fig 1.) It consists of a Spectra Physics air-cooled Ar ion laser, Ocean Optics USB2000 fluorescence spectrometer, focusing optics, and a sample stage. Fluorescence is coupled into the spectrometer with an optical fiber. This project requires very clean, evaporated films of Au and Ag. Purchased pre-evaporated Ag and Au microscope slides from EMF Corporation.

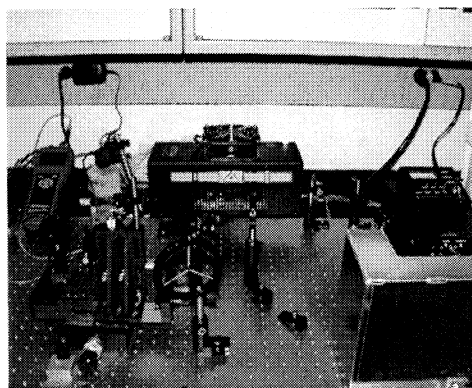


Figure 1: Newly constructed and fully functional FRET setup, consisting of an air-cooled Ar laser, USB2000 fluorescence spectrometer, housing etc.

For simplicity we chose to begin measurements with dyes rather than bacterial membranes. We chose to use

Fluorescein (“F”, the donor) and Tetramethylrhodamine 668 (“T”, the acceptor) because the absorption band of F is matched to the 488 line from the Ar laser. These were purchased from Molecular Probes. We have also already obtained purified plasma membranes of rhodobacter Spheroides from the Shapleigh lab, though these will remain in the deep freezer until we complete a set of measurements on dyes.

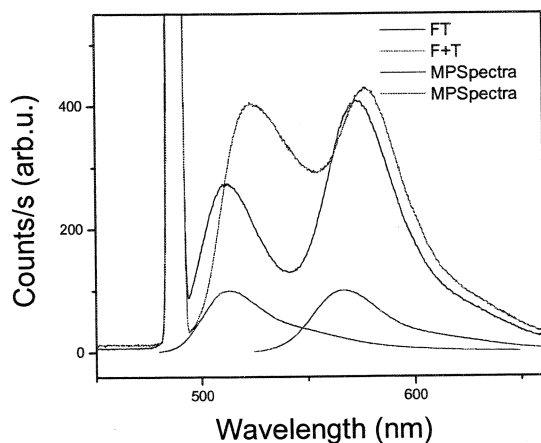


Figure 2: Fluorescence measurements in solution from F and T. (blue) Spectra from independent dyes. (red) The sum of independent F and T spectra. (black) Spectra from a mixed solution of F and T. The enhanced peak at 575 nm indicates FRET energy transfer between the dyes.

The first fluorescence measurements from F and T, taken in solution, are displayed in Figure 2. After some experimentation we were able to observe the signature of FRET in these measurements, which is enhanced emission from the acceptor dye.

We went on to begin measurements of dyes deposited on Ag and Au surfaces. T and F

were deposited on substrates using the solvent technique described. Surprisingly, we were unable to detect fluorescence from these samples as the fluorescence from the dyes was being quenched by contact with the metal surface. Preventing this requires placing an optically inactive buffer layer between the metal film and the dyes, which can also enhance the interaction with surface plasmons by placing the dyes in the peak of the evanescent field. For this purpose we are in the process of spin coating our substrates with polymethyl methacrylate (PMMA), which is insulating, optically inactive and whose thickness can easily be controlled. Once this is complete we should be able to obtain surface measurements.

PMMA in addition to acting as a spacer layer, provides a means to pattern the surfaces, which will allow us to control the geometry of dyes on the surface. This will also eventually help us to explore device-relevant geometries.

In the next year we anticipate observing FRET on an appropriately buffered surface and obtaining some systematics on the influence of surface plasmons. We plan to also begin experimenting with patterning the PMMA.

SPECIFIC ACCOMPLISHMENTS:

None

LDRD FUNDING:

FY 2005	\$79,321
FY 2006 (budgeted)	\$80,000

Intense THz Source and Application to Magnetization Dynamics

G. Lawrence Carr

05-044

D. A. Arena

PURPOSE:

Despite continuous progress in developing laser-based sources of coherent THz radiation pulses over the past 15 years, these THz sources have been limited mostly to linear spectroscopy. The issue is the low intensity of the THz pulses, whether derived from photoconductive switch sources or produced by electro-optic rectification. It is now recognized that the coherent THz from relativistic electrons can be orders of magnitude larger, opening the possibility for studying materials in the “high field regime” (E-field greater than 10^5 V/cm). In this project, we are developing an innovative coherent THz source based on relativistic electrons from the Source Development Lab (SDL) linac of the NSLS. In preliminary work, we have observed extremely intense and ultrashort THz pulses from this linac source. Our intention is to fully characterize the source, and then initiate a set of measurements where the intense THz pulses are used to produce rapid excitations in magnetic thin films. Other measurements being planned or considered include ultra-fast current transients in superconductors and non-linear optical effects in polar crystals (e.g., perovskites) or carbon nanotubes that are induced by the intense THz fields. The successful implementation of these plans will provide BNL with the basis to develop a vibrant new user community based on the use of intense, ultra-short THz pulses.

APPROACH:

The SDL linac-based THz source uses ~120 MeV, 350 fs long electron bunches (~ 800 pC). The THz radiation is produced as “transition radiation” when the electrons are incident onto a metal mirror. Because the electron bunch is less than 1 ps in duration, the emitted radiation pulse is coherent for frequencies up to 1 to 2 THz. The energy in such a THz pulse is about 100 μ J, about a factor of 100X higher than what has been achieved using photoconductive switch sources. When strongly focused, the electric field is expected to peak near values of 1 MV/cm. This makes the SDL THz source an ideal instrument for investigating strong-field properties of materials on ultra-fast time scales. The transient magnetic field, with values greater 1 kG, can also be used for the practical study of magnetization dynamics, which is a primary theme for this project.

The initial phase of the scientific plan is to develop the optical apparatus to more fully characterize the THz source. This involves designing and constructing THz collection and focusing optics and incorporating a facility to co-propagate an ultra-short laser pulse that will be used for electro-optic sampling of the THz fields.

After the THz fields are well characterized, experiments involving a type of magnetic “imprinting” will be conducted. In these measurements, magnetic thin films are exposed to the THz pulses, which should result in a re-orientation of the magnetic domain pattern. The resulting domain pattern can be imaged *ex-situ* and the results compared to images of the domain pattern of unexposed samples. We have initiated a collaboration with researchers at NIST in Gaithersburg, MD. They will perform the imaging of the magnetic domain patterns as this capability is not available at BNL. After demonstrating the efficacy of the THz pulses

as an excitation source for magnetization dynamics, we will modify the set-up to conduct time-resolved magneto-optic Kerr effect (TR-MOKE) measurements of hard ferromagnets. TR-MOKE is a standard technique used in studies of ultrafast magnetization dynamics, but is typically limited to studies of soft ferromagnets. The THz pulses can extend the range of TR-MOKE to harder ferromagnetic materials.

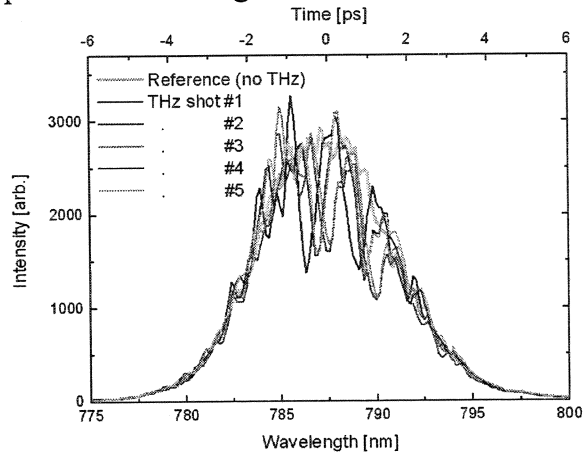
In addition, we plan to study THz-induced excitations in superconductors and correlated electron systems. For this work, the large electric field of our THz pulses would be used to drive super currents in excess of the critical value, leading to a new type of non-equilibrium state. Our E-field strengths of 10^5 to 10^6 V/cm exceed estimates for the required field by more than an order of magnitude.

TECHNICAL PROGRESS AND RESULTS:

To date, technical efforts have proceeded along two paths. First, for the magnetization imprinting studies, we have grown thin, epitaxial Fe films on MgO(100), which is a substrate that is transparent to THz radiation (to avoid some of the complications that arise from strong THz reflections at the film/substrate interface). Also, without imprinting, these films have been examined by our collaborators at NIST to determine the native domain pattern of the films.

In parallel with these efforts, we have been implementing the electro-optical detection technique needed to characterize the spatial and temporal profile of the THz pulse. This effort involves collecting and focusing the coherent THz onto a ZnTe crystal and co-propagating a polarized, chirped laser pulse with the THz pulse. The large electric field of the THz pulse induces a birefringence in the ZnTe, which in turn modifies the

polarization of the laser pulse. Spectral analysis of the modified laser pulse can be directly related to the instantaneous electric field of the THz. Examples of preliminary measurements using these techniques are presented in the figure below:



A post-doctoral research associate was hired (D.A. Arena) to conduct the magnetization dynamics experiments and help implement the electro-optical sampling of the THz pulses. We prepared and characterized an initial set of ferromagnetic films for use in the transient dynamics study (D. Arena). Successfully implemented and collected a complete E-field waveform by single-shot electro-optic detection.

SPECIFIC ACCOMPLISHMENTS:

Hosted a workshop (May '05) on Applications of Intense THz Pulses from the SDL Linac. Spectroscopy with Coherent THz Pulses at the NSLS SDL Linac. Carr, G. L.; Loos, H.; Sheehy, B.; Arena, D.; Smith, R. J.; Kao, C. -C.; Tsang, T.; Murphy, J. B.; Watanabe, T.; and Wang, X. -J., BNL Workshop on Intense Coherent THz Pulses, Upton, NY, May 10-11, 2005.

LDRD FUNDING:

FY 2005	\$ 50,175
FY 2006 (budgeted)	\$100,000

Nano-Imaging of Whole Cells with Hard X-Ray Microscopy

Lisa M. Miller

05-048

PURPOSE:

The objective of this work is to develop 3-dimensional, high-resolution, hard x-ray imaging for the study of whole living (frozen) cells. This project takes advantage of the high brightness and coherence of synchrotron light and recent advances in new x-ray imaging technology (i.e. hard x-ray zone plates). To date, other imaging techniques are limited by sample thickness, e.g. soft x-ray microscopy is limited to <1 μm and electron microscopy is limited to < 100 nm. In this work, we aim to improve the sample penetration depth to 50 – 100 μm (the thickness of typical cells) and the spatial resolution to <20 nm by using hard x-rays for 3-D imaging. The NSLS has several beamlines that are well suited for developing hard x-ray microscopy and also has an accomplished user base for the development and implementation of x-ray zone plates. This new technique will become a key element in the ongoing development of a Biomedical Imaging program at the NSLS.

APPROACH:

Currently, confocal microscopy with visible light is the most common method of imaging biological processes in living cells. However, the primary drawback to this technique is the diffraction-limited spatial resolution of ~300 nm. This resolution can be used to image large sub-cellular organelles but cannot be used to study smaller sub-cellular structures such as cell membranes and individual protein complexes.

Other imaging techniques with higher spatial resolution, such as electron microscopy and soft x-ray microscopy, have limited sample penetration depths so that only small cells and/or particles can be studied. We are working towards the development of an x-ray microscope that surpasses any other at the NSLS in both spatial resolution and sample penetration depth. This type of spatial resolution will enable cellular processes, such as apoptosis and mitosis, to be studied in the native cellular environment to provide new insight into the way cells behave as “molecular machines.” Moreover, the development of this nanoscale tool will not only be applicable to biological systems, but will be valuable for the study of numerous other nanoscale structures in the chemical, materials, and environmental sciences fields.

The specific aims of this proposal are: (1) to customize and test a hard x-ray zone plate to a NSLS bending magnet beamline, (2) to develop cryogenic cooling techniques, (3) to adapt current electron microscopy biochemical tags for hard x-ray microscopy, and (4) to apply the newly developed technique to image cellular processes such as mitosis or apoptosis.

TECHNICAL PROGRESS AND RESULTS:

In FY 2005, Meghan Ruppel developed methods for combining epifluorescence microscopy with hard x-ray microprobe in collaboration with Dr. Antonio Lanzirotti (University of Chicago). This was the work of Ms. Ruppel's M.S. thesis (SBU Dept of Materials Science and Engineering). In late FY 2005, Ms. Ruppel set up a cell culture laboratory at the NSLS and tested methods for growing fibroblasts (human skin melanoma cells) on x-ray transparent materials including formvar, silicon monoxide, and silicon nitride.

Also in FY 2005, in collaboration with Dr. Yen-Fang Song at the National Synchrotron Radiation Research Center (NSRRC) in Taiwan, we collected hard x-ray microscopy images of microdamaged bone samples in both absorption and phase contrast mode. These experiments were performed to test the technology on samples that were not radiation-sensitive. Based on the results of these experiments, additional beamtime has been awarded at the NSRRC in March 2006 to continue the work on whole fibroblasts. These experiments will be performed at the NSRRC while the appropriate technology is developed at the NSLS.

In FY 2006, we will begin to adapt immunogold tags (standard antibody-conjugated labels) for x-ray microscopy and test them at the NSRRC and NSLS. We will begin to examine methods for cryogenic sample cooling. In collaboration with Dr. Ken Evans-Lutterodt, we will investigate other methods of phase contrast imaging.

SPECIFIC ACCOMPLISHMENTS:

Publications:

FY 2005: L.M. Miller, M.E. Ruppel, C.H. Ott, A. Lanzirotti. (2005) Development and

Applications of an Epifluorescence Module for Synchrotron X-Ray Fluorescence Imaging. *Rev. Sci. Instr.*, **76**: 066107.

Abstracts:

FY 2005: R. Smith, Q. Wang, L.M. Miller. "Combining IR Microscopy and X-ray Fluorescence Microprobe Using a Patterned Sample Substrate." 2005 NSLS Users Meeting, May 23-25, 2005.

M.E. Ruppel, D.B. Burr, L.M. Miller. "Chemical Makeup of Microdamaged Bone Differs from Undamaged Bone." 2005 NSLS Users' Meeting, May 23-25, 2005.

Thesis:

FY 2005: M.E. Ruppel. "Development and Applications of an Epifluorescence Module for Synchrotron X-ray Fluorescence Imaging." Master of Science, Department of Materials Science and Engineering, Stony Brook University.

LDRD FUNDING:

FY 2005	\$19,496
FY 2006 (budgeted)	\$80,000

Study to Convert the NSLS VUV Ring to Coherent IR Source

Boris Podobedov

05-050

PURPOSE:

The IR user program based on the NSLS VUV/IR ring is presently the strongest in the world. As we move forward with the NSLS-II Project, we would like to preserve and expand the infrared (IR) and THz capabilities for this vibrant user community. To this end we propose to move the existing NSLS VUV/IR ring to be part of the NSLS-II complex and to operate it with top-off injection. The ring would serve the IR user community exclusively, while the present VUV (vacuum ultra-violet and soft X-ray users would migrate to the new NSLS-II ring.

With an eye toward expanding the capabilities of our workhorse IR source, we are investigating the potential of operating the NSLS VUV/IR ring as a coherent IR facility by adding a high frequency superconducting RF (SCRF) system. We are exploring the various coherent synchrotron radiation (CSR) emission regimes possible for both the existing and the upgraded VUV/IR ring. Broadly formulated, the definition of success for this LDRD is the feasibility determination of a future VUV/IR ring upgrade with the added coherent mode of operation, as well as the choice of the optimal RF system and other accelerator hardware necessary for this upgrade.

APPROACH:

While potentially capable of providing the users with far-IR and THz spectral ranges that are several orders of magnitude higher in photon flux compared to the standard

incoherent mode of operation, the performance in this configuration is not easily estimated. In fact, only one ring in the world (BESSY, Germany) has recently achieved this mode of operation and there is still intense debate in the accelerator community as to what exactly limits the performance. The primary factors defining the photon flux are the maximum achievable current and minimum achievable bunch length. These in turn depend on complexities of electron beam dynamics in the ring and are usually limited by various instabilities.

The RF system is one of the primary elements affecting longitudinal beam dynamics including instability thresholds, and therefore one of the primary outcomes of this LDRD would be a recommendation of the optimal RF system to provide the best performance in this new mode of operation. Generally the RF system choice is constrained due to engineering and operational issues such as the availability of cavities and power sources, injection system compatibility, as well as cost and other factors. First, however, there is still an unresolved accelerator physics question being addressed by this LDRD, as to what is the optimal RF system choice within the aforementioned constraints for the future VUV/IR ring upgrade.

Dynamics of very short and intense electron bunches in storage rings, when they are significantly interacting with emitted CSR as well as vacuum chamber components, is not entirely understood. Existing theories are fairly complex and yet they usually deal with very simplified models of the impedance. This is why in our view the experimental work as well as computer simulations must be performed.

In particular, to probe the short bunch length regime experimentally, we will do (or have already done) the following:

- 1) exploit the flexibility of the NSLS VUV ring magnet lattice, which allows orders of magnitude reduction in momentum compaction,
- 2) store small beam currents with just the 4th harmonic (211 MHz) RF cavity,
- 3) perform similar studies at the MIT-Bates ring which incorporates a unique 2856 MHz RF system allowing for very short bunches (few orders of magnitude shorter than what's available in the present NSLS VUV/IR ring).

Future studies will include impedance and instability studies, calculations and set up of an optimal magnetic lattice, measurement of coherent emission and the assessment of the operational impact of the proposed upgrade. We will examine the possibility of using an SCRF system identical to the NSLS-II SCRF system which could allow us to prototype the ring RF system and get an early start on coherent IR operation on the IR ring.

TECHNICAL PROGRESS AND RESULTS:

Most of the work performed to-date was experimental in nature and took place in the MIT-Bates South Hall Ring as mentioned in item 3) above. This timeline was significantly influenced by the Bates running schedule. Specifically, as the Bates nuclear physics program was nearing completion, the accelerator operation was about to cease.

Our technical progress to date can be briefly summarized as follows. For the first time in the history of the Bates facility, longitudinal beam dynamics has been extensively characterized, using the hardware and expertise from BNL. Low momentum compaction lattices, that should provide

significantly shorter bunches than the nominal 18 ps rms bunch length used for nuclear physics experiments have been established. With these lattices, bunches as short as a few ps rms have been measured (see Figure 1, taken from [3] below). To observe CSR emissions from these short bunches, a beam line off one of the bending magnets has been built. Subsequently, CSR emissions with their characteristic quadratic dependence on beam intensity were measured applying several different techniques developed earlier at the NSLS. The spectral and time structure of these emissions have been extensively characterized [3].

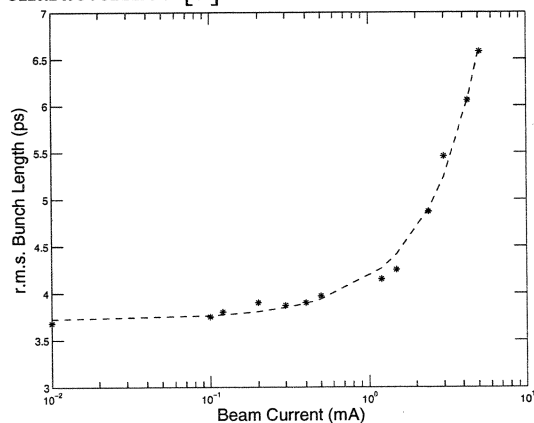


Figure 1: Bunch length measured with a streak camera vs. beam current.

So far the CSR emissions have only been observed in the so-called bursting mode, where the intensity of emitted photons drastically fluctuates on a tenth of a second time scale. While interesting from an accelerator physics point of view, this bursting mode significantly degrades the quality of the photon beam available to the users. Our final goal at the NSLS is to control the onset of this bursting mode as well as being able to operate the accelerator below the bursting mode threshold. Presently, the existence of this bursting mode is believed to be due to an instability caused by the CSR and the regular vacuum chamber impedance combined.

One of the most intriguing findings of significant relevance to the future NSLS IR ring is that the instability threshold appears to be a factor of about 40 lower than what is predicted by the present theories using the best known model of the Bates ring impedance.

As a result of these studies a clear pathway forward has been established for the Bates part of this research. It includes establishing single bunch injection capability, further work on lattices, improvement in diagnostics, identification and removal of harmful impedance components, etc. When this is completed future experimental runs at MIT-Bates with BNL participation to address unresolved issues in beam dynamics could take place. However, all future experimental work at Bates is dependent on its ability to attract funding to operate the accelerator which is presently shut down.

This fiscal year we are switching to the rest of the items listed in the Approach Section above, which will be performed at the existing NSLS VUV/IR ring or via computer simulations.

SPECIFIC ACCOMPLISHMENTS:

Non-refereed publications

[1] F. Wang, D. Cheever, W. Franklin, W. Graves, M. Farkhondeh, E. Ihloff, J. Van der Laan, C. Tschalar, D. Wang, D.F. Wang, T. Zwart, L. Carr, B. Podobedov, F. Sannibale, "Terahertz Coherent Synchrotron Radiation in the MIT Bates South Hall Ring," Proceedings PAC2005.

[2] D. Cheever, W. Franklin, W. Graves, M. Farkhondeh, E. Ihloff, J. Van der Laan, C. Tschalar, D. Wang, D.F. Wang, F. Wang, T. Zwart, B. Podobedov, "Very Short Bunches in MIT Bates South Hall Ring," Proceedings PAC2005.

Refereed publications

[3] F. Wang, D. Cheever, M. Farkhondeh, W. Franklin, E. Ihloff, J. Van der Laan, B. Mcallister, R. Milner, C. Tschalar, D. Wang, D.F. Wang, A. Zolfaghari, T. Zwart, L. Carr, B. Podobedov, F. Sannibale, "Coherent THz Synchrotron Radiation from a Storage Ring with a High RF Frequency System," submitted for publication to Physical Review Letters, Oct. 2005

LDRD FUNDING:

FY 2005	\$ 49,261
FY 2006 (budgeted)	\$130,000

Superconducting Undulator Technology

George Rakowsky

05-051

PURPOSE:

Short-period superconducting undulators (SCUs) have been proposed as the ultimate X-ray sources for Protein Crystallography (PX) beamlines in NSLS-II and other high-brightness synchrotron radiation sources. Current technology of short period SCUs is limited by (a) low critical current of conventional NbTi superconductors, (b) quenching in presence of electron beams and synchrotron radiation, and (c) lack of means for "shimming" to correct field errors. In this project we seek to demonstrate technologies that may overcome these limitations and provide a basis for the design of long (up to 5 m) SCUs that will meet the demanding requirements of NSLS-II.

APPROACH:

Task (a): In-vacuum permanent-magnet undulators, pioneered at NSLS and Spring8, are the current baseline technology proposed as photon sources for PX beamlines in NSLS-II. However, the peak fields obtainable with permanent magnet technology are too low to provide the 3:1 tuning range needed for full spectral coverage by the fundamental, third and higher undulator harmonics in the multi-keV photon energy range of interest to PX. Higher fields have been achieved in SCUs wound with conventional NbTi, but these fall short in peak field and tunability. Other National Labs (LBNL, in particular) are attempting to achieve the required high fields using Nb₃Sn to build SCU models. Nb₃Sn does operate at higher J_c, but it is very brittle, and the wind-and-react

construction technique used with Nb₃Sn is more difficult.

A promising SC material with higher J_c is NbTi with artificial pinning centers (APC-NbTi). Since it is not yet available commercially, we have contracted with the patent holder to develop an APC-NbTi superconductor to our specifications, with high enough J_c to achieve the required high field. A practical advantage of this material is that it is insulated and handled like ordinary NbTi, without a high-temperature react cycle or the brittleness of Nb₃Sn. We plan to demonstrate on a short model that the required higher SCU fields can be achieved using APC-NbTi.

This task includes magnetic and mechanical design of the SCU model, acquisition of machining and CAD/CAM capability to fabricate the bifilar helical yoke geometry, and adapting and programming our coil winding apparatus to wind the conductors in the complex helical pattern.

Task (b): Cryogenic cooling of SCU magnets presents a technical challenge. Immersion of SCU yokes in liquid helium (LHe) is not an option in an electron storage ring, since a single, thin wall between LHe and ultra-high vacuum in the beamtube is not permitted. Direct conduction-cooling of SC windings by a "cold finger" to a cryocooler, as in recent industry-built SCUs, has proven inadequate to handle the heat induced by even very low electron beam currents. Nb₃Sn models built at other National labs have somewhat higher thermal margins due to the higher critical temperature (T_c) of Nb₃Sn, but, with just conduction cooling of the superconductor, they will likely also prove incapable of handling the tens of watts/meter of beam-induced heating in modern synchrotron light sources. We plan to demonstrate a novel SCU cooling design by co-investigator John

Skaritka of NSLS. The design employs a beampipe cooled by cryogenic (10-20K) helium gas, to intercept the beam-induced heat at a higher temperature where it can be removed more efficiently than at 4K. The NbTi windings are thermally isolated from the beampipe and maintained below the critical temperature (T_c) by helium gas, sub-cooled to $\sim 4K$, circulating in embedded cooling channels under the windings. A dual helium gas circulation and heat exchange system with a cryocooler will be designed for this purpose. Thermal isolation of the beampipe requires a slight increase of the magnetic gap. Consequently, the coils must be operated at somewhat higher current to achieve the required field, so the higher J_c of APC-NbTi is crucial. This task includes cryogenic thermal analysis of the beampipe cooling design to verify adequacy of thermal isolation between the beampipe and the SC windings and to calculate the helium gas flow rates needed for operation.

Task (c): Recent advances in thin- and thick-film MgB_2 high-temperature superconductors (HTS) are being pursued by co-investigator Lance Cooley of the Material Sciences Department with the goal of producing HTS printed conductor patterns for field error correction in SCUs. The films can be in contact with the beampipe, since MgB_2 has a T_c of $39^\circ K$. We have contracted with the developer of a MgB_2 film deposition process to supply thin films on various substrates as well as to print conductor patterns by photo-lithography. Laser cutting of patterns will also be explored. These test samples will be evaluated at the Materials Science Department's facilities.

A short prototype SCU incorporating APC-NbTi wire and our thermal intercept cooling design will be designed and fabricated and will be tested in the NSLS Vertical Test

Facility located in the Superconducting Magnet Division.

TECHNICAL PROGRESS AND RESULTS:

Task (a): We have designed an SCU prototype, consisting of two low-carbon steel yokes wound with APC-NbTi wire in a bifilar, modified helical pattern to produce a planar undulator field with a 15 mm period. The magnetic design has been modeled in 3D using the code Radia.

In order to fabricate the yokes, we have purchased and installed a 4th axis head on our CNC machine and acquired 3D CAD/CAM software to program the cutting of the complex bifilar helical conductor channels in the ferromagnetic yokes. The software translates AutoDesk Inventor 3D models into a 4-axis computer numerical control (CNC) machine commands. Wax and aluminum "proofs" of a 5-period yoke have been successfully cut to verify the programming. Low-carbon steel is on hand and the actual yokes will be cut next.

The APC-NbTi superconductor has been fabricated by the patent holder, L. Motowidlo, at Supra-Magnetics, Inc. The extrusion of the wire with a 0.5 x 1.0 mm rectangular cross-section was done at Hyper-Tech Research, Inc. The vendor is researching suitable polyamide and ceramic insulation coatings. Copper "practice" wire of the same dimensions, drawn through the same dies as the SC wire, has been received. Research Associate, S. Chouhan, has begun practice winding of this conductor on the aluminum version of the yoke in our coil-winding machine.

Task (b): To determine the effectiveness of the thermal intercept concept, a cryogenic thermal analysis of the beamtube with beam heating and helium gas cooling was

subcontracted to Topsfield Engineering Services, Inc. Initial 2D conduction analysis has been completed and shows that with 30 W/m heat input to the beamtube's top and bottom inner surfaces, 29.9 W/m is removed by the helium cooling tubes, with only a 10° rise between the "hot spot" in the beamtube and the helium tube. Classical radiative heat transfer across the 0.1 mm gap between the beamtube and yoke is also very small. Quantum-mechanical heat transfer at 4K was estimated to contribute an additional 20%.

Co-investigator, J. Skaritka, has completed a preliminary design of the dual helium gas circulation and heat exchange system, including selection of a cryogenic gas circulation pump and a cryocooler. A contract has been let to Janis Research, Inc. for an independent review of the cryogenic design and for a detailed design and cost estimate of a cryocooler-based system for cooling short SCU models, up to 1/3 m long, with simulated beam heating. The system could be stand-alone or used in conjunction with our SCU Vertical Test Facility.

Task (c): We have contracted with Superconducting Technologies, Inc. (STI) in Santa Barbara, CA, to fabricate MgB₂ thin and thick films on various substrates. We have received an assortment of MgB₂ thin film samples from STI for initial evaluation by co-investigator, L. Cooley, at the end of FY2005. Patterning and characterization is underway in the Materials Science Department. These films will serve as a baseline for evaluating thicker films to be deposited on flexible substrates and patterned in the shim coil configuration.

Encouraged by reports of improvements in J_c in MgB₂ wires by Hyper-Tech Research (funded independently by a SBIR contract),

we contracted Hyper-Tech to draw prototype lengths of MgB₂ wires in Nb, in several variants: (1) MgB₂ with no additives; (2) MgB₂ doped with either NaSiO₄ or ZrB₂, which are known to raise J_c; and (3) two wires doped with promising additives, such as CaB₆, BaB₆, NaB₂, or others suggested by L. Cooley, after evaluating samples (1) and (2). We received the prototype wires at the end of FY05 and they are presently being evaluated by Cooley.

The work planned for 2006 includes: (a) winding and testing of the APC-NbTi SCU model in our Vertical Test Facility at SMD; (b) demonstration of the thermal intercept scheme; (c) lithography of MgB₂ thin and thick films into conductor patterns and evaluation of their current carrying capacity; evaluation of MgB₂ wires and measurement of their engineering J_c.

SPECIFIC ACCOMPLISHMENTS:

Invention Disclosure by L.D. Cooley, with G. Rakowsky and J. Skaritka: "Small Gap High Temperature Superconducting Undulator," submitted 06/20/2005.

Invited presentation: L.D. Cooley, "MgB₂ activities at BNL," Workshop on high-field MgB₂, University of Wisconsin, 10-12 August 2005

LDRD FUNDING:

FY 2005	\$189,451
FY 2006 (budgeted)	\$175,000

Characterization and Imaging of Amyloid Plaques Using Diffraction Enhanced Imaging

Zhong Zhong

05-057

PURPOSE:

The goal of this LDRD has been to explore the potential of Diffraction Enhanced Imaging (DEI) for early detection of amyloid beta peptide deposition in Alzheimer's disease (AD). Since the appearance of these plaques, a hallmark feature of AD, precedes clinical symptoms by many years, there is great interest to develop methods for their early detection.

DEI is a novel radiography method that introduces fine selectivity for the angular deviation of x-rays traversing the subject. DEI's angular sensitivity allows measuring the gradient of the x-ray index of refraction in soft tissues as well as the yield of "small angle scattering" (extinction contrast). The organized structure of amyloid plaques is expected to exhibit certain extinction contrast, thus allowing their distinction from healthy brain tissues by DEI.

APPROACH:

The technical aims of the program include improvement of the mechanical stability of the DEI system at the NSLS's X15A beamline and the development of DEI-CT capability. Because the DEI imaging contrast from the amyloid plaques are expected to be small, these two steps are crucial to enable imaging of these plaques. DEI's effectiveness will then be tested by characterization of the extinction properties of amyloid plaques and that of healthy brain tissue and by establishment of a correlation

between the DEI images, the infrared spectroscopy images, and the histological analysis. The project was undertaken by a multi-disciplinary team consisting of the investigators A. Dilmanian, L. Miller, and C. Muehleman, and the graduate students C. Parham and D. Connor, and the summer students J. Chen, E. Mahajna, and A. Wu.

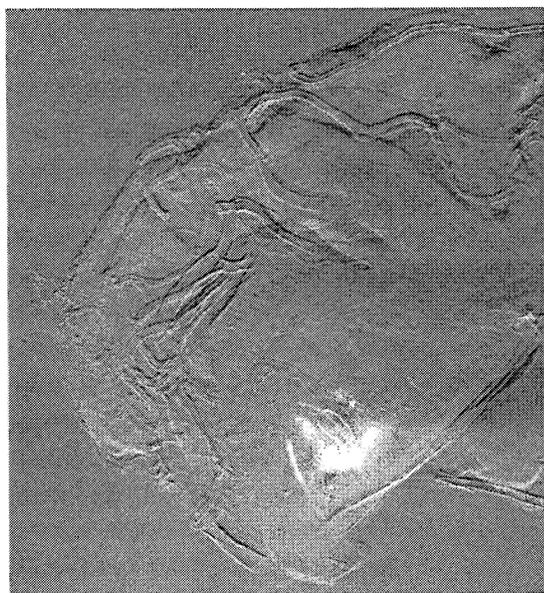
TECHNICAL PROGRESS AND RESULTS:

The DEI system was upgraded to improve the stability of the system as the stability of the monochromator and analyzer at sub-microradians is key for DEI-CT at high spatial resolution. The system's drift before the upgrade was 6 microradians. After the upgrade, which included installation of a new water-cooled mount for the second crystal of the monochromator and modification of the white beam filter assembly, this drift was reduced to below 0.02 micro-radians as measured by analytical techniques. The improved system already was used by several X15A collaborating users to image a variety of samples, including specimens of human breast cancer and osteoarthritis.

Specimens of the TG mice AD model, provided by Helene Benveniste, were imaged. The images showed no obvious AD plaques. The studies indicated that a high-resolution detector would be necessary for such a study.

It was decided to acquire detectors of 10 and 30-micron pixel sizes. A vendor was identified and an evaluation was performed with a demonstration unit. The new 30-micron detector was commissioned in July of 2005. A method to integrate this detector into the DEI system to perform robust DEI-CT imaging, including multiple imaging

radiography (MIR)-CT, was subsequently established using this detector.



Soon afterward, five AD brain specimens and two control specimens were acquired from Rush University Medical Center through Carol Muehleman and her collaborators. The DEI extinction properties of the specimens were characterized. Notably, at high x-ray energies (> 40 keV) that are required to penetrate the skull, DEI proved to be capable of yielding a significant extinction contrast for micro-calcifications (shown as white dots in figure above acquired at 40 keV) in diseased brains. In comparison, conventional x-rays at the same x-ray energy and dose yielded no contrast for the micro-calcifications.

Approval from the BNL Institutional Animal Care and Use Committee (IACUC) was sought and gained to perform in vivo DEI-CT imaging of an AD mouse model. A commercial transgenic mouse model and age-matched wild-type mice for control were identified.

This project involves animal vertebrates (BNL IACUC protocol 305) and specimens from human subjects (IRB 15)

SPECIFIC ACCOMPLISHMENTS:

Patents:

M.N. Wernick, L.D. Chapman, O. Oltulu, and Z. Zhong, "Imaging method based on attenuation, refraction and ultra-small-angle-scattering of x-rays," US patent #US 6,947,521 B2, issued on Sept. 20, 2005.

Peer reviewed publications :

1. M.O. Hasnah, C. Parham, E.D. Pisano, Z. Zhong, O. Oltulu and D. Chapman, "Mass Density Images from the Diffraction Enhanced Imaging Technique," *Phys. Med. Bio.*, **32(2)** (2005) 549-552.
2. J. Li, J.M. Williams, Z. Zhong, K.E. Kuettner, M. Aurich, J. Mollenhauer, and C. Muehleman, "Reliability of Diffraction Enhanced Imaging for Assessment of Cartilage Lesions, Ex Vivo," *Osteoarthritis and Cartilage* **13(3)** (2005) 187-197.
3. D.M. Connor, D. Sayers, D.R. Sumner, and Z. Zhong, "Identification of fatigue damage in cortical bone by Diffraction Enhanced Imaging," *Nucl. Instrum. Meth. Phys. Res. A* **548** (2005) 234-239.

Papers in press and in review:

1. Muehleman, C.; Li, J.; Zhong, Z.; Brankov, J.; Wernick, M.N.; "Multiple Image Radiography for soft tissue," *J. Anatomy*, in press.
2. Wernick, M.N.; Yang, Y.; Mondal, I.; Chapman, D.; Parham, C.; and Zhong, Z.; "Computation of mass density

images from refraction-gradient images,” *Phys Med Biol.* in press.

3. Muehleman, C.; Li, J.; Zhong, Z.; “Preliminary study on diffraction enhanced imaging for a canine model of cartilage damage,” *Osteoarthritis and Cartilage*, in review.
4. D.M. Connor, D. Sayers, D.R. Sumner, Z. Zhong. “Diffraction enhanced imaging of controlled defects within bone, including bone-metal gaps.” *Phys. Med. Bio.*, in review

Conference Proceedings:

1. Wernick, M.N.; Brankov, J.G.; Chapman, D.; Yang, Y.; Pisano, E.; Parham, C.; Muehleman, C.; Zhong, Z.; Anastasio, M.A.; “Multiple-image radiography and computed tomography,” *Proc. SPIE*, 5535: 369-379, 2005.
2. Brankov, J.G.; Khelashvili, G.; Chapman, D.; Anastasio, M.A.; Yang, Y.; Zhong, Z.; and Wernick, M.N.; “Physical model of image formation in multiple-image radiography,” *Conf. Record of the 2005 IEEE Nuclear Science Symposium & Medical Imaging Conference*, in press.

Abstracts and presentations:

1. Z. Zhong, 399th Brookhaven Lecture, Brookhaven National Laboratory, Upton, New York, December 17, 2004, “Diffraction Enhanced Imaging: Seeing X-Rays as One Sees the Light,” Invited Talk.
2. Z. Zhong, *NIH Fibrosis workshop*, NIH Campus, Building 31, Bethesda, Maryland, March 29, 2005, “DEI and its applicability to liver fibrosis,” invited talk.

3. J. Chen, C. Parham, A. Wu, D. Connor, A. Dilmanian, J. Li, E. Mahajna, L. Miller, C. Muehleman, H. Zhong, and Z. Zhong, “Preliminary Characterization of Alzheimer’s Disease Brains using Diffraction Enhanced Imaging,” submitted to *Synchrotron Radiation Instrumentation Conference, SRI05*.

4. A. Wu, E. Albanis, D. Connor, J. Chen, S. Friedman, C. Parham, H. Zhong, and Z. Zhong, “Imaging of a Rat Model of Liver Fibrosis: A Preliminary Study,” submitted to *Synchrotron Radiation Instrumentation Conference, SRI05*.

5. D. M. Connor, H. Hallen, D. R. Sumner, Z. Zhong. “Comparison of diffraction-enhanced computed tomography and monochromatic synchrotron radiation computed tomography of human trabecular bone,” submitted to *Synchrotron Radiation Instrumentation Conference, SRI05*.

6. J. Li, Z. Zhong, K. E. Kuettner and C. Muehleman, “Detection of tendon lesions with diffraction enhanced x-ray imaging,” 51st Annual Meeting of the Orthopaedic Research Society, February 20 - 23, 2005, Washington, D.C.

7. C. Muehleman, J. Li, K.E. Kuettner, and Z. Zhong, “Diffraction enhanced x-ray imaging of musculoskeletal lesions,” 51st Annual Meeting of the Orthopaedic Research Society, February 20 - 23, 2005, Washington, D.C.

Reports:

Mahajna Ebrahim, “Characterization of the Brain Calcification with DEI – MIR,” 10-page report was submitted to DOE as part of requirements for summer internship at BNL.

Related grant proposals:

1. "Design of multiple-image radiography of the breast," Wernik (PI), Pisano and Zhong, NIH, funded \$20k/yr for BNL, October 2005 – October 2008.
2. "2D CCD detector for NSLS X15A beamline," Muehleman (PI), and Zhong, NIH equipment grant, funded \$100k, Feb 2005 – Feb 2006.
3. "Novel x-ray imaging technologies for degenerative joint disease," Muehleman (PI), Wernik (PI for IIT), and Zhong (PI for BNL), NIH, pending, \$80k/yr for BNL, Oct 2006 – October 2011.
4. "A synchrotron based apparatus for long term tracking of therapeutically implanted single cells." Menk (PI), Schultke, Chapman, Zhong, Lewis, Hall, and Yagi, HFSP, not funded. \$100k/yr requested for BNL, October 2005 – October 2009.

LDRD FUNDING:

FY 2005	\$100,793
FY 2006 (budgeted)	\$100,000

Development of Methodologies for Analyzing Transcription Factor Binding in Whole Genomes

Carl W. Anderson

05-058

PURPOSE:

The goal of this program is to develop a robust method for identifying and characterizing protein binding sites and epigenetic markers in whole genomes of eukaryotic cells. We developed a method, Serial Analysis of Chromatin Occupancy (SACO), for profiling the functional chromatin binding sites of proteins in cells across whole genomes (Impey et al., 2004). A variation of this procedure, Paired-End SACO (PE-SACO) will be developed that simplifies the basic SACO procedure and makes it robust for potential automation. PE-SACO also will be extended by coupling it with a highly sensitive methylated-CpG island recovery assay, MIRA, to identify epigenetic markers in DNA that regulate chromatin function. The PE-SACO procedure will be validated through identification and analysis of the binding sites for the human tumor suppressor protein p53 in primary human epithelial cells following DNA damage (e.g. exposure to ionizing radiation) and by analyzing the methylation status of one or more characterized cell lines. The technology is relevant to developing a systems understanding of the cellular responses of human and mouse cells to low doses of ionizing radiation for DOE's Low Dose Radiation Program. This will require determining how and where radiation and other genotoxic stresses induce changes in transcription factor binding, chromosome structure and whether epigenetic changes such as methylation of cytosine residues occurs in the DNA. The methodology also

is applicable to understanding the complex physiological and behavioral systems coordinated by a central nervous system and, therefore, complements BNL's institutional strategy on understanding brain function. Our methodology also will have broad applicability to understanding chromatin function in many fields including for DOE programs in energy biosciences in GTL: Genomes-to-life.

APPROACH:

Two major principles underlie the Genome Signature Tag (GST) method (Dunn et al., 2002) that forms the basis for SACO. First, short DNA GST sequences (21 bp) are sufficient to identify unique sites within a genome; second, the concatenation of these short DNA sequences greatly increases the efficiency of identification through high throughput sequencing. SACO combines the GST methodology with a technique called **chromatin immuno-precipitation** (ChIP), in which proteins bound to DNA are reversibly crosslinked to the DNA segment to which they are bound with formaldehyde. The crosslinked chromatin is then fragmented into ~500 bp fragments by sonication, and the DNA to which any given protein is bound is recovered using antibodies that specifically recognize that protein. For a human cell a typical transcription factor might bind to several thousand sites within the entire human genome. Thus, ChIP is expected to extract perhaps a million bp of sequence (500 bp x ~2000 binding sites), i.e. 0.3% of the total human genome, with which a given transcription factor is bound. For SACO, Genome Sequence Tags are then created from these fragments, concatenated, and sequenced to produce a quantitative profile of the loci to which the transcription factor was bound at the time the cells were treated with the crosslinking agent.

PE-SACO simplifies the SACO procedure and makes it more robust. For PE-SACO the ~500 bp ChIP fragments will be first cloned into a specially constructed vector that has *Mme* I restriction sites (or sites for other suitable restriction enzymes) flanking the cloning site. The *Mme* I restriction enzyme cleaves DNA 20 or 21 base-pairs (bp) away from its recognition site, thereby creating ~20 bp sequence tags from each end of each ChIP fragment. The cleaved vectors are then relegated to create a ~42 bp insert, a "di-tag," containing ~20 bp from each end of a ChIP fragment. The di-tags then may be amplified using the polymerase chain reaction (PCR). The PCR fragments are then digested with another restriction enzyme that cleaves sites in the PE-SACO vector flanking the *Mme* I sites to release each di-tag. Di-tags are then concatenated, cloned into a sequencing vector, the inserts are sequenced, and bioinformatics is then used to extract each sequence tag and determine the location in the genome from which it was derived.

An advantage of the PE-SACO methods is that for factor binding, loci are recovered many times. The factor-binding site must be found with the segment that is common to all recovered DNA fragments corresponding to the locus. This feature of the method will reduce the segment that must be examined for factor binding sites from ~2000 bp to perhaps 100 bp.

The method also can be used to identify modified DNA segments in chromatin such as segments that are epigenetically marked with methylated cytosines. Chromatin segments containing methylated cytosines are recovered using a protein, such as the DNA binding segment of MeCP2, that specifically binds methylated DNA sequences in place of an antibody to a protein that recognizes DNA. Gerd Pfeifer, Beckman Research Institute of the City of

Hope, has developed a highly sensitive protocol for isolating methylated DNA fragments. We will collaborate with Pfeifer's group to adopt his procedure for PE-SACO and to validate its use for identifying epigenetically marked DNA in human cells. We also will explore methods for the subtractive analysis of methylated DNA segments that would more readily permit identification of changes in epigenetic marks. If resources permit we also will explore the use of single-chain antibodies for ChIP isolation of DNA fragments. Unlike polyclonal antibodies, single-chain antibodies have a well-characterized binding specificity that are readily produced in laboratory systems and can be made available to the scientific community cheaply.

To validate the PE-SACO technique we will prepare and characterize a PE-SACO library corresponding to the bindings sites of the p53 human tumor suppressor protein in human epithelial cells following treatment with ionizing radiation. p53 is a 393 amino acid, tetrameric, transcription factor that regulates the expression of genes which control cell cycle progression, the induction of apoptosis and senescence, DNA repair, and other functions involved in cellular responses to stress and maintenance of genome integrity. p53 is the most commonly mutated gene in human cancers, and loss of p53 function, either directly through mutation or indirectly through several other mechanisms, plays a central role in the development of cancer. Genomic approaches have shown that p53 induces or inhibits the expression of more than 1500 human genes. The p53 monomer binds a consensus DNA sequence, 5'-RRRC(A/T)-3', which commonly is repeated as pairs of inverted repeats separated by 0 to 14 bp to create a 20 bp binding site for tetrameric p53. Thus, p53 specifically recognizes the consensus sequence 5'-RRRCWWGYYY (N

= 0-14) RRRCWWGYYY-3' where R stand for a purine base (A or G), Y stands for a pyrimidine base (T or C) and W stands for either A or T. For p53 as well as for most other transcription factors, the degenerate nature of the DNA binding consensus sequence makes it difficult to predict and identify authentic binding motifs in whole genomes by simply scanning the sequence (there are >65,000 unique sequences that match the p53 consensus sequence excluding the 0-14 bp spacer); in addition, not all consensus sites (p53 responsive elements, p53REs) are competent for p53 binding *in vivo*. p53 also promotes the expression of some genes through elements that are of limited similarity to the consensus binding motif (e.g. the *PIG3* gene). The nuclear concentration of p53 increases about two orders of magnitude, from a few hundred molecules per cell to several 10's of thousands of molecules per cell, in response to certain genotoxic and non-genotoxic stresses. Protein modifications and the presence of binding partners and their concentration all are thought to modulate p53's ability to transcriptionally activate or conversely repress target genes. Understanding which sites in chromatin are bound by p53 after genotoxic stress is critical for understanding how p53 prevents cancer and may lead to improved cancer treatments.

TECHNICAL PROGRESS AND RESULTS:

The first technical hurdle that needed to be overcome was the design, construction, and testing of a special DNA cloning vector which was based on the pSCANS vector developed at BNL. pSCANS was modified for efficient cloning of single DNA fragments in a manner that places them immediately adjacent to oppositely oriented *Mme* I recognition sequences. These are the only *Mme* I sites in the vector. Two *Bbs* I

sites were placed between the *Mme* I sites in opposite orientations such that when the vector is cut with *Bbs* I, the linearized vector DNA will have non-self ligatable ends with 4 nucleotide (nt) overhangs (5'-GTTCG-3').

Synthetic double-stranded DNA cassettes were designed to append simultaneously *Btg* ZI and *Bbs* I sites to the ends of blunt-ended chromatin immuno-precipitated (ChIP) DNA fragments. Cutting with these cassettes with either *Btg* ZI or *Bbs* I generates 4 bp overhangs (5'-CGAC-3') on the ends of the linkered DNA that are complementary to the overhangs of the *Bbs* I cut vector. Standard DNA ligation generates recombinant plasmids with only single inserts. The clones contain an *Mme* I site (TCCGAC) at the 5' side of the DNA insert, and another *Mme* I site on the minus strand, at the 3' end of the insert. The *Mme* I restriction enzyme was used to cleave these clones 20-21bp into the inserts from both their 5' and 3' ends. Consequently, despite the variable sizes of the inserts, the vector-plus-20-21bp DNA signature tags on each end of all DNA clones are of a constant size (approx. 4490bp) that can be easily recognized upon agarose gel electrophoresis and can be purified from the unwanted cDNA fragments that are a by-product of the *Mme* I digestion. In the next step, the gel-purified linearized vector-plus-tags was ligated with a 16-fold degenerate *Bcl* I linker. This step captures the sequence information on each of the two 3' overhangs left after *Mme* I digestion. It also leaves a *Bcl* I recognition site as a punctuation sequence between di-tag pairs. The linkered DNA was self-ligated to form circles which were gel purified and electroporated into electrocompetent *E. coli* D1210 cells to form the di-tag library. Plasmid DNA was isolated and the di-tags excised by digestion with the restriction enzyme *Bam* HI. After purification the di-tags were self-ligated to form concatemers which were then cloned,

sequenced and the data then used to map the genomic segments recovered during the immunoprecipitation. A computer algorithm, p53MH, developed at The Rockefeller University, was used successfully to identify the putative p53 transcription factor DNA-binding sites in these sequences.

Our initial experiments used samples that had p53 induced by a DNA-damaging chemical. In the second year of this project, responses to ionization radiation will be investigated to distinguish radiation response from other agents. Other anticipated accomplishments include the development and validation of methods for obtaining PE_SACO di-tags from methylated DNA segments, and development of single-chain antibodies and their comparison for use in PE_SACO, validation of the use of antibodies that recognize protein modifications for PE_SACO, and the development of double-ChIP methods that will allow, e.g. the identification of p53 binding sites in methylated DNA sequences.

References:

Impey, S.; McCorkle, S. R.; Cha-Molstad, H.; Dwyer, J. M.; Yochum, G. S.; Boss, J. M.; McWeeney, S.; Dunn, J. J.; Mandel, G.; and Goodman, R. H. Defining the CREB regulon: A genome-wide analysis of

transcription factor regulatory regions. *Cell* 119, 1041-1054 (2004).

Dunn, J. J.; McCorkle, S. R.; Praissman, L. A.; Hind, G.; van der Lelie, D.; Bahou, W. F.; Gnatenko, D. V.; and Krause, M. K. Genomic signature tags (GSTs): A new system for profiling genomic DNA. *Genome Res.* 12(11), 1756-1765 (2002).

SPECIFIC ACCOMPLISHMENTS:

A BNL Record of Invention filed by J.J. Dunn on August 19, 2005 entitled "Vectors and procedures for producing ditags and ditag arrays."

Follow-On Funding:

KP1102020, BO-129, Whole Genome Analysis of Transcription Factor Binding in Response to Low Doses of Radiation, C. W. Anderson and J. J. Dunn (PIs), DOE, 4/1/05 – 9/30/07, \$900,000 for 3 years. This is a follow-on pilot project to show that a SACO library of p53 binding loci can be prepared from human cells after low dose ionization and that the resulting data can be interpreted.

LDRD FUNDING:

FY 2005	\$ 92,970
FY 2006 (budgeted)	\$112,000

Application of Endophytic Bacteria to Improve the Phytoremediation of TCE and BTEX Using Hybrid Poplar

Daniel van der Lelie

05-063

PURPOSE:

To improve the phytoremediation of volatile organic contaminants by using endophytic bacteria to complement the metabolic properties of their host plant.

APPROACH:

The approach is to complement the metabolic properties of poplar, a plant species frequently used for phyto-remediation of groundwater contaminated with organic solvents, by that of associated endophytic bacteria. This should result in an improved degradation of contaminants. To do so poplar was inoculated with the endophyte *Burkholderia cepacia* VM1468. This strain, which has yellow lupine as its natural host, possesses the pTOM-Bu61 plasmid encoding for constitutively expressed toluene degradation. As controls, non-inoculated plants or plants inoculated with the soil bacterium *B. cepacia* Bu61 (pTOM-Bu61) were used. After 10 weeks the growth of the plants in the presence and absence of toluene was examined. We also analyzed the release of toluene via transpiration in the atmosphere. Finally, we analyzed the endophytic communities associated with poplar in order to determine the successful establishment of the inocula.

TECHNICAL PROGRESS AND RESULTS:

Beneficial effect of inoculation. Inoculation of poplar with the *B. cepacia* strains had a positive effect on plant growth in the presence of toluene and reduced the amount of toluene released via evapotranspiration. This effect was more

dramatic for VM1468, the endophytic strain, than for Bu61. These results confirm our earlier observations with yellow lupine that endophytic bacteria, equipped with the proper degradation pathway, are able to protect their host plant against the phytotoxic effect of toluene. The results also show that degradation of toluene by the endophytic bacterium results in a reduced release of toluene in the atmosphere.

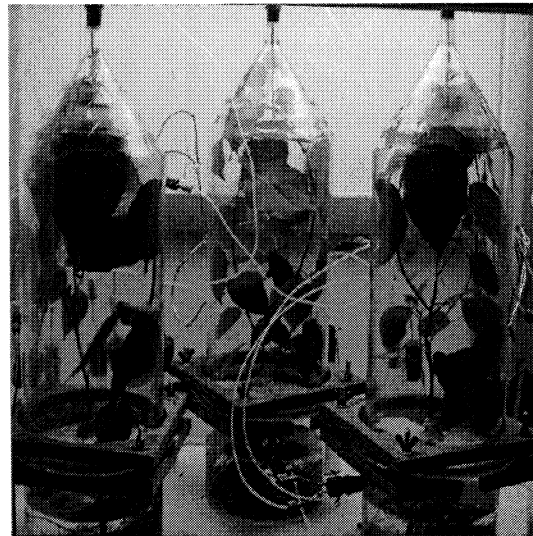


Figure 1: growth of poplar in a two-compartment system to study the evapotranspiration of toluene.

Horizontal gene transfer of pTOM-Bu61. We analyzed the composition of the endophytic communities associated with the inoculated poplar plants in order to determine if the inocula succeeded in successfully establishing themselves in the endogenous endophytic communities. To our surprise, none of the strains succeeded in establishing itself at detectable numbers within the endophytic community, but horizontal gene transfer of pTOM-Bu61 occurred to different members of the endogenous endophytic community, both in the presence and absence of toluene. This work is the first report on *in planta* horizontal gene transfer among plant associated endophytic bacteria and demonstrates its possibility to adapt natural endophytic microbial communities to improve the remediation of environmental insults.

SPECIFIC ACCOMPLISHMENTS:

During the course of our experiments we noticed that the presence of endophytic bacteria had a general beneficial effect on plant growth. This observation was used to successfully apply for funding to further exploit the phenomenon: Understanding the Effects of the Interactions Between Poplar and its Endophytic Microbial Partners on Plant Biomass Production and Below-Ground Carbon Cycling. S. Taghavi (PI) and D. van der Lelie (co-PI). DOE-OBER, KP1102010, BO-131, \$580,424, FY 2006-2008.

FY 2005 Publications:

Response to Newman: New uses of endophytic bacteria to improve phytoremediation. van der Lelie, D.; Barac, T.; Taghavi, S.; and Vangronsveld, J. Trends in Biotech. 23(1), 8-9 (2005).

Horizontal gene transfer to endogenous endophytic bacteria from poplar improves phytoremediation of toluene. Taghavi, S.; Barac, T.; Greenberg, B.; Vangronsveld, J.; and van der Lelie, D. Appl. Environ. Microbiol. (in press).

Endophytic bacterial diversity in poplar trees growing on a BTEX-contaminated site: The characterization of isolates with potential to enhance phytoremediation. Moore, F. P.; Barac, T.; Borremans, B.; Oeyen, L.; Vangronsveld, J.; van der Lelie, D.; Campbell, C. D.; and Moore, E. R. B. Systematic & Appl. Microbiol. (accepted).

Endophytic bacteria and their potential application to improve the phytoremediation of contaminated environments. Mastretta, C.; Barac, T.; Vangronsveld, J.; Newman, L.; Taghavi, S.; and van der Lelie, D. Biotech. Genetic Engin. Rev., Vol. 23 (submitted).

LDRD FUNDING:

FY 2005	\$212,900
FY 2006 (budgeted)	\$220,000

Design and Build Two Dimensional Protein-Lipid Thin Film: A First Step Toward Novel Biochips

Yinan Wei

05-064

PURPOSE:

In this proposed research, we will perform structural and functional studies of metal transporter proteins and develop the technique to “polymerize” these proteins in their fully functional states into a two-dimensional matrix. Subsequently, phospholipids will be incorporated into the gaps of the protein matrix to form a bioactive thin film. Insight acquired during this proposed research will benefit the development of general methodologies for membrane protein expression, purification, and characterization. The bioactive two-dimensional (2D) protein-lipid thin film to be constructed may bring new opportunities into the development of biotechnology.

APPROACH:

The marriage of biology and nanoscience yields the burgeoning field of biochips. Usually no larger than a fingernail, these biochips can be designed to perform reactions or detections with high quality and efficiency. The research of protein biochips starts with the attachment of protein molecules to a surface in an ordered manner. We plan to invent a structural based protein engineering approach to assemble membrane protein molecules into 2D films. In the current stage we carried out detailed biophysical characterization of the target membrane protein, *Escherichia coli*. Zn²⁺ transporter YiiP. YiiP is picked as building blocks for the films due to its ability to transfer heavy metal ions across the

membrane, which may facilitate applications such as pollution control of heavy metal ions. After necessary structural information being acquired, a docking unit will be introduced into the protein at designated positions by mutagenesis. Next biophysical properties of the modified protein molecules will be examined and active candidates with the best stability will be used in the polymerization study.

TECHNICAL PROGRESS AND RESULTS:

During FY 2005, we have made the following technical progress:

Experimentally established a topological model for YiiP.

Elucidated the functional role of the highly conserved residue Asp157 in metal binding and transport with direct biophysical measurements.

Established a direct structural connection between substrate selection and translocation across the membrane.

In summary, we have greatly advanced our understandings about the structure of protein YiiP, which is the foundation for the structural based design of docking sites.

During FY 2006, more biophysical studies will be carried out to probe the structure and function of YiiP. Docking sites will be designed and created based on the structural information; and the stability and activity of the modified proteins will be tested.

SPECIFIC ACCOMPLISHMENTS:

FY 2005 Publication:

Selective metal binding to a membrane-embedded aspartate in the *Escherichia coli*

metal transporter YiiP (FieF). Wei, Y. and Fu, D. J. Biol. Chem. 280(40), 33716-33724 (2005).

LDRD FUNDING:

FY 2005	\$61,342
FY 2006 (budgeted)	\$60,000

Positron Labeled Stem Cells for Non-Invasive PET Imaging Studies of In-Vivo Trafficking and Biodistribution

Suresh Srivastava

05-068

L. Pena

PURPOSE:

The overall goal of this project is to develop methods for radiolabeling progenitor stem cells for noninvasively tracking their behavior and fate *in vivo* through PET imaging. If successful, these investigations would lead in the long run to the development of a generally practical, convenient, and reliable method for following the distribution, differentiation, and survival of stem cells in a quantitative fashion. This project has the potential to significantly enhance and broaden our understanding of the mechanisms of stem cell involvement in health and disease. It involves the use of the very sensitive PET radiotracer imaging technique, which has had DOE support at BNL for over four decades. The proposed work fully conforms to the DOE's mission to advance the radiotracer technology to provide critical insights into biological phenomena including stem cell development and differentiation, and will open up an important new area for further investigations of interest to both DOE and the NIH.

APPROACH:

The overall *rationale* of this project derives from the following. Published reports identify the need for a practical, reliable, and cost-efficient way of marking progenitor stem cells to non-invasively evaluate their distribution and survival following transplantation. Our preliminary results and work from multiple laboratories suggest that radiolabeling anti-bodies that are specific to subpopulations of progenitor stem cells, with

positron emitters to allow PET imaging, is perhaps the most efficient and economical way to follow stem cell trafficking, survival, and differentiation *in vivo*.

The general approach for cell labeling involves preparing a radioimmunoconjugate of the appropriate cell-specific monoclonal antibody (MAb) first with the PET radionuclide (e.g, I-124 and Co-55 proposed in this investigation) and then stably and irreversibly attaching the resulting radio-immunoconjugate to the progenitor stem cell under study. The initially selected model was the bipotential glial stem cell line, CG-4, and the monoclonal antibody A2B5, which targets an antigen present specifically on the glial cell surface. After initial experimentation, it became clear that the level of A2B5 expression in these glial progenitor cells (CG4) was rather low. We began looking for another cell type with high levels of A2B5 expression to use as a positive control. The best candidate turned out to be the RIN-m5F cells. These cells are derived from a rat insulinoma model.

This work is expected to accomplish the first steps towards fulfilling the above stated unmet need for a noninvasive imaging methodology for following stem cell trafficking, survival, and differentiation *in vivo*.

In addition to the P.I.s, the other investigators involved in this project were M. Rao (NIH, Consultant), G. Meinken, Scientific Associate, and D. White, Technical Assistant.

TECHNICAL PROGRESS AND RESULTS:

During FY 2005, our initial steps involved developing the methodology for preparing milligram amounts of MAb A2B5 from an appropriate hybridoma cell line and to radioiodinate it with commercially available I-131 (as a surrogate for the positron emitter I-124) using an increasing number of iodine

atoms per MAb molecule (1.33 or no-carrier-added, 5, and 10). The next step was to prepare a slot blot of cell lysates from test and control cell lines. The procedure for determining the binding efficiency and the retention of biological activity of the immunoconjugate included incubating the blots with the radioiodinated A2B5, and autoradiography using a Phosphor Imaging System.

We achieved the preparation of the MAb A2B5 by implementing the following steps. We grew hybridoma cells that secrete MAb A2B5 in a cell culture, optimized conditions for cell growth and for harvesting the medium, carried out affinity purification #1 using a T-Gel Column (that enriches thiophilic proteins including MAbs), performed affinity purification #2 using a Protein L Column (to enrich immunoglobulins, particularly IgM), and carried out an ultrafiltration procedure (100K cutoff) for quantification (concentration and buffer exchange in one step). Using the above optimized methodology we were successful in scaling up the production MAb A2B5 to the required milligram quantities.

Next, we optimized the iodination (with both I-125 and I-131) of A2B5 with good labeling efficiency (50 – 80%) and determined the retention of biological activity of radioiodinated A2B5 using positive glial cell controls. Due to the rather low expression of A2B5 MAb on the glial cell surface and in addition, possibly because of the low specific activity of I-131, our results were not entirely clear. These experiments will require the use of I-125 and/or the use of the RIN-m5F cells as the positive control. The schematic description of these studies is shown in Figure 1.

Our plans for FY 2006 are to finish the remaining Specific Aims 2 - 4 and develop methods for labeling the antibody with the commercially available Co-57 (as a surrogate for positron emitter Co-55). We will optimize for the highest radioisotope loading

efficiency (I-125, I-131, and Co-57) without loss of biological activity. We will determine in vitro stability of the radiolabeled MAb A2B5 and label the CG-4 cells. Finally, conditions will be optimized for maximum radiolabeled A2B5 loading per 10,000, and per 50,000 CG-4 cells.

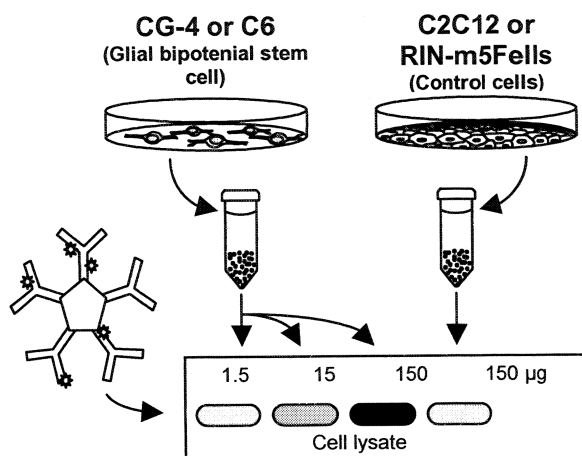


Figure 1. Schematic representation of the experiments for determining biological activity retention of the radioimmunoconjugates.

Future plans also include optimizing the retention of biological activity of the radioactive A2B5-labeled RIN cells, as a function of increasing A2B5 and isotope concentrations. We will use differentiation effects in vitro, and unlabeled RIN cells as controls.

The in vivo behavior (biodistribution and kinetics) in rats, following both intravenous and regional administration of the radiolabeled CG-4 cells, will be studied using micro PET, tissue counting, and autoradiography. The results will be compared with those obtained with Tc-99m-RBC as a control system.

This project involves vertebrate animals.

LDRD FUNDING:

FY 2005	\$ 63,600
FY 2006 (budgeted)	\$165,000

Breaking the Millimeter Resolution Barrier in fMRI

Dardo Tomasi

05-069

PURPOSE:

The effective relaxation time of the tissue magnetization is very short (~40 ms) and limits the number data samples in fast magnetic resonance imaging (MRI) acquisition methods. As a consequence, spatial resolution is limited in functional MRI, preventing the study of hemodynamic/neural processes at the sub-millimeter scale in humans. To overcome this limitation we propose to speed up MRI by using parallel imaging acquisition techniques and high performance readout gradient pulses. This novel data acquisition approach will allow functional MRI (fMRI) with increased spatial resolution and promote highly innovative and exploratory research in physiology and medicine at BNL and elsewhere.

APPROACH:

A faster sampling rate is needed to increase spatial resolution in fMRI. Partially parallel imaging (PPA) with *receiver coil arrays* use combinations of simultaneously acquired signals from multiple surface coils with different spatial sensitivities to produce images with enhanced spatial resolution. Using phased arrays with 4-8 radio frequency (RF) coils and PPA acquisition/reconstruction methods, spatial resolution can be increased by a factor that ranges from 2 to 6. High spatial resolution can be achieved in fMRI by using *high performance gradient coils* that can deliver strong and fast-switching readout gradient fields, allowing the use of a higher acquisition bandwidth. Commercially available gradient coils for head imaging

produce gradient pulses of 75 mT/m with a rise time of 0.2 ms. Coils with higher gradient efficiency and lower inductance can produce gradient pulses with double the amplitude and quarter the rise time at sub magnetic stimulation threshold levels and further speed up acquisition by a factor of 4.

Therefore, we aim to develop a hybrid system composed of a high performance gradient coil and an 8-channel RF-coil array to collect functional images of the human brain with sub-millimeter resolution. The project involves the development of 1) a gradient coil, 2) RF-coils, 3) a parallel MRI-receiver to collect multiple signals from the coils, and 4) the system integration with the MRI instrument at BNL.

TECHNICAL PROGRESS AND RESULTS:

We designed, constructed, and tested at low power levels a novel insertable high performance gradient coil. The coil can produce gradient pulses of 150 mT/m with a rise time of 0.03 ms; gradient uniformity is better than 5% in a 15cm-diameter spherical volume; thus, it allows whole brain imaging with minimal distortion. Second, we developed an 8-channel Nuclear Magnetic Resonance (NMR) digital receiver to acquire multiple MRI signals coming from RF-coil arrays. We used two general-purpose 32-channel narrowband digital receivers VIM-4 modules (Pentek 6230, Pentek, inc.), which were interconnected to a PMC/VIM Carrier PMC7455/57 PowerPC Processor VME Boards (Pentek 4205, Pentek, inc.) for high performance I/O and processing (Ethernet 100Mb), and controlled by a PC using the eCos, and Ready Flow software packages. Third, the parallel acquisition/reconstruction methods were numerically simulated to evaluate the feasibility for achieving high acceleration factors. The simulation algorithm was developed for PC platforms

using Visual Basic and C++ languages to optimize the geometry of the parallel coil arrays. Gaussian noise was introduced in the calculations to evaluate the effect of noise in the reconstruction. Fourth, we developed a 4-channel phased array. Fifth, we developed primary visual and auditory stimulation paradigms for fMRI.

We did not integrate the new head gradient coil with our gradient system yet because electrical connections have to be done at 4Tesla magnetic field, and OSHA regulations limit magnetic field exposure to 2Tesla, for BNL employees; an exemption was requested to allow workers to enter zones of higher magnetic fields than 2Tesla.

This project involves the use of animal vertebrates and/or human subjects.

SPECIFIC ACCOMPLISHMENTS:

Publications:

1. The Effect of Small Rotations on R2* with Echo Planar Imaging. Caparelli, E.C.; Tomasi, D.; and Ernst, T. *NeuroImage* 24, 1164-1169 (2005).
2. fMRI-acoustic noise alters brain activation during working memory tasks. Tomasi, D.; Caparelli, E.C.; Chang, L.; and Ernst, T. *NeuroImage* 27, 377-386 (2005).
3. Machine Learning for Clinical Diagnosis from Functional Magnetic Resonance Imaging. Zhang, L.; Samaras, D.; Tomasi, D.; Volkow, N.D.; Goldstein, R.Z. *Computer Vision and Pattern Recognition, 2005. IEEE Computer Society Conference* 1: 1211 – 1217 (2005).
4. Magnetic Field Shift due to Mechanical Vibration in Functional MRI. Foerster, B.; Tomasi, D.; and Caparelli, E.C. *Magn Reson Med* 54: 1261-1267 (2005).
5. Exploiting Temporal Information in Functional Magnetic Resonance Imaging Brain Data. Zhang, L.; Samaras, D.; Tomasi, D.; Alia-Klein, N.; Cottone, L.A.; Leskovjan, L.C.; Volkow, N.D.; Goldstein, R.Z. *Medical Image Computing and Computer Assisted Intervention – MICCAI, Proceedings, Part I. Lecture Notes in Computer, Science* 3749 Springer, ISBN 3-540-29327-2, 679-687 (2005).
6. Common deactivation patterns during working memory and visual attention tasks: An intra-subject fMRI study at 4 Tesla. Tomasi, D.; Ernst, T.; Caparelli, E.C.; and Chang, L. *Human Brain Mapp* (in press).
7. A simple theory for vibration of MRI gradient coils. Tomasi, D.; and Ernst, T. *Braz J Phys* (in press). Optimization of biplanar gradient coils for magnetic resonance imaging. Tomasi, D. *Braz J Phys* (in press).
8. The human immunodeficiency virus reduces network capacity: acoustic noise effect. Tomasi, D.; Chang, L.; Caparelli, E.C.; and Ernst, T. *Ann Neurol* (n press).
9. Loss of sensitivity to relative saliency of money in cocaine users is associated with disrupted activity in lateral orbitofrontal cortex. Goldstein, R.Z.; Tomasi, D.; Cottone, L.A.; Telang, F.; Caparelli, E.C.; Zhang, L.; Samaras, D.; Leskovjan, A.C.; Chang, L.; Ernst, T.; and Volkow, N.D. *Neuroimage* (submitted).
10. Intra-vascular contamination in activation patterns of working memory. Tomasi, D. and Caparelli, E.C. *Neuroimage* (submitted)
11. Decreased prefrontal cortical sensitivity to monetary reward in cocaine addiction is associated with impaired motivation and self-control. Goldstein, R.Z.; Alia-Klein, N.; Tomasi, D.; Cottone, L.A.; Zhang, L.; Maloney, T.; Telang, F.;

Caparelli, E.C.; and Volkow, N.D. *Am J Psychiatry* (submitted)

12. Different activation patterns for working memory load and visual attention load. Tomasi, D.; Chang, L.; Caparelli, E.C.; and Ernst, T. *J Magn Reson Imaging* (submitted).

Book Reviews:

1. Tomasi, D. *Health Physics* 89, 95-96, 2005.

Grant applications:

1. "Fast EPI readout for mapping whole brain connectivity," PI: D. Tomasi. Total costs: \$499,516, agency: NIH, 1 R21 NS050175-01A1, Dates: 04/01/06-03/31/08. Pending.

Conference Proceedings:

1. Loss of sensitivity in appraising the relative saliency value of money in drug abusers is associated with disrupted activity in orbitofrontal cortex. Goldstein, R.Z.; Tomasi, D.; Cottone, L.A.; Telang, F.; Caparelli, E.C.; Zhang, L.; Leskovjan, A.C.; Chang, L.; Ernst, T.; and Volkow, N.D. SFN, 34th Annual Meeting, San Diego, CA, October 23-27, 2004
2. The word "NO" activates areas associated with negative emotion and inhibitory control. Alia-Klein, N.; Goldstein, R.Z.; Tomasi, D.; Cottone, L.A.; Wang, G.J.; Fowler, J.; and Volkow, N.D. SFN, 34th Annual Meeting, San Diego, CA, October 23-27, 2004
3. Role of genotype in cingulate function and inhibitory control: A functional magnetic resonance imaging (fMRI) study. Alia-Klein, N.; Goldstein, R.Z.; Tomasi, D.; Cottone, L.A.; Fowler, J.; Wang, G.J.; Volkow, N.D. *J Cogn Neurosci*: 33-34 Suppl. S 2005
4. Modulation of neural response in the prefrontal cortex and cerebellum by

monetary reward and instrumental response on a GO/NO-GO task. Leskovjan, A.C.; Tomasi, D.; Zhang, L.; Cottone, L.A.; Telang, F.; Caparelli, E.C.; Samaras, D.; Chang, L.; Ernst, T.; Volkow, N.D.; Goldstein, R.Z. *J Cogn Neurosci* 36-36 Suppl. S, 2005

5. Iterative Phase Correction to Minimize Signal Loss in EPI. Caparelli, E.C.; Tomasi, D.; Ernst, T. ISMRM Workshop on Methods for Quantitative Diffusion of Human Brain, 13-16 March, Alberta, Canada, 2005
6. Role of Genotype in Cingulate Function and Inhibitory Control: a Functional Magnetic Resonance Imaging (fMRI) Study. Alia-Klein, N.; Goldstein, R.Z.; Tomasi, D.; Zhang, L.; Cottone, L.A.; Fowler, J.; Wang, G.J.; Volkow, N.D. CNS Annual Meeting, New York, NY, April 9-12, 2005.
7. Modulation of neural response in the prefrontal cortex and cerebellum by monetary reward and instrumental response on a GO/NO-GO task. Leskovjan, A.C.; Tomasi, D.; Zhang, L.; Cottone, L.A.; Telang, F.; Caparelli, E.C.; Samaras, D.; Chang, L.; Ernst, T.; Volkow, N.D.; and Goldstein, R.Z. CNS Annual Meeting, New York, NY, April 9-12, 2005.
8. Acoustic Interference on working memory in HIV patients. Tomasi, D.; Chang, L.; Caparelli, E.C.; Foerster, B.; and Ernst, T. ISMRM, Thirteen Annual Meeting, Miami, FL, May 7-13, 2005.
9. Brain deactivation during attention-demanding tasks: inhibition or blood flow compensation. Tomasi, D.; Ernst, T.; Caparelli, E.C.; and Chang, L. ISMRM, Thirteen Annual Meeting, Miami, FL, May 7-13, 2005.
10. Correction for magnetic field shift due to mechanical vibration in EPI functional imaging. Foerster, B.; Tomasi, D.; Caparelli, E.C. ISMRM,

- Thirteen Annual Meeting, Miami, FL, May 7-13, 2005.
11. A Critical Comparison of Different Methods of Analysis for Individual Variability Studies Utilizing fMRI Regions of Interest. Korgaonkar, M.S.; Greenberg, T.; Tomasi, D.; Wagshul, M.E.; Mujica-Parodi, L.R. ISMRM, Thirteen Annual Meeting, Miami, FL, May 7-13, 2005.
 12. Mapping the phase component of the fMRI signal: Macro- and micro-vascular effects during working memory tasks. Tomasi, D.; Caparelli, E.C.; Foerster, B.; Telang, F. OHBM, Eleventh Annual Meeting, Toronto, Canada, June 12-16, 2005.
 13. Acoustic noise changes fMRI activation during visual attention task. Tomasi, D.; Caparelli, E.C.; Chang, L.; Ernst, T.; and Telang, F. OHBM, Eleventh Annual Meeting, Toronto, Canada, June 12-16, 2005.
 14. Increased amygdala and decreased anterior cingulate responses to a signal to stop behavior (emphatic vocalizations of the word "No!") in aggression-prone individuals. Alia-Klein, N.; Goldstein, R.Z.; Tomasi, D.; Zhang, L.; Cottone, L.A.; Fowler, J.; Volkow, N.D.; Wang, G.J. OHBM, Eleventh Annual Meeting, Toronto, Canada, June 12-16, 2005.
 15. Machine Learning for Clinical Diagnosis from Functional Magnetic Resonance Imaging. Zhang, L.; Samaras, D.; Tomasi, D.; Volkow, N.; Goldstein, R.Z. IEEE Computer Vision and Pattern Recognition, San Diego, CA, June 20-25, 2005.

LDRD FUNDING:

FY 2005	\$109,920
FY 2006 (budgeted)	\$110,000

Novel Multi-Modality MRI and Transcranial Magnetic Stimulation to Study Brain Connectivity

Elisabeth de Castro Caparelli 05-070

PURPOSE:

In this work we propose to develop a revolutionary methodology integrating transcranial magnetic stimulation (TMS) and interleaved acquisition of functional magnetic resonance imaging (fMRI) and diffusion tensor imaging (DTI), using BNL's 4T MR scanner, so as to provide the unique windows on brain function and connectivity. TMS can, non-invasively and painlessly, transiently disrupt activity in focal brain regions; fMRI is a well established technique used to measure changes in blood oxygenation level dependent (BOLD) signals in brain regions, which reflects changes in neuronal activity; and DTI permits the visualization of the tracts or bundles of neuronal axons that connect different parts of the brain. Thus, with this novel combination of TMS and multi-modality of MRI techniques in a high magnetic field we will be able to answer fundamental questions relating to brain behavior and its anatomical basis. This will promote the conduct of highly innovative and exploratory research and advance medical sciences at BNL.

APPROACH:

Background: Boning et al. (2000) applied single-pulses TMS over the motor cortex in healthy volunteers during fMRI studies in a 1.5T MR scanner. They verified that interleaved TMS/fMRI can be used in averaged single-pulse trials, and BOLD

responses to single-pulse TMS which can be detected under the TMS coil.

Guye et al. (2003) combined fMRI and DTI, to explore primary motor cortex (M1) connectivity in the human brain. The results demonstrated strong connections from M1 to the pyramidal tracts, premotor areas, parietal cortices, thalamus, and cerebellum, showing that the combination of fMRI and DTI is a promising tool to study the structural basis of functional networks in the human brain in vivo.

Aim: Integrate TMS and MRI technologies for the first time in a 4-T MRI scanner. Map brain activation produced by TMS-pulses, when applied over the motor cortex area using fMRI. Map structural connectivity within the TMS-activated neural networks using DTI.

Method: TMS will be applied through a nonferromagnetic double cone coil (70-mm outer wing diameter), connected to a Magstim Rapid stimulator (The Magstim Company, Wales, UK). The fixation and placement of the TMS coil will be done using a custom-made adjustable coil holder that will attach to the MRI head coil. fMRI will be performed using an EPI-GRE sequence, and data analysis will be performed in SPM2. DTI will be acquired using an EPI-SE sequence and data analysis will be performed using the medical imaging display and analysis group (MIDAG) package.

Collaborators: Dardo Tomasi, Ph.D., Gene-Jack Wang, M.D. and David Ansel, M.D.

References:

Bohning D.E. et al., JMRI 2000; 11: 569
Guye M. et al., NeuroImage 2003; 19:1349

TECHNICAL PROGRESS AND RESULTS:

During this first year the technical implementation of TMS inside the high field MRI scanner has been initiated. The Magstim Rapid, model 220, which is composed of a main unit and a booster, and an MRI compatible 70 mm figure of eight TMS coil, has been purchased. The stimulator is able to reach a peak of 2 T and a maximum repetition rate of 1 Hz. The MRI compatible TMS coil can produce a maximum magnetic field of 0.91 T.

The interaction of the static magnetic field with the magnetic field generated by the TMS coil results in additional force acting over the TMS coils. For this reason a safe adjustable holder was made with wood to attach the TMS coil inside of the RF-coil. The holder was tested in the MRI to ensure physical safety to any subject prior to use. Piezoelectric has been used to detect TMS coil vibration, in order to verify the holder quality.

A standard TMS coil, also 70 mm figure of eight, to be used outside the MRI during the experiment to previously determine the site of stimulation and motor threshold for each subject was purchased. Quality tests of both TMS coils and calibration have been performed with a pickup coil. Possible interferences of the TMS with the image acquisition started to be explored. Susceptibility artifacts were observed in a phantom image, due to the presence of the TMS coil. DTI technique has been incorporated in the 4 T MRI scanner: the pulse sequence and image reconstruction has been developed. MIDAG package has been implemented for post-processing. A new environmental safety review (ESR) was generated and approved. The protocol, which will use 20 healthy volunteers, was also approved.

SPECIFIC ACCOMPLISHMENTS:

Publications:

1. The Effect of Small Rotations on R2* with Echo Planar Imaging. Caparelli, E.C.; Tomasi, D.; and Ernst, T. *NeuroImage* 24, 1164-1169 (2005).
2. Can Motion Artifacts be Completely Removed from fMRI-Activation Maps? Caparelli, E.C.; *Current Medical Imaging Reviews*, 1, 253-264 (2005)
3. fMRI-acoustic noise alters brain activation during working memory tasks. Tomasi, D.; Caparelli, E.C.; Chang, L.; and Ernst, T. *NeuroImage* 27, 377-386 (2005).
4. Magnetic Field Shift due to Mechanical Vibration in Functional MRI. Foerster, B.; Tomasi, D.; and Caparelli, E.C. *Magn Reson Med* 54: 1261-1267 (2005).
5. Common deactivation patterns during working memory and visual attention tasks: An intra-subject fMRI study at 4 Tesla. Tomasi, D.; Ernst, T.; Caparelli, E.C.; and Chang, L. *Human Brain Mapp* (in press).
6. The human immunodeficiency virus reduces network capacity: acoustic noise effect. Tomasi, D.; Chang, L.; Caparelli, E.C.; and Ernst, T. *Ann Neurol* (n press).
7. Loss of sensitivity to relative saliency of money in cocaine users is associated with disrupted activity in lateral orbitofrontal cortex. Goldstein, R.Z.; Tomasi, D.; Cottonec L.A.; Telang, F.; Caparelli, E.C.; Zhang, L.; Samaras, D.; Leskovjan, A.C.; Chang, L.; Ernst, T.; and Volkow, N.D. *Neuroimage* (submitted).
8. Intra-vascular contamination in activation patterns of working memory. Tomasi, D. and Caparelli, E.C. *Neuroimage* (submitted)
9. Decreased prefrontal cortical sensitivity to monetary reward in cocaine addiction is associated with impaired motivation

and self-control. Goldstein, R.Z.; Alia-Klein, N.; Tomasi, D.; Cottone, L.A.; Zhang, L.; Maloney, T.; Telang, F.; Caparelli E.C.; and Volkow, N.D. Am J Psychiatry (submitted)

10. Different activation patterns for working memory load and visual attention load. Tomasi, D.; Chang, L.; Caparelli, E.C.; and Ernst, T. J Magn Reson Imaging (submitted).

Conference Proceedings:

1. E. C. Caparelli et al, ISMRM Workshop on Methods for Quantitative Diffusion of Human Brain, Alberta, Canada, 2005
2. Leskovjan, A.C.; Tomasi, D.; Zhang, L.; Cottone, L.A.; Telang, F.; Caparelli, E.C.; et al. J Cogn Neurosci: 36-36 Suppl. S, 2005
3. Leskovjan, A.C.; Tomasi, D.; Zhang, L.; Cottone, L.A.; Telang, F.; Caparelli, E.C. et al. CNS Annual Meeting, NY, 2005.
4. Tomasi, D.; Chang, L.; Caparelli, E.C. et al. ISMRM, 13 Annual Meeting, FL, 2005.
5. Tomasi, D.; Ernst, T.; Caparelli, E.C.; and Chang, L. ISMRM, 13 Annual Meeting, Miami, FL, 2005.
6. Foerster, B.; Tomasi, D.; Caparelli, E.C. ISMRM, 13 Annual Meeting, FL, 2005.
7. Tomasi, D.; Caparelli, E.C. et al., OHBM, 11 Annual Meeting, Toronto, Canada, 2005.
8. Tomasi, D.; Caparelli, E.C. et al., OHBM, 11 Annual Meeting, Toronto, Canada, 2005.

Grant Applications:

1. "Fast EPI readout for mapping whole brain connectivity," PI: D. Tomasi, Total costs: \$499,516, agency: NIH, 1 R21, Dates: 04/01/06-03/31/08, Pending
2. "Development of new magnetic resonance imaging contrast agents" PI: M. Miura, Technology Maturation Project. Total Cost: \$ 97,100 Pending

LDRD FUNDING:

FY 2005	\$105,571
FY 2006 (budgeted)	\$112,000

Ovarian Hormone Modulation of ICP: MRI Studies

Anat Biegon

05-071

PURPOSE:

The invasive nature of current methods used for the measurement of intracranial pressure (ICP) precludes the investigation of physiological modulators of this parameter in healthy individuals. The specific aims of this project are: 1. To develop and optimize a new non-invasive, robust method for measuring ICP by high-field MRI. 2. Generate new data on the range and direction of ICP changes across the human menstrual cycle 3. Generate new data on the effect of estrogen alone or in combination with progesterone on ICP. 4. Generate new data on the connection between hormone-dependent increases in ICP, changes in brain water content and common complaints associated with the premenstrual period, such as headache, depression, irritation and decreases in performance of cognitive tasks.

The ultimate goal of this proposal is to develop and validate a sensitive and reliable non-invasive method of measuring intracranial pressure so it can be safely applied to the study of ICP in the wider context of brain water dynamics in a variety of physiological (e.g. menstrual cycle, pregnancy) and pathological (e.g. head injury, stroke, hydrocephalus, brain tumors) conditions.

APPROACH:

Increased intracranial pressure is a dangerous and sometimes fatal phenomenon. Annually, over 1.5 million people in the United States alone suffer from neurological problems stemming from traumatic brain

injuries, hydrocephalus, intracranial hemorrhages, tumors, and other disorders that are associated with abnormal intracranial pressure. At present, ICP measurement techniques are highly invasive, requiring insertion of a catheter into the brain tissue or a cerebral ventricle. Insertion of these catheters damages brain tissue and carries risks of intra cerebral bleeding and infection. Despite the risks, the tests are used because intracranial pressure is such an essential clinical parameter. However, due to these problems, ICP is usually monitored only in severely head injured patients, in a clinical setting and only for limited periods. All of these restrictions could be relaxed if a non-invasive ICP measurement system were to be made available. A non-invasive procedure may provide a substantial risk reduction and improved quality of life in the patient groups currently getting monitored and open a whole new field of research regarding the possible effect of demographic factors (age, sex, race, ethnic origin) on ICP and the correlation and possible causal relationship between transient, moderate increases in ICP and changes in normal brain function such as mood and cognition. We chose to adopt and optimize an MRI-based non-invasive technique developed for a moderate (1.5T) strength magnet by Alperin and colleagues at UI and apply it to a higher field magnet such as the BNL 4T and the SBU 3T magnets. This work is done in collaboration with Drs. Mark Wagshul, an MRI physicist; and Michael Egnor, a neurosurgeon, both of SBU.

ICP at any given time is determined by brain water content and fluid dynamics; and ovarian hormones are known to exert significant influence on water balance, including swelling and water retention, in target organs such as the uterus and breast. We found that after traumatic brain injury, young women are significantly more likely to develop edema (brain swelling) and

elevated ICP than young men. Women are also significantly more likely than men to develop idiopathic intracranial hypertension, migraines, depression, and multiple sclerosis with exacerbations known to increase in frequency in the late phase of the normal menstrual cycle when progesterone and estrogen are declining from peak levels.

Taken together, these observations suggest that fluctuating levels of ovarian hormones may result in ICP fluctuations, rendering women more vulnerable to developing intracranial hypertension during discrete phases of the menstrual cycle. Experiments were designed to test this hypothesis using the new technique.

TECHNICAL PROGRESS AND RESULTS:

In the first experiment we tested and optimized various MRI sequences on a flow phantom constructed at BNL and testing MRI sequences to the point where flow rate measured by MRI was similar to actual calibrated linear flow rate over an acceptable range of values (5-65cm/sec), representing the expected range of flow rates in human CSF, veins and arteries.

The optimization work was continued in human subjects at SBU on a clinical 3T magnet. The optimized sequence was tested using different coils (head coil VS. 2 surface coils) and different gating approaches (peripheral pulse VS. ECG). Signal to noise was better with the head coil and ECG.

Overall, we performed eight MRI flow (venous, arterial and CSF flow in each

session) measurement experiments on 7 subjects and calculated the elastance index and the ICP. The results are summarized in Table 1. As can be seen from the table, all healthy subjects had ICP values within the normal range (<15 mmHg) and the only abnormal value was measured in one patient.

Based on these encouraging preliminary results, we have written and submitted a protocol to CORIHS for using this technique to measure ICP in young women at different phases of the menstrual cycle and older postmenopausal women who are or are not taking hormone replacement therapy in conjunction with measurement of hormone levels in plasma and a short neuropsychological assessment of mood and cognition. This protocol was provisionally approved in October 2005.

Table 1. MRI-derived elastance and ICP in six Healthy Subjects and one hydrocephalus patient

elastance index	Sex	Age	calc ICP ~
0.022	female	58	1.57
0.095	female	22	6.80
0.115	female	50	8.17
0.079	female, retest	50	5.65
0.040	male	24	2.85
0.172	male	32	12.24
0.065	male	40	4.68
0.214	HC patient-female	15	15.20

This project involves human subjects.

LDRD FUNDING:

FY 2005	\$107,120
FY 2006 (budgeted)	\$112,200

Feasibility of CZT for Next-Generation PET Performance

Paul Vaska

05-072

PURPOSE:

We aim to demonstrate the feasibility of using cadmium zinc telluride (CZT) as a gamma-ray detector for medical imaging with positron emission tomography (PET). CZT has been discussed in this context for years and the quality and availability of CZT detectors has steadily increased, but a broad team of detector and imaging scientists is required to overcome a number of technical obstacles. This work is in the field of Medical Imaging as well as at the interface of Life and Physical sciences, two recent initiatives within the BNL institutional strategy.

APPROACH:

CZT has great potential for PET because of its potentially high spatial resolution (1 mm or less, including in depth which is important to minimize parallax problems), high-energy resolution (to reject scattered radiation), favorable geometry (no photosensor, compact), and insensitivity to magnetic fields (to permit simultaneous imaging with PET and MRI). The main hurdles are poor timing (required to reject random coincidences) and relatively low stopping power at 511 keV. The high-risk element of the project lies in our ability to mitigate these shortcomings.

To demonstrate feasibility we have developed methods to overcome these hurdles with an exceptionally qualified, interdisciplinary team of experts from the areas of solid state detector and nuclear

medicine research. The team includes one of the best CZT research groups in the world (Aleksy Bolotnikov, Giuseppe Camarda, Gabriela Carini, and Ralph James), low-noise electronics expertise (J.-F. Pratte and Paul O'Connor), and experienced imaging physicists (Avraham Dilmanian, Sang-June Park, and Paul Vaska).

The general approach is to first develop methods to overcome the timing and sensitivity drawbacks of CZT using actual CZT devices and then incorporate the optimized methods and measured detector performance into a realistic Monte Carlo simulation of a full PET system to estimate the ultimate performance of CZT for PET.

TECHNICAL PROGRESS AND RESULTS:

We have been able to evaluate a number of different CZT crystals in terms of coincidence timing and have achieved 10–20 ns full width at half maximum (FWHM) time resolution depending on the specific detector. The cathode waveform is digitally sampled and a fitting algorithm applied to estimate the time of occurrence of the event as shown in Fig. 1.

To satisfy the imaging requirement as well as provide sufficient sensitivity, we have procured 2 ~1 cm³ pixel detectors from eV Products, with an anode array pitch of 2.5 mm. We designed and built a readout board and electronics for these detectors and characterized them in terms of uniformity of response to both X-rays (at the NSLS – Fig. 3) and gamma-rays (511 keV, not shown). The results from both measurements demonstrated excellent detector quality.

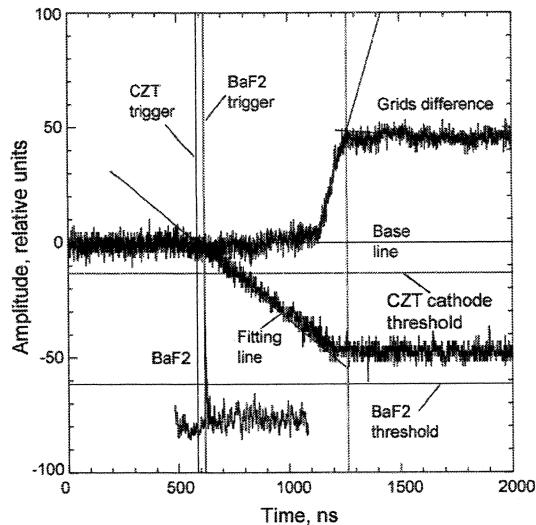


Fig. 1. Pulse waveforms from 7.5 mm thick coplanar grid CZT detector irradiated with 511 keV gamma rays, including the fits used for time estimation.

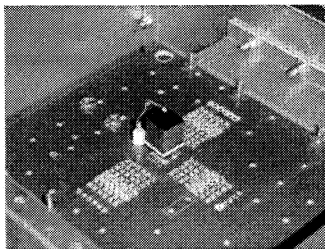


Fig. 2. Pixel detector on custom PC board.

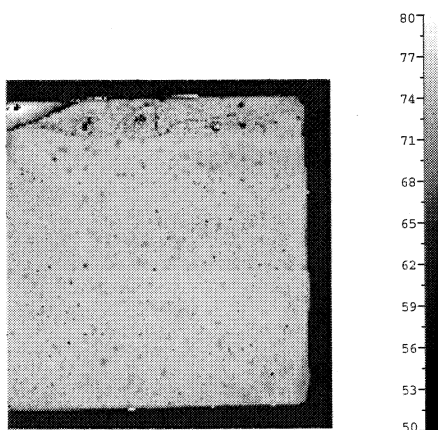


Fig. 3. Uniformity of energy response from CZT pixel detector from scan of X-ray beam across cathode.

Accurate Monte Carlo simulations of a full PET system employing these pixel detectors are being developed using the GATE package (which is based on GEANT4) which has been installed and benchmarked.

Finally, the Instrumentation Division has developed a full data acquisition system to simultaneously read out all anode and cathode channels from 2 pixel detectors. It takes advantage of a unique peak-detect Application Specific Integrated Circuit (ASIC) developed at BNL. Adapting this system to our CZT detectors involved yet another custom PC board design which was recently completed.

In FY06, we plan to analyze the performance of the pixel detectors using the new peak-detect data acquisition system, optimize coincidence timing algorithms, and demonstrate full PET performance via simulation. Some preliminary PET images may be acquired from this system.

SPECIFIC ACCOMPLISHMENTS:

Studies of CZT for PET Applications, P. Vaska, A. E. Bolotnikov, G. Carini, G. S. Camarda, J.-F. Pratte, F. A. Dilmanian, S.-J. Park, and R. B. James, IEEE Nuclear Science Symposium and Medical Imaging Conference, Fajardo, Puerto Rico, Oct. 24-29, 2005.

LDRD FUNDING:

FY 2005	\$111,425
FY 2006 (budgeted)	\$110,000

Biology on Massively Parallel Computers

James W. Davenport

05-074

J. Glimm

D. Keyes

Y. Deng

PURPOSE:

This is a proposal to develop new algorithmic approaches for computational biology on massively parallel computers. The aim is to make effective use of machines such as the 12,000 processor Quantum Chromodynamics on a Chip (QCDOC) and the 131,000 processor BlueGene/L (BG/L) requiring a combination of algorithms and applications.

The algorithmic research includes the development of efficient molecular dynamics (MD) codes which take account of data non-locality and apply explicit routing protocols suitable for both QCDOC and BG/L.

The applications involve molecular dynamics simulations of several small proteins including the adenovirus protease studied structurally by Mangel and co-workers and Botulinum neurotoxin studied by Swaminathan and co-workers both at the NSLS.

APPROACH:

Molecular dynamics simulations require large amounts of computer time in addition to efficient algorithms. To deal with these a new MD code specifically adapted to QCDOC is being developed. The time limitations are usually due to the long-range nature of the forces between atoms. These are evaluated by fast Fourier transforms

(FFTs), which are known to be slow on massively parallel machines. Hence an important component of this research is the development of communication routines for FFTs which is being carried out by Y. Deng and students at Stony Brook. Application to the proteins mentioned above uses the AMBER suite of codes. The adenovirus work is being performed at BNL, the Botulinum at Stony Brook.

TECHNICAL PROGRESS AND RESULTS:

The FFT code has been written and shows excellent scaling in tests on QCDOC up to 4096 processors. The new MD code has been written and is undergoing tests. More than 10 nsec of simulated time has been calculated for the adenovirus protease and more than 50 nsec for the botulinum. Structural changes associated with the activation of adenovirus have been found in the simulations. Changes in the structure of Botulinum have been studied as a function of pH. In 2006, these simulations will be further analyzed and compared with experiments.

SPECIFIC ACCOMPLISHMENTS:

Publications:

B. Fang and Y. Deng, *Performance of 3D FFT on 6D QCDOC Torus Parallel Supercomputer*, J. Comp. Phys. Submitted:

LDRD FUNDING:

FY 2005	\$168,787
FY 2006 (budgeted)	\$177,801

Ionic Liquids in Biocatalysis and Environmental Persistence

Arokiasamy J. Francis

05-078

S.V. Malhotra

C. Zhang

C.J. Dodge

PURPOSE:

The overall goal of this project is to determine the application of ionic liquids (ILs) in industrial, agricultural, and environmental remediation processes, leading to improved or new green chemistry based methodologies. Initial efforts are focused on their ability to form complexes with uranyl ion, a major contaminant in DOE wastes. The persistence of the U(VI) ILs in the environment due to inadvertent release is also being investigated in this study.

APPROACH:

We investigated the interaction of uranium with ILs N-ethylpyridinium tetrafluoroborate (EtPyBF₄), ethylpyridinium trifluoroacetate (EtPyCF₃COO), and 1-butyl-3-methylimidazolium hexafluorophosphate (BMIMPF₆). The two ethylpyridinium based ILs are hydrophilic and have great potential applications in organic synthesis and biocatalysis, whereas BMIMPF₆ is a widely used hydrophobic IL.

Equimolar 1:1 U(VI)-IL mixtures (5.78 mM) were prepared by mixing uranyl nitrate and IL solution in 25ml volumetric flasks and allowed to stabilize for 24 hours in the dark to prevent photodegradation reactions. Similar methods were used to prepare 1:2 U(VI) - IL mixtures. The interaction between uranium and the IL was determined by a combination of several analytical methods

including potentiometric titration, UV-vis spectrophotometry, liquid chromatography-mass spectrometry (LC-MS), and x-ray absorption spectroscopy at the NSLS. X-ray absorption near edge structure (XANES) and extended x-ray absorption fine structure (EXAFS) analyses were used to determine the speciation of uranium and the molecular structure of the U-IL complex.

TECHNICAL PROGRESS AND RESULTS:

Potentiometric Titration. Figure 1 A-C shows the effect of 0.01 N sodium hydroxide additions on the complexation of uranyl ion with the ILs. The coincidence of the titration curves for the U:EtPyBF₄ (Figure 1A) and the U:BMIMPF₆ (Figure 1B) complexes with uranyl nitrate alone indicate no complex formation is evident between the metal and the IL. Addition of one-fold excess IL had no effect on the complexation. However, titration of the U in the presence of EtPyCF₃COO (Figure 1C) shows a release of protons into the medium as indicated by the increase in inflection point with increasing pH. This indicates there is an interaction of the uranium with the IL. The interaction increases with addition of one-fold excess IL.

UV-Vis Spectrophotometry. The UV-Vis absorption spectrum of the free uranyl ion is given in figure 2A in the range 300 nm to 500 nm. The spectra show a weak absorption band in the range 350 nm and 480 nm with a characteristic fine structure. Above 480 nm no further absorption bands were observed. The shape of the uranium absorbance is identical following 24-h incubation with maximum absorbance at 413 nm, and two side shoulders at 402 and 425 nm. The pH was adjusted to 2.12 (similar to U: EtPyCF₃ mixture) by 0.1N nitric acid to elucidate the pH effect on UV

absorbance. The results showed that the pH change did not alter the shape of the absorbance and that the decrease in absorbance was due to the addition of nitric acid.

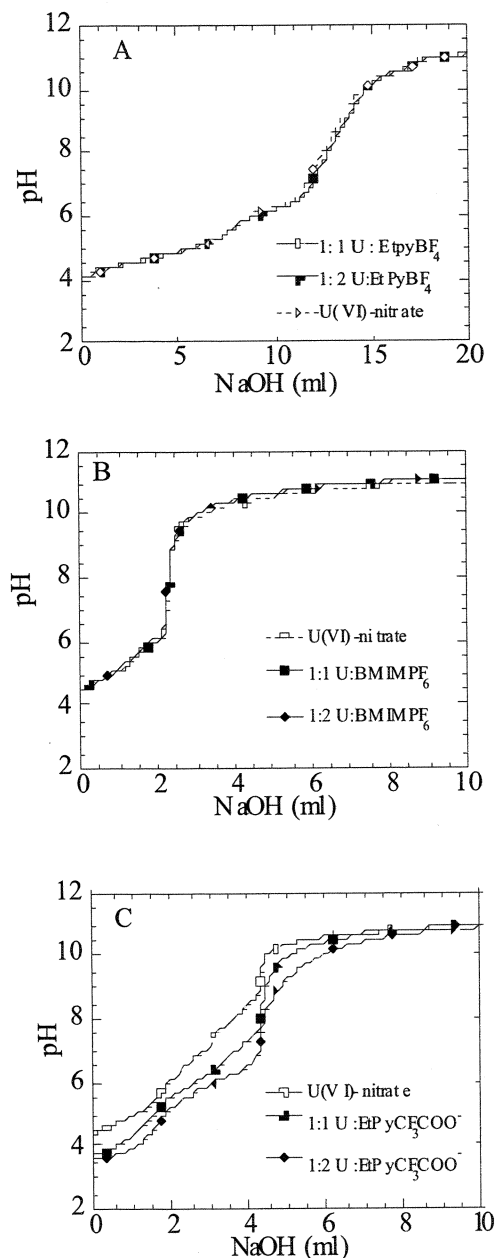


Figure 1. Potentiometric titration curves of U with various ionic liquids.

UV absorbance change for the U in 1:1 U:EtPyBF₄ and 1:2 U:EtPyBF₄ mixtures are shown in Figure 2B. The spectra are similar to that found for the U(VI)-nitrate indicating

no evidence of complexation of the IL with U. The 1:1 and 1:2 U:BMIMPF₆ mixtures also have the same absorbance as uranium itself (Figure 2C) indicating no complexation occurs in the presence of uranium. However, in the U:EtPyCF₃COO mixture, maximum absorbance has shifted to 408 nm and 419 nm (Figure 2D).

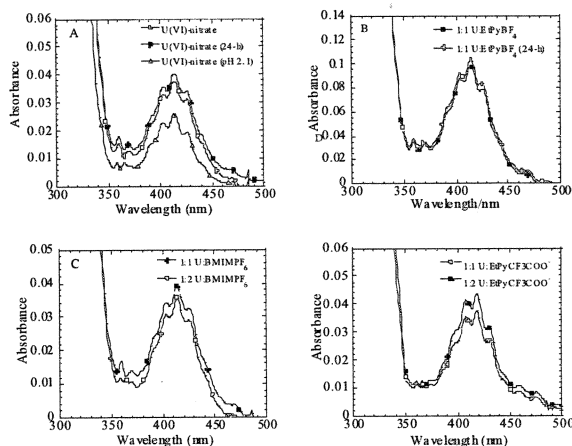
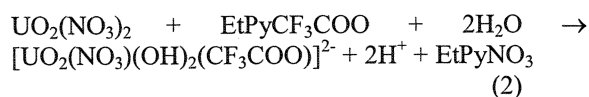
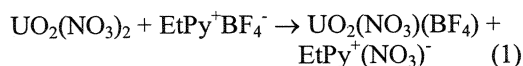


Figure 2. UV-vis spectrophotometry of U-nitrate (A), U:EtPyBF₄ (B), U:BMIMPF₆ (C), and U:EtPyCF₃COO (D).

The complexes were also analyzed in solution phase using Liquid Chromatography Mass Spectrometry in the negative ion mode. Anion exchange products were identified for reaction between U and EtPyBF₄ (Reaction 1) and EtPyCF₃COO⁻ (Reaction 2).



X-ray absorption near-edge spectroscopic (XANES) analysis. XANES measures the oxidation state of the central atom by determining the shift in absorption edge compared to a known standard. Analysis of the absorption edge energies for U(VI)-

nitrate and mixtures of U(VI)-nitrate and various IL's revealed they had the same absorption edge energy (17175 eV) (Figure 3). This confirms that the U(VI) added to the IL's solution was present as U(VI) species and not reduced to U(IV).

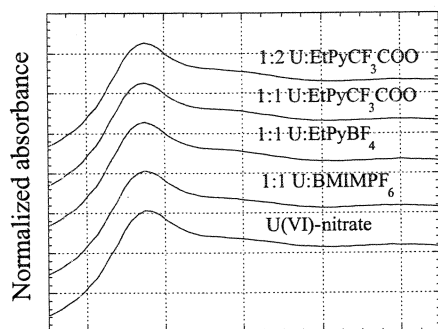


Figure 3. Normalized XANES spectra showing oxidation state of U in the presence of various ILs.

Extended X-ray absorption fine structure (EXAFS) analysis. EXAFS spectroscopy measures the x-ray absorption as a function of energy and determines the local arrangement of atoms around a given absorbing atom. Analysis of the EXAFS data allows the determination of the type of atom, the number of neighboring atoms, and their distances from the central scattering atom. EXAFS measurements at the complexed metal absorption edge can also distinguish between the different functional groups. The k^3 -weighted and Fourier-transformed data for uranyl nitrate and the U:IL complexes is presented in Figure 4.

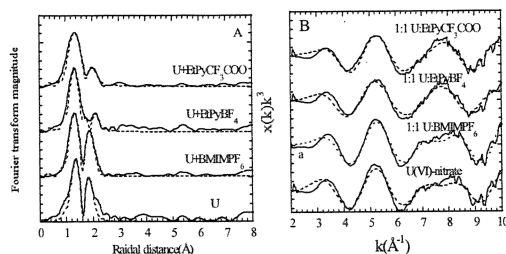


Figure 4. EXAFS analysis at the U L_{III} edge showing (A) raw k^3 -weighted (2.0 - 12.0 \AA^{-1}) and (B) Fourier-transform data for uranium and different ILs mixtures. Experimental data (-); fitted data (- -).

EXAFS analysis of uranium in water indicates structural parameters for the oxygen atoms associated with the uranium and consisted of 2 axial oxygens at $1.77 \pm 0.01 \text{ \AA}$ and $4.5 \pm 1.5 \text{ O}_{eq}$ at 2.33 \AA , which is consistent with the expected values for a hydrated uranyl sample (Figure 5a).

In the 1:1 U:BMIMPF₆ mixture the best fit model is almost the same as the hydrated uranyl moiety (Figure 5b). Because of the low solubility of BMIMPF₆ in aqueous solution, less PF₆⁻ was present in the water, and the complex concentration was too small to obtain a detectable signal. However, examination of the literature show the formation of UO_2PF_6^+ complex confirmed by time resolved emission spectroscopy (TRES).

The data presented in this study clearly show there is a complex formed between (i) U and EtPyBF₄ consisting of the BF₄⁻ component of the IL (Figure 5c) and, (ii) U and EtPyCF₃COO consisting of the CF₃COO⁻ component of the IL (Figure 5d).

In 1:1 U:EtPyBF₄ mixture, 3.5 ± 1.3 equatorial oxygen were found at $2.45 \pm 0.02 \text{ \AA}$ and 1.4 ± 0.4 fluoride atoms were found at $2.22 \pm 0.01 \text{ \AA}$, which suggested the presence of a monodentate complex.

In $\text{UO}_2\text{CF}_3\text{COO}^+$ complex 2.4 ± 0.1 a O_{ax} was found at $1.77 \pm 0.03 \text{ \AA}$ with a $4.6 \pm 2.5 \text{ O}_{eq}$ atom at $2.40 \pm 0.03 \text{ \AA}$, and $1.4 \pm 0.8 \text{ C}$ atom at $2.92 \pm 0.02 \text{ \AA}$. Normally a monodentate complex the O_{eq} distance is from 2.30 to 2.35 \AA , and bidentate carboxylate bonding is from 2.40 to 2.50 \AA . Therefore, the 2.40 \AA in our experiment is typical of bidentate complex. Due to the low complex constant or the dissociation of EtPyCF₃COO, addition of more EtPyCF₃COO would not change the U complex formation.

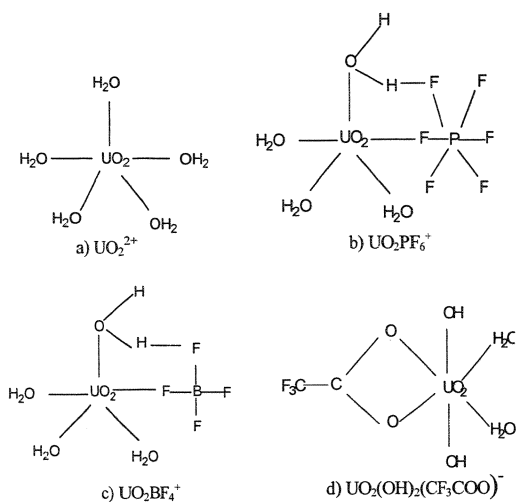


Figure 5. Proposed structures of uranium complexation with ILs.

Based upon the LC-MS and EXAFS results we propose the following structures for ionic liquid complexes with uranium (Figure 5).

SPECIFIC ACCOMPLISHMENTS:

1. Malhotra, S.V.; A.J. Francis, C. Zhang. Biocatalysis in ionic liquids for environmental application. Paper presented at 24th Rare Earth Research Conference, Keystone Colorado, June 26-30, 2005.
2. Zhang, C.; S.V. Malhotra, A.J. Francis. Interaction of ionic liquids with uranium and its implication on bioreduction. Paper presented at 230th ACS National Meeting, Washington D.C., August 28-September 1, 2005.
3. Zhang, C.; S.V. Malhotra, A.J. Francis. Effects of ionic liquids on uranium bioreduction. Paper presented at Pacificchem 2005 International Chemical Congress of Pacific Basin Societies, Honolulu, Hawaii, December 15-20, 2005.

LDRD FUNDING:

FY 2005	\$ 99,464
FY 2006 (budgeted)	\$100,000

Single Particle Laser Ablation Time-of-Flight Mass Spectrometer (SPLAT-MS) Enhancements: Aerosol Optical Properties And Increased Particle Detectivity

Gunnar Senum

05-082

PURPOSE:

SPLAT-MS is an aerosol mass spectrometer developed by Dan Imre and Alla Zelenyuk which has been on loan to PNNL. This instrument has now been returned to BNL. The purpose of this program is to reassemble SPLAT at BNL and examine several enhancements that could be applied to SPLAT to improve its value for measurements in the DOE aerosol/climate program. These include measuring the aerosol Mie scattering pattern with increased spatial resolution to possibly determine aerosol particle refractive index and asphericity and a second enhancement which is an improvement in the timing algorithms that controls the firing of the ablation laser. This would extend the aerosol particle sampling diameter range.

APPROACH:

When SPLAT-MS was at BNL before the loan to PNNL, I worked with Dan Imre and Alla Zelenyuk on this instrument. I participated in a field experiment with SPLAT-MS and consequently disassembled and reassembled SPLAT several times. During this period I performed many experiments on SPLAT, both in field experiments and in lab characterization of SPLAT for future publications. This allowed me to become quite familiar with the operation and theory of the instrument. Also I observed some of the deficiencies in

SPLAT. This has led to this LDRD which will either improve or explore the feasibility of enhancements to remove the timing deficiency and to explore the feasibility of enhanced spatial resolution of the Mie scattering patterns. The approach will be to use my expertise to reassemble SPLAT and to examine the feasibility of these enhancements. Art Sedlacek is a collaborator.

TECHNICAL PROGRESS AND RESULTS:

A request was made to PNNL to end the loan of SPLAT (which had expired in May 2004) and return it to BNL at the start of FY 2005 so that work on this LDRD could start. However, SPLAT was not delivered in a timely manner, and not until May 2005, just about one year later than anticipated. Consequently, no LDRD work was done or LDRD funds expended until May 2005. At that time SPLAT was unpacked and inventoried. All of the major parts of SPLAT were found to have been returned to BNL. Further work did not start until September 2005 at which time reassembly of SPLAT was initiated. Progress included examination of the computers to find that all of the SPLAT software was there; closer examination of the returned SPLAT parts indicated that many of the smaller parts, such as flange bolts, PMT shrouds, vacuum fittings, hoses, clamps, signal cables, etc., were not returned, consequently plans were made to purchase these needed items. At this time it was also noted that SPLAT had been totally deconstructed for its return to BNL, which made reassembly a more difficult task though not insurmountable. Plans were made for the reassembly of SPLAT regarding needed electrical power, venting, and lab location. The lab space was prepared, and the major sections of SPLAT were moved into the lab.

The most significant quantifiable accomplishment of FY 2005 was the actual return of the SPLAT to BNL. The small amount of work performed in FY 2005 was mostly of inventorying and planning for work in FY 2006. Discussions were held in FY 2005 for some experiments to be performed on SPLAT once it is assembled.

SPECIFIC ACCOMPLISHMENTS:

None

LDRD FUNDING:

FY 2005	\$ 97,705
FY 2006 (budgeted)	\$100,000

Transition Metals in Oil and Gas Exploration

Appathurai Vairavamurthy

05-088

PURPOSE:

The overall purpose was to conduct exploratory research in petroleum geochemistry, focused on improving our knowledge of the science and technology for recovering and utilizing petroleum (natural gas and oil), primarily based on analytical capabilities at BNL's NSLS. The specific objective was to enhance the fundamental understanding of the science of gas and oil exploration and exploitation, building on our expertise on x-ray absorption spectroscopy.

APPROACH:

The primary goal was to better understand the significance of transition-metal catalysis in generating natural gas in sediments. Conventionally, the generation of gas from oil was thought to be thermally induced. But some giant gas deposits occur in shallow low-temperature reservoirs suggesting catalysis could be involved. Based on laboratory experiments, it was proposed that zero-valent-transition metals, particularly nickel, catalyze this conversion. Thus, our goals were (1) verify the occurrence of Ni(0) in late diagenetic sediments using x-ray spectroscopy, and (2) examine the potential mechanisms of Ni(0) formation under conditions appertaining to deep sediments.

A second research area focused on improving the science of heavy oils and tar sands. The presence of macromolecular polar compounds containing sulfur and nitrogen is a major hindrance to economically recovering heavy oils. The geochemistry of this polar fraction is poorly known because of problems in analyzing

complex molecules. Thus, an important aim of this research was to use the non-destructive X-ray Absorption Near Edge Structure (XANES) spectroscopy to shed new light on the composition of sulfur compounds in heavy oils and tar sands.

Ni Speciation in Sediments

To explore the significance of Ni(0) in gas generation, we examined the speciation of nickel in two well-known petroleum source/reservoir rocks where catalytic conditions for natural gas formation could prevail: (1) the Miocene Monterey Formation, California, U.S.A., and (2) the Kimmeridge Clay Formation, Dorset, England (main source rocks of the North Sea oil). Using synchrotron-radiation based x-ray absorption spectroscopy, we probed the chemical state of nickel non-destructively. The shale samples were obtained through collaboration from the United States Geological Survey (USGS).

The K-edge x-ray absorption spectra (EXAFS) of nickel were collected in the fluorescence mode at the X-18B beamline, NSLS, using a Si(111) channel-cut monochromator. The EXAFS were analyzed using the IFEFFIT software package involving standard procedures. To establish the spectroscopic behavior of different types of nickel-containing bonds and molecules, we also collected spectra from several model compounds.

Mechanistic Studies on Ni Transformation

These experiments tested the hypothesis that zero-valent nickel could have been formed from the reduction of Ni(II) by reduced organic sulfur compounds in the sediments. Our approach was to react Ni(II) with various reduced organic sulfur compounds at temperatures relevant to sediments (closed system, 150-250 °C) and to monitor changes in the chemical speciation of the metal and

sulfur using XANES and EXAFS spectroscopies.

TECHNICAL PROGRESS AND RESULTS:

EXAFS Analysis of Nickel Speciation in Shales

X-ray absorption spectroscopy did not reveal any elemental nickel in the sediment samples, but rather showed it existed predominantly as Ni(II). Oxygen appeared to be the main ligand in the first coordination shell, although sulfur also constituted a significant fraction in the organic-rich sediments from the Monterey Formation, probably as nickel sulfide.

Although our methodology did not show the presence of zero-valent nickel in these two well-known petroleum source/reservoir rocks where catalytic conditions for natural gas formation potentially could exist, it could be there at low levels, e.g., < 1 ppm, at which the method would not detect it. Further zero-valent nickel could have existed in the original catalytic sediments but have been destroyed subsequently, probably through reactions with oxygen, thereby oxidizing it to Ni(II). Thus, while our results did not directly support the hypothesis that zero-valent nickel was the active catalyst for generating natural gas in sediments, they did not entirely rule out the possibility that it could be involved. Indeed, a different form of nickel, or a different transition-metal species, other than zero-valent nickel, might catalyze the generation of natural gas in sediments. We are pursuing this further.

Mechanistic Studies

Heating a mixture of a reduced sulfur compound, for example, cysteine, and Ni(II) (nickel chloride) in the presence of water around 225 °C in a closed reactor led to the copious production of gas as evidenced by the buildup of intense pressure. XANES analysis of the residue revealed that Ni(II) was converted to nickel sulfide (NiS). The gas was shown to be mainly hydrogen and carbon

dioxide (>90%), along with small amounts of low-molecular-weight hydrocarbons. Our inference is that the reaction of reduced sulfur with Ni(II) generated a catalytically active form of NiS that transformed the organic molecule into hydrogen, carbon dioxide, and pyrobitumen.

These results are remarkable because the catalytic potential of nickel sulfides in geochemical processes were not recognized earlier, despite their widespread distribution in reducing organic-rich sediments. In continuing studies, we will explore the effect of *in situ* generated NiS in transforming biomass derived molecules, such as glucose, to useful fuel products.

Speciation of sulfur in heavy oils

We assembled and collected sulfur XANES spectra from several heavy oils and tar sands from the Western Canada Sedimentary Basin. Our initial results showed that thiophenes and sulfides accounted for more than 70% of the total sulfur in most oils. Further work on sulfur speciation in heavy oils is in progress.

SPECIFIC ACCOMPLISHMENTS:

"X-ray absorption spectroscopic speciation of nickel in organic shales: implications for catalysis in natural gas generation" was submitted to *Applied Geochemistry*.

We submitted a proposal titled "Speciation of Sulfur and Nitrogen in Heavy Oils" to the Office of Fossil Energy, U.S. Department of Energy in March 2005. The Program could not consider this proposal for funding at that time because of its uncertain future directions. We may resubmit a revised proposal in FY 2006. The petroleum industries are considering some support for the proposed work in FY 2007.

LDRD FUNDING:

FY 2005	\$128,489
FY 2006 (budgeted)	\$135,000

An Innovative Infiltrated Kernel Nuclear Fuel for High- Efficiency Hydrogen Production with Nuclear Power Plants

Jacopo Saccheri

05-092

B. Bowerman

PURPOSE:

This project will demonstrate the feasibility of a new manufacturing process for an innovative nuclear fuel: the Infiltrated Kernel Nuclear Fuel (IKNF). The IKNF process deposits nuclear fuel into the naturally occurring porosity in graphite. IKNF consists of infiltrating uranyl nitrate dissolved in an organic solvent into the graphite and then heat-treating the sample to remove the solvent and convert the uranyl nitrate to UO_2 at low ($<300^\circ C$) temperatures. Complete conversion to UC_2 can be accomplished by heating to temperatures higher than $3000^\circ C$. IKNF is extremely flexible: it is appropriate for very high temperature applications and heating the infiltrated product to intermediate temperatures ($\sim 900^\circ C$) produces nuclear fuel with a range of chemistries in the U-C-O system (similar to the current US TRISO fuel). It is believed that the process can also be used to produce fuel containing transuranics.

Graphite infiltration involves a few, easily measurable and controllable variables, it is reproducible and predictable. It is believed that the IKNF process will be less expensive, more robust, and more suitable for on-line monitoring than the current sol-gel fabrication technique. The technology used by IKNF was developed in the late '80s at BNL for the Space Nuclear Thermal Propulsion program (SNTP). BNL is

currently fabricating IKNF fuel using surrogate material (natural uranium) and will be characterizing the microstructure of the new material.

APPROACH:

The experimental procedure to produce IKNF consists of four steps:

1. *Uranyl Nitrate Infiltration.* Uranyl nitrate, $UO_2(NO_3)_2$, is dissolved in methyl alcohol and infiltrated into the nuclear grade graphite. After infiltration, the alcohol is removed by vacuum drying.
2. *Uranyl Nitrate Conversion to Uranium Oxide.* The infiltrated graphite is heated to convert $UO_2(NO_3)_2$ to UO_2 ($300^\circ C$ for 30 minutes).
3. *Uranium Oxide Conversion to Uranium Carbide.* The infiltrated graphite is further heated to convert the UO_x molecules into UC_2 . During this chemical conversion, CO_x gases (mainly CO) are also released, which further increases the porosity of the graphite matrix. The conversion occurs at approximately $900^\circ C$. By controlling the time and temperature it is possible to control the amount of UO_x converted to UC_2 .
4. *Uranium Carbide Melting and Kernel Formation.* The graphite is further heated to above the melting temperature of UC_2 ($3000^\circ C$). The molten UC_2 is drawn inside the graphite by capillary action to form the inner fuel kernel. The outer surface of the graphite is relatively clean for subsequent coating processes.

The uranium loading in the graphite is quantitatively predictable from the solution concentration, graphite density, and extent of conversion to UC_2 .

TECHNICAL PROGRESS AND RESULTS:

Experimental Achievements

The experimental apparatus necessary for the uranyl nitrate infiltration was set up (Figure 1) and the corresponding experimental safety review (ESR) documentation submitted and approved. Infiltration of two rod shaped samples of nuclear grade graphite were carried out with the experimental apparatus shown in Figure 1. A glass vessel was designed and fabricated in which the graphite can be submerged in uranyl nitrate/methyl alcohol and subsequently dried at room temperature through a vacuum pump (Figures 2a and 2b).

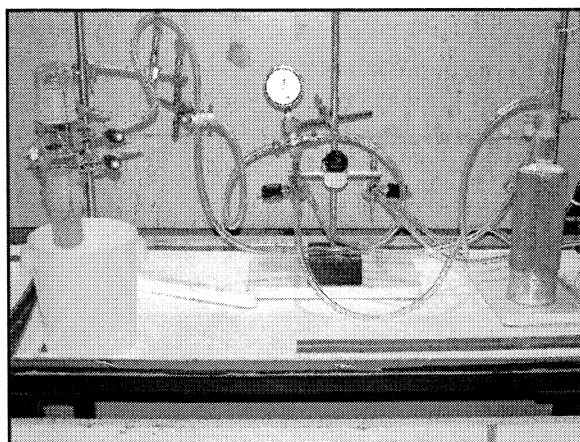


Figure 1 - Photograph of the glass infiltration vessel, tubing for argon gas and vacuum system, and cold trap.

The samples were heated to 300°C for 30 minutes to evaporate any remaining solvent and their mass was measured (Figure 3.a). The infiltration and drying procedure was performed 3 times on each sample. The increase in mass of the graphite samples is shown in Table 1.

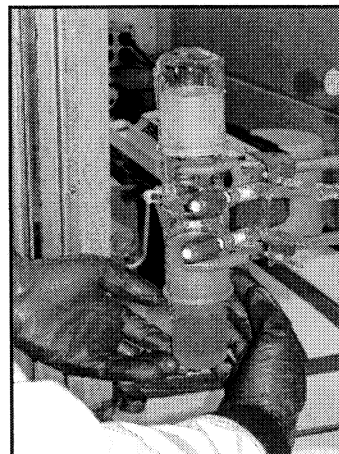


Figure 2.a - Glass infiltration vessel with uranyl nitrate/methyl alcohol solution.



Figure 2.b - Graphite rods submerged in uranyl nitrate solution in the infiltration vessel.

<i>Graphite Rod Mass (g)</i>		
	Sample 1	Sample 2
Initial Mass	1.49603	1.50097
1 st Infiltration + Drying	1.57154	1.57922
2 nd Infiltration + Drying	1.61854	1.58488
3 rd Infiltration + Drying	1.64330	1.62282
High Temper. Drying	1.63230	1.59371

Table 1. Increase in mass after each sample infiltration and 300°C drying. The final mass was measured after the 850°C heat treatment.

After the 3rd infiltration the samples were heated to 850°C for 1 hour. Based on the color of the samples (Figure 3.b), it is believed that the uranium is present as UO₂, or a mixed UO₂/U₃O₈ material. The increase in mass after each infiltration is consistent with the SNTP experiments conducted at BNL in the late 1980s. Work is in progress to achieve conversion of the UO₂ into UC₂.

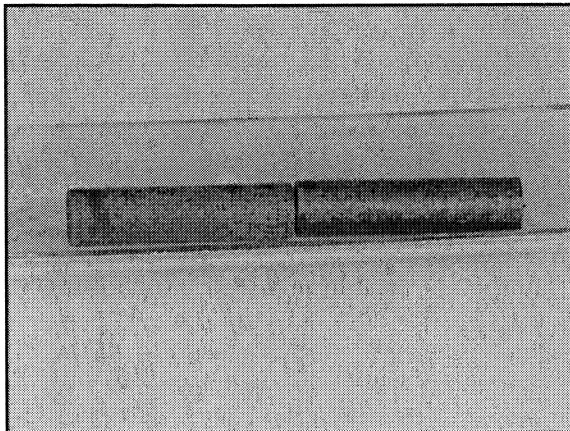


Figure 3.a - Graphite samples after 300°C heat treatment. The orange powder is believed to be U₃O₈.

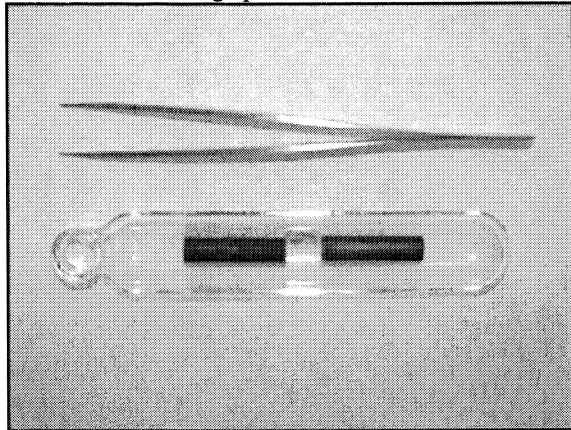


Figure 3.b - Graphite samples after 850°C heat treatment. It is believed that U₃O₈ have been converted to UO₂, which is black in color.

Quantitative Predictions of Weight Gain

A simple physical model to predict the increase in mass (uranium loading) after each infiltration step was developed and compared to data from the previous SNTP experiments. The model estimates the

amount of uranyl nitrate within the graphite from the infiltration solution concentration and the porosity available to the solution. A comparison of the model to the previous data is shown in Figure 4.

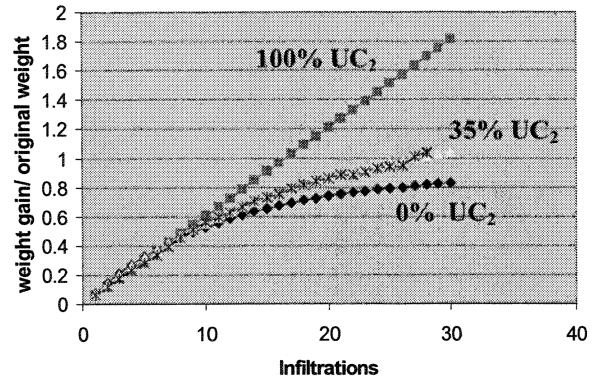


Figure 4. Predicted increases in mass assuming 0% UC₂ conversion, 35% UC₂ conversion and 100% UC₂ conversion. For the 35% case, the experimental data from the SNTP experiments basically overlap with the predicting curve.

Future Work

In FY06 the plan is to address the following issues:

- Complete the high temperature heat treatment using an induction furnace. This will fully convert the fuel to UC₂ and form a UC₂ rich inner fuel kernel within the graphite.
- Characterize the microstructure of the new material and determine the chemical compounds present (UO₂, U₃O₈, UC, U₂C₃, UC₂, UCO) using X-ray diffraction
- Investigate, using surrogate material for transuranics, to assess whether IKNF can be used for new fuel types.

SPECIFIC ACCOMPLISHMENTS:

Presentations

- L. Blake, L. Ecker, J. Saccheri, B. Bowerman, and H Ludewig. "Weight Gain Predictions for Infiltrated Kernel Nuclear

Fuel.” Murdock Conference, Nampa, Id.
Nov 11.

Storage of Fission Products Following
Aqueous Separation of Spent Nuclear
Fuel.” (submitted for NERI)

Proposals

- BNL White Paper to DOE – “An Infiltration Manufacturing Process for Nuclear Fuels.”
- Letter of Intent with Columbia University “Graphite Infiltration Techniques for Nuclear Fuel Fabrication and Long-Term

LDRD FUNDING:

FY 2005	\$130,393
FY 2006 (budgeted)	\$130,000

Development of Green Processes: Catalytic Hydrogenation in Water Utilizing *In Situ* Biologically-Produced Hydrogen

Devinder Mahajan
D. Van der Lelie

05-094

PURPOSE:

Hydrogenation reactions vital to the manufacture of numerous products in practice require fossil fuel-derived hydrogen, an organic solvent, high pressures, high temperatures, and stirring for efficient gas/liquid/solid mixing to attain fast reaction rates. Green Chemistry is a sensible approach to develop the next generation processes to achieve sustainable development. A challenge then is to develop a concept that can allow hydrogenation reactions to operate in an aqueous phase using hydrogen produced from a renewable source.

APPROACH:

We are pursuing an integrated approach that combines a biological hydrogen production strategy with a hydrogenation process that uses a homogeneous transition metal catalyst operating in an aqueous phase. For proof-of-concept we have selected a renewable hydrogen production source and a water-soluble catalyst/olefin system. For the biological hydrogen production we are using *Thermotoga neapolitana*, a thermophilic bacterium of the order *Thermotogales* that is able to produce clean (CO-free) hydrogen gas from a variety of carbon sources under a broad range of physiological conditions. Hydrogen produced *in situ* is readily available for subsequent hydrogenation of an

olefin on the catalyst that is dissolved in the same aqueous solution.

TECHNICAL PROGRESS AND RESULTS:

We initially conducted a set of baseline hydrogen production runs with *Thermotoga neapolitana* extremophile. The cultures were grown in a 1977 ATC medium, of which 1 mL was transferred to a 160 mL glass bottle (110 mL medium, 50 mL head space) that was incubated at 70°C and ambient atmosphere and hydrogen evolution was monitored as a function of time.

In order to develop a catalytic system that is effective for olefin hydrogenation in an aqueous phase, various rhodium-based catalysts (rhodium is known to be an efficient hydrogenation catalyst) were evaluated for hydrogenation of itaconic acid (Table 1). Since $\text{RhCl}_3 \cdot 3\text{H}_2\text{O}/\text{TPPTS}$ yielded the fastest reaction rate, this system has been selected for further evaluation.

Table 1. Screening potential catalysts for effective hydrogenation activity (catalyst: 3mM; Ligand: TPPTS = 10mM; Solvent: Water = 100 mL; Substrate: Itaconic Acid; 500 mM; Gas: 99.9% H_2 ; T: 70°C; Initial pressure: 2.0 MPa; Reactor volume: 300 mL). TPPTS is a water-soluble ligand.

Catalyst	Ligand	Reaction time,	% Hydrogenation
$\text{Rh}[(\text{C}_8\text{H}_{14})_2]_2$	TPPTS	120	0
$\text{RhCl}_3 \cdot 3\text{H}_2\text{O}$	TPPTS	18	86
$\text{NiCl}_2 \cdot 6\text{H}_2\text{O}$	TPPTS	120	0

Work continues to screen other extremophiles for hydrogenation production, transition metal catalysts for effective hydrogenation and integration of the two systems to develop a green process.

SPECIFIC ACCOMPLISHMENTS:

Refereed Publications

Presentations

1. Application of Nanocomposites In Biomimetic Hydrogen Production. Mahajan, D.; Anjom, M.; Van der Lelie, D.; and Taghavi, S. 12th International Conference on Composites and Nano Engineering (ICCE-12), Tenerife, Spain, Aug. 1-6, 2005.

2. Biological H₂ Production from Carbonaceous Sources Using Extremophiles. Mahajan, D. Invited Lecture at the Agriculture Research Service, U.S. Dept. of Agriculture, Florence, South Carolina, May 16, 2005.

3. Biological Processing of Carbonaceous Sources Using Extremophiles for CO₂-Neutral Ultra-Pure Hydrogen Production. Anjom, M.; Dong, B.; Van Ooteghem, S.A.; Van der Lelie, D.; Taghavi, S.; and Mahajan, D. 5th Topical Conference on Natural Gas Utilization Advanced Gas Conversion and Hydrogen Production. AIChE Spring National Meeting, Atlanta, GA. April 10-14, 2005.

LDRD FUNDING:

FY 2005	\$274,561
FY 2006 (budgeted)	\$288,000

Fast Neutron Imaging Detector

James R. Lemley

05-098

PURPOSE:

The project will demonstrate feasibility of a directionally sensitive detector for fast neutrons that has practical detection sensitivity at ranges sufficient to search large areas for improvised nuclear explosive devices (IND) or nuclear materials that could be used to manufacture INDs. The neutron sensitive medium is a polymer emulsion containing microscopic drops of superheated Freon. Neutrons striking the medium release the stored chemical energy to form a macroscopic bubble in the polymeric medium of the detector plane. Since fast neutrons cannot be easily focused, the coded-aperture technique will be used to encode the directionality to the source as a spatially varying pattern in the planar bubble medium. The coded-aperture is a redundant array of open areas and blocks made of neutron thermalizing and absorbing materials that cast a pattern on the detector plane. The bubble pattern in the detector plane will be recorded for analysis by illuminating with visible light and photographing with a digital camera or if necessary by other means. The pattern of varying optical intensity due to the bubbles will be digitized and deconvolved to recreate the image of the neutron source and the direction to its location. To spatially modulate a flux of fast neutrons, the coded aperture must be rather thick, compared to coded apertures for thermal neutrons made of cadmium metal. The pixel size and corresponding image will be somewhat coarse. Nevertheless, the directional information about source location should be superior to that provided by currently available neutron detectors consisting of

large slabs of polyethylene with imbedded ^3He tubes. Pressurizing the bubble medium to collapse the bubbles and re-liquefy the Freon regenerates the bubble medium for reuse. Design of sufficiently thin mask elements to efficiently attenuate fast neutrons is a key element of the project. When produced in large quantities, the SHE medium is expected to be significantly less expensive than electronic detectors for fast neutron. When feasibility of this novel application of Superheated-emulsion (SHE) technology has been demonstrated, the project should be of interest to DOE, DHS, and collaborating international partners who would support development of a full-scale prototype and its commercialization.

APPROACH:

SHE technology is available commercially, most commonly as pencil-shaped personal neutron dosimeters and is used in various configurations and combinations for neutron spectroscopy. In a previous LDRD project E. Kaplan, J. Lemley, and T. Tsang developed electronic readout technology that would enable neutron bubble dosimeters to be deployed in counterterrorism applications such as instrumentation of multi-mode shipping containers for detection of neutron-emitting materials during transit. As a result of this work BNL became the only US participant in a project organized by a manufacturer of SHE technology [Bubble Technology Industries (BTI)] to test instrumented bubble detectors. The Government of Canada has funded the project, but BNL has been unable to find means to accept the Canadian funds.

In other work at BNL, P. Vanier, et al., developed a coded-aperture imaging detector for thermal neutrons. The fission neutron spectrum of weapons-usable materials (e.g., plutonium) contains more fast neutrons than thermal neutrons. Since fast neutrons are

more penetrating than thermal neutrons, they can potentially be detected at greater distances. Since SHE are sensitive only to fast neutrons and can be manufactured in a planar array, development of an imaging detector for fast neutrons seemed feasible.

Materials to attenuate fast neutrons are being investigated both experimentally and through Monte Carlo calculations. Superheated emulsions in the form of disks have been acquired from BTI. Practical means to digitally encode (read out) the pattern of bubbles in a planar array of SHE are also being investigated.

TECHNICAL PROGRESS / RESULTS:

In a separate LDRD project in FY 2003-4, electronic readout capability for SHE dosimeters was developed, and the capability to transmit dosimeter readings electronically was demonstrated. In FY 2005, the first year of the current project, BNL acquired planar SHE media from BTI. A versatile digital camera was purchased. Skill has been developed to manipulate the SHE disks so that neutron induced bubbles can be distinguished from bubbles and imperfections appearing at the container interfaces. H. Ludewig and A. Mallon used Monte Carlo codes to evaluate materials and configurations for mask materials. These calculations supported the feasibility of an imaging fast-neutron detector by showing that a fission-spectrum neutron flux could be attenuated by at least a factor of two with mask materials of acceptable thickness for use in a practical detector.

A manufacturer of SHE media with the superheated droplets suspended in aqueous gels has been located. This medium may be more appropriate for the present application because it is fluid and can be poured to fill containers of the desired shape.

In FY 2006 we will demonstrate experimentally that fast neutrons can generate a useful pattern of coded-aperture components in a detector plane consisting of the bubble medium. Image recording by simple photographic techniques and other means will be investigated. Components to complete a prototype will be constructed or procured. The readout system will be developed. Image digitization, processing, and deconvolving will be undertaken.

SPECIFIC ACCOMPLISHMENTS:

A Record of Invention for the fast-neutron imaging detector based on SHE technology was filed with the BNL Intellectual Property Office in September 2004 when LDRD funding for FY 2005 was received.

The fast-neutron imaging-detector concept based on SHE technology was included in a proposal to DOE/NA-22 in April 2005. No part of the proposal has been funded.

The fast-neutron imaging detector has been included in briefings primarily about other applications of SHE technology presented to DOE/NA-22 (October 2005) and to ITT and Yale University (November 2005).

A proposal currently in preparation will be submitted to the Domestic Nuclear Detection Office (DNDO) of the Department of Homeland Security (DHS) by mid-December 2005.

LDRD FUNDING:

FY 2005	\$124,052
FY 2006 (budgeted)	\$144,000

Giant Proximity Effect (GPE) in High-Temperature Superconductors

Ivan Bozovic

05-104

PURPOSE:

We are investigating systematically the Giant Proximity Effect (GPE) in high-temperature superconductors (HTS) using the atomic-layer-by-layer molecular beam epitaxy (ALL-MBE) system newly acquired by BNL. The atomic-layer engineering capability allows us to synthesize atomically perfect HTS films and fabricate precise multilayers and superlattices. We proved that GPE is real and intrinsic to HTS, and this imposed a new experimental constraint on the theory of HTS. We are tightening this further by determining quantitative dependence of the proximity-induced superconductivity on a number of parameters.

APPROACH:

Our strategy is to synthesize a series of SN' bilayers and SN'S junctions; here, S denotes an optimally doped HTS compound and N' an underdoped or overdoped HTS material with a reduced T_c' . [GPE is observed at temperature $T_c' < T < T_c$.] We can vary systematically the doping level x , the temperature T , the external magnetic field H , the power P of microwave radiation, etc. Combinatorial synthesis and parallel testing greatly increase the density of data points; this is a novelty in physics experiments. G. Logvenov, V. Butko, A. Gozar and A. Bollinger are also participating in this project.

TECHNICAL PROGRESS:

The MBE system was assembled, debugged, and calibrated. The ozone distillation and delivery system was designed to conform to BNL safety standards, constructed, tested extensively, and used routinely. So far we ran

31 growth experiments. $R(T)$ and $\chi(T)$ measurement setups were completed. Every film was characterized by reflection high-energy electron diffraction (RHEED), transport measurements (resistivity and susceptibility as a function of temperature down to 4.2 K), and atomic force microscopy (AFM). Selected ones were also characterized by Rutherford back-scattering. Some films were atomically smooth; this milestone was reached faster than the most optimistic expectations. [One-two years is more typical.]

The plan for FY 2006 is to synthesize by MBE a number of atomically smooth SN' bilayer films and SN'S trilayer films, characterize them by RHEED, x-ray diffraction, and AFM. In addition, we will perform variations of transport measurements, measurements of the dependence of I_c and $\chi(T)$ on thickness, doping levels (x), temperature (T), magnetic field (H), and the power of microwave radiation (P), and thus extract the dependence of induced coherence length ξ_n on x , T , H , and P .

SPECIFIC ACCOMPLISHMENTS:

In FY 2005, the group published 10 refereed papers and presented 11 invited talks at research conferences as follows:

Publications:

1. Giant Proximity Effect in cuprate superconductors. I. Bozovic, G. Logvenov et al. Phys. Rev. Letters 93, 157002 (2004). [Highlighted in Physics World, Dec. 2004, pp. 19-20.]
2. Ultrafast light generates coherent sound. I. Bozovic et al. Phys. Rev. B 69, 132503 (2004). [Highlighted in Science Today, Virtual Journal of Ultrafast Science and Virtual Journal of Applications of Superconductivity.]
3. Combinatorial molecular beam epitaxy of $\text{La}_{2-x}\text{Sr}_x\text{CuO}_4$. G. Logvenov, I. Sveklo and I. Bozovic. Proc. SPIE Proceedings 5932, 2005.
4. Structure and transport properties of the charge-transfer salt coronene – TCNQ. X.

- Chi, V. Y. Butko, et al. *Chemistry of Materials* 16, 5751 (2004).
5. Crystallization of charge holes in the spin ladder $\text{Sr}_{14}\text{Cu}_{24}\text{O}_{41}$. P. Abbamonte, A. Gozar, et al. *Nature* 431, 1078 (2004).
 6. Nano-engineered multi-layer films and superlattices of cuprates and other complex oxides. I. Bozovic. Proc. ICCNE-11 (2005).
 7. Highly conductive nanolayers on strontium titanate produced by preferential ion beam etching. W. Reagor and V. Y. Butko. *Nature Materials* 4, 593 (2005).
 8. Low-temperature field effect in a crystalline organic material. V. Y. Butko, J. C. Lashley and A. P. Ramirez. *Phys. Rev. B* 72, 081312 (2005).
 9. Symmetry and Light Coupling to Phononic and Collective Magnetic Excitations in $\text{SrCu}_2(\text{BO}_3)_2$. A. Gozar et al. *Phys. Rev. B* 72, 064405 (2005).
 10. Evolution of Superconductivity in Electron-Doped Cuprates: Magneto-Raman Spectroscopy. M. M. Qazilbash, A. Gozar, et al. Accepted for publication in *Phys. Rev. B*.
- Presentations:
1. Atomically layered cuprates. I. Bozovic. Aspen Winter Conference on High Temperature Superconductivity, 9-15 January 2005, Aspen, Colorado.
 2. Nano-Film Density of States and Transport at the Metal Insulator Transition. V. Butko. Workshop on Physics of Ultra Thin Films Near the Metal Insulator Transition II, 6-7 Jan. 2005, BNL, New York.
 3. High quality crystalline pentacene and rubrene FETs. V. Butko, APS Meeting, 20-25 March 2005, Los Angeles, California.
 4. Ultrafast pump-probe experiments on high- T_c cuprates. I. Bozovic. Workshop on Spectroscopic Studies of Nanoscale Systems, May 25, BNL, New York.
 5. Atomic-layer engineering and the physics of high-temperature superconductors. CERC-ERATO Workshop on Phase Control of Correlated Electron Systems, 7-11 June 2005, Maui, Hawaii.
 6. Artificial superlattices grown by MBE: can we design novel superconductors? G. Logvenov. Workshop on Room Temperature Superconductivity, 10-11 June 2005, Notre Dame University, Indiana.
 7. Combinatorial molecular beam epitaxy of $\text{La}_{2-x}\text{Sr}_x\text{CuO}_4$. I. Bozovic. American Conference on Crystal Growth and Epitaxy, 9-16 July 2005, Big Sky Resort, Montana.
 8. Shaping the beam fluxes for combinatorial molecular beam epitaxy of $\text{La}_{2-x}\text{Sr}_x\text{CuO}_4$. G. Logvenov, International Conference on Strongly Correlated Electron Materials: Physics and Nano-engineering, 31 July – 4 August 2005, San Diego, California.
 9. Atomic-layer engineering of high-temperature superconductors and other strongly correlated oxides. I. Bozovic. 2005 YUCOMAT, 12-16 September 2005, Herceg Novi, Serbia and Montenegro.
 10. Giant proximity effect. I. Bozovic. 18th ISS, October 24-26, 2005, Tsukuba, Japan.
 11. Strong electron-phonon coupling in high-temperature superconductors. I. Bozovic. International Workshop on Electron State and Lattice Effects in Cuprate High Temperature Superconductors, October 27-28, 2005, Tsukuba, Japan.
- Three new DOE grants were awarded; the total of \$1,930,558 was received in FY 2005. U.S. DOE project: Molecular Beam Epitaxy of Complex Materials, \$115,000; U.S. DOE project: Molecular beam epitaxy and nanostructuring of perovskite oxide materials toward an understanding of strongly correlated systems, \$1,362,337; and U.S. DOE capital equipment grant of \$453,221. The funding is secured for two more years.
- LDRD FUNDING:**
- | | |
|--------------------|-----------|
| FY 2005 | \$267,837 |
| FY 2006 (budgeted) | \$275,000 |

Development of an Observation Based Photochemical-Aerosol Modeling System

Douglas Wright

05-105

PURPOSE:

The objective of this project is to develop a modeling system for evaluation of the chemical and aerosol components of chemical transport and climate models by extensively incorporating field observations and observation-derived model constraints. The modeling system was conceived as a unique integration of datasets collected in major field campaigns and their subsequent incorporation into state-of-the-art chemical transport models, and should provide a unique tool tailored to upcoming field experiments such as those involving the DOE Atmospheric Science Program. Implicit in this objective was an examination of current possibilities and limitations in the use of such datasets to evaluate aerosol models, and how data collection and associated modeling might better coordinate with each other in future campaigns.

APPROACH:

Recent advances in data collection and instrumentation, as well as the appearance of more sophisticated models, make possible a new degree of integration of observations with models. We approached this integration in an innovative way in that the models are constrained by one subset of the observations and evaluated by another, rather than proceeding entirely from first principles and a handful of poorly known initial conditions with the hope that model results will in some respects resemble the observations. Given that the detailed

models used in this study require a large amount of input and evaluation data, a serious concern and risk in this undertaking is that the observations will still prove to be inadequate for model evaluation beyond what can already be done more readily by other means. Further, until the observations are studied in detail it is not known what opportunities for model evaluation the collected datasets will present: i.e., if the formation of new particles or organic aerosol in the atmosphere was not observed, model representation of these important but poorly understood processes cannot be evaluated with these datasets.

To investigate this approach to model-observation integration, the present study examined the extent to which the datasets obtained onboard the DOE G-1 aircraft during the NorthEast Aerosol eXperiment (NEAX) in the summer of 2004 which included chemical, aerosol, and meteorological quantities, could be used to evaluate detailed models of aerosol evolution, focusing on processes that shape the particle size distribution.

A modeling system was designed and tailored to the flight plans and datasets of NEAX, and introduced model constraints forcing the model to match the observations for most all processes except those governing aerosol microphysical evolution. These constraints permitted model examination to focus on the aerosol microphysical processes governing the particle size distribution.

Development of the modeling system was greatly aided by the several scientists in the Atmospheric Sciences Division responsible for data collection, processing, and the building of instruments deployed during NEAX (S.R. Springston, J. Wang, Y.-N. Lee). In this connection, Larry Kleinman

was a close collaborator in the strategy and design of this project.

TECHNICAL PROGRESS AND RESULTS:

The core model component, a photochemical-aerosol box model developed at Caltech and the Atmospheric and Environmental Research Corporation, was implemented in the Environmental Protection Agency's chemical transport model, the Community Multiscale Air Quality Modeling System (CMAQ). New aerosol process modules were added to CMAQ, and 1- and 2-dimensional variants of the 3-dimensional CMAQ system were developed. Data readers and processors for the observational datasets were created, as well as modules to synthesize the observations for mapping to the model domain. Observation-derived model constraints appropriate to point sources such as power plant plumes were implemented. As the net result of these accomplishments a 'version 1' of the modeling system was completed and applied to the 9 August 2004 field experiment, the most promising of the

NEAX flights from the point of view of analysis.

In FY 2006 additional aerosol process modules will be incorporated into the modeling system, probably focusing on new particle formation and the growth of the smallest particles. In light of the upcoming MAX-Tex field campaign near Houston in summer 2006, which presents unique opportunities to study organic aerosol formation at point sources of hydrocarbon emissions, additional modules for organic aerosol formation may also be incorporated.

SPECIFIC ACCOMPLISHMENTS:

Modeling aerosol evolution in power plant plumes during the NEAX 2004 study. Wright, D. L.; Kleinman, L. I.; Springston, S. R.; Wang, J.; Lee, Y.-N. (and others) Atmospheric Chemistry and Physics, (under review)

LDRD FUNDING:

FY 2005	\$109,033
FY 2006 (budgeted)	\$ 79,000

Exploring Root Physiology in Relation to Uptake of Groundwater Pollutants

Richard A. Ferrieri
M. Thorpe

05-106

PURPOSE:

There is a growing concern over continued elevated levels of chlorocarbon contaminants in groundwater which present human health risks as potential carcinogens. Carbon tetrachloride (CCl₄), one of several compounds in this class of contaminants, has been targeted for environmental remediation. Unlike many organic compounds, chlorocarbons can persist in the environment for decades. Use of poplar trees to clean up such groundwater contaminants is cost-effective, but we still face the challenge of minimizing foliar emissions of volatile chlorocarbon compounds as they can become atmospheric pollutants capable of depleting the ozone layer. Our research is focused on elucidating the mechanistic pathways through which plants naturally metabolize certain chlorocarbon compounds and on improving these processes. One strategy we have been exploring is to heighten a plant's natural defense system using treatments of specific compounds known to be biosynthesized as part of the plant's defense processes.

APPROACH:

We have developed a suite of short-lived radiolabeled substances that can be administered to intact plants while maintained under tight environmental controls, and we can administer ¹¹C₂ to leaves. Rapid turnover to mobile radiolabeled sugar allows us to explore how contaminants change the way plants utilize

their carbon resources. Further, we have successfully radiolabeled the contaminant ¹¹CCl₄ and administered it to plants to assess the dynamics of uptake and whole-plant distribution. Our developing work in plant biology represents a natural outgrowth for new applications of radiotracers and imaging in life science. The short-lived positron-emitting isotope, carbon-11 (t_{1/2} 20.4 min) allows for non-destructive and repeated measurement of the spatial distribution and transport dynamics of plant carbon as well as contaminants. Further, the annihilation gamma radiation from tracer decay (511keV) penetrates plant tissue, allowing detection of *in vivo* tracer.

TECHNICAL PROGRESS AND RESULTS:

Using radiographic imaging, leaf export and partitioning of [¹¹C]-photosynthate between apex and lower stem was quantified and compared with baseline responses for control and CCl₄ treated plants (Figure 1).

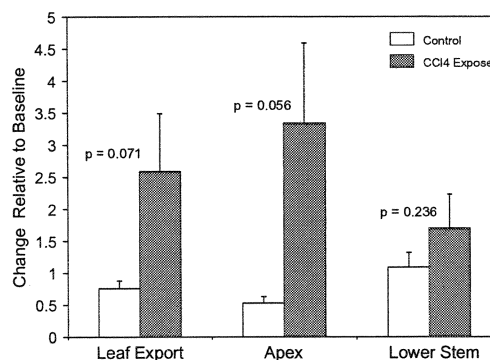


Figure 1. Partitioning (shown means \pm SE from n=3 replicates) of [¹¹C]-photosynthate from poplar clones (OP637).

We have shown that there is a statistically significant increase in leaf export of [¹¹C]-photosynthate from mature leaves of plants exposed to CCl₄ for 24 hours, whereas control plants exhibited no significant change. Further, most of the increase in transported carbon was preferentially partitioned to the apex. These results

indicate that rapid changes occur in leaf metabolism and whole-plant partitioning of newly acquired carbon upon exposure to the contaminant. However, we note that the increased partitioning of carbon to the apex is not typical of a defense posture. For instance, our work in *Populus* has shown that response to exogenous jasmonate treatment (a known plant defense hormone) or to insect herbivory leads to increased mobile sugar pools and increased carbon partitioning belowground. Hence, the increased carbon partitioning to younger sink leaves suggests that their demand for newly acquired carbon increased as a consequence of their having to accumulate and/or metabolize CCl₄.

Further, we observed diurnal variation in leaf emissions for both isoprene and CCl₄ (Figure 2).

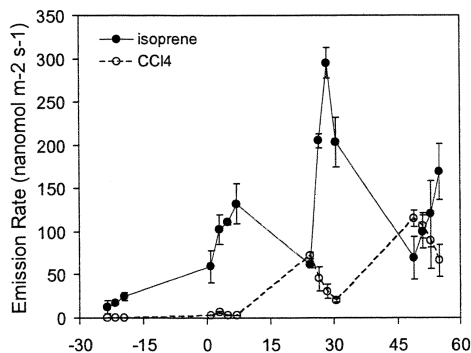


Figure 2. Leaf emissions of isoprene and CCl₄ from baseline to 3 days after continued exposure to CCl₄. Data (means ± SE for n=3 replicates) is presented as a function of the time in hours from the zero time when CCl₄ exposure began.

Isoprene emission in untreated plants increased from 15-to-30 nmol m⁻² s⁻¹ during the course of the day which is typical for this species, and reflects a change in leaf carbon pool size where approximately 80% of the carbon that is utilized in biosynthesizing isoprene derives from newly acquired carbon. Further, isoprene emissions were elevated 2-to-3 fold within a few hours of plant exposure to CCl₄, and continued to

exhibit diurnal variation with time of day. Continued elevations in emission were noted on subsequent days as well. These results support our contention that there is a rapidly changing demand within the plant for newly acquired carbon that coincides with the accumulation of CCl₄. Furthermore, CCl₄ emissions exhibited an opposite trend to isoprene, being highest in the early morning when carbon pools were small and lower later in the day as carbon pools increased.

Interestingly, we did not begin to see leaf emissions of CCl₄ until 24 hours after root exposure, and then continued elevation in emission levels was noted with each subsequent day of exposure. As a test to determine whether CCl₄ transport within the xylem was somehow hindered, we administered doses of ¹¹CCl₄ to both rooted and cut stems of saplings and then imaged for radioactivity distribution 60 minutes later. Results indicated rapid xylem transport of ¹¹CCl₄ within this time period with rapid diffusion of tracer out of the xylem and into surrounding leaf tissue. No significant difference was noted between rooted and cut stems indicating that root assimilation is not rate limiting. Therefore, the delay in leaf CCl₄ emissions may be due to the plant's ability to effectively balance contaminant metabolism in the early stages of exposure.

Subsequent studies using ¹¹CO₂ followed by a metabolic analysis of leaf tissue revealed that carbon-11 was incorporated into trichloroacetic acid (TCA), a known metabolite of CCl₄ that is not volatile. The combined observations reported here support a direct association between the plant's ability to metabolize CCl₄ and its newly acquired carbon. Further, this suggests that it should be possible to amplify contaminant metabolism, thereby lowering leaf CCl₄ emissions by altering the way a plant utilizes carbon.

Knowing that jasmonate treatment will elevate sugar intermediate pools, we might expect plants that had been treated with methyl jasmonate to have increased TCA production. Indeed, when we treated the entire foliage of intact poplar plants with a 1 mM solution of methyl jasmonate (MeJA), foliar CCl₄ emission was reduced 2-fold relative to controls while the TCA level was increased 1.7-fold relative to controls (Figure 3).

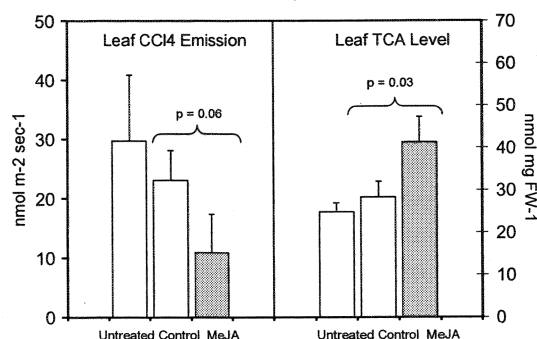


Figure 3. Left-side panel shows average leaf CCl₄ emission rates for untreated, control treated and 1 mM MeJA treated plants exposed to 520 ppm CCl₄ for 24 hr. Right-side panel shows average leaf TCA levels for untreated, control treated and 1 mM MeJA treated plants at the same point in time.

This work demonstrates that plant metabolism of CCl₄ by poplar clones (OP637) involves newly acquired carbon. Furthermore, an increase in the size of the leaf carbon pool – and particularly the size of the mobile sugar pool or its intermediates – will increase the extent of CCl₄ metabolism thereby impacting leaf emission of the contaminant. We also demonstrated that the extent of this metabolism can be manipulated through treatment with the defense signal chemical, methyl jasmonate. It is unclear whether persistent up-regulation of plant defenses will continue to have beneficial effects on plant phytoremediation of CCl₄. Furthermore, the key regulatory control points for metabolism have yet to be explored. Identification of specific genes involved in this regulatory pathway could

lead to viable molecular engineering strategies for designer plants with enhanced metabolic function.

SPECIFIC ACCOMPLISHMENTS:

5 Peer reviewed papers in review and/or in press:

1. Jasmonic acid induces rapid changes in carbon transport and partitioning in *Populus*. Babst, B.; **Ferrieri, R.A.**; Gray, D.W.; Thorpe, M.R.; Lerdau, M.; Schlyer, D.; Schueller, M.; Orians, C.M. *New Phytologist* **167**: 63-72, 2005
2. Use of carbon-11 shows that exogenous jasmonic acid influences carbon sources for isoprene biosynthesis in *Populus*. **Ferrieri, R.A.**; Gray, D.W.; Babst, B.A.; Schueller, M.J.; Schlyer, D.J.; Thorpe, M.R.; Orians, C.M.; Lerdau, M. *Plant Cell & Environment* **28**: 591-602, 2005.
3. Synthesis of the phytohormone [¹¹C]methyl jasmonate via methylation on a C₁₈Sep Pak™ cartridge. Herth, M.M.; Thorpe, M.R.; **Ferrieri, R.A.** *Journal of Labelled Compounds and Radiopharmaceuticals* **48(5)**: 379-386, 2005.
4. Up-regulating plant defenses in *Populus* increases phytoremediation capacity for carbon tetrachloride. Ferrieri, A.P.; Thorpe, M.R.; **Ferrieri, R.A.** *8th International Symposium on Remediation*, June (2005), Batelle Press (2005).
5. Stimulating Natural Defenses in *Populus* Increases their Metabolism of Carbon Tetrachloride. Ferrieri, A.P.; Thorpe, M.R.; **Ferrieri, R.A.** *Int. J. Phytoremediation* (in review).

3. Papers/poster presented at scientific conferences:

1. Ferrieri, R.A.; Ferrieri, A.P.; Thorpe, M.R., Up-regulating Plant Defenses in *Populus* Increases Phytoremediation of Carbon Tetrachloride. Abstract accepted to 8th International Symposium on In-Situ and On-Site Bioremediation, June 2005.
2. Ferrieri, A.P.; Thorpe, M.R.; and Ferrieri, R.A.; The Chemistry of Communication: How Certain Defensive Signals are Perceived by Plants. DOE-SULI Poster and student invited presentation (Aug 2005).
3. Ferrieri A.P.; Thorpe, M.R.; and Ferrieri, R.A.; The Chemistry of Communication: How Certain Defensive Signals are Perceived by Plants. Holy Cross College student research symposium (Sept 2005).

Grant proposals submitted:

1. Enhancement of Carbon Sequestration by Jasmonate Mediation of Sugar Transporters. DOE/OBER Announcement LAB 05-10 (not funded).
2. Resource Flow and the Rhizosphere: Insights from Integrating Routes of Exchange. NSF: Frontiers in Biological Research (not funded).

LDRD FUNDING:

FY 2005	\$165,365
---------	-----------

X-ray Absorption Spectroscopic Method for Studying Environmentally- relevant Reaction Kinetics

Jeffrey Fitts

05-108

PURPOSE:

The initiative's chief objective is to develop resources at the NSLS required to conduct world-class molecular environmental science research. This LDRD has been used to produce unique research applications by combining the suite of tools developed as part of the EnviroSuite initiative. The LDRD research objective is to combine microspectroscopy and quick-scanning x-ray absorption spectroscopy in order to understand the kinetics of contaminant transformations in heterogeneous sediments.

APPROACH:

We propose to combine synchrotron-based microspectroscopy and Quick-scanning X-ray absorption spectroscopy (XAS) measurements made in parallel on identical samples in order to follow the time-dependent chemical transformations of a metal ion contaminant (in the initial case either nickel or chromium) in a heterogeneous sediment. This work is intended to bring together the unique information provided by two state-of-the-art synchrotron-based methods that are currently under development by National Synchrotron Light Source staff scientists, James Ablett and Wolfgang Caliebe, in collaboration with EnviroSuite scientists based in the Environmental Research and Technology Division.

This novel approach will enable detailed chemical kinetics studies of contaminant

metals and radionuclides as they react with heterogeneous samples; our current understanding of these processes is based on studies of idealized model systems (a metal reacted with a single type of mineral) or empirical measurements of real-world sediments, in which case the results do not provide the fundamental chemical information necessary to reliably predict contaminant transformations.

Both the development of the individual synchrotron-based methods and the combined experimental approach represent novel efforts underway at the NSLS with an eye toward taking advantage of the unique attributes of the NSLS-II. This approach is intended to address the scientific challenges faced by the DOE mission of providing long-term stewardship of the large volumes of sediments contaminated with metals and radionuclides.

TECHNICAL PROGRESS AND RESULTS:

The EnviroSuite Initiative has assumed at least partial management of four end stations at the NSLS during the course of this LDRD. This role has enabled EnviroSuite scientists to develop new resources (e.g., a microprobe at beamline X27A) and specifically to tailor three XAS beamlines (X15B, X11A, and X11B) to provide a unique suite of synchrotron-based tools.

The X-ray microprobe at beamline X27A came on-line in November 2004 and after significant conditioning became available for the first experiments in August 2005 with a 10 micron resolution. The microprobe enabled us to determine the spatial variation (on the order of individual sediment grains) of the chemical state and bioavailability of nickel contaminated sediments collected from the Oak Ridge Field Research Center.

Quick scanning XAS measurements were demonstrated using solid model compounds and achieved a time resolution of approximately three seconds per scan. This work was carried out by NSLS scientist, Wolfgang Caliebe, who unfortunately accepted a job in Germany.

SPECIFIC ACCOMPLISHMENTS:

Follow-on funding:

Molecular-Scale Kinetic Controls on Metal and Radionuclide Fate and Transport. PI Fitts, J. P.; White paper submitted to DOE OBER ERSD (funded March 2004; \$50K for 1 yr.).

Composition Of Microbial Communities Used For In Situ Radionuclide Immobilization: Natural Gene Transfer To Develop Resistance To Metal Toxicity. co-PI's Fitts, J. P.; and van der Lelie, D.; submitted to DOE OBER NABIR program March 9, 2004 (funded July 2004; \$300K/yr for 3 yrs).

Developing EnviroSuite Resources at the NSLS. PI Fitts, J. P.; proposal submitted to DOE OBER June 30, 2004 (funded August 2004; \$250K/year for 4 years; \$225K end-of-year capital equipment).

Environmental Molecular Science Institute (EMSI) Support for the Center for Environmental Molecular Science; PI Kalb, P. D.; White paper presented to Teresa Fryberger in Germantown March 31, 2004, (funded April 2004, \$250K/year for 3 years).

EnviroSuite Contributing User Agreement with the NSLS for the Microprobe Beamline at X27A. PI Fitts, J. P.; Proposal requesting 25% of experimental time for a three-year period beginning Winter cycle 2006; 15% of experimental time rewarded by NSLS Science Advisory Committee for 3 years.

Refereed Publications:

In-situ Grazing-Incidence EXAFS Study of Pb(II) Chemisorption on Hematite (0001) and (1-102) Surfaces. Bargar, J. R.; Trainor, T. P.; Fitts, J. P.; Chambers, S. A.; Brown, Jr., G. E. *Langmuir*, 20, 1667-1673 (2004).

Adsorption of Trace Metals on Glass Fiber Filters. Fuhrmann, M.; Fitts, J. P.; *Journal of Environmental Quality*, 33, 1943-1944 (2004).

Emissions and Encapsulation of Cadmium in CdTe PV Modules during Fires. Fthenakis, V.M.; Fuhrmann, M.; Heiser, J.; Lanzirrotti, A.; Fitts, J.; and Wang W., *Progress in Photovoltaics: Research and Applications*, August (2004).

Electrostatic Surface Charge at Aqueous/ α -Al₂O₃ Single-Crystal Interfaces as Probed by Optical Second-Harmonic Generation. Fitts, J. P.; Shang, X.; Flynn, G. W.; Heinz, T. F.; and Eienthal, K.B.; *J. Phys. Chem. B* 109 (16): 7981-7986 (2005).

Second harmonic generation and theoretical studies of protonation at the water/ α -TiO₂ (110) interface. Fitts, J. P.; Machesky, M. L.; Wesolowski, D. J.; Shang, X.; Kubicki, J. D.; Flynn, G. W.; Heinz, T. F.; and Eienthal, K.B.; *Chemical Physics Letters* 411, 4-6, 339-403 (August 15, 2005).

Molybdate polymerization at the FeOOH-water interface. Chusuei, C. C.; Fitts, J.P.; and Herbert, B.; submitted to *Langmuir* (September 2005).

LDRD FUNDING:

FY 2005	\$92,733
---------	----------

Global Cloud Analysis Technologies (G-CAT)

Andrew Vogelmann

05-109

PURPOSE:

The objective of this LDRD is to address a pressing issue in the climate community by architecting a framework within the Earth Systems Science Division (ESSD) Cloud Properties Group that would 1) enable the requisite acquisition of voluminous, global data sets, and 2) explore novel methods for efficiently integrating the information content of data from diverse sensors.

APPROACH:

The past decade marks an explosion of new atmospheric data from sophisticated surface-based instrumentation and satellites that have ushered in a new era in climate change research. The DOE Atmospheric Radiation Measurement (ARM) Program will soon have acquired a decade of data at each of its sites. Passive satellite remote sensing is nearing 30 years of observations, and their sophistication is crowned by the recent Earth Observing System (EOS) launches. These measurements contain a climate-scale record of cloud and atmospheric properties that can unlock the answers to unresolved climate and climate change problems. However, no single sensor can provide all of the information needed to resolve these issues and, while we may be data rich, the sophistication and sheer volume of these data have outstripped standard analysis capabilities and methods. While the volume of data from the existing passive sensors already represents an analysis bottleneck, new active sensors that are now being deployed have data rates that are even several orders of magnitude larger.

The objective of this LDRD is to address a pressing need to develop new computational and integrated techniques that can harvest the wealth of climate knowledge contained within these diverse emerging data streams. The result of these integrations is to provide a self-consistent picture of the atmospheric state.

The ESSD personnel that were involved with this project were Dr. M. Miller, Dr. M. Jensen, E. Luke, and M.-J. Bartholomew.

We focus on developing methods to enhance abilities to acquire new massive data sets, and develop new computational technologies for efficient integration and analyses with particular emphasis on bottlenecks that prevent the use of global cloud observations for climate analyses:

- 1) Data acquisition. A key bottleneck is in the acquisition of satellite data from NASA's data distribution centers. The system is fine for obtaining small amounts of data, but quickly becomes overpowered when data for long time periods or large spatial areas are needed for climate studies.
- 2) Automated cloud analysis. Current approaches to analyzing cloud data typically involve simple statistics that ignore the cloud structure or cloud morphology, which is essential for understanding cloud behavior. We will take full advantage of the cloud data by developing a fully automated cloud identification and analysis tool that can quality control the data fields, and then use an artificial intelligence (AI) scheme to pick over the valid data regions and locate the particular type of cloud fields of interest.
- 3) 3D data corrections. Recent literature has indicated that many satellite-based cloud products are adversely impacted by 3D radiative transfer effects that are

not treated in the retrievals. We will investigate this phenomena and its possible impact on our cloud morphology studies.

- 4) Trajectory analysis. Cloud properties are heavily influenced by the airmass in which they formed, and understanding the underlying dynamical interactions requires use of a trajectory model. Such a model is straightforward to run on a case-by-case basis, but is prohibitively cumbersome for obtaining the needed long-term statistics. We will develop an automated method to stage the data, run the model, interpret the output, and place it in the same time and space framework as the satellite data.

TECHNICAL PROGRESS AND RESULTS:

Programmatically, we developed the *BNL Clouds and Precipitation Science Initiative*, which is chartered to address the compelling question: How will clouds and precipitation respond to global climate change? The initiative is planned to take advantage of BNL expertise in surface radar, lidar and satellite remote sensing of cloud systems. The challenge is to develop an integrated surface-satellite analysis and modeling approach to determine cloud-climate: relationships, processes, feedbacks, and teleconnections. The initiative was adopted and merged with the Aerosols Initiative.

To address the technological bottlenecks described before, we developed the Cloud Interaction, Modeling And Trajectory Ensemble (CLIMATE). CLIMATE is a suite of analysis capabilities for global, multi-parameter active and passive sensor integration needed to observe and understand cloud-climate interactions with the following components:

1. Automated NASA Data Acquisition

Associated investigator: E. Luke

To address the bottleneck that exists in acquiring large volumes of NASA satellite data, we developed a multi-user, automated acquisition web interface. The system is built from Perl scripts around a central MySQL database, and is designed for maximum throughput efficiency by managing multiple user IDs for ordering, and a queue system that preferentially loads orders during periods when the NASA DAAC is most responsive (*i.e.*, is underutilized). The system enabled the efficient acquisition of six terabytes of pixel-level NASA data needed by the Cloud/Aerosols group for climate studies (Peak rate = 250 GB/day, Median= 75 GB/day). Its reporting flexibility has proved useful in providing statistics about NASA ordering/response patterns and audit information for occasional troubleshooting.

2. AI Automated Cloud Analysis Capability

Associated investigators: E. Luke, M. Jensen, and M. Miller

To take advantage of this wealth of cloud data, we developed a set of automated cloud identification and analysis algorithms that selects marine boundary layer cloud scenes from data. The algorithm applies rigorous quality control so that scenes are not contaminated by cirrus or frontal clouds, sunglint, or other possible sources of error. We applied the algorithms to analyze the 6 TB of cloud data obtained from NASA in scenes 300 km x 300 km (equivalent to GCM grid size used in climate studies). The algorithm identified over 53,600 marine boundary layer scenes, which enables thorough statistical analyses of the cloud properties that have never been accomplished before.

To coordinate the running of cloud satellite data analysis programs, we developed an

automated scheduler. It is a distributed client/server software wrapper package that optimizes the runtime of a computationally intensive analysis algorithms by managing and balancing the computational load across multiple network Linux machines. In so doing, it reduced the time required for a complete analysis from weeks to days.

This NASA data acquisition and analysis suite of tools also assisted efforts by the ARM Mobile Facility (AMF) Chief Scientist (M. Miller), by demonstrating the representativeness of the AMF deployment location at Pt. Reyes, relative to the nearby marine boundary layer clouds, based on the analysis of multi-year MODIS cloud properties relative to distance from the coastline.

3. Cloud Edge and 3D Data Corrections

Associated investigators: E. Luke, M. Jensen

Satellite-derived cloud properties of pixels that reside at the edges of clouds are more problematic to accurately obtain because of possible contamination by partially filled cloud pixels, or 3D radiative transfer effects that are not treated in the cloud retrievals. Either effect might introduce false variability in our results (as well as those by others). We address this problem using a morphological erosion technique, whereby pixels near cloud edge are removed successively one 'ring' of cloud pixels at a time, and the resulting distributions analyzed. This can be computationally time-consuming, but our automated scheduler minimized the additional runtime. We found that successive ring removal preferentially removes smaller optical depths that tend to contain the greatest share of the variability within the cloud scene. If left unaccounted, this variability would confuse our interests that typically are to best define the measures of central tendency within the scenes.

4. Ensemble Trajectory Analyses

Associated investigator: M.-J. Bartholomew and M. Miller

To enable ensemble statistics from the trajectory model needed to interpret the observed cloud or aerosol state, we developed an automated method to stage the data, run a back trajectory model. The back trajectories are computed using the HYSPLIT (HYbrid Single-Particle Lagrangian Integrated Trajectory) model, which is the newest version of a complete system for computing simple air parcel trajectories to complex dispersion and deposition simulations. The model was acquired from the NOAA Air Resources Laboratory and has recently been upgraded with improved advection algorithms, updated stability and dispersion equations, a new graphical user interface, and the option to include modules for chemical transformations. Without the additional dispersion modules, HYSPLIT computes the advection of a single pollutant particle, or simply its trajectory.

The automated scripts were successfully applied to the problem of projecting the paths taken by airmasses that originate over the Saharan desert, and how trajectories are associated with surface observations from an oceanic research vessel and satellite precipitation observations.

SPECIFIC ACCOMPLISHMENTS:

Grant Proposals

- 1) "Parameterizations of Cloud Microphysics and Indirect Aerosol Effects," co-PI (PI Mark Miller, BNL), submitted to the DOE Atmospheric Radiation Measurement (ARM) Program. Awarded \$2,344,100 (total) for FY06-FY08, #TBD.
- 2) "ARM Mobile Facility Site Science," co-PI (PI Mark Miller, BNL), Renewal submitted to the DOE Atmospheric

Radiation Measurement (ARM) Program. Awarded \$1,527,300 (total) for FY06-FY08, #5524.

- 3) "The Influence of Aerosol on Arctic Climate," co-PI (PI Dan Lubin, SIO), Renewal submitted to the DOE Atmospheric Radiation Measurement (ARM) Program. Requested \$158,000 (total, BNL component) for FY06-FY08. Not funded.
- 4) "Cirrus-climate interactions in the tropics - A collaborative effort between Brookhaven National Laboratory and NASA GISS," Submitted to the NASA Ice Cloud and Land Elevation Satellite (ICESat) Science Team. Requesting \$702,031 (total) for 3 years. Pending.
- 5) "The Influence of Aerosol on Arctic Climate: A Unique Role for ICESat," co-PI (PI Dan Lubin, SIO), Submitted to the NASA Ice Cloud and Land Elevation Satellite (ICESat) Science Team. Requesting a total of \$159,608 (total, BNL component) for 3 years. Pending.
- 6) "Investigation of Precipitation Systems Using Integrated A-train Observations," co-I (PI Pavlos Kollias, BNL), Submitted to the NASA CloudSat Science Team. Requesting \$748,000 (total) for 3 years. Pending.

Presentations:

- 1) Collins, W. D.; A. M. Vogelmann, M. P. Jensen, G. Zhang, and E. Luke, 2005: Marine Stratus Analysis and Parameterization using MODIS

Observations. Presented at the Cloud Modeling Workshop, Marriott Hotel, Fort Collins, 6-8 July.

- 2) Jensen, M. P.; A. M. Vogelmann, and W. D. Collins, 2004: Regional and Seasonal Variations in Stratus Cloud Properties from MODIS Observations. Proceedings of the AGU Fall Meeting, San Francisco, 13-17 December.
- 3) Jensen, M. P.; A. M. Vogelmann, W. D. Collins, G. Zhang and E. Luke, 2005: Radiative Effects of Subgrid Scale Variability in Stratus Cloud Properties from MODIS Observations. Proceedings of the 5th International Scientific Conference on the Global Energy and Water Cycle, Westin Hotel, Orange County, California, 20-24 June.
- 4) Vogelmann, A. M.; M.P. Jensen, and W.D. Collins, 2004: Radiative Effects of Stratus Cloud Subgrid Scale Variability Observed by MODIS. Proceedings of the AGU Fall Meeting, San Francisco, 13-17 December.
- 5) Vogelmann, A. M.; M.P. Jensen, E. Luke, and E.R. Boer, 2005: Tropical Cloud Overlap Structure and Cloud Area. Proceedings of the Fifteenth Atmospheric Radiation Measurement (ARM) Science Team Meeting, Daytona Beach, Florida, 14-18 March.

LDRD FUNDING:

FY 2005	\$92,858
---------	----------

Computational Science

James W. Davenport

05-110

D. Keyes

K. Kang

Y. Deng

J. Glimm

PURPOSE:

This is a project to develop new basic parallel algorithms for the efficient solution of large linear systems, both sparse and dense and to apply them to the electronic structure of nanoscale clusters of atoms. Our density functional theory (DFT) codes solve coupled Schrodinger and Poisson equations using localized basis sets. Thus, they naturally lead to large linear systems. We use techniques developed through our DOE SciDAC project TOPS (Terascale Optimal Partial Differential Equation Simulation, www.tops-scidac.org). Application is to palladium clusters, with potential use in hydrogen storage, and to gold clusters which are important catalysts.

APPROACH:

Most DFT calculations apply to small molecules or to crystals. The approach here provides a new capability for finite clusters. We utilize a localized augmented basis set consisting of Slater type orbitals outside atom centered spheres and numerical solutions of the radial Schrodinger equation inside. Solutions of the Poisson equation in the region between spheres is carried out numerically on an overset grid. Inside the spheres the charge density and potential are given in a spherical harmonic expansion which naturally describes the rapid variation in these quantities near the nuclei. A key step here is the incorporation of modern grid based techniques including multigrid and

sparse matrix solvers into a usable, massively parallel, code.

TECHNICAL PROGRESS AND RESULTS:

The parallel LASTO code has been written and is undergoing testing. Results have been obtained for small palladium clusters and for small clusters of cobalt-nickel. On completion of testing, the applied mathematics issues associated with finite basis set errors and larger matrix diagonalization will be explored. Applications will be extended to hydrogen metal systems associated with hydrogen storage. Performance of several of the SciDAC codes which will be utilized has been evaluated on BlueGene/L and the TeraGrid. The technique of all-gather for massively parallel computing is important both for electronic structure calculations and for molecular dynamics.

SPECIFIC ACCOMPLISHMENTS:

Publications:

R. Rissland and Y. Deng, All-gather on QCDOC, *Parallel Computing*.

LDRD FUNDING:

FY 2005	\$109,776
FY 2006 (budgeted)	\$126,000

Structural Study of the gamma-Secretase by Cryo-EM

Huilin Li

05-111

PURPOSE:

γ -Secretase is an unprecedented intramembrane-cleaving aspartyl protease required for the normal development of metazoans because it processes Notch within cellular membranes to release its intracellular signaling domain. The protease is also causally implicated in Alzheimer's disease, as it releases the neurotoxic amyloid β -peptide ($A\beta$) from its large precursor, Amyloid Precursor Protein (APP). γ -Secretase constitutes a high molecular weight complex comprised of Presenilin (bearing the active site aspartates), Nicastrin, Aph-1 and Pen-2, and enzymatic activity can be fully reconstituted with only these four proteins. No structural information has been reported for γ -secretase or any other intramembrane protease. This hinders the understanding at the molecular level of the notch signaling pathway and the development of anti-neurodegenerative disease agents targeting the unique protease as well. Our purpose is to gain mechanistic insight of the γ -secretase through structural studies.

APPROACH:

γ -Secretase was first recognized as the proteolytic activity responsible for generating $A\beta$ via cleavage of APP within cellular membranes. Inherited mutations in Presenilin, the active site component of γ -secretase, modulate the intramembrane cleavage of APP to increase levels of the highly amyloidogenic $A\beta_{42}$ peptide in humans. APP, Notch and other γ -substrates must undergo shedding of their large

ectodomains by one of the α -secretases, or by β -secretase, before they can be processed within the membrane by γ -secretase. Beyond the intense interest in γ -secretase function for normal cell biology, the enzyme has emerged as a key therapeutic target for Alzheimer's disease, and inhibitor design would be much facilitated by structural information about the proteolytic mechanism. No structural information has been reported for the γ -secretase complex or any other intramembrane protease, and the presence of at least 18 transmembrane domains will make crystallographic approaches challenging. We decided to determine the molecular architecture of the γ -secretase by cryo-electron microscopy, a method that requires a minimum amount of purified sample, and without a need for crystallization.

We have established collaboration with D. Selkoe at Harvard Medical School and Brigham and Women's Hospital. He is one of the world leaders in neuron degenerative disease research, and a founder of the pharmaceutical company ELAN.

TECHNICAL PROGRESS AND RESULTS:

- (1) Unlike most proteins, γ -secretase is very difficult to prepare at a high-grade level that is pure and homogeneous enough for a rigorous structural study. Working with our collaborators at Harvard, our first major breakthrough of the project was obtaining purified γ -secretase that was active and produced physiological ratios of $A\beta_{42}$ and $A\beta_{40}$.
- (2) The second result was the three-dimensional reconstruction of the γ -secretase structure from electron microscopy (EM) images. The resolution we achieved was 15 Å and demonstrated that γ -secretase has

an elongated globular structure, with the longest dimension being ~120 Å (in the membrane) and the other two dimensions perpendicular to the long axis being about 70-80 Å each. A major feature of the 3D map was a belt-like density ~60 Å high circumferentially around the particle that is very likely to be the transmembrane portion of γ -secretase. There is a low-density central chamber with a diameter of 20-40 Å. The extracellular density at the top of the map can be attributed to part of the large (669 amino acid) ectodomain of NCT, as it comprises a long extracellular polypeptide (~70 kDa) onto which N-linked oligosaccharide groups are attached. At the display threshold, we observed two openings to the interior chamber: one of ~20 Å size facing up toward the exterior of the cell, and the other about 10 Å in size facing down toward the cytoplasm.

(3) To determine the basic orientation of the complex in the membrane and ascertain whether the top surface in our 3D map faces the extracellular or the cytoplasmic space, we localized the extracellular domain of the enzyme complex by taking advantage of the fact that multiple N-linked oligosaccharide groups occur exclusively in the Nicastrin ectodomain, and that the plant lectin, Concanavalin A, can bind their mannose and glucose residues highly specifically.

The most enigmatic feature of γ -secretase and other intramembrane proteases is their location within the hydrophobic environment of the membrane and yet has a requirement for water molecules to accomplish peptide bond hydrolysis. The observed interior chamber and apical and basal pores in the EM structure would allow the entry of water molecules and their sequestration from the lipid surrounded by the proteinaceous microenvironment provided by the many transmembrane domains. The two thin-density regions in

the transmembrane portion may represent sites which could be opened up transiently to enable entrance of the α -helically conformed substrates,

SPECIFIC ACCOMPLISHMENTS:

Follow-On Funding:

Develop a Hybrid Electron Cryo-Tomography Scheme for High Throughput Protein Mapping in Whole Bacteria, H. Li and J. Hainfeld (co-PIs), DOE, KP1102010, BO-122, \$1,700,000 for FY 2005-2007.

Publications:

Structural role of glycine in amyloid fibrils formed from transmembrane α -helices. Liu, W.; Crocker, E.; Zhang, W.; Elliott, J. I.; Luy, B.; Li, H.; Aimoto, S.; and Smith, S. O. *Biochemistry* **44**, 3591-3597 (2005).

Structure of the CED-4-CED-9 complex provides insights into programmed cell death in *Caenorhabditis elegans*. Yan, N.; Chai, J.; Lee, E. S.; Gu, L.; Liu, Q.; He, J.; Wu, J. W.; Kokel, D.; Li, H.; Hao, Q.; Xue, D.; and Shi, Y. *Nature* **437**, 831-837 (2005).

Electron microscopic structure of purified, active γ -secretase reveals an aqueous intramembrane chamber and two pores. Lazarov, V. K.; Fraering, P. C.; Chen, Z.; Ye, W.; Wolfe, M. S.; Selkoe, D. J.; and Li, H. *Proc. Natl. Acad. Sci. USA* (submitted).

LDRD FUNDING:

FY 2005 \$191,280

Structural Analysis of Bacterial Pilus Biogenesis

Huilin Li

05-112

PURPOSE:

Gram-negative bacterial pathogens have evolved multiple pathways for the assembly and secretion of virulence factors across their outer membranes (OM). The basic workings of these pathways are beginning to be understood, but detailed knowledge of the molecular mechanisms governing secretion, particularly across the OM, is lacking. Structural information is essential for a thorough understanding of the secretory process.

APPROACH:

In this project, we apply high-resolution electron microscopy (EM) techniques to elucidate the structural basis of secretion in Gram-negative bacteria. We focus on the chaperone/usher pathway that is dedicated to the assembly and secretion of a superfamily of virulence-associated surface structures. The prototypical organelles assembled by this pathway are the adhesive P and type 1 pili of uropathogenic *Escherichia coli*.

The PapC usher is an integral OM protein that has been shown to assemble into an oligomeric, ring-shaped complex. However, the oligomeric state of the complex has not been defined and the 3D structure is unknown. Purified usher protein will be reconstituted back into lipid bilayers – their native environment – for the generation of two-dimensional (2D) crystals. The 2D crystals will be used to determine the oligomeric state of the usher complex and to generate a 3D structure of the usher at medium resolution by electron crystallography. In addition, three-

dimensional crystallization and X-ray crystallography will be attempted for the wild type PapC usher.

The usher serves not only as a secretion channel, but also as a platform for the ordered assembly of subunits into the pilus fiber. Procedures have been established for the co-purification of *in vivo* pilus assembly intermediates with the usher, representing various stages of pilus biogenesis. These complexes will be analyzed by single-particle cryo-electron microscope (EM) techniques to determine the mechanism of pilus assembly and secretion by the usher. Cryo-imaging will also be used to analyze pilus assembly intermediates generated *in vitro*.

Collaborated with D. Thanassi at Stony Brook University who is a microbiologist with extensive research experience in pathogenic bacterial appendage studies. Our close collaboration ensures that we are getting the right bacterial clones and many PapC and assembly intermediate mutants for structural studies. Also established a collaboration with J. St. Geme III, Department Chair and Pediatrician in Purdue University, on the studies of a membrane protein called HMW1 from *Haemophilus influenzae*, which is responsible for the secretion of adhesin.

TECHNICAL PROGRESS AND RESULTS:

(1) Through 2D crystallization and electron crystallographic work, we found that wild-type PapC formed a dimer in the lipid bilayer, instead of the previously believed hexamer. We further confirmed by other biophysical characterizations, such as dynamic light scattering and direct single particle EM observation, that wild-type PapC was in the dimeric form in detergent solution.

(2) A large C-terminal deletion mutant, PapC640D (lacking 169 amino acid residues), inserts properly in the outer membrane and forms a stable β -barrel structure similar to wild-type PapC. This C-terminal domain is not required for *in vitro* chaperone-subunit interaction, but is essential for *in vivo* pilus biogenesis. We also successfully grew 2D crystals of the PapC mutant, and found the C-terminal deletion mutant of PapC formed a twin-pore dimer with altered packing as compared to the wild type dimer.

(3) In order to obtain a high-resolution structure of the PapC usher, we have started the 3D crystallization effort. Preliminary 3D crystals have been obtained. The crystals are small and not at the diffraction-quality yet. More work is needed to improve the quality.

(4) For the adhesin secreting membrane protein HMW1B, we have obtained a low resolution EM structure through a single particle method. We have recently obtained 2D crystals, and a medium resolution structure has been calculated from EM images of the 2D crystals.

Major conclusion from our structural studies of PapC usher and the HMW1B was that both outer membrane proteins formed dimeric structures, and the secretion channels were located inside the proteinacious β -barrels, not between the dimer interface.

SPECIFIC ACCOMPLISHMENTS:

Follow-On Funding:

Develop a Hybrid Electron Cryo-Tomography Scheme for High Throughput Protein Mapping in Whole Bacteria, H. Li and J. Hainfeld (co-PIs), DOE, KP1102010, BO-122, \$1,700,000 for FY 2005-2007.

Publications:

Characterization of a *Mycobacterium tuberculosis* proteasomal ATPase homologue. Darwin, K. H.; Lin, G.; Chen, Z.; Li, H.; and Nathan, C. F. *Molec. Microbiol.* 55(2), 561-571 (2005).

Protein secretion in the absence of ATP: the autotransporter, two-partner secretion and chaperone/usher pathways of Gram-negative bacteria (Review). Thanassi, D. G.; Stathopoulos, C.; Karkal, A.; and Li, H. *Mol. Membrane Biol.* 22(1-2), 63-72 (2005).

ATPase-dependent cooperative binding of ORC and Cdc6 to origin DNA. Speck, C.; Chen, Z.; Li, H.; and Stillman, B. *Nature Struct. Mol. Biol.* (in press).

LDRD FUNDING:

FY 2005	\$208,405
---------	-----------

Study of High- T_c Nanostructures

Ivan Bozovic

05-114

PURPOSE:

We are investigating systematically the effects of reduced dimensionality and confined geometries on high-temperature superconductors (HTS). This allows us to attack some of the most basic questions in the HTS physics such as what are the spin and the charge of free carriers and what is the nature of superconducting transition. We will determine if Cooper pairs form and condense at T_c or else do the pairs formed at some higher temperature T^* undergo Bose-Einstein condensation at T_c - and is the presence of dynamic stripes a necessary condition for HTS to occur. If we demonstrate that HTS can be sustained in mesoscopic samples (such as nanowires or nanodots), this would rule out a large class of theoretical models currently under active investigation and narrow down the playing field; this could be an important step towards elucidation of the mechanism of HTS.

APPROACH:

We use the state-of-the art atomic-layer-by-layer molecular beam epitaxy (ALL-MBE) system to synthesize atomically smooth HTS films, multilayers and superlattices. Electron-beam nanolithography allows fabrication, from such films, of a variety of mesoscopic (nanoscale) devices such as nanowires, nanorings, and nanodots. Measurements of transport properties of these nanostructures reveal their critical temperature T_c , the critical current density j_c , etc. It is important to make as perfect samples as possible in order to discriminate between extrinsic and intrinsic causes of T_c reduction. Other participants in this project are G. Logvenov, V. Butko, A. Gozar, and A. Bollinger.

TECHNICAL PROGRESS:

The MBE system was assembled and calibrated. The ozone distillation system was designed in conformity to BNL safety standards, constructed, and used routinely. So far we ran 31 growth experiments. $R(T)$ and $\chi(T)$ measurement setups were built. Every film was characterized by reflection high-energy electron diffraction (RHEED), transport measurements (resistivity and susceptibility as a function of temperature down to 4.2 K), and atomic force microscopy (AFM). Selected ones were also characterized by Rutherford back-scattering. Some films were atomically smooth; this milestone was reached faster than the most optimistic expectations. [One-two years is more typical.]

The plan for FY 2006 is to synthesize by MBE a number of atomically smooth HTS films, characterize them by RHEED, x-ray diffraction, AFM, and transport measurements; install and calibrate lithographic equipment, design, acquire and test lithographic masks, fabricate testing structures, build the setup for measurement of I-V characteristics of micro and nano-structures, perform measurements, and analyze the results.

SPECIFIC ACCOMPLISHMENTS:

Refereed Publications:

1. Giant Proximity Effect in cuprate superconductors. I. Bozovic, G. Logvenov et al. *Phys. Rev. Letters* 93, 157002 (2004). [Highlighted in *Physics World*, Dec. 2004, pp. 19-20.]
2. Ultrafast light generates coherent sound. I. Bozovic et al. *Phys. Rev. B* 69, 132503 (2004). [Highlighted in *Science Today*, *Virtual Journal of Ultrafast Science and Virtual Journal of Applications of Superconductivity*.]
3. Combinatorial molecular beam epitaxy of $\text{La}_{2-x}\text{Sr}_x\text{CuO}_4$. G. Logvenov, I. Sveklo, and I

- Bozovic. Proc. SPIE Proceedings 5932, 2005.
4. Structure and transport properties of the charge-transfer salt coronene – TCNQ. X. Chi, V. Y. Butko, et al. Chemistry of Materials 16, 5751 (2004).
 5. Crystallization of charge holes in the spin ladder $\text{Sr}_{14}\text{Cu}_{24}\text{O}_{41}$. P. Abbamonte, A. Gozar, et al. Nature 431, 1078 (2004).
 6. Nano-engineered multi-layer films and superlattices of cuprates and other complex oxides. I. Bozovic. Proc. ICCNE-11 (2005).
 7. Highly conductive nanolayers on strontium titanate produced by preferential ion beam etching. W. Reagor and V. Y. Butko. Nature Materials 4, 593 (2005).
 8. Low-temperature field effect in a crystalline organic material. V. Y. Butko, J. C. Lashley and A. P. Ramirez. Phys. Rev. B 72, 081312 (2005).
 9. Symmetry and Light Coupling to Phononic and Collective Magnetic Excitations in $\text{SrCu}_2(\text{BO}_3)_2$. A. Gozar et al. Phys. Rev. B 72, 064405 (2005).
 10. Evolution of Superconductivity in Electron-Doped Cuprates: Magneto-Raman Spectroscopy. M. M. Qazilbash, A. Gozar, et al. Accepted for publication in Phys. Rev. B.
- Correlated Electron Systems, 7-11 June 2005, Maui, Hawaii.
6. Artificial superlattices grown by MBE: can we design novel superconductors? G. Logvenov. Workshop on Room Temperature Superconductivity, 10-11 June 2005, Notre Dame University, Indiana.
 7. Combinatorial molecular beam epitaxy of $\text{La}_{2-x}\text{Sr}_x\text{CuO}_4$. I. Bozovic. American Conference on Crystal Growth and Epitaxy, 9-16 July 2005, Big Sky Resort, Montana.
 8. Shaping the beam fluxes for combinatorial molecular beam epitaxy of $\text{La}_{2-x}\text{Sr}_x\text{CuO}_4$. G. Logvenov, International Conference on Strongly Correlated Electron Materials: Physics and Nano-engineering, 31 July – 4 August 2005, San Diego, California.
 9. Atomic-layer engineering of high-temperature superconductors and other strongly correlated oxides. I. Bozovic. 2005 YUCOMAT, 12-16 September 2005, Herceg Novi, Serbia and Montenegro.
 10. Giant proximity effect. I. Bozovic. 18th ISS, October 24-26, 2005, Tsukuba, Japan.
 11. Strong electron-phonon coupling in high-temperature superconductors. I. Bozovic. International Workshop on Electron State and Lattice Effects in Cuprate High Temperature Superconductors, October 27-28, 2005, Tsukuba, Japan.

Invited Talks:

1. Atomically layered cuprates. I. Bozovic. Aspen Winter Conference on High Temperature Superconductivity, 9-15 January 2005, Aspen, Colorado.
2. Nano-Film Density of States and Transport at the Metal Insulator Transition. V. Butko. Workshop on Physics of Ultra Thin Films Near the Metal Insulator Transition II, 6-7 Jan. 2005, BNL, New York.
3. High quality crystalline pentacene and rubrene FETs. V. Butko, APS Meeting, 20-25 March 2005, Los Angeles, California.
4. Ultrafast pump-probe experiments on high- T_c cuprates. I. Bozovic. Workshop on Spectroscopic Studies of Nanoscale Systems, May 25, BNL, New York.
5. Atomic-layer engineering and the physics of high-temperature superconductors. CERC-ERATO Workshop on Phase Control of

Three new DOE grants were awarded and the total of \$1,930,558 was received in FY 2005. The funding is secured for two more years as follows:

1. US DOE project: Molecular Beam Epitaxy of Complex Materials, \$115,000
2. US DOE project: Molecular beam epitaxy and nano-structuring of perovskite oxide materials toward an understanding of strongly correlated systems \$1,362,337
3. US DOE capital equipment grant, \$453,221

LDRD FUNDING:

FY 2005	\$265,787
FY 2006 (budgeted)	\$275,000

Appendix A

2006 Project Summaries

Appendix A BNL FY 2006 Projects

- (06-071) Development of a Cloud Condensation Nucleus Separator
J. Wang (FY 2006 Funding \$52,500)

Plan to develop a novel Cloud Condensation Nucleus Separator (CCN separator) that separates CCN and non-CCN under climatically important supersaturations.

- (06-074) Aluminum Hydride - An Ideal Hydrogen Source for Small Fuel Cells
J. Graetz (FY 2006 Funding \$100,000)

Involves the synthesis and fundamental characterization of the seven crystalline aluminum hydride (AlH₃) polymorphs. The crystallographic structures and the thermodynamic properties of each of the phases will be determined and used to establish the relative stabilities of the different AlH₃ polymorph structures and how phase transitions occur between polymorphs.

- (06-087) Gamma Ray Imager for National Security Applications
P. E. Vanier (FY 2006 Funding \$100,000)

A next-generation coded-aperture gamma ray imager for nuclear materials detection will be developed by integrating expertise in national security technology, medical imaging physics, and electronics development. The gamma-ray detector portion of the imager is based on a similar device developed for Positron Emission Tomography applications, consisting of custom-designed application-specific integrated circuits for pixel-by-pixel readout of arrays of avalanche photodiodes that detect scintillation light from commercially available scintillator materials.

- (06-088) Neurogenomics: Collaboration Between the Biology Department and the Brookhaven Center for Translational Neuroimaging to Investigate Complex Disease States
J. S. Fowler/N. Alia-Klein (FY 2006 Funding \$113,000)

Establish vital tools that combine genetics and neuroimaging to find causes for human disease. Will target genotypes that encode different levels of the major neurotransmitters of Dopamine and serotonin (5-HTT), that are known to regulate brain functioning and may confer vulnerability to certain disease.

- (06-092) Nanoparticle Labeled Neural Stem Cell Tracking In Vivo by Magnetic Resonance Microscopy
H. Benveniste (FY 2006 Funding \$83,000)

Develop and implement new technology using stem cells, nanoparticles coated with organic moieties, and high-resolution magnetic resonance microscopy to track the fate of neuronal stem cells on a bio-systems level in vivo.

Exhibit A

Director's Office
Laboratory Directed Research and Development Program



Building 815E
P.O. Box 5000
Upton, NY 11973-5000
Phone 631 344-4467
Fax 631 344-2887
newman@bnl.gov

managed by Brookhaven Science Associates
for the U.S. Department of Energy

Memo

date: March 7, 2005

to: Distribution

from: L. Newman L.N.

subject: Laboratory Directed Research & Development Program (LDRD) Proposals

We are now soliciting proposals for the annual LDRD competition. Proposals must be submitted **electronically by email** through your respective Chairperson and Associate Laboratory Director to Kevin Fox (kjfox@bnl.gov) by April 15, 2005. The revised version of the Proposal Information Questionnaire (PIQ) submission form **must** be used, and it can be obtained electronically by going to <https://sbms.bnl.gov/standard/3c/3c02e011.htm> or from greco@bnl.gov. A copy is attached for your convenience. The BNL LDRD Policy, which defines the LDRD Program, can be reviewed at this web site. In my capacity as Scientific Director for LDRD, I am available to counsel individuals to aid them in their preparation of a successful proposal.

Please note that we require an abstract to fit on the first page of the form and a proposal that is not more than three pages in length. Also, note that LDRD projects are restricted to a maximum of three years. However, projects and their budgets should be tailored to no more than a two-year schedule. Along with your proposal you are requested to include a one-page vita and a milestone schedule of activities to be completed with planned accomplishments and dates of completion of for example: lab setups, test runs or trials, compiled data sets, reports to be issued on results, etc. In each year there is a mid- year review of all programs to assess the extent of progress.

Research conducted under the LDRD Program should be highly innovative, and an element of high risk as to success is acceptable. This year we will be especially pleased to receive innovative new projects in support of RHIC and the Light Source and any of the Strategic Initiatives listed at the LDRD web site, www.bnl.gov/ldrld. The total amount of money for new starts in FY 2006 has not yet been determined.

The Selection Committee will be chaired by the Scientific Director for LDRD and includes the Deputy Director for Science and Technology along with the Associate Laboratory Directors and is augmented by selected distinguished scientists. The committee hopes to conclude the selection process by the end of June.

Exhibit A

For your convenience and planning purposes, note the following calendar for LDRD activities.

March 7, 2005	Call for FY 2006 Proposals
April 15, 2005	FY 2006 Proposals Due
May 2 – 6, 2005	FY 2005 Mid-Year review
May 25 – June 30, 2005	Selection of FY 2006 Projects
August 15, 2005	FY 2006 Plan Due to DOE
October 1, 2005	Funding of FY 2006 Projects
October 11, 2005	Call for FY 2005 Annual Reports
November 14, 2005	FY 2005 Annual Reports Due

LN:kjf
Attachment

Distribution:

Level I & II Managers

cc: P. Looney
N. Narain

Exhibit B

BROOKHAVEN NATIONAL LABORATORY PROPOSAL INFORMATION QUESTIONNAIRE LABORATORY DIRECTED RESEARCH AND DEVELOPMENT PROGRAM

PRINCIPAL INVESTIGATOR _____

PHONE _____

DEPARTMENT/DIVISION _____

DATE _____

OTHER INVESTIGATORS _____

TITLE OF PROPOSAL _____

PROPOSAL TERM (month/year) From _____ Through _____

SUMMARY OF PROPOSAL

Description of Project:

Expected Results:

INSTRUCTIONS

Under **Description of Project**, provide a summary of the scientific concept of the proposed project including the motivation for the undertaking and the approach that will be used to conduct the investigation. Also indicate how the project meets the general characteristics of the LDRD Program and how it is tied to the DOE Mission. Under **Expected Results**, clearly enunciate what are the expected results and how they will impact the science. These items should not exceed the space remaining on this page, using the given font and size. Follow this page with an extended Proposal of no more than three (3) pages in length plus a Milestone Schedule. In addition, include a one-page Vita of the Principal Investigator; fill out the page with citations to recent pertinent publications. Do not include any additional attachments, as these will be discarded. Complete the Questionnaire, obtain the required approvals, and provide a Budget in the format on the form supplied. Break down the funding by fiscal year and by the broad categories of labor, materials and supplies, travel (foreign & domestic), services and subcontracts. LDRD funds cannot be used to purchase capital equipment. Indicate the intent to use collaborators, postdoctoral research associates, and/or students. Identify the various burdens applied, i.e., organizational, materials, and contracts. Include any other charges but the Laboratory G&A should not be applied. Go to the LDRD web site (www.bnl.gov/ldr/) for further information. **(This paragraph should be deleted before you input the requested information.)**

Exhibit B
PROPOSAL

Exhibit B

VITA (Principal Investigator)

Exhibit B
LDRD MILESTONE SCHEDULE

Date	Planned Accomplishments
6 months	
1 year	
18 months	
2 years	
30 months	
3 years	

Exhibit B

1. HUMAN SUBJECTS (Reference: DOE Order 1300.3)

Are human subjects involved from BNL or a collaborating institution?

If **yes**, attach copy of the current Institutional Review Board Approval and Informed Consent Form from BNL and/or collaborating institution.

Y/N _____

2. VERTEBRATE ANIMALS

Are vertebrate animals involved?

Y/N _____

If **yes**, has approval from BNL's Animal Care and Use Committee been obtained?

Y/N _____

3. NEPA REVIEW

Are the activities proposed similar to those now carried out in the Department/Division which have been previously reviewed for potential environmental impacts and compliance with federal, state, local rules and regulations, and BNL's Environment, Safety, and Health Standards? (Therefore, if funded, proposed activities would require no additional environmental evaluation.)

Y/N _____

If **no**, has a NEPA review been completed in accordance with the Subject Area National Environmental Policy Act (NEPA) and Cultural Resources Evaluation and the results documented?

Y/N _____

(Note: If a NEPA review has not been completed, submit a copy of the work proposal to the BNL NEPA Coordinator for review. No work may commence until the review is completed and documented.)

4. ES&H CONSIDERATIONS

Does the proposal provide sufficient funding for appropriate decommissioning of the research space when the experiment is complete?

Y/N _____

Is there an available waste disposal path for project wastes throughout the course of the experiment?

Y/N _____

Is funding available to properly dispose of project wastes throughout the course of the experiment?

Y/N _____

Are biohazards involved in the proposed work? If yes, attach a current copy of approval from the Institutional Biosafety Committee.

Y/N _____

Can the proposed work be carried out within the existing safety envelope of the facility (Facility Use Agreement, Nuclear Facility Authorization Agreement, Accelerator Safety Envelope, etc.) in which it will be performed?

Y/N _____

Exhibit B

If **no**, attach a statement indicating what has to be done and how modifications will be funded to prepare the facility to accept the work.

5. TYPE OF WORK

Select Basic, Applied or Development _____

6. LINK TO LABORATORY STRATEGIC INITIATIVES

Identify below if the proposal is in support of RHIC, the Light Source, or any of the Strategic Initiatives that can be found listed at the LDRD web site, www.bnl.gov/ldrdr.

7. POTENTIAL FUTURE FUNDING

Identify below the Agencies and the specific program/office, which may be interested in supplying future funding. Give some indication of time frame.

APPROVALS

Department /Division Administrator _____

Print Name

Department Chair/Division Manager _____

Print Name

Cognizant Associate Director _____

Print Name

Exhibit B

BUDGET REQUEST BY FISCAL YEAR

Department

Title

PI

(Note: Funding for more than 2 years is unlikely and cannot exceed 3 years)

COST ELEMENT	FISCAL YEAR _____	FISCAL YEAR _____	FISCAL YEAR _____	TOTAL COST
Labor* Fringe Total Labor Organizational Burden @ _____ %				
DISTRIBUTED TECHNICAL SERVICES				
Materials Supplies Travel Services Total MST Materials Burden @ _____ %				
TECHNICAL COLLABORATORS/ CONSULTANTS				
Sub-contracts Contracts Burden @ _____ %				
Electric Power Other (specify)				
TOTAL PROJECT COST				
*Labor (give levels of effort with names, or if unknown indicate TBD) <u>Scientific & Professional</u> <u>Post Doc</u> <u>Other</u>				
<u>Note:</u> The Budget Office covers 20% of the Post Doc's salary/fringe.				
List all Materials Costing Over \$5,000				

Exhibit C

LDRD DATA COLLECTION FORM

Read and then remove the instructions before attempting to complete this form and return it electronically to D. J. Greco (greco@bnl.gov)

LDRD PROJECT NUMBER:

PROJECT TITLE:

PRINCIPAL INVESTIGATOR(S):

PUBLICATIONS

TOTAL _____

List all refereed publications originating in whole or in part from this LDRD including those that have been submitted, but do not include any that are in preparation during the fiscal year.

Example of style

Ozone production in the New York City Urban Plume. Kleinman, L. I., Daum, P. H., Imre, D. G., Lee, J. H., Lee, Y. -N., Nunnermacker, L. J., Springston, S. R., Weinstein-Lloyd, J., and Newman, L. J. *Geophys. Res.*, 105, 14,495-14,511 (2000).

MEETINGS, PROCEEDINGS, AND ABSTRACTS

TOTAL _____

List all formal presentations originating in whole or in part from this LDRD presented during the fiscal year.

Example of style

Ozone production in the New York City urban plume. Kleinman, L., Daum, P. H., Imre, D., Klotz, P., Lee, J. H., Lee, Y. N., Nunnermacker, L. J., Springston, S., Weinstein-Lloyd, J., and Newman, L. American Geophysical Union Fall Meeting, San Francisco, CA, Dec. 8-12, 1997.

REPORTS

TOTAL _____

List all formal reports originating in whole or in part from this LDRD including those that have been published during the fiscal year.

PATENTS AND LICENSES

TOTAL _____

List all patents and licenses originating in whole or in part from this LDRD during the fiscal year. Provide the total number above.

Exhibit C

COPYRIGHTS

TOTAL _____

List all copyrights (other than publications) originating in whole or in part from this LDRD granted during the fiscal year. Provide the total number above.

INVENTION DISCLOSURES

TOTAL _____

List all invention disclosures submitted during the fiscal year to the Laboratory's Office of Intellectual Property & Sponsored Research that were either directly derived from this LDRD or from any follow-on efforts.

PROJECT REVIEWS

TOTAL _____

List all formal review presentations that pertain to this work conducted during the fiscal year. Include the name of the reviewing body and date of review, title of presentation, and names of presenters. Do not include the mid-year LDRD program reviews. Provide the total number above.

STUDENTS AND RESEARCH ASSOCIATES

TOTAL _____

Provide names of all graduate students and Research Associates supported during the fiscal year and give the number of months that they were supported. Provide the total number above combined as full-time equivalents, rounded to the nearest month.

NEW HIRES

TOTAL _____

Provide names of any new staff that were hired during the fiscal year as a direct result of this LDRD. Provide the total number above.

FOLLOW-ON FUNDING

TOTAL _____

List all requests for funding submitted during the current and prior fiscal years including any that have been rejected. Give the title of the project, the Principal Investigator, date of submission, the name of the agency, action taken, amount funded or requested per year, and the duration. Provide the total number above.

AWARDS

TOTAL _____

Provide information on any national awards or recognitions received during the fiscal year that are attributable in whole or in part to the LDRD project. For each award, describe (in 150 words or less) its significance and the role that LDRD played in achieving it. Provide the total number above.